Development of methods for retinal ganglion cell replacement in glaucoma

MEGAN FRANCES JONES

Thesis submitted to University College London for the degree of Doctor of Philosophy

UCL Institute of Ophthalmology

University College London

June 2013

Declaration

I, Megan Frances Jones confirm that the work presented in this thesis is my own. Where the information has been derived from other sources, I confirm that this has been indicated in the thesis.

June 2013

Acknowledgements

The work presented in this thesis would not have been possible without the help of many people. I would like to thank Professor Astrid Limb for the opportunity to carry out this research and the NIHR for funding my PhD. Her eternal support and guidance during my research was invaluable and I am extremely grateful for her supervision and her mentorship. Thank you Astrid for your kind words and endless care and encouragement, you are an inspiration, as a scientist and as a woman. I would also like to thank Professor Karl Matter for his direction through the molecular biology and the suggestions during my project.

I would like to thank the Müllers, old and new, who have always been a tremendous support and for making my PhD less traumatic, always providing comic relief and technical support. Thanks to DrDr, DrDr B, FP, Silke, Karen, Dan, Joey, Stefano, Aman, Phil, Na, Hussam and Angshu. A special thank you to Ha-ri, for being a constant rock to me, I would not have been able to get through the last few years without your help, thanks for being my PhD buddy. I would also like to acknowledge the Müller fountain of knowledge EM (efficient Müller) or Phillippa for all the help with PCRs, Westerns, ERGs, cell culture, electrospining, PC, as well as answering all my questions. I also want to thank Sudershana for her friendship as well as Naheed, Claire, Joanne and Aida, who have all made my life at the institute run smoothly. I would like to thank the BRU staff for their guidance and help during the *in vivo* experiments and Dan Frampton and Douglas King for their technical expertise with the miRNA analysis for this thesis.

I would like to thank everyone in the Ocular Regeneration and Biology department. In particular, the students, as well as Anne Snowling and Professor Pete Coffey for their faith and friendship during my time as one of the student reps.

I am extremely grateful to my friends and family for their belief, encouragement and constant love. In particular, I am indebted to my Mum (Mama-Meg aka my hero), who has always been my one constant champion. Although I may not say it enough, I am grateful for all you have done for me, especially during the past few years, enduring my numerous highs and lows, THANK YOU. I want to express my thanks to my Granddad, Rae, who has always been enthusiastic and encouraged my interest in biology. I would also like to acknowledge my Uncle Mick, without whom, I would not have had the opportunities given to me, you have always believed in me from a very young age and are an incredible man and inspiration. Finally, I would like to give my appreciation to all the babies I have helped over the years. I am privileged to have been part of your journeys into adulthood and am so proud of you all. You have kept me sane (and cool) and have always inspired me to do more. I dedicate this thesis to you guys, the next generation.

Abstract

A sub population of human Müller glia contained within the neural retina is known to exhibit stem cell characteristics. Previous studies in the host laboratory have investigated their ability to differentiate into different retinal populations *in vitro,* providing a potential source of cells for development of therapies to treat retinal degenerative diseases. This study investigated molecular factors involved in differentiation of retina ganglion cells (RGCs) derived from human Müller stem cells. It also aimed to explore the feasibility of transplanting RGC derived from Müller stem cells into large mammalian eyes, using collagen based cellular scaffolds. These objectives ultimately aimed to study the potential application of Müller stem cells for treatment of late stage glaucoma.

As determined by microarray analysis of total RNA specimens, *in vitro* culture of Müller stem cells undergoing Notch inhibition in the presence or absence of bFGF, led to alteration in microRNA (miRNA) profiles. These are short RNA molecules synthesised within cells that play a role in various cellular processes. MicroRNAs associated with Notch signalling, cell cycling and differentiation, were enriched in Müller cell populations undergoing Notch inhibition, conditions previously shown to induce RGC development. Elevated expression of these specific miRNAs suggests the emergence of novel targets under the regulation of the Notch pathway in Müller stem cells. These constitute factors that could be potentially used to develop therapies which facilitate endogenous neural differentiation of the latent Müller stem cell population in the human neural retina.

Collagen based cellular scaffolds were developed to deliver RGCs derived from Müller stem cells onto the inner retina of the large mammalian eye. Collagen is a ubiquitous protein found within numerous tissues types, acting as a framework for cellular support and adhesion. Delivery of grafted cells onto retinal explants *in vitro,* and transplantation of scaffolds into the rabbit

eye *in vivo,* was examined by confocal microscopy and showed that plastic compressed collagen scaffolds served as a potential suitable substrate for transfer of cells to the host retina. Integration was observed in some cases and rarely observed into host tissue, facilitated by degradation of the extracellular matrix by chondroitinase ABC and by the use of the anti-inflammatory agent triamcinolone *in vivo*.

In conclusion, the present study showed that standardised protocols used to differentiate Müller stem cells into RGC promoted alterations in Müller stem cell miRNAs associated with RGC development and maturation. In addition, compressed collagen scaffolds were shown to aid delivery of RGCs onto the inner retinal surface. These observations pave the way for further investigations to promote endogenous retina regeneration and refinement of transplantation strategies to apply these cells to the development of human therapies.

Table of Contents

Contents

List of Figures

Chapter 1

Chapter 2

Chapter 3

List of Result Tables

List of Abbreviations

Ago: Argonaut Protein

AMD: Age-related Macular Degeneration

Ash-1a: Achaete/scute homologue 1a

AsPC-1: Human pancreas adenocarcinoma cell line

ATOH7: Atonal homolog 7

BDNF: Brain-derived neurotrophic factor

bHLH: Basic helix-loop-helix

BMP: Bone morphogenetic protein

BSA: Bovine serum albumin

cAMP: Cyclic adenosine monophosphate

CDK2: Cyclin-dependent kinase 2

CDKN1b: Cyclin-dependent kinase inhibitor 1B

ChABC: Chondroitinase ABC

CHX10: ceh-10 homeo domain containing homolog

CMZ: Ciliary marginal zone

CNS: Central Nervous System

CNTF: ciliary neurotrophic factor

CRALBP: Cellular Retinaldehyde-Binding Protein

CREB: cAMP response element-binding protein

CRX: Cone-rod homeobox protein

CSL: CBF1/RBP-Jkappa, Suppressor of Hairless, Lag-1

CSPG: Chondroitinase Sulphate Proteoglycans

DAPT: N-[N-(3,5-Difluorophenylacetyl)-L-alanyl]-S-phenylglycine t-butylester

DGCR8: DiGeorge Syndrome Critical Region 8

DLL-4: Delta like ligand 4

DMEM: Dulbecco's Modeified Eagle's Medium

DMSO: Dimethyl Sulfoxide

DNA: Deoxyribonucleic Acid

dNTP: Deoxyribonucleotide Triphosphate

DR: Diabetic Retinopathy

DRG: Dorsal root ganglia

DSHB: Developmental Studies Hybridoma Bank

ECM: Extracellular matrix

EDC: 1-Ethyl-3-(3-dimethylaminopropyl)carbodiimide

EDTA: Ethylenediaminetetraacetic acid

EGF: Epidermal Growth Factor

EGF-R: Epidermal growth factor receptor

EMT: Epithelial-mesenchymal transition or transformation

EpCam: Epithelial cell adhesion molecule

ERG: Electroretinography

ESC: Embryonic stem cell

FBS: Foetal Bovine Serum

bFGF: Basic Fibroblast Growth Factor

GAG: Glycosaminoglycans proteoglycans

GCL: Ganglion cell layer

GFAP: Glial Fibrillary Acidic Protein

GFP: Green Fluorescent Protein

GMP: Good Manufacturing Practice

GTA: Glutaraldehyde

HA: Hyaluronic acid

HCC: Hepatocellular carcinoma

Hes1: Hairy and enhancer of split-1

Hes5: Hairy and enhancer of split-5

HFIP: Hexa-fluoro-isopropanol

HSCs: Hematopoietic stem cells

HuD: Human antigen D

HUVEC: Human umbilical vein endothelial cells

ICM: Inner Cell Mass

IGF: Insulin-like growth factor

IKNM: Interkinetic nuclear migration

ILM: Inner limiting membrane

INL: Inner Nuclear Layer

IOP: Intraocular Pressure

iPS: Induced Pluripotent Stem Cell

Islet-1: Insulin gene enhancer protein

JAG-1: Jagged 1 protein

KH: K Homology

KHSRP: KH-type splicing regulatory protein

Klf4: Kruppel-like factor 4

Lag1: Longevity-assurance gene

LH: Lister Hooded

MAML: Mastermind-like

MB: Mellanoblastoma

miRNA: Micro Ribonucleic Acid

mRNA: Messenger Ribonucleic Acid

MSCs: Mesenchymal stem cells

mTOR: Mammalian target of rapamycin

MYBL2: Myb-related protein B

NF-κB: Nuclear factor kappa-light-chain-enhancer of activated B cells

NGF: Nerve growth factor

NHS: *N*-Hydroxysuccinimide

NICD: Notch Intracellular Domain

NMDA: N-Methyl-D-Aspartic Acid

NR: Neural retina

NR2E3: Nuclear receptor subfamily 2, group E, member 3

NRL: Neural retina leucine zipper

NTF: Neurotrophic Factor

OCT: Optimum cutting temperature

Oct4: Octamer-binding transcription factor 4)

OEC: Olfactory ensheathing cell

ON: Optic nerve

ONL: Outer Nuclear Layer

OTX2: Orthodenticle homeobox 2

P107: Retinoblastoma-like protein 1

PACT: Cellular protein activator of PKR

PAX6: Paired box gene 6

PC: Plastic Compression

PCR: Polymerase Chain Reaction

PEDF: Pigment epithelium derived factor

PEG: Polyethylene glycol

PIP_3: Phosphatidylinositol (3,4,5)-triphosphate

PLA: Polylactic acid

PLGA: poly(lactic-*co*-glycolic acid)

PLK1: Serine/threonine-protein kinase PLK1

PLR: Pupillary Light Reflex

PMSF: Phenlymethyl Sulfonylfluoride

PNIPAAm: Poly(*N*-isopropylacrylamide)

pre-miRNA: Precursor micro ribonucleic acid

pri-miRNA: Primary micro ribonucleic acid

PTEN: Phosphatase and tensin homolog

PVR: Proliferative Vitreoretinopathy

RAM: RBP-Jkappa-associated module

Ran-GTP: RAs-related Nuclear protein-Guanosine-5'-triphosphate

RBP-J: Recombining binding protein suppressor of hairless

RCS: Royal College of Surgeons

RGC: Retinal Ganglion Cell

RISC: RNA-induced silencing complex

RP: Retinitis pigmentosa

RPE: Retinal pigment epithelium

RT: Reverse transcription

Rx: Retinal Homeobox

SCI: Spinal Cord Injury

SDS: Sodium dodecyl sulphate

Shh: Sonic hedgehog

siRNA: Small interfering

SMAD-4: Human Homolog of the *Drosophila* Mothers against decapentaplegic-4

Sox2: SRY (sex determining region Y)-box 2

STAT3: Signal transducer and activator of transcription 3

SVZ: Subventricular zone

TA: Triamcinolone

TACE: Tumour Necrosis factor Alpha-converting Enzyme

TGF-β: Transforming growth factor beta

TM: Trabecular Meshwork

TRBP: HIV-1 TAR RNA binding protein

UTR: Untranslated region

Wnt: Wingless

ZEB: Zinc finger E-box-binding homeobox

Chapter 1: General Introduction and Objectives

1.1. Retinogenesis

Cell lineages contained within the vertebrate eye have been extensively conserved in many species (Andreazzoli, 2009), where the majority of molecular regulation of cell fate is mediated by transcription factors, which are able to control RNA transcription. Many of these factors act synergistically to yield specification to the retinal progenitor population at birth. Researchers in the regenerative medicine field are currently targeting molecular and epigenetic regulators to develop ocular degenerative therapies. Knowledge of the coordinated processes involved in retinogenesis will improve our understanding of age-related or inherited retinal diseases and will aid in the design of regenerative therapies for degeneration of specific cell niches.

There are seven types of cells born during ocular organogenesis; six neurons and one glial population, namely the Müller glia. Synchronised development of the retina involves transcriptional and translational control which is governed by intrinsic or environmental mechanisms. The eye structure is defined within the ectoderm germ layer, specifically involving the anterior neural plate and its cellular content. This region undergoes repression of Wingless (Wnt1) and bone morphogenetic protein (BMP), by its inhibitor Noggin, and is coupled with increased production of basic fibroblast growth factor (bFGF) and insulin-like growth factor (IGF) (Pera et al., 2001, Delaune et al., 2005). This single region separates to give origin to distinct retinal compartments. The newly born retinal primordial tissues then gives rise to the optic vesicles (Chow and Lang, 2001, Rembold et al., 2006) which house the neuroblasts that will undergo cell division to form the different retinal cell layers. Cellular proliferation causes the tissue to evaginate laterally, yielding two optic cups where the pigmented RPE lines the outer surface, surrounding the developing neural retina (Andreazzoli, 2009).

The formation of the mature retina involves an evolutionary conserved time-competent generation of neurons and glia by the retinal progenitors. Broadly, the retinal ganglion cells (RGCs) are produced initially, followed by cones and horizontal cells, and at a later stage amacrine cells, rods and bipolar cells. Finally, the Müller glia are produced (Figure 1.1). The different retinal neurons are all derived from the same population of progenitors that pass through various proliferative states (Livesey and Cepko, 2001, Marquardt and Gruss, 2002). These cell states are regulated by organisational signals provided within the tissue, whether extrinsic or intrinsic. Early retinal progenitors are all primarily plastic and able to produce all retinal cell sub-types, whilst later progenitors have a limited potency and have the capacity to produce post-mitotic neural populations that are generated during the later stages of organogenesis. The early progenitors are elongated bipolar-like cells, which span the final width of the retina, their nuclei are housed within the central domain of the retinal microenvironment and are able to migrate basally or apically during development, this is commonly known as interkinetic migration (IKNM) (Baye and Link, 2007). Early division is asymmetrical, where progenitors give rise to two variant daughter cells, one becoming an early post-mitotic neuron being ganglion, cone or horizontal in fate, whilst the other replenishes the progenitor pool and retains its mother's potency. This mode of division lasts a short time. However, in larger mammals it can be a prolonged process before the later neurons are born (LaVail et al., 1991). Once early RGCs are generated, they commence differentiation into mature ganglion morphologies by developing radial extensions towards the inner basal layer. These initially act to anchor the cell body into the inner lamina, where they then send extensive axonal outgrowths adjacent to the progenitor end feet, directed towards the future optic nerve (Hinds and Hinds, 1974). Late progenitors produce the late-born post-mitotic neurons, as well as the glial population. The late progenitors are similar in their phenotypes to young Müller glia, which retain an elongated

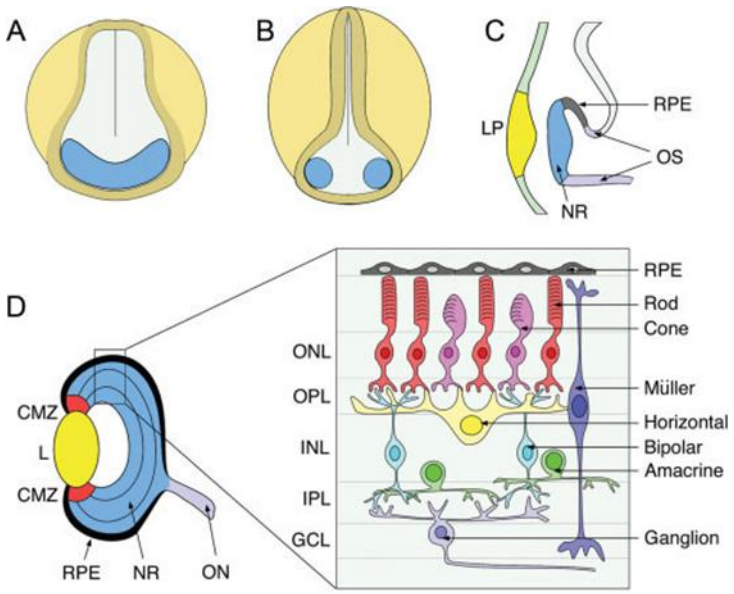

Figure 1.1: Eye field specification and retinogenesis diagrams. A) Eye field determination (blue) from the neural plate B) Following neuralation and eye field specification, the two retinal territories separate. C) Evagination of retinal territories, creating optic vesicles with neural retina (NR), RPE and optic stalk. D) mature organisation of the ocular tissues and neural retina containing the ganglion cell layer (GCL), inner nuclear layer (INL), inner plexiform layer (IPL), outer nuclear layer (ONL), and optic nerve (ON) (Adapted from Andreazzoli, 2009).

bipolar morphology. They also produce late born bipolar and amacrine cells, as well as provide the solid scaffold which neurons use to travel towards their final destinations within the growing neuroepithelium (Meller and Tetzlaff, 1976, Reichenbach et al., 1994a, Reichenbach et al., 1994b). Müller glia also facilitate the outgrowth of ganglion cell dendrites into the inner plexiform layer (Bauch et al., 1998), in order to create synapses with other proximal neurons. This is a very similar process utilised by other neural retinal cells when developing interlinking signalling networks, such as those observed between bipolar cells and both populations of photoreceptors. Müller glia guide the cells during late retinogenesis, but also ensure the formation of synapses between neurons born both early and late. Once migration and proliferation has concluded, the two plexiform-synaptic layers are formed. These separate the three retinal nuclear layers to create the final retinal mosaic.

1.1.1. Transcriptional regulators of retinal progenitors

The signalling and molecular controls imposed on retinogenesis have in part been attributed to two synergistic paths, one which down-regulates the expression of factors that promote differentiation, whilst the other acting to promote multipotency and proliferation. Together these mechanisms work to maintain a pool of self-renewing and undifferentiated cells during organogenesis. Transcription factors are proteins that act in a sequential manner to control the maintenance of adult tissue or the development of embryonic tissues. Pax6 is a paired homeobox transcription factor that has been termed a “master controller” of eye development, it has been shown to regulate the proliferative rate of early progenitors during eye development, ensuring enough cells are created to satisfy the cell numbers required for retinogenesis. Knockout Pax6 murine models only produce amacrine cells following organogenesis, demonstrating the vital role that Pax6 has (Marquardt et al., 2001) in retinal development.

Sex determining region Y (SRY)-box 2 (Sox2), is another transcription factor that regulates early retinal progenitors (Bhatia et al., 2011b) and appears to have a direct positive action on the Notch signalling pathway and its downstream target Hairy and enhancer of split-1 (Hes1) (Taranova et al., 2006). Its constitutive activation causes suppression of genes that induce cell commitment down a neural lineage, preventing proliferation and self-renewal.

Notch signalling demonstrates how the microenvironment can be employed to alter the fate of different sub-sets of cells within a population of potent cells. Increasing the cellular expression of the Notch antagonist Delta, progenitors can self-induce differentiation which represses their internal Notch signalling, creating a negative feedback loop for their own production. This hinders the triggering of the signalling cascade, and in this way can commit a population of potent cells to mature (Andreazzoli, 2009). Furthermore, Notch signalling has demonstrated a control over apical-basal spatial differentiation in both zebrafish and mice, where cells born from progenitors within the basal region will become post-mitotic and undergo symmetrical division. In contrast, those born proximal to the apical domain will undergo asymmetric division, where one daughter cell will maintain its Notch signalling and retain a potent ability (Del Bene et al., 2008).

It has been shown recently that some molecules can intrinsically monitor and alter the phenotypes of retinal progenitors. These are known as micro RNAs, which can control the extent of translation and/or the degree of proteomic expression within a plastic retinal population (Slack et al., 2000, Moss et al., 1997). These agents have been shown to be involved in layer formation, apoptosis and the timing of cellular maturation.

Müller cells give rise to rod progenitors during normal development in the zebrafish. However in dystrophic retina, Müller glia are able to de-differentiate, regenerate and repopulate injured retina (Bernardos et al., 2007). This was first observed in lower vertebrates and amphibians, but

more recent studies have identified this regenerative potential in mammalian species (Fischer and Reh, 2001, Fischer and Reh, 2003). Rat retinal progenitors have been isolated and incubated under *in vitro* conditions and it has been suggested that their over expression of Notch1 and Hes1 appears to induce generation of Müller glia (Blackshaw et al., 2004). Murine models transplanted with activated Müller glia due to injury, have demonstrated the capacity to produce neurons of all retinal laminations which is attributed to the alteration of their Notch1 profile (Das et al., 2006). These findings suggest that Müller glia within mammals, do retain some stem cell characteristics, and appear to react under the guidance of the Notch signalling pathway. Understanding the mechanisms and factors implicated in retinogenesis may aid in the design of novel strategies to target retinal degenerations.

1.2. Retinal Degenerative Diseases

Retinal degeneration is a feature of diseases that affect the posterior segment of the eye specifically the retina and choroid. Degeneration of the retina leads to neuronal loss and is the predominant cause underlying visual loss (Figure 1.2). The eye, in addition to the highly organised system of neurons, also houses a complex network of vasculature. Problems within the vasculature may lead to leakage or ischaemia, whilst neuropathies lead to progressive neuronal atrophy. Loss of vision generally involves an abnormality in either or both of these networks.

Based on the estimated figures released by the World health organisation in 2010 (Pascolini and Mariotti, 2012), 284 million people are considered visually impaired, with over 39.3 million being completely blind. Retinal degeneration accounts for 14% of the world's blind population with 51% due to cataract. In developed countries such as the United Kingdom, where blindness caused by cataract is no longer a main problem, retinal degenerative diseases, such as glaucoma, diabetic retinopathy and age-

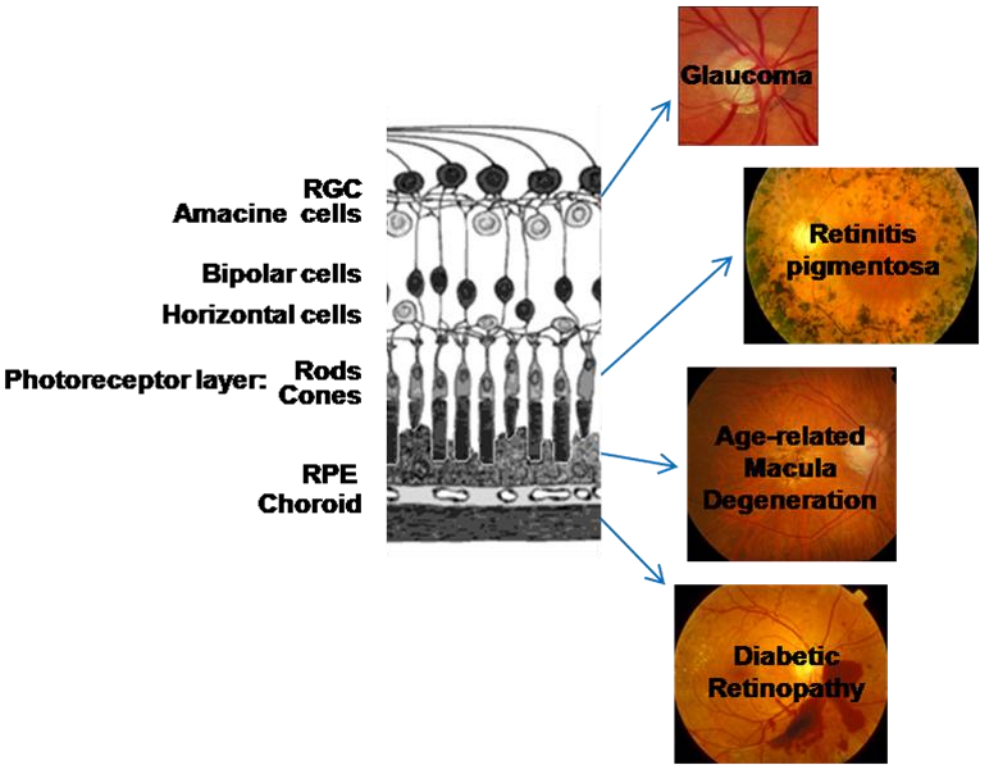

Figure 1.2: Retinal structures affected by the common causes of retina-associated visual loss and their clinical presentation. Glaucoma occurs as a consequence of retinal ganglion cell degeneration, Retinitis Pigmentosa (RP) is a combination of genetic mutations leading to malfunctions within the photoreceptors and retinal pigment epithelium (RPE), Age-related Macular Degeneration (AMD) is caused by the abnormalities of the RPE and choroid leading to secondary photoreceptor degeneration and Diabetic Retinopathy is caused by vascular leakage and retinal ischaemia.

related macular degeneration (AMD) are significantly more prominent. At present pharmacological interventions used to treat these disorders are aimed at controlling their progression, but in many cases, progression cannot be halted and patients may go on to develop total and permanent visual loss.

Diabetic retinopathy (DR) is a condition caused by complications of either poorly controlled or a lengthy duration of diabetes mellitus. Hyperglycaemia is associated with pericyte loss in the retinal vasculature (Chistiakov, 2011). This leads to thickening of the connective tissue, causing retinal vessels to become increasingly permeable resulting in localised vascular leakage (Hudson, 1996, Wilkinson et al., 2003). As the blood supply becomes more restricted retinal ischaemia develops and may be associated with secondary neural degeneration as well leading to later sequelae such as neovascularisation, haemorrhage and tractional retinal detachment.

AMD is a leading cause of irreversible blindness that first affects the retinal pigmented epithelium (RPE). The ageing process within RPE layer appears to trigger a cascade of events that results in neural degeneration. Atrophy of RPE manifests in the eventual depletion of photoreceptors and finally loss of visual acuity (de Jong, 2006). Lipid containing lesions, known as drusen, are deposited between the choroid and RPE at the posterior pole, and are one of the earliest manifestations of the disease. Damage is focused on the macula region and therefore diminishes the central field of vision. In dry AMD the onset is of slow progression, but in wet AMD, the exudative form of the disease, the progression may be rapid with sudden and devastating visual impairment.

Primary retinal degenerative diseases include congenital defects that affect the development and maturation of the neural retina itself. Retinitis Pigmentosa (RP) is usully an inherited condition leading to photoreceptor degeneration affecting the rods more than cones and is of a progressive nature. It has diverse modes of inheritance where the photoreceptors

deteriorate, coupled with secondary degeneration of the RPE (Berson, 2007). Other congenital defects that lead to macular degeneration and neuronal loss are Stargardt's disease (Kapadia, 2000) and Leber's Congenital Amaurosis (Maguire et al., 2008). All these conditions are associated with progressive visual loss with no proven treatments currently available.

1.3. Glaucoma

Glaucoma is characterised by a progressive optic neuropathy associated with loss of RGCs within the inner retina. It is the leading cause of blindness in the world after cataract, accounting for 8% of the total blind population. This neuropathy is commonly associated with increased intraocular pressure (IOP) which results in atrophy of RGCs and their axons, together with the clinical observation of optic nerve head cupping (Levin, 2005, Singh, 2005). RGCs have long axonal processes which converge collectively to form the optic nerve. The optic nerve serves as the nerve channel that relays sensory information gathered by the eye to the brain. It acts by transducing the pattern of electrical impulses collected within the retina to the visual cortex. Generally there is a ratio of 100 cones and rods transmitting visual data to one RGC depending on the retinal region. Hence, RGC death or damage can lead to loss of vision, if prolonged, to complete blindness.

The mechanisms which lead to the onset of glaucoma include cell death within the ganglion cell population, which ultimately impacts on the complex network of the neural retina as well as the efficiency of phototransduction to the visual cortex. Peripheral vision is lost initially and complete blindness can ensue if not treated. Treatments used to reduce IOP and arrest progression of the disease are both medical and surgical. Medical treatments currently target the trabecular meshwork (TM) or the ciliary body. These act by increasing outflow mechanisms of the TM and reducing aqueous humour production in order to reduce IOP, such as Lumigan. Surgical intervention is

used when medical treatments are no longer effective and involve laser treatment of the TM to increase aqueous outflow or filtration procedures to divert the aqueous humour into the subconjunctival space. Evidence suggests that patients that have advanced glaucoma with extensive nerve fibre degeneration of greater than 90% are still able to perform tasks to look after themselves and maintain a reasonable quality of life (Alward, 1999). This suggests that 1% of functional ganglion axons are able to retain sufficient central vision and can be the difference between being blind and being able to perform day to day tasks.

1.4. Potential of cell-based therapies for Glaucoma

In order to develop cell based therapies for retinal degenerations, anatomical constrictions need to be considered. Studies have mainly concentrated on RPE and photoreceptor delivery, due to the accessibility of this region for transplantation. Sub-retinal delivery of cells for RPE or photoreceptor disease are not dependent upon migration into the neural retina and y do not need to form neurite outgrowths for synaptic connections. Hence direct injection adjacent to the host RPE layer delivers the cells to their site of activity and need. However, cellular transplantation for inner retinal disease faces different obstacles compared to photoreceptor or RPE delivery.

Tissue engineering is required in order to ensure maximum cellular integration of transplanted cells within the inner retina when considering cell replacement therapies for. Intravitreal injection of cells into the rat eye does appear to ensure adequate therapeutic delivery of cells into the inner retina (Bull et al., 2011, Johnson et al., 2009, Singhal et al., 2012). However, this approach of cellular transplantation onto the inner retinal surface using intravitreal injection into larger mammalian eyes is likely to be less successful. Rodents have a comparatively large lens; occupying approximately over half of the intraocular volume, compared to larger mammals, including humans (Hughes, 1979). It is therefore possible that the

presence of a large lens in rodents may serve as a scaffold to maintain cellular orientation of transplanted cells onto the retina. On this basis, cellular scaffolds have been proposed for use to physically support transplanted cells onto the retina. The use of scaffolds has also been investigated for non-stem cell derived RPE grafting (Falkner-Radler et al., 2011).

Cellular environments are crucial to the development and growth of cells and can direct maturation and differentiation. Hence transplanting cells into dystrophic retinal tissue may hinder the regenerative capacity of the cells, within its diseased architecture. The extent of integration undergone by transplanted stem cells appears to depend on the state of cellular maturation. This has been demonstrated by the ability of grafted cells to integrate more efficiently when differentiated (Ong and da Cruz, 2012, Tibbetts et al., 2012, Stern and Temple, 2011, MacLaren et al., 2006). This indicates that pre-differentiation of stem cell populations would be a pre-requisite for optimal integration and therapeutic efficacy.

Cellular therapies targeted for glaucoma would aim to differentiate cells towards an RGC fate. Stem cell therapies for this group of neurons may also intend to regenerate the optic nerve itself, which is a far more challenging objective. There are five main subdivisions of RGCs; midget, parasol, bistratified, photosensitive and finally a group of ganglions cells that are involved in fast eye movements.

When considering cell replacement of RGCs the mode of delivery is pivotal as it is important that transplanted cells are able to move into the ganglion cell layer and are able to migrate within it. This would ensure optimal integration into host tissue, maximising the degree of potential cell replacement. Following integration within the inner retina, cells would also need to form synaptic connections with the host tissue. Synapse formation within the ganglion cell layer itself, as well as within the inner plexiform layer

is essential for true RGC function. In addition in order to regenerate the optic nerve, cells face the immense challenge of creating long neurite processes that must migrate towards the lateral geniculate nucleus of the host brain. These steps would be required for fulfilment of adequate cell replacement therapies and to date have not all been achieved.

The enhancement of RGC function observed after stem cell transplantation in experimental glaucoma may be due to the secretion of neurotrophic factors by the transplanted cells. This therapeutic response is seen across the whole central nervous system when stem cells are transplanted, and potentially constitute another avenue for cell based therapies (De Feo et al., 2012).

Stem cells derived from the bone marrow have been investigated for possible use in cell based therapies for glaucoma. Human mesenchymal stem cells (MSCs) have been injected into the vitreous of optic nerve axotomised rats (Johnson et al., 2010) and have proved to significantly reduced ganglion cell death. Ganglion cell survival was further enhanced by inducing the cells to express neurotrophic factors (NTFs). Similar observations were seen with human MSCs in another rat model of glaucoma (Levkovitch-Verbin et al., 2010). In this instance IOP was increased using laser to scar the TM in order to reduce aqueous outflow. The MSCs rescued the retinal ganglions cells from further axonal damage and were also identified as releasing NTFs within the degenerative retinal environment. These studies however did not show improvement in optic nerve atrophy or cupping. Another bone marrow derived MSC population; with extensive stromal phenotype, were transplanted into glaucomatous Wistar rats. This model was achieved by cautery of the episcleral veins. Transplanted cells did not integrate within the host ganglion layer but instead lined along the inner limiting membrane. The cells survived for the duration of the experiment and expressed high levels of NTFs. Higher levels of ganglion cell survival were observed within the

injected glaucomatous eyes compared to their controls of increased IOPs (Levkovitch-Verbin et al., 2010).

Multipotent adult stem cells have also been proposed as a tool for retinal ganglion cell regeneration. Recent work has demonstrated that adult human Müller stem cells have the ability to restore RGC function in a rodent model of glaucoma. This stem cell population was able to refine their gene expression pattern to that of a ganglion cell precursor invitro prior to transplantation. Functional data within this rat model of glaucoma consisting of ganglion cell depletion, has demonstrated the ability of these cells to partially restore ganglion cell function (Singhal et al., 2012). An alternative adult cell population used in experimental studies to treat glaucoma-like disease is the olfactory ensheathing cells (OECs), isolated from rat cadaveric nasal tissue. These cells when injected into eyes with optic nerve transection had a neuroprotective effect, which appears to be mediated by the secretion of Brain-derived neurotrophic factor (BDNF) (Li et al., 2003).

Debates about the pathological progression and cause of glaucoma have led to development of different experimental models. This has built controversy on the extent of rescue delivered by these cell therapies. Methods for gathering data of ganglion cell survival and optic nerve protection are vast and researchers in this field use different outcome measures, including ganglion cell numbers, optic nerve head cupping, pattern electroretinograms and scotopic negative threshold responses. On this basis, to avoid variations in the analysis of stem cell uses, standardised methods need to be employed. Specifically when assessing the real functional benefit provided by cell therapies for glaucoma.

Replacing or improving the health of the resident RGCs, even by a small proportion can have a large impact on a patient’s quality of life. Replacing such a low number of the RGCs is a simpler task than repopulating the whole ganglion cell layer and would be a significant advance for those who are

afflicted with advanced glaucoma. Glaucoma patients may potentially benefit from the repopulation of small areas of the central retina, which could potentially improve the range of tasks the patients could perform. This assumption may require the combination of stem cells therapy and tissue engineering.

1.5. Stem Cells

Stem cells are able to maintain an undifferentiated state as well as having the ability to continuously divide and self-renew. These cells can produce daughter cells that can commit to lineages of a variety of cell types, and therefore have the potential to regenerate any type of tissue.

Stem cells taken from different mature or immature tissues represent cells with different competencies and plasticity, based upon their development, source and birth. Cells taken from adult tissue that possess the stem cell attribute of self-renewal and ability to maintain their population, are able to re-enter the cell cycle, but are not always capable of generating cells from all the primary embryonic tissues.

Mammalian stem cells can be sourced from either embryos or post natal tissues. Post natal stem cells include cells isolated from infant or adult bone marrow and visceral tissues. Therefore it is conceivable that cell based therapies could provide a viable option for patients facing terminal vision loss.

1.5.1. Embryonic stem cells

Embryonic stem cells (ESCs) derive from the internal cells of the developing embryo at the blastocyst stage. These cells can be taken from the inner cell

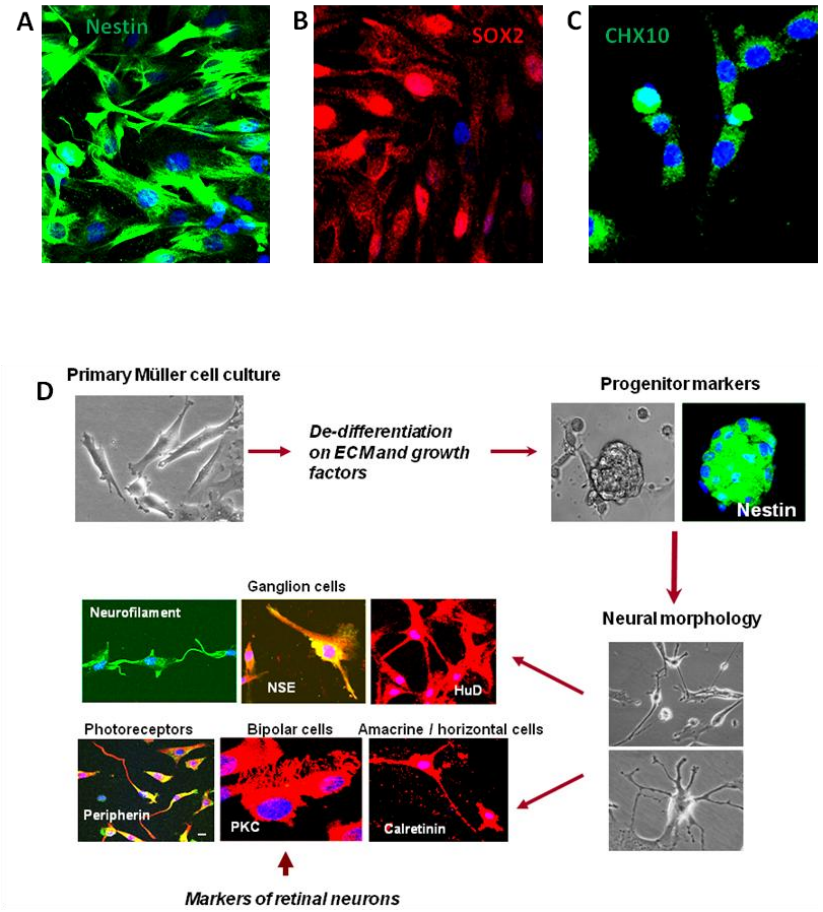

Figure 1.3: A sub-population of Müller glia from adult human post mortem retinal tissue express markers of neural stem cells *in vitro*. Müller stem cells in culture express **(A)** the intermediate filament nestin, a marker of neural stem cells, **(B)** SOX2 which is a marker of all neural stem cells and including those of the retina, and **(C)** the early retinal progenitor marker CHX10. **(D)** These cells can be grown indefinitely and form neurospheres of Nestin positive cells. Following culture under differentiating conditions, they express neural morphology and markers of various retinal neurons (Figure adapted from Bhatia et al., 2010 and Lawrence et al., 2007)

mass (ICM) and exhibit the capacity to develop into all mature cells types present within an adult (Evans and Kaufman, 1981). This pluripotent nature is coupled with the ability to continuously proliferate, for which they can theoretically be made to propagate infinitively *in vitro*. This poses an attractive source of cells for cell-based therapies, as ESCs are able to adapt their morphology and phenotype *in vitro* in order to generate all adult cell types upon specific conditions in culture. As such, this led to the conclusion that these cells would be able to differentiate into specific cell lineages, using well defined external factors. Such lineages have included the production of hepatocytes (Watt and Forrester, 2006), retinal pigmented epithelium (Hirano et al., 2003), cardiomyocytes (Zhang et al., 2002), neurons (Bibel et al., 2004) and glia (Vadivelu et al., 2005). Human ESCs (hESCs) have also shown the ability to differentiate into photoreceptor progenitors, mature photoreceptors and RPE (Lamba et al., 2009, Idelson et al., 2009), determined by their pattern of gene expression. Transplantation of RPE differentiated cells into a rodent model of photoreceptor depletion, was shown to induce functional improvement in response to light stimuli *in vivo* (Lamba et al., 2009). Although ESCs can potentially generate a multitude of cell types, the ethical restraints and the use of allogeneic material is still being deliberated. The main moral argument against this type of therapy lies with the use of embryos as a source of cells. Like induced pluripotent cells (iPS), ESCs have the ability to over proliferate under standard cultural protocols, and to form teratomas (Hentze et al., 2009). Classification and validation of this stem cell source still requires many investigations before designing cell based therapies for retinal degenerations.

1.5.2. Induced pluripotent stem cells

Within the last 5 years, a new group of pluripotent stem cells has been generated *in vitro*; these cells are known as induced pluripotent stem (iPS) cells. These originate from terminally differentiated somatic cells that have

undergone genetic reprogramming, arbitrated by either vector or non-vector means. Keratinocytes or fibroblasts from skin biopsies, are coaxed into continuously expressing a combination of different transcription factors; Octamer 3/4, Oct4, cellular myelocytomatosis oncogene, c-Myc, Krüppel-like factor 4, Klf4 and Sox2. Alternatively, they can be induced by only four factors Oct4, Sox2, Nanog and Lin28 (Takahashi and Yamanaka, 2006, Okita et al., 2007). Generation of these "artificial stem cells" remove some of the controversy surrounding the use of embryonic stem cells as they can be engineered from the patient's own cells. The use of these cells may also limit some of the difficulties found when harvesting tissue-specific adult stem cells, or when using allogeneic donor strategies. Hence, iPS cells would remove the restraint of the use of immunosuppressive drugs to maintain the survival of non-autologous transplanted cells. iPS cell therapy potentially can be optimised to expand cells of a required lineage under standardised protocols using exogenous factors, such as mitogens and basement proteins.

iPS cells like embryonic stem cells are pluripotent and harbour the capacity to produce a variety of cell types spontaneously. However, due to the methods used to generate these cells, iPS cells may not be proved safe for transplantation. This is due to the risks faced when transforming these cells, as inducing the cells to up-regulate oncogenes has been shown to promote teratoma formation and the onset of uncontrollable proliferation. *Ex vivo* teratomas produced from iPS cultures have been shown to contain normal tissues of all three embryonic germ layers in an unorganised, sporadic pattern. Up-regulation of c-Myc has been shown to encourage the establishment of proliferation at an abnormal rate. Due to the increased rate of cell cycling there is an increased possibility of random genomic integration of these genes following transduction which can lead to oncogenesis and malignancy (Nakagawa et al., 2008). Improving methods of reprogramming have partly reduced the risk of promoting over proliferation. In addition,

reduction in the number of reprogramming genes used, as well as the regimes undertaken to induce pluripotency, has minimised the incidence of teratoma formation. Alternative induction methods have included the use of non-vector or -viral mediated transduction; whether by non-integrating gene processes or small molecules (Okita et al., 2008). However, to date the methods have not yielded complete success when eradicating the risk of inducing severe genomic alterations and unwanted cellular division.

In relation to the application of iPS cells for retinal therapies, a type of cell that can be spontaneously produced using iPS cells are RPE cells, characterised by pigment production and atypical tight cell-cell interactions accompanied by expression of RPE markers (Carr et al., 2009). Alternative, differentiating regimes have also produced neural and glial-like cells (Dimos et al., 2008, Tokumoto et al., 2010, Jang et al., 2010).

1.6. Adult tissue-derived stem cells

Adult stem cells are found within most mature tissues where they are thought to repair and maintain tissues of the body. Examples of these cells are those found within the crypts of Lieberkuhn in the ileum (Al-Dewachi et al., 1979), and the Limbus within the ocular surface of the cornea (Thoft et al., 1989). Cell culture of adult stem cells can develop into finite lineages that can potentially be used to replenish specific cell niches such as haematopoietic, nerve or muscle. Although adult stem cells are multipotent, their function is generally limited to their location when induced to differentiate. Retinal stem cells or progenitors isolated from the adult or foetal human ocular tissue have been explored as a possible source for stem cell therapies directed for retinal degenerations (Lawrence et al., 2007, Klassen et al., 2004). They retain the ability to produce multiple cell types contained within the retina. It had been previously shown that the tissue from which retinal stem-like cells originate is the early post natal ciliary margin (Xu et al., 2007) within the xenopus and zebrafish. Tropepe et al. later showed that in mice these cells were contained

within a similar region to the amphibian ciliary marginal zone, and had the innate ability to differentiate into a range of retinal neurons as well as, to lesser extent, RPE cells (Tropepe et al., 2000). However, more recent studies have identified stem cells within the neural retina itself, which has been shown to be a sub-population of Müller glia (Bhatia et al., 2009, Bhatia et al., 2010, Bhatia et al., 2011a, Lawrence et al., 2007).

1.6.1. Müller stem cells

Müller cells are the main glial cells of the retina and are located throughout its whole structure. They provide biochemical support to the neurons and blood vessels of the retina, as well as structural support. The cell bodies of Müller glia are found within the inner nuclear layer, with cytoplasmic projections extending laterally and transversely throughout this layer, enabling interactions between themselves and other neural cell bodies. These interactions ensure that Müller cells can participate in neural homeostasis within the retinal microenvironment. Müller cells are characterised by the expression of epidermal growth factor receptor; EGF-R, glutamine synthetase, vimentin and cellular retinaldehyde binding protein; CRALBP.

Within the developing mammalian adult brain, radial glia have been found to have the ability to repopulate both the neural cell populations as well as the glial population itself (Merkle et al., 2004). Other pools of glia within the CNS have also shown neural stem cell traits. Bergmann glia housed in the cerebellum of adult mice express the neural stem cell markers Sox1 and Sox2 (Sottile et al., 2006).

Müller glial stem cells could provide a possible tool for the design of cell based therapies to regenerate the human retina (Lawrence et al., 2007). Müller stem cells have been shown to regenerate the retina after damage in various species, including post natal chick (Fischer and Reh, 2001, Fischer

and Reh, 2000), rodents (Das et al., 2006) and zebrafish (Yurco and Cameron, 2005, 2012). It had been thought that these innate characteristics had not been conserved within adult humans, despite the retina harbouring this cell type. Recent evidence in our laboratory has shown that these cells upon transplantation can partially restore retinal function in rat models of retinal degeneration, including neurotoxic damage to the ganglion cell layer (Singhal et al., 2012).

Like most adult stem cells, human Müller stem cells appear to be multipotent and therefore tissue specific and restricted to producing different retinal cell subtypes. They express Sox2, Pax6, Chx10 and Notch1 (Lawrence et al., 2007, Bhatia et al., 2011b). Immortalised cells cultured *in vitro* are able to differentiate into a variety of retinal neurons, which in turn express distinctive markers. These include; peripherin, a marker of photoreceptors, Protein Kinase, a marker of bipolar cells, calretinin, a marker of both amacrine and horizontal cells along with Brn3b; an early marker of committed RGC precursors (Lawrence et al., 2007, Singhal et al., 2012, Bhatia et al., 2011b). These cells are also able to form neurospheres that express Nestin, a protein marker of early stem cell differentiation (Figure 1.3). The formation of neurospheres and subsequent ability to differentiate *in vitro* is achieved using bioactive growth factors such as basic fibroblast growth factor (bFGF), epithelium growth factor (EGF) or insulin.

Sourcing human Müller stem cells is a relatively easy procedure as they can be obtained from cadaveric donor tissues and can be induced to undergo extensive expansion *in vitro*. Use of these cells for human therapies would eradicate the ethical and moral objections to embryonic stem cell based therapies and merits investigations.

1.6.1.1. Differentiation of Müller stem cells into retinal ganglion cells

Committing the Müller stem cell population to a RGC fate involves inhibiting the Notch signalling pathway, one of the early regulatory signalling cascades that prevent specification of both early and late retinal progenitors (Andreazzoli, 2009). This pathway involves a family of transmembrane protein receptors that act to suppress differentiation of stem cells and maintain a constant level of proliferation. When a Notch ligand binds the receptor, an intracellular domain of the protein activates and triggers a cascade reaction (Jadhav et al., 2006). By upregulating its target genes, the pathway causes inhibition of differentiation by down regulating factors that encourage neural development. Progenitors and stem cells maintain their pluripotent state during development by maintaining this signalling pathway active. Hence in order to differentiate, signalling via this pathway must be prevented.

Human Müller stem cells treated with a Notch inhibitor undergo a significant adaptation to a proneural state. When this state is exploited by the subsequent addition of bFGF, it causes the cells to downregulate their gene expression of markers of Müller cells and convert to the expression of markers an early RGC precursor, demonstrating their ability to revert back to the mitotic phase and differentiate towards a RGC phenotype (Singhal et al., 2012).

Over the last ten years investigators have found another group of translational modulators, in the form of microRNAs (miRNA), active during development and adulthood. microRNAs are short sequences of RNA that are simultaneously generated alongside their messenger RNA (mRNA). They function by suppressing the translation of proteins by steric hindrance or degradation of the mRNA preventing translation. miRNAs are involved in the regulation of the downstream targets of Notch, and have also been

targeted themselves by Notch, preventing differentiation (Garzia et al., 2009). Investigating their capacity within Müller stem cells could potentially be used to promote differentiation of latent Müller glia within dystrophic retina, removing the need for invasive therapy of cellular scaffolds.

1.6.2. Bone marrow derived stem cells

The bone marrow houses a heterogeneous population of stem cells that perform specific duties. The two main subsets of stem cells present in the bone marrow are haematopoietic and mesenchymal stem cells. Use of autologous bone marrow cells eliminates the potential risk of allogenic transplantation, which in many cases necessitates lifelong immunosuppression. Haematopoietic stem cells (HSCs) are able to induce differentiation down various haematopoietic lineages giving rise to all the blood cells of the circulatory system, whilst maintaining a pool of blood stem cells and progenitors. Mesenchymal stem cells represent a population that exhibit large mononuclei and have the ability to adhere to plastic culture surfaces. These cells have also been retrieved from non-bone marrow sources derived from tissue originating from the mesoderm, such as adipose tissue, as well as non-mesoderm tissues including liver, umbilical cord, cord blood and placenta. MSCs possess cellular features typical of cells contained within both the stroma and mesenchyme. These are the connective tissues which surround the organs of the body. Whilst the stroma imparts structural support, the mesenchyme forms loosely around the organs and contains highly mobile cells. These stem cells have been shown to differentiate into a wide range of cells, displaying pluripotent ability (Shakhbazau et al., 2011, Chen et al., 2012, Khlusov et al., 2011). It was assumed that MSCs would exhibit only a multipotent capability, only differentiating into restricted lineages. However these cells are able to produce daughter cells that possess cellular attributes characteristic not only of the mesoderm, but also the ectoderm and endoderm germ layers. Bone marrow derived stem cells

demonstrate a potential pool of cells that can undergo multipotent differentiation for possible retinal degeneration applications.

1.7. Retinal ganglion cell differentiation

RGCs are the first cells generated during mammalian retinogenesis from the primary retinal neuroblasts, following initial formation of the optic cups from the neural plate at embryonic day (E) 8.0 (Young, 1985). The neuroblasts present then proliferate under the influence of Pax6 (Livesey and Cepko, 2001, Marquardt et al., 2001). RGCs appear in the mouse at E11.5, when the stem cells begin to divide asymmetrically producing a progeny of daughter cells which have exited cell cycling (Young, 1985). These primary RGC precursors do not all develop into ganglion cells but this early specification begins within the temporal, central region of the young retina and spreads out to the anterior periphery (Hu and Easter, 1999). This primary proliferation is prompted by the secretion of Shh which follows a route to the outer regions of the retina and has been evidenced in zebrafish, in which it appears to be the main factor responsible for RGC specification. The next stage involves a refinement period of cell competence that determines their development; this comprises the expression of basic helix-loop-helix (bHLH) transcription factors Ath5 and NeuroD at E13.5 in the mouse, that induce these precursors to commit to RGC fate (Brown et al., 1998, Pennesi et al., 2003). In addition, inhibitors of the cell cycle; $p27^{Kip1}$ and $p57^{Kip2}$ are also expressed within these precursor cells, and are charged with hindering the activity of cyclin kinases (Dyer and Cepko, 2001). The exact combination of gene expressions that contribute to RGC precursor development does not appear to be completely defined due to the early birth of this population. The scenario may involve RGC precursor commitment being determined during early progenitor proliferation, where a progenitor competent in becoming any retinal cell decides to devote its lineage to a ganglion fate. Alternatively postmitotic cells become ganglion cells when all

the progenitor divisions have concluded. Despite this we see genes, consecutively involved in the tailoring of retinal cell genesis. Specifically for RGCs we find Pax6, Six3, Rx, Chx10 and the Notch pathway including the Ath5 and the Brn3 family (Mu and Klein, 2004, Marquardt et al., 2001). These factors determine the correct spatial patterning of the ganglion cell layer and ensure its networking organisation is correctly established.

The Notch pathway prevents the expression of proneural genes and triggers the expression of an alternative set of bHLH factors; Hes1 and Hes5 which have been shown to target the Ath family for repression. Ath5 is essential for RGC production and alterations in its expression is manifested in changes in the amount of ganglion cells made during retinogenesis. Overexpression of Ath5 results in an excess of RGCs made at the expense of other neurons and glia in chick (Liu et al., 2001) and xenopus (Kanekar et al., 1997) retinae. Knock-out experiments in mice (Wang et al., 2001) and zebrafish (Kay et al., 2001) for Ath5 homologs ended with the almost complete lack of RGCs and a surplus of both cones and amacrine cells. Though Ath5 expression is essential for RGC initiation and determination and all cells committed to a ganglion fate expressed Ath5, not all the Ath5-expressing cells become RGCs, suggesting the upstream roll of this bHLH in RGC specification as well as the presence of other influential cues involved in ganglion differentiation. Hence the over production of RGCs observed in knock-in studies indicates the creation of a larger cohort of proliferative progeny competent to generate RGCs.

Downstream targets of Ath5 are the earliest determinant switches of RGC differentiation. The class IV POU domain transcription factor; Brn3b is similar to other transcription factors. Like Pax6, Brn3b has a bipartite DNA binding domain (Liu et al., 2000) and it has been reported that Brn3b expression is vital for RGC development and maturation. BRN3B knockout mice fail to produce a normal population of ganglion cells, losing 70% viability (Liu et al.,

2000). Brn3b expression occurs rapidly, once the progenitors of the retina have exited the cell cycle and have committed to a RGC specification. Ath5 proceeds the expression of Brn3b in competent ganglion cell progenitors, whilst Brn3b expression is exclusively found in post mitotic RGC precursors as well as mature ganglion cells (Gan et al., 1999). It is thought Ath5 commences Brn3b expression, however its maintenance involves other cues once Ath5 production ceases, indicative of the presence of cofactors that lie between the two genes and may act to maintain Brn3b independently of Ath5, or in association. Apoptosis of ganglion cell progenitors coincides with a depression of BRN3B, indicating a close synergy between RGC maturation and BRN3B expression.

Final differentiation entails the spatial localisation of the RGC and the development of functional axons, dendrites and synapses. This organisation requires genes able to orchestrate ion channel formation, axon guiding agents and synaptic neurotransmitters. Cells undergoing differentiation commit to migrate to the inner layer of the neuroepithelium and become polarised in morphology and send out axonal projections which ultimately converge together to from the optic nerve. 87 genes have been reported, which are under the regulation of Brn3b are the controllers of the final differentiation of RGC and are involved in their maturation and maintenance of function (Mu and Klein, 2004). Brn3b also has a negative impact on Shh secretion and acts to prevent abnormal amounts of proliferation once maturation has commenced (Zhang and Yang, 2001). The transcriptional control of ganglion cells gives an insight into how stem cell differentiation may be influenced to follow a neural lineage, as well as how control of the transcription factors by epigenetic targeting may be induced.

1.8. Tissue Engineering for Stem Cell Transplantation into the Eye

The eye is considered to be an extension of the brain, and as such is part of the central nervous system (CNS). Damage within the CNS is irreversible

due to the lack of regenerative cells and the non-permissive architecture of these tissues (Jacobs and Fehlings, 2003). Regeneration of the retina may not be possible, but studies are aimed at improving function by either replacing damaged cells or promoting survival and regeneration of the remaining cells. To this effect, cell delivery to replace neural populations, would need to achieve differentiation, integration and survival with the host tissue (Mason and Dunnill, 2008). Encouraging residual dystrophic cells to survive and maintain their inherent functionality may also be achieved by delivery of cells that release trophic factors, as well as injections of therapeutic drugs, genes or factors. Tissue engineering aims to enhance, restore or maintain tissue function and involves the application of various disciplines in the biological, engineering and medical fields.

Natural polymers are favoured by tissue engineers due to their inherent biocompatibility with the body, and have been extensively employed clinically to create *in vivo* substrates, such as lubricants, dermal and wound sealants, surgical sponges and dermal fillers (Johl and Burgett, 2006, Lapcik et al., 1998). Cell delivery by such polymers has been studied using astrocytes, Schwann cells and neural progenitors, and these potentially can be used for retinal cell transplantation.

Collagens are an important source of natural polymers and are a family of ubiquitous proteins, which constitute a significant proportion of the basement membrane and support tissue structures. Type I collagen is used currently in the clinic in the form of surgical sponges for swabbing and wound dressings, and has also been used for drug delivery in this form (Bai et al., 2010). Both collagen hydrogels and electrospun matrices have also been studied for clinical application. Since both collagen gels and scaffolds are inherently weak, similar to other natural polymers following extraction processes, they require structural reinforcement (Matthews et al., 2002, Pieper et al., 2002). Chemical crosslinkers are currently the prime candidate used to improve

durability and give strength to such matrices. Glutaraldehyde (GTA) is an aldehyde derivative used in laboratory settings as a fixative which has the ability to crosslink cellular proteins, and as such is used to strengthen collagen matrices. However the use of such chemicals is cytotoxic when implanted *in vivo*, due to the release of residual reactive moieties from GTA. In addition, to chemical crosslinkers, non-toxic crosslinking catalysts are also used to enhance collagen robustness as well as other natural polymers (Macaya and Spector, 2012). Genipin is sourced from gardenia plants and is an aglycone (non-saccharide sugar component) which constitutes a natural protein crosslinker that catalyses protein fibre coupling. Following crosslinking, collagen matrices have been studied for its factor loading capabilities where evidence demonstrated the ability of collagen being able to stably release ciliary neurotrophic factor (CNTF) to proximal rat neural stem cells, safeguarding their proliferation and survival, under culture conditions (Yang et al., 2010).

An alternative source of natural material is hyaluronan (HA), which like collagen is found extensively in connective tissues and within cellular supportive matrices. It has an innate feature which enables cells to grow and proliferative *in vivo* as well as aiding wound healing processes (Pakulska et al., 2012). HA is intrinsically weak and unlike other natural polymers, it is unable to polymerise once it has been extracted from native tissues and is prone to digestion unless exhaustively crosslinked or blended with other polymers which impart strength to the mixture (Ji et al., 2006, Zheng Shu et al., 2004). One such example is the blending of methylcellulose and HA for gels containing bFGF and EGF for transplantation for spinal cord (Kang et al., 2009) and stroke (Cooke et al., 2011) degenerations. It was initially evident that in order to sustain factor loading of HA mixed matrices would require further modulation, as factors were seen to leach fully within 24 hours following loading. To sequester the factors suitably poly(lactic-*co*-glycolic acid (PLGA) nanoparticles were made to incorporate the factors which were

then included into the matrices, which improved the release profile of these factors (Baumann et al., 2009).

Synthetic materials have also been proposed, and have generally been used in the past as co-polymers; however researchers are examining the potential of their standalone application for drug and cell delivery. The processing of such polymers gives researchers the opportunity to synthesise materials from the bottom up, where the features can be tailored for a distinct use. Both BDNF and NT-3 have been incorporated into synthetic materials composing of poly-(N-isopropylacrylamide) (PNIPAAm) with the addition of poly-(ethylene glycol) (PEG) functional groups. Constructs were found to release the two factors over a period of 30 days *in vitro* (Vernengo et al., 2008). Poly-(lactic acid) (PLA) is usually used in biology as a co-polymer. Modification of its monomer sequence can be made to include agents such as NT-3, which can subsequently prolong its release for up to 14 days in murine models of spinal cord injury (SCI) (Piantino et al., 2006). Retinal progenitors have been cultured on synthetic PLA, and its derivatives (Tomita et al., 2005), polycaprolactone (PCL) (Sodha et al., 2011) and poly-(glycerol-sebacate) (PGS) (Neeley et al., 2008) have been investigated for their potential to support cells for transplantation.

Construct-tissue dynamics has been shown to be integral to the survival of grafted cells, integration into host tissue and prevention of necrosis of local cell populations. Preventing cellular aggregation of transplanted cells and encouraging cellular distribution on a tissues surface has been shown to promote cell survival and host integration (Pakulska et al., 2012). Whilst uniform distribution of grafted cells can favour survival of transplants, the presence of a cellular support which provides an adherent surface for grafted cells limits anoikis (a form of cell death) (Frisch and Francis, 1994, Frisch and Screaton, 2001) and suggests an advantage over cell suspension delivery.

An ideal engineered construct needs to have an *in vitro* 3D structure able to regulate and control cell function. Proteins of the basement membrane have been used as a 2D planar culture layers or in a 3D form, and this includes extracellular membrane proteins reconstituted from the basement membrane. These are aimed to support cell growth, attachment and differentiation. The extent to which uniform cellular integration occurs throughout the whole inner surface of the retina following transportation has so far been limited in our laboratory with an uneven distribution of transplanted cells observed upon injection of cell suspensions. Cellular scaffolds or nanostructures have been proposed to address this problem, whilst supporting the cells structurally and assisting in their delivery onto the damaged retina. Employing a cellular scaffold involves engineering a structure which has biocompatibility and bio mimicry.

There is therefore the need to create a vehicle for cell delivery in order to regenerate the retinal ganglion cell population after degeneration, the major pathology of glaucoma. The creation of a suitable construct would provide a platform for uniform cellular distribution which would aim to promote host integration and cell survival. This project favoured the use of Collagen Type-I as a natural polymer, which has recently been modified by non-toxic processing involving physical crosslinking removing the need for using chemicals. Collagen scaffolds produced by plastic compression (PC) (Brown et al., 2005) can be produced that have a geometrical conformation resembling the *in vivo* dimensions of a basement membrane. Type-I Collagen is a readily sourced protein that can be tailored to build these matrices to provide biological support to cells. Stem cell transplantation studies to repair degenerated retina have not yet achieved adequate cellular distribution across the neural retina. This is partly attributed to the anatomical features of the retina and surrounding tissues that prevent optimal migration and integration of injected cells. There is therefore the need to develop

methods that can efficiently and safely deliver cells into the retina as a tool for cell based therapies to treat retinal disease.

1.9. Objectives of this thesis

Based on the current knowledge within the field of stem cell biology and transplantation, and the need for the design of cell based therapies to treat end stage glaucoma, it is important to define parameters to ensure optimal differentiation of retinal ganglion cells (RGCs) from Müller stem cells, as well as to design appropriate methods to ensure widespread delivery of these cells into the RGC layer. To validate previous protocols used for RGC generation *in vitro* this study investigated molecular mechanisms known to promote RGC differentiation during development. The project also aimed to develop collagen-based scaffolds for cellular delivery onto the retina *in vitro* and *in vivo*, and examined the interaction between Müller stem cell-derived RGCs and the scaffolds.

The following objectives were therefore formulated.

1. To investigate downstream targets involved in the Notch signalling pathway that lead to differentiation of Müller stem cells into RGCs in vitro. This part of the study involved the examination of miRNA expression by cells undergoing Notch inhibition, as well as the determination of transcription factors controlled by Notch activation, and upregulation of known RGC markers.

2. To develop protocols for the design of cellular scaffolds to facilitate uniform transplantation of RGCs onto the inner retina. This research involved the use of electrospinning protocols as well as compression methods to produce collagen scaffolds which could serve as supports for cell transplantation. Various crosslinking agents as well as their affect on cell viability, proliferation and differentiation were used in the study.

3. To determine the capacity of cellular scaffolds to support migration and integration of RGCS into the retina. This part of the study examined the ability of scaffolds to facilitate migration of RGCs onto the human retinal explants *in vitro* and onto rabbit retina *in vivo.*

Chapter 2: Changes in MicroRNA Expression during Retinal Ganglion Cell Differentiation of Müller Stem Cells

2.1. Müller Glia with stem cell characteristics in the adult retina

Adult retinal stem cells have been identified within the mature human retina. Investigations into the features of this population have identified them as a population of Müller glia. These cells appear to remain quiescent within adult tissue and are unable to regenerate retina, however they constitute a population that has the potential for establishing cell-based therapies for retinal degenerations. To understand this capacity, a better understanding of the properties of retinal stem cells within the Müller population is required.

RGCs are the first cells to be born in the retina, with Müller glia being generated last. In fish and amphibians Müller cells are able to repair retinal damage incurred even during adulthood (Bernardos et al., 2007). It is thought that the cohort of cells that possess the capacity to regenerate retinal tissue in these species are a population of late radial glial progenitors that appear to have retained their progenitor potential, and are able to re-enter the cell cycle (Walcott and Provis, 2003, Seigel et al., 1996, Das et al., 2006). They also retain their predecessors' morphology of elongated bipolar-like structures, which during development aids with the migration of young neurons to their various retinal laminae (Meller and Tetzlaff, 1976). Retinogenesis involves two distinct histogenic periods, one involves early neuronal development and the second involves the generation of late born neurons and the glial population. Assuming that the radial glial progenitors are conserved within the mature Müller population, it could imply that these cells would be restricted in producing progeny born later during retinogenesis. However in fish and amphibians this is not the case.

In response to injury, quiescent Müller stem cells in amphibians have the ability to undergo phenotypic adaptations to permit de-differentiation, controlled proliferation, migration to damaged lamina and differentiation into new neurons (Reh and Fischer, 2001, Ooto et al., 2004). Both fish and amphibian retinae can undergo neural growth through the proliferation of

Müller stem cells in the ciliary marginal zone (CMZ) (Mack et al., 1998), which is the junction at which the neural retina and ciliary body meet. Müller stem cells are also housed within the main body of the teleost fish retina and largely yield RGCs following damage, although the primary production of new cells is co-ordinated from the CMZ (Julian et al., 1998, Kassen et al., 2008). Amphibian retina can also undergo regeneration through trans-differentiation of their RPE (Raymond, 1991), as well as the stem cells of the CMZ (Umino and Saito, 2002). The outer nuclear layer (ONL) of the adult fish contains rod precursors able to respond to rod photoreceptor damage, and can stimulate proximal Müller stem cells to proliferate into photoreceptors and migrate into the ONL along the surface of non-plastic residual Müller glia (Reh and Levine, 1998, Morris et al., 2008, Otteson and Hitchcock, 2003). In zebrafish Müller cells express the “master controller” transcription factor Pax6, cone rod homeobox (CRX) and α1-tubulin (Fausett and Goldman, 2006, Fausett et al., 2008), indicative of the innate capacity of these cells to enable production of all retinal neurons in the post-natal period (Bernardos et al., 2007). Müller glia from zebrafish constitutively upregulate the expression of the basic helix-helix (b-HLH) transcript achaete-scute homolog-1a (ash-1a), which is thought to assist in the transformation of dormant Müller stem cells into potent progenitors, encouraging a pro-neuronal, cell cycling state (Fausett et al., 2008).

Whilst adult cold blooded vertebrates demonstrate the innate ability to regenerate the neural retina, warm blooded animals show a restricted capacity, which in most cases ceases rapidly following birth. When damaged, the young chick retina has the ability for a cohort of Müller glia to alter their expression profile to that of a pro-neuronal state. This behaviour is mediated by the ash-1a homolog CASH-1, Pax6 and Chx10. These cells mainly generate other Müller cells with or without progenitor features, however a number of them are able to exit the cell cycle and differentiate into retinal neurons, demonstrating their regenerative capabilities (Fischer and Reh,

2001, Fischer and Reh, 2003). However this regenerative ability becomes less potent over time and decreases with increasing age. The anatomical region housing the majority of the progenitor-like cells diminishes over time, and is observed to regress to the more peripheral retinal domains.

In vivo de-differentiation and proliferation of the latent Müller stem cell population can be induced by bFGF and insulin injections (Fischer et al., 2002). Expression of NeuroD contributes to neuronal differentiation of chick Müller stem cells, but it is thought that the relatively low degree of glial to neuronal differentiation is due to the presence of pro-glial signalling mediated by bone morphogenetic proteins (BMPs) within injured retinal tissue (Fischer et al., 2004b, Fischer et al., 2004a). Notch is also a major contributory factor to the progenicity of Müller stem cells following injury. Its constitutive signalling maintains the proliferative and undifferentiated state of the Müller stem cell population, and also limits the extent of neuronal de-differentiation by Müller glia within the retina (Hayes et al., 2007).

Mammalian retinae have also exhibited evidence of a restricted level of retinal regeneration, driven by a sub-population of Müller cells in early post-natal life (Blackshaw et al., 2004). Both rat and murine retina have been shown to contain a cohort of Müller cells that express the homeodomain transcription factors Pax6 and Chx10 (Rowan and Cepko, 2004), with murine Müller cells directing their plasticity via their expression of Notch and Nestin (Roesch et al., 2008). Various markers of neuronal development have been also found to be upregulated within rodent Müller stem cells following injury. The adult human retina also harbours a population of Müller cells that express proteins of early retinal progenitors such as, Sox2, Chx10 and Pax6, as well as markers of retinal glia and neurons (Bhatia et al., 2011b).

The main pathways involved in co-ordinating Müller-derived retinal regeneration in mammalian retina have been identified as the Notch and Wnt/β-catenin signalling cascades (Das et al., 2006, Osakada et al., 2007).

Wnt3a promotes proliferation of Müller stem cells in murine models of photoreceptor deficiency, whilst in humans Notch-1 has been shown to play a role in maintaining cell cycling and an undifferentiated state *in vitro.* Inhibition of this pathway in human Müller stem cells has been shown to induce RGC differentiation (Singhal et al., 2012).

2.1.1. The Notch pathway

The Notch pathway has been shown to play a significant role within the development of the central nervous system. Since the Notch-1 pathway is an integral component of Müller stem cell differentiation, the understanding of how Notch controls RGC maturation is crucial in determining the extent of RGC development *in vitro,* as well as the mechanisms involved in such a process.

The Notch pathway involves the constitutive signalling of a heterodimeric transmembrane receptor within stem cell populations, and is a highly conserved signalling mechanism observed in many species (Yu et al., 2008). This pathway mediates the maturation as well as the maintenance of stem cell niches, especially those involved in neurogenesis. The Notch receptor family of proteins span the plasma membrane in a characteristic single pass fashion where the extracellular domain, consisting of multiple EGF-like motifs, is involved in the ligand binding process (Faigle and Song, 2013) (Figure 2.1). There are four members of the Notch family, identified by the number of EGF repeat motifs. In *Drosophila* the protein receptor is activated by the binding of its extracellular domain by its ligand, either Serrate or Delta on adjacent cells (Louvi and Artavanis-Tsakonas, 2006). These ligands have either an excitatory or inhibitory mode of action, depending on the state and or maturation of neighbouring cells. Serrate inhibits the Notch cascade whilst Delta and its mammalian homologues, Jagged and Delta-like, activate the pathway (Stump et al., 2002). Following binding and activation, both the

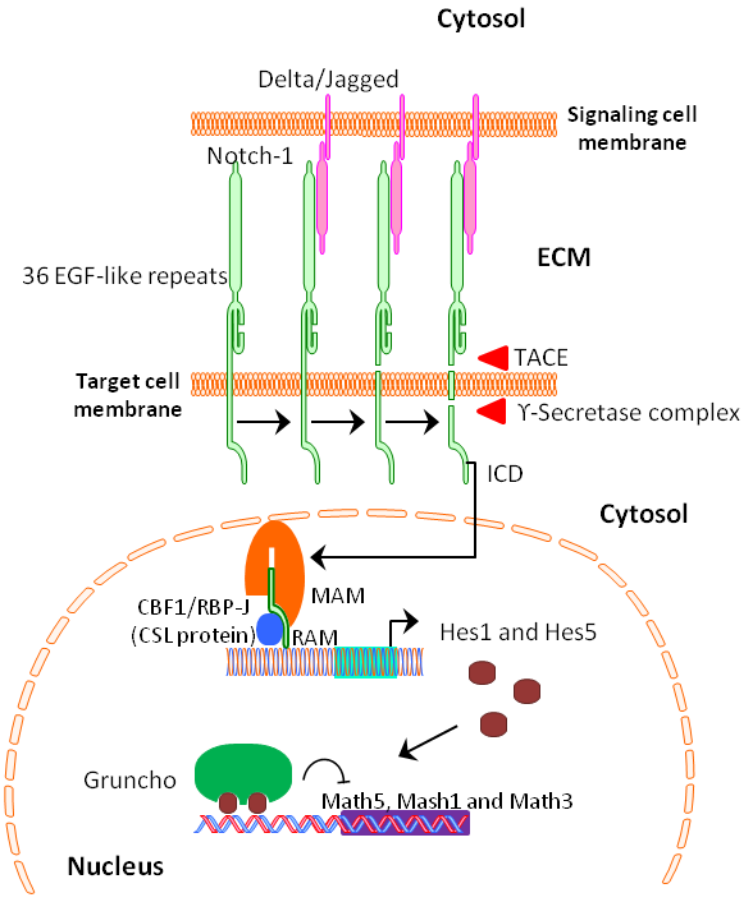

Figure 2.1: Processing and activation of Notch-1 by proteolytic cleavage. Upon binding with its ligands (Delta or Jagged) the Notch receptor is activated, both the intracellular (ICD) and extracellular domains of the receptor are cleaved. The ICD is released by the action of gamma secretase and translocates to the nucleus, where it initiates the transcription of Hes1 and Hes5, mediated by CSL proteins. Hes1 and Hes5 act as transcriptional repressors of pro-neural genes, attenuating neural differentiation. (Modified from Hakateyama and Kageyama, 2004, using Motifolio)

extracellular and intracellular domains undergo enzymatic cleavage. The ligand-bound extracellular domain is cleaved by the tumour necrosis factor alpha-converting enzyme (TACE) and is in turn endocytosed along with its ligand, into the ligand expressing cell. Subsequently the Notch intracellular domain (ICD) is also cleaved upon activation, mediated by the enzyme presenilin gamma secretase (Miele et al., 2006a, Miele et al., 2006b).

Upon cleavage from the transmembrane receptor, the Notch ICD translocates to the nucleus where it interacts with a member of the CBF1/RBP-J kappa, Suppressor of Hairless, Lag-1 (CSL) transcription factor family. This association is thought to be mediated by the RBP-J kappa-association molecule (RAM) of the Notch ICD (Miele et al., 2006a, Miele et al., 2006b, Okuyama et al., 2008, Deregowski et al., 2006). A number of genetic targets have been identified as housing CSL binding sites that propagate the Notch signalling cascade for cellular regulation. These include Hairy enhance of split-1 (Hes-1), NF-kB, Cyclin D1 and c-Myc. Some are present in all tissue types whilst others are limited to specific tissues (Okuyama et al., 2008, Miele and Osborne, 1999).

Activation of the transcription of Hes1 and subsequently of Hes5 by the Notch ICD is followed by their interaction with the transcription repressor Groucho (Nagel and Preiss, 2011). This results in the suppression of transcription of downstream pro-neuronal genes, hindering differentiation during development (Hatakeyama et al., 2006, Das et al., 2005, Ohsawa and Kageyama, 2008). The activity of Notch in repressing neural development is also synchronised with continuous self-renewal, allowing stem cells to remain within the cell cycle. Cyclin D1 and CDK2 transcription factors are directly activated by Notch signalling, and when activated via CSL binding, their levels of mRNA have been shown to increase in neuroepithelial and cancer cells (Ronchini and Capobianco, 2001). Notch signalling plays a regulatory role in Müller glial differentiation and maintenance of the glial state (Nelson et

al., 2011, Nelson and Hyde, 2012). In addition, downregulation of Notch signalling in human Müller glia with stem cell characteristics has been shown to induce RGC differentiation (Singhal et al., 2012).

2.1.2. The Role of the Notch-1 Pathway in Müller Stem Cells

Ocular development encompasses a range of developmental processes including gliogenesis, neurogenesis and vascularisation in a conserved, well-ordered manner.

Notch 1 expression has been identified within the developing eye, with expression being located on the inner surface of the optic cup. During development Notch activity is down regulated once progenitors begin differentiation and maturation, which is followed by migration to their respective layers within the retina. Ganglion cells being the first to be born are the first population where Notch signalling is down regulated. This is an essential step for RGC maturation in both Chick and *Xenopus* retinae (Ohsawa and Kageyama, 2008). The loss of Notch activity and its downstream effector Hes1 favours an intrinsic establishment of pro-neural gene expression inducing differentiation. In terms of the RGC population, this involves the upregulation of the human gene ATOH7, as well as its murine equivalent Math5 and Mash1. Notch signalling within the initial progenitor pool prevents the onset of ganglion cell neurogenesis and aids the development of Müller glia during gliogenesis (Gaiano et al., 2000). Prior to rod, bipolar and glial differentiation the late progenitors transform into a resilient radial glial subtype which retains the bipolar elongated morphology and proliferative capacity of their earlier predecessors, ensuring their ability to produce glia and neurons. Evidence in *Xenopus* development has demonstrated that cells produced during late retinogenesis that originate from late-radial glial progenitors and are able to maintain Notch activity, develop into Müller glia (Dorsky et al., 1995). Although these cells require Notch signalling to commit initially to gliogenesis, in order to terminally

differentiate, Notch signalling must ultimately be repressed (Dorsky et al., 1995). This mode of progenitor development may be the reason why in lower mammals and amphibians Müller glia are able to de-differentiate and re-enter the cell cycle in response to neuronal damage.

2.1.3. MicroRNA function and phenotype regulation

Neural stem cell renewal and maturation has also been linked to a range of external and internal control mechanisms during development. Recent research has begun to define the processing cues that act as molecular regulators of protein expression profiles by means of restricting or enhancing transcript production. These endogenous regulators are known as microRNAs (miRNAs). There have been over 1,000 miRNAs identified in the human genome. They function to repress translation by targeting gene coding transcripts and altering their conformation, ultimately causing steric hindrance of their target messenger RNA (mRNA). This changes the gene patterning within a cell which can in turn promote different cellular activities, for example division, differentiation, potency or apoptosis (Guo et al., 2010, Takada and Asahara, 2012).

miRNAs are short single stranded sequences of RNA which can range between 10-22 nucleotides (nt) long, and are encoded within intronic or intergenic regions of genomes in a conserved manner between eukaryotic species. The transcription of miRNAs provides an extra layer of control on post-transcriptional and translational processes, resulting in a system that functions to regulate the extent of protein activity. The majority of this control is reflected on the production of protein, and manifests at the mRNA level by mediating the stability of the mRNA structure. Unlike small interfering RNAs (siRNAs), miRNAs are made from single-stranded transcripts rather than long double-stranded sequences. Targeted genes undergo transcription by Polymerase III which simultaneously triggers the production of miRNA transcripts via the action of Polymerase II. This yields a short sequence

adjacent to the target gene, producing a hairpin structured primary microRNA (pri-miRNA) sequence 72-100 nucleotides (nt) long. Prior to exiting the nucleus miRNAs are modified via cleavage of the hairpin ends, which is performed by associating with Drosha (RNase III enzyme), DGCR8 (in vertebrates) or Pasha (in non-vertebrates), producing smaller hairpin/stem-loop structures. These are known as precursor microRNA (pre-miRNA) duplex comprising of 65-70nt, or less, with 2-5nt 3' overhangs (Liu et al., 2008, Okamura et al., 2008a, Okamura et al., 2008b). The molecule then exits the nucleus and enters the cytoplasm through the nuclear pores aided by Exportin-5 complexes, powered by Ran-GTP. Upon entry into the cytosol, pre-miRNAs form complexes with Dicer, which consequently remodels and cleaves the RNA molecule to produce mature miRNAs, approximately 22nt long (Khvorova et al., 2003, Schwarz et al., 2003). The resulting duplex binds RNA-induced silencing complex (RISC) as well as Argonaut proteins, namely Ago1, Ago2, Ago3 and Ago4, to aid the stabilisation of the short RNA molecule. This causes the complementary strand of the small hairpin to be discarded (Parker and Barford, 2006). The binding is mediated by RNA binding proteins such as HIV-1 TAR RNA binding protein (TRBP) and Cellular protein activator of PKR (PACT), and supports the association between the two molecules. Dependent on the complementary nature of the mature miRNA sequence to its mRNA target, it is able to cause degradation of the mRNA transcript upon its binding to Ago2 (Takada and Asahara, 2012). When miRNA sequences are not fully complementary there is semi-efficient binding of the complex to its targets, resulting in mRNA retention for either gene silencing or translational inhibition (Figure 2.2). The mechanisms by which miRNA finally degrades mRNA or disrupts translation is by binding to the 3' untranslated regions (UTRs) of target mRNAs. miRNAs are able to target and suppress multiple mRNA transcripts, whilst one mRNA can be targeted by numerous miRNAs depending on their location, maturation and function.

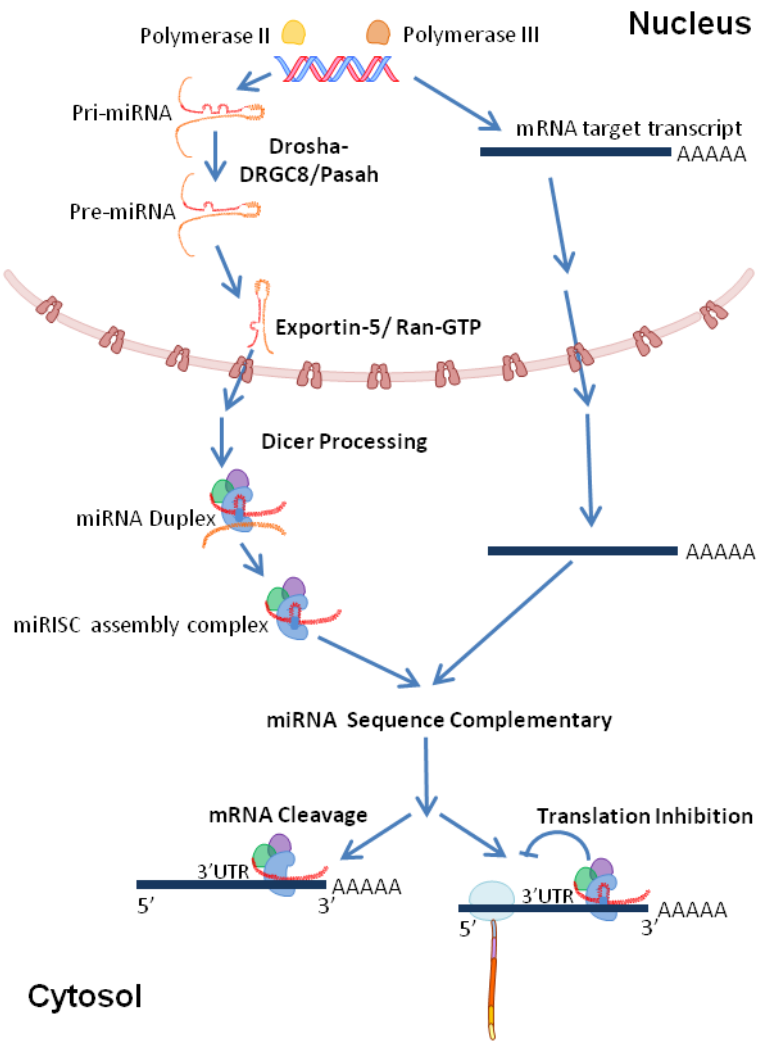

Figure 2.2: microRNA biogenesis. The primary miRNA hairpin structure is synthesised via the action of RNA polymerase II, which is then modified by DRGC8/Drosha complex, resulting in the production of the precursor miRNA molecule. The RNA molecule is exported out of the nucleus and undergoes cleavage by Dicer. One of the final, mature strands associates with RNA induced silencing complex (RISC), where the miRNA and its transcript target interact, which either leads to translation suppression or mRNA degradation. (Modified from Liu et al, 2008, using Motifolio).

Although mature miRNAs are regulatory agents within translational processes, they themselves have been shown to be under regulation by other components of the gene expression machinery. The majority of miRNA modulation involves their repression in the nucleus by transcription factors, cofactors and other miRNAs. Transcription factors determine the expression of mature miRNA by preventing pri-miRNA production (Rodriguez et al., 2004). Cofactors involved in miRNA maturation can prevent or enhance their production. Proteins recruited to hinder miRNA maturation alter the cleavage of immature miRNAs by Drosha or Dicer and the Argonaut proteins (Zhang and Zeng, 2010). Enhancing miRNA generation involves proteins facilitating cleavage by either Dicer or Drosha. KH-type splicing regulatory protein (KHSRP) contains several multifunctional RNA-binding sites intended to aid both Drosha and Dicer recruitment of a number of RNA transcripts, especially pre-miRNAs and pri-RNAs (Trabucchi et al., 2009). Other auxiliary protein expression, involved in miRNA production can alter their generation, including Argonaut proteins (Zhang et al., 2009) and the nuclear pore protein Exportin-5 (Yi et al., 2005). These can all effect cellular proliferation, differentiation and maturation within different tissues.

2.1.4. MicroRNA Expression in the Retina

miRNAs are extensively expressed within mammalian brain tissue, indicative of their possible role in neural function and development. Different families of miRNAs have demonstrated the ability to refine neural progenitor differentiation, directing their fate and function (Wienholds et al., 2005, Du and Zamore, 2005, Krichevsky et al., 2003). miR-124 and miR-128 are highly expressed in adult brain neurons, whilst miR-23 is primarily expressed in astrocytes. Additionally, miR-9 and miR-125 are constitutively found across all neuronal sub-types (Smirnova et al., 2005). miRNAs are attractive targets for controlling the onset of neurogenesis and lineage-specific gene expression within neural stem cells, as well as retinal stem cells. Inducing

dysfunctional expression of miRNAs contained within the brain during development showed altered population densities within this tissue. Forced ectopic expression of miR-9, miR-124 and miR-128 in late neural precursors reduced the production of astrocytes whilst reducing miR-9 activity, either in combination with miR-124 or alone, hindered neural generation. It is thought that both miRNAs exert their control by regulating the signalling pathways of STAT3 and Notch, which are involved in the proliferative and neurogenic ability of stem cells (Krichevsky et al., 2006). Let-7 is another miRNA expressed in stem cells within the murine brain and it is suggested to have a role in early neural specification (Wulczyn et al., 2007). Notable miRNA differences have been found between post-natal mouse brain and retina. These include, miR-9, miR-335, miR-31, miR-106, miR-129, miR-3p, miR-691and miR-26b (Huang et al., 2008, Loscher et al., 2007).

Whole eye analysis has indicated the enriched presence of miR-204 and miR-96 in both mice (Lagos-Quintana et al., 2003) and zebrafish tissue (Wienholds et al., 2005), suggesting an important role for eye function. However, extraction of murine embryonic retinal tissue at E.10.5, demonstrated different expression profiles. miR-204 was highly expressed in the ciliary body, lens and RPE, whilst miR-184 was absent from retinal tissue but was expressed in the lens and cornea. The developing optic cup demonstrated enriched expression of miR-124a miR-9, miR-29 and miR-181a at E10.5, with their adult expression profiles confined to the retina (Karali et al., 2007). Within postnatal P7 mouse retina, miR-181 was found within the ganglion and inner plexiform layer only and miR-204 was located in the RPE and ciliary body regions (Ryan et al., 2006). One month old murine retinas showed distinct locations of three retinal miRNAs: miR-182 was detected within the ONL and let-7 and miR-181a were identified in the INL, and in the mature RGCs(Loscher et al., 2007).

2.1.5. MicroRNA regulation of the Notch-1 Pathway

To understand and fully utilise miRNAs in mature and developing retina for regenerative therapies, it is important to predict and verify their targets. miRNAs have been shown to interact with the Notch pathway, by either regulating it up- or down- stream of its locus, impacting on its functional role in both oncogenic and stem cells. The majority of evidence demonstrating Notch and miRNA interaction is from studies involving tumorigenesis or development. Like the genetic transcripts involved in tumour progression, miRNAs can be either ontogenetic or tumour-suppressive in their action. Upstream modulators of Notch include miRNAs that act as tumour-suppressor agents that inhibit the expression genes involved in the translation of Notch or factors involved in its signalling (Figure 2.3).

In the *Drosophila* miR-1 targets Notch via Delta repression preventing activation and nuclear translocation of its ICD (Kwon et al., 2005). miR-1 also suppresses the Notch pathway in murine ESCs during development (Ivey et al., 2008). Another tumour-suppressive agent involved in Notch regulation is miR-34. This has been shown to arrest Notch-1 and -2 signalling in gastrointestinal pancreatic cancer cells and appears to prevent cellular self-renewal and abnormal growth (Ji et al., 2009, Ji et al., 2008). miR-124a activity is preferentially expressed in neurons, and has been implicated in neurogenesis and differentiation in the subventricular zone (SVZ), where it represses Sox9 during neural development. Following focal cerebral ischemia in adult rats miR-124a was shown to markedly decrease in the SVZ, coupled with the onset of Notch activation. Forced the expression of miR-124a in SVZ cells led to Jagged-1 (JAG-1 the Delta ligand homolog) repression, which acts normally to activate Notch (Liu et al., 2011). This resulted in decreased proliferation of neural progenitors but enhanced differentiation.

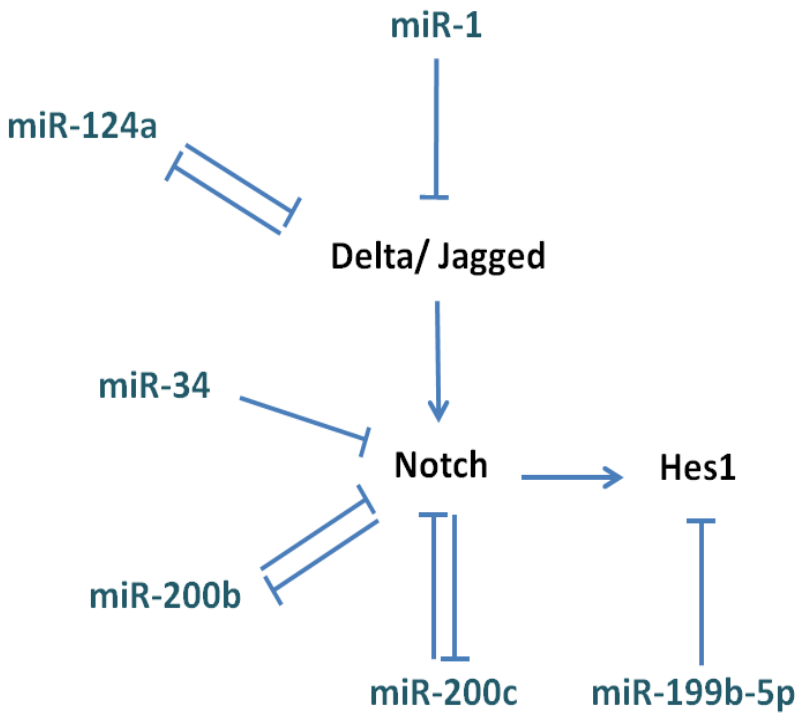

Figure 2.3: Regulation of the Notch signaling pathway by miRNAs. A schematic illustration of Notch targeting for miRNA silencing by both upstream and downstream mature miRNAs, based on up to date oncogenetic studies.

In contrast, miRNAs are also able to repress downstream targets of the Notch pathway, preventing propagation of its signalling. The miR-199 family negatively regulates Notch targets, and acts downstream of Notch, inhibiting their activity by promoting differentiation rather than maintaining an undifferentiated state. Downregulation of the miR-199 family has resulted in the progression of different cancers. Specifically miR-199a expression is markedly reduced in both hepatocellular carcinoma (HCC) (Murakami et al., 2006) and ovarian cancers (Iorio et al., 2007) and has been shown to prevent cell cycling by acting at the G2/M phase. miR-199b-5p targets Hes-1 to inhibit transcription of pro-differentiating genes in medulloblastoma (MB) cancer cells. MB patients that presented with metastatic tumours had reduced levels of miR-199b-5p compared to non-metastatic patients, indicating that this miRNA is an important onco- and Notch- suppressive agent (Andolfo et al., 2012, Garzia et al., 2009).

Lastly, the miR-200 family has been shown to act as a Notch-1 antagonist in cancer stem cells undergoing epithelial-mesenchymal transition (EMT) (Burk et al., 2008). Notch-1 promotes the activation of the zinc-fingered E-box binding homeobox (ZEB) proteins, ZEB1 and ZEB2, as well as CD44, EpCam and Hes-1 in different cancer cell lines, including the human pancreatic cancer cell line AsPC-1 (Korpal et al., 2008, Park et al., 2008, Gregory et al., 2008). When these cells are induced to ectopically express Notch-1 miR-200b and miR-200c are reduced significantly. Conversely, when the expression of these two miRNAs was upregulated, EMT diminished, Notch signally ceased and E-cadherin, a cell attachment protein, increased (Bao et al., 2011, Kong et al., 2010, Li et al., 2009). These observations indicate that miR-200 family and Notch act antagonistically, inhibiting each other's expression depending on the cellular state.

Emerging evidence suggests that miRNAs are potential agents that could be targeted for novel therapy strategies in cancer or regenerative medicine.

Human Müller stem cells, which appear to lie dormant in the human retina *in vivo,* regulate their renewal and progenicity through Notch-1 signalling *in vitro* (Singhal et al., 2012). Therefore Notch constitutes a target for either induction of endogenous regeneration *in vivo* or regulation of cell differentiation for *in vivo* grafting. The extent of miRNA control is yet to be examined in these cells and understanding the roles these molecules may play in Müller stem cell differentiation *in vitro*, may aid in the development of regenerative therapies using these cells. On this basis, this chapter aimed to investigate the expression of miRNAs by Müller stem cells following differentiation into RGC phenotypes.

2.2. Objectives and experimental design

The aim of this chapter was to investigate changes in miRNA expression by Müller stem cells following a differentiation protocol aimed at inducing Notch downregulation to yield an enriched population of RGC precursors. Current research suggests that miRNAs involved in neural stem cell differentiation are controlled by other miRNAs and various co-factors and transcription factors. The epigenetic control of neural cell populations by miRNAs has identified some signalling pathways, illustrating a control of transcription and downstream expression of neuronal genes. It was therefore important to identify changes in miRNA expression profiles during human Müller stem cell differentiation into RGCs *in vitro*. Understanding the role of these molecules and the timing of generation may aid in the design of cell therapies to replace RGC damaged by degeneration.

The general objectives of this chapter were:

1. To identify the downstream Notch pathway targets that lead to differentiation of human Müller stem cells into RGC *in vitro*.
2. To investigate changes in microRNA expression profiles following inhibition of the Notch pathway in human of Müller stem cells.
3. To investigate changes in microRNA expression following inhibition of the Notch pathway in the presence of bFGF in Müller stem cells.

To fulfil the above objectives, the following experiments were performed:

1. Investigation of the effect of Notch inhibition with **N-[N-(3,5-Difluorophenacetyl)-L-alanyl]-S-phenylglycine t-butyl ester (DAPT) in the presence of bFGF,** on Hes1 and retinal ganglion cell markers by differentiated Müller stem cells. This was assessed using RT-PCR, immunocytochemistry and western blotting techniques.

2. Evaluation of differentially expressed miRNAs in undifferentiated Müller stem cells and comparison with cells undergoing Notch inhibition in the absence of bFGF, using microarray analysis with Agilent platform.
3. Evaluation of differentially expressed miRNAs in undifferentiated Müller stem cells in comparison with cells undergoing Notch inhibition in the presence of bFGF, a protocol known to induce RGC differentiation of Müller stem cells, using microarray analysis, performed as indicated above.

2.3. Results

2.3.1. The effect of Notch inhibition in Müller stem cells cultured in the absence of bFGF

Cells were cultured for one week in the presence of 50μM DAPT with or without ECM. The ECM gel used was composed primarily of laminin, collagen type IV, heparan sulfate proteoglycan and entactin, and was used to facilitate the differentiation of RGC-derived Müller stem cells, as previously demonstrated by our laboratory (Singhal et al., 2012). This treatment was observed to induce morphological cell changes consistent with acquisition of neural features. These included formation of long cytoplasmic projections and branching occurring on cultured cells, coupled with the appearance of phase-bright nuclei (Figure 2.4A) suggestive of neural differentiation. These projections were measured and demonstrated the induction of neurite development with Notch inhibition, which was significantly increased in the presence of ECM (Figure 2.4B).

Notch inhibition was also examined by gene expression analysis of various genes involved in the Notch pathway during normal stem cell maturation. This investigation demonstrated that in the DAPT treated cells Notch-1 expression in Müller stem cells was not modified, either in the presence or absence of ECM, as compared with the DMSO control (Figure 2.5). In contrast, Hes-1, a downstream factor of the Notch pathway, was significantly decreased by culturing Müller stem cells with DAPT in the presence or absence of ECM. Analysis of Hey2 (another factor of the Notch pathway) expression showed that Notch inhibition with DAPT caused a decrease in mRNA levels of this molecule. Culture of these cells on ECM caused increased expression of Hey2, but lower levels were observed when DAPT was added to cells cultured on ECM, as compared with controls. Marked elevations were observed in mature transcripts involved in RGC development, namely Brn3b and Islet-1 (Figure 2.6). Brn3-b is a member of

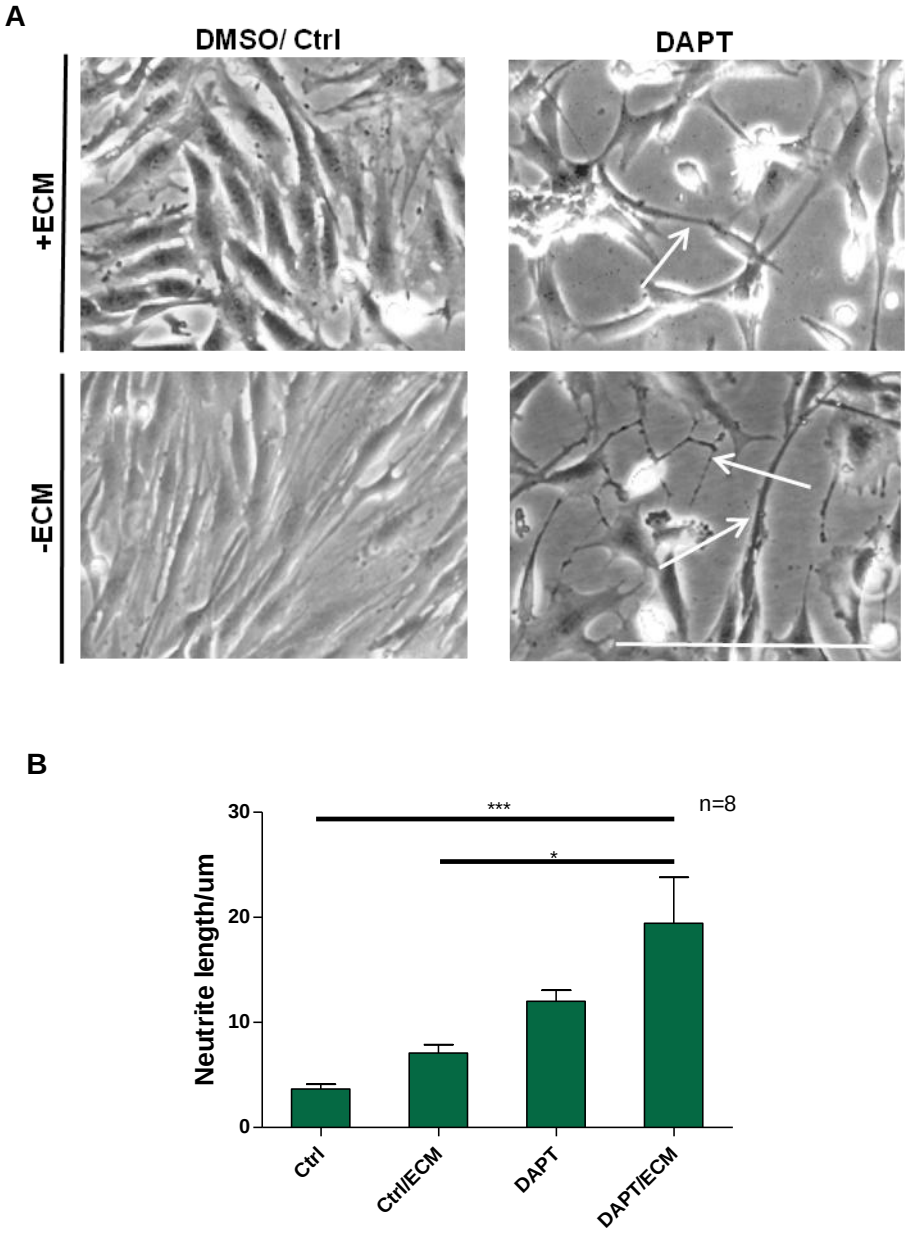

Figure 2.4: Effect of Notch inhibition in the absence of bFGF on Müller stem cell morphology. Phase-contrast imaging of Müller stem cells cultured under control conditions (no treatment), in the presence of DMSO (vehicle), and in the presence of DAPT, either with or without ECM coating. In this Müller stem cell population DAPT induced morphological changes, with development of phase-bright nuclei and outgrowth of long neurites (white arrow). Freehand measurement of the cellular projections, using a calibrated image J scale enabled analysis of neurite length which was markedly increased in the presence of DAPT in presence and absence of ECM. Scale bar=100µm

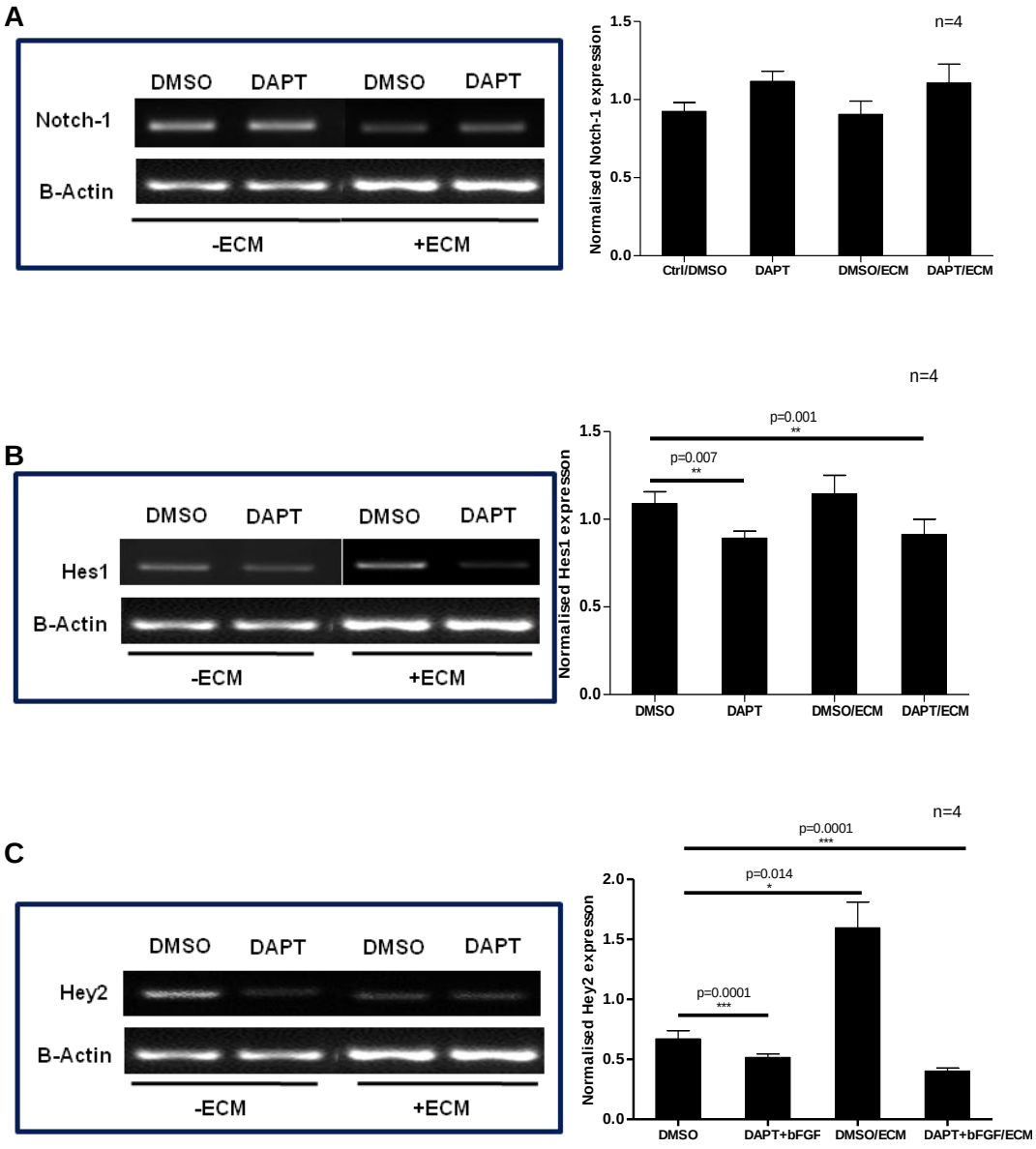

Figure 2.5: Expression of transcription factors of neural development by Müller stem cells, following Notch inhibition in the absence of bFGF. RT-PCR showing expression of genes involved in Notch signaling, specifically Notch-1, Hes1, and Hey2, following culture with DAPT for 7 days with or without ECM. A) Notch-1 remained unaltered following treatment with DAPT. Beta actin was used as the housekeeping gene to normalise gene expression levels. B) Treatment with DAPT induced decreased expression of Hes1 in the presence and absence of ECM. C) Hey2 expression levels decreased significantly with DAPT treatment in the absence of ECM, however a marked increase in its expression was observed in cell cultured without DAPT in the presence of ECM Gel images are representations of the expression of these factors, whilst histograms represent the mean ± SEM of 4 experiments.

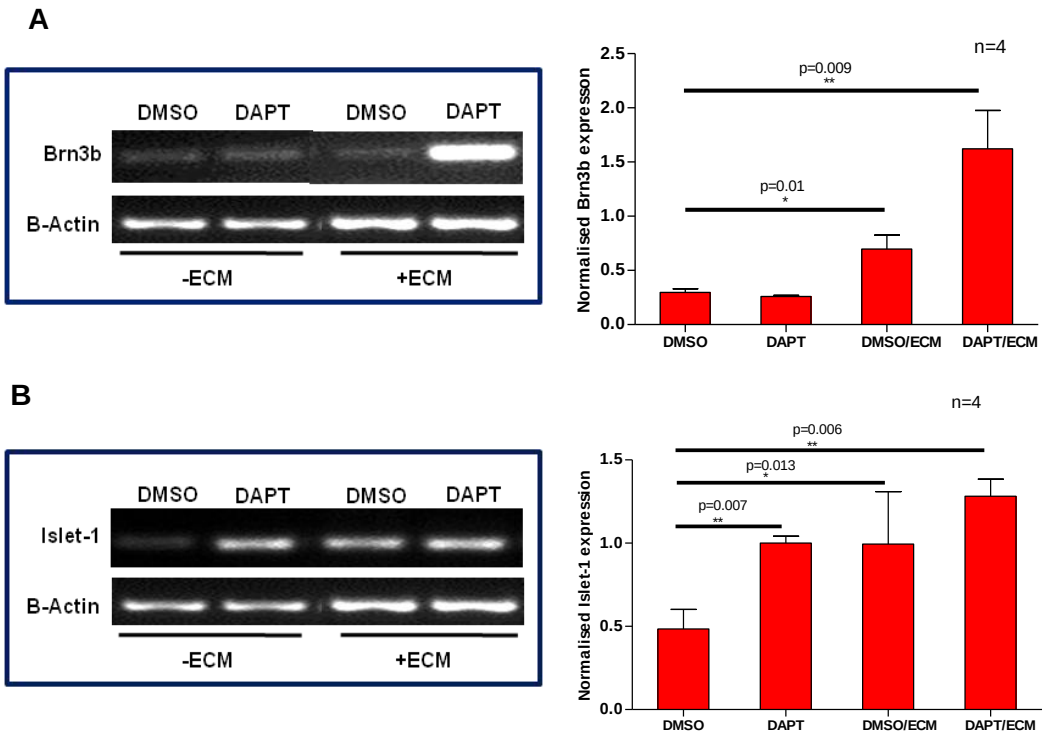

Figure 2.6: Markers of RGC precursors following Notch inhibition in Müller stem cells in the absence of bFGF. RT-PCR demonstrating the expression of Brn3b and Islet-1.Following Notch repression with DAPT after 7 days culture with or without ECM coatings. A) DAPT induced Brn3b to elevate significantly in the presence of ECM, although ECM coating also induced marked elevations of Brn3b expression. B) Treatment with DAPT induced an increase in mRNA expression of Islet-1 either in the presence and absence of ECM. Beta actin was used as the housekeeping gene to normalise gene expression levels. The results are the mean ± SEM of 4 experiments

the POU-domain family and serves as a neuronal transcription factor during the early stages of RGC development. Islet-1 is a LIM-homeodomain transcription factor and is thought to have a synergistic function with Brn3-b during the early stages of retinogenesis and RGC maturation (Mu et al., 2008). These factors were used to determine the effect of the Notch pathway on the development of RGC-derived Müller stem cells. Raised levels of Brn3b were only observed when cells were cultured in the presence of DAPT and ECM.

Following initial examination of Hes1 and Notch1 expression at the mRNA transcript level, western blotting and immunocytochemical analysis were performed on cell populations cultured with the Notch inhibitor DAPT. Protein preparations were made by lysis of cells cultured in the presence or absence of DAPT. Untreated cells showed elevated baseline expression of Notch (Figure 2.7B) and Hes1 (Figure 2.8B) proteins, as compared with treated cells. Cells cultured with the Notch inhibitor DAPT demonstrated depletion of Notch ICD whilst Hes1 expression was also decreased, although not significantly (Figure 2.8B). Immunocytochemistry depicted the localisation of both Hes1 and Notch within cell cultures. Untreated cells exhibited Notch and Hes1 localisation in the nuclear and cytoplasmic domains suggesting that Notch signalling pathway is active within these cell populations (Figure 2.7A and 2.8A). Treatment with DAPT resulted in decreased cellular expression of Notch (Figure 2.7A) and Hes1 (Figure 2.8A) in the nuclei of these cells. However, Notch remained within the cytoplasm and Hes1 continued to be located within the perinuclear domains, although its intensity appeared to decrease with DAPT treatment.

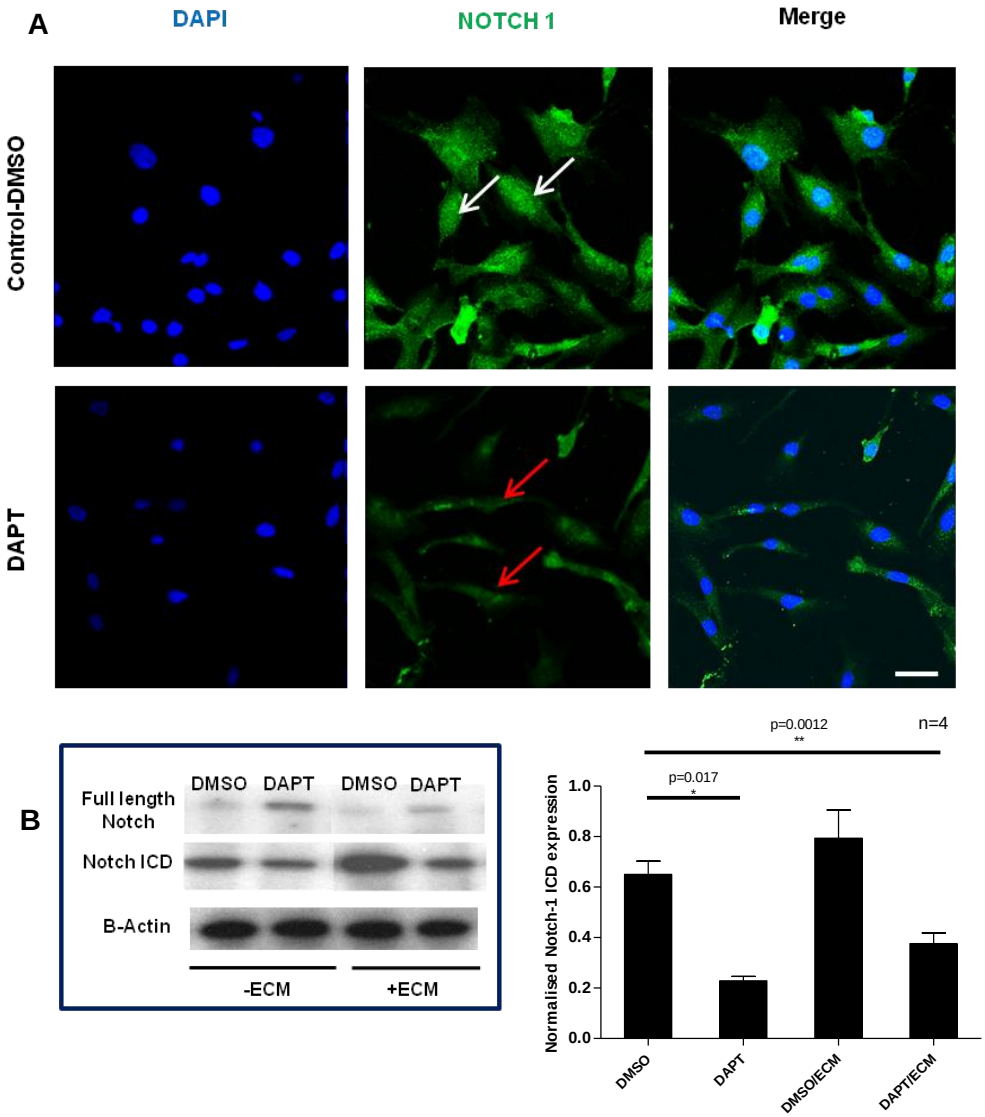

Figure 2.7: The effect of Notch inhibition on Notch-1 protein expression in Müller stem cells. (A) Immunostaining of control (untreated cells) for Notch-1 showed widespread intracellular localization of this factor within the cells. Staining was observed in both the nuclei (white arrows) and cytoplasm. Staining of cells treated with DAPT showed a decreased intracellular expression of this protein. Notch-1 expression within the perinuclear domains and nuclear regions diminished with DAPT treatment (red arrows). (B) Western blotting detected the presence of ICD within control and treated cells, although a lower quantity was found in DAPT treated cells, with or without ECM. The results are the mean ± SEM of 4 experiments. Scale bar=50µm.

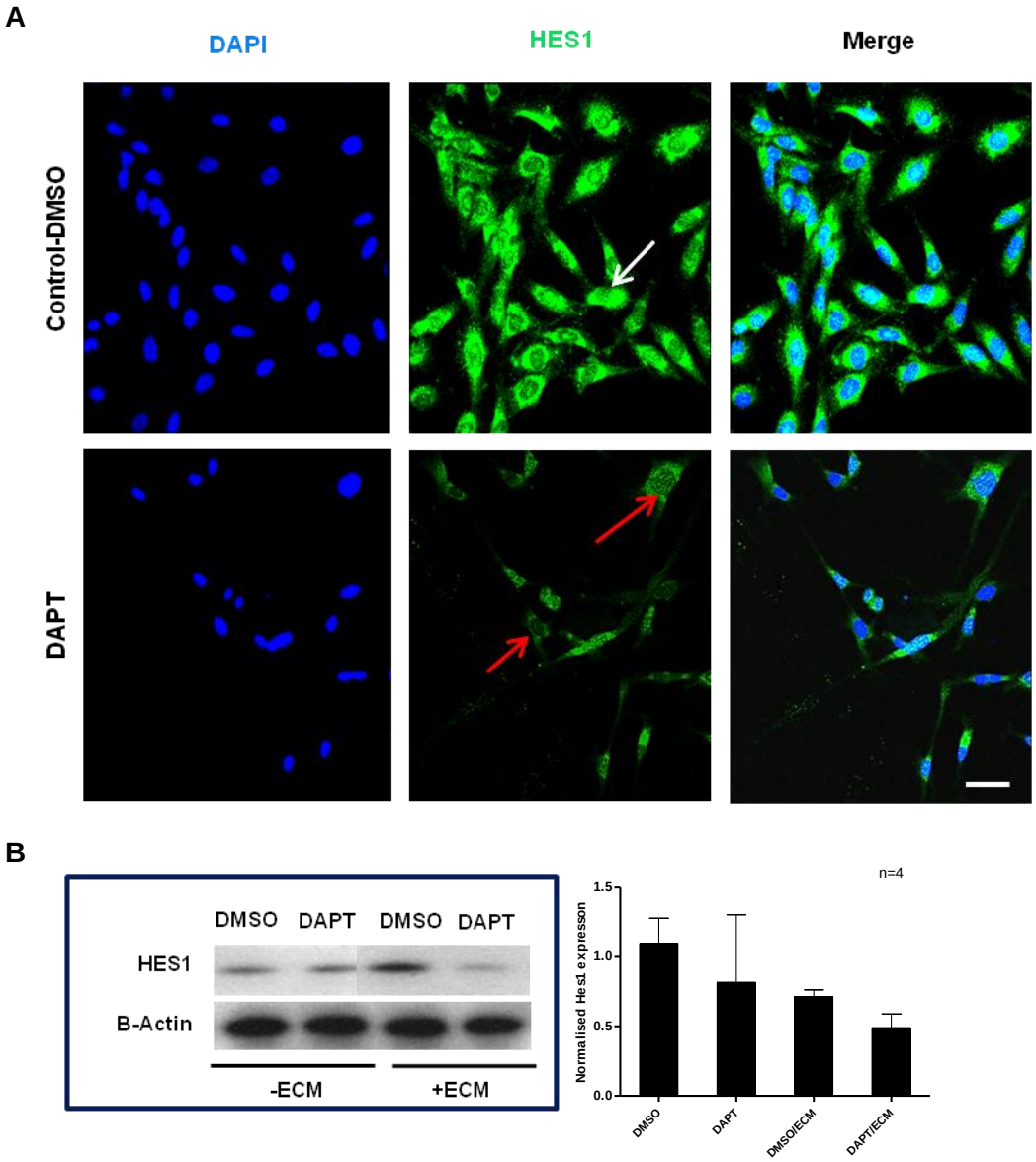

Figure 2.8: The effect of Notch inhibition on Hes1 protein expression in Müller stem cells. (A) Immunostaining of untreated cells with Hes1 antibody demonstrated the localization of the transcription factor within the perinuclear and nuclear domains of the cells (white arrow). However, staining of cells treated with DAPT showed a decreased cellular expression of this factor, there was a marked decrease in nuclear and perinuclear staining (red arrows). (B) Western blotting confirmed the trend of Hes1 depletion following Notch inhibition, although not significant. The results are the mean ± SEM of 4 experiments. Scale bar=50µm

2.3.2. The effect of Notch inhibition in Müller stem cells cultured in the presence of bFGF

Following culture of Müller stem cells on ECM with the addition of DAPT (50μM) and bFGF (20ng/ml), a RGC differentiation protocol previously developed in our laboratory, cells exhibited neurite outgrowth with primary and secondary branching of cellular projections as observed under light microscopy (Figure 2.9A). Measurement of the cellular projections demonstrated marked increase of neurite length in the presence of DAPT+bFGF in both the presence and absence of ECM (Figure 2.9B) indicative of a neural morphology and characteristic of *in vitro* differentiation. As previously seen with cells treated with DAPT in the absence of bFGF, cells cultured with this Notch inhibitor in the presence of bFGF did not exhibit significant changes in their mRNA expression of Notch. However, gene expression analysis demonstrated a significant decrease of Hes1 ($p<0.0001$ without ECM and $p<0.0002$ with ECM) and Hey2 transcripts in RNA samples taken from cells treated with DAPT and bFGF, in the presence or absence of ECM, as compared to untreated cells (Figure 2.10). This suggests that knock-down of Notch and its downstream effectors were evident, and that its signalling pathway was also altered. Markers that indicate the development of RGC precursors, increased following Notch inhibition in the presence of bFGF. Islet-1 increased with differentiating protocols in both the presence and absence of ECM coating (Figure 2.11B). However, the early RGC marker Brn3b increased significantly when treated cells were cultured on ECM coated flasks (Figure 2.11A).

Notch ICD protein expression markedly decreased with DAPT and bFGF treatment in the presence of ECM (Figure 2.12B). Hes1 protein levels also depleted significantly upon culture with DAPT and bFGF, in both the absence and presence of ECM (Figure 2.13B).

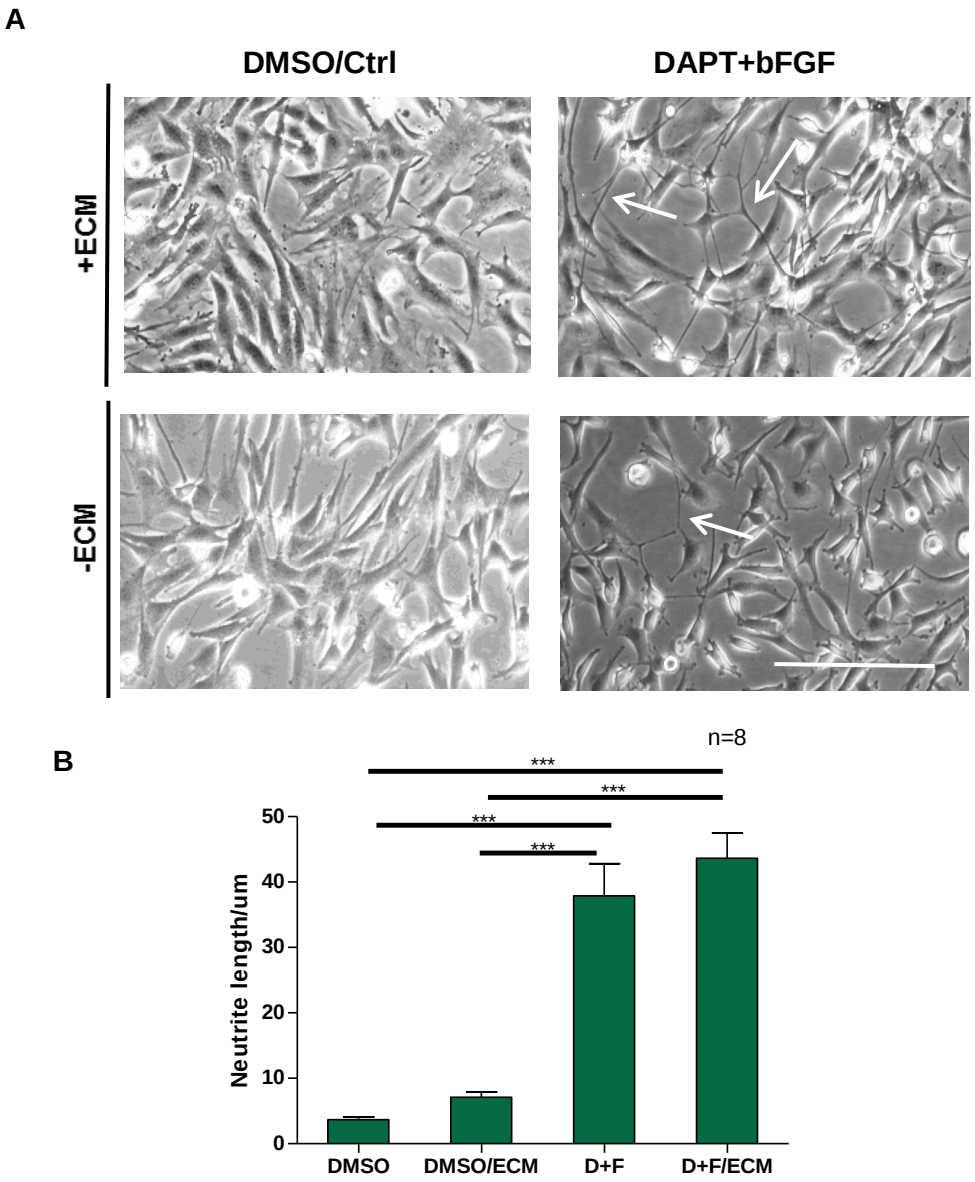

Figure 2.9: Effect of Notch inhibition following culture with bFGF on Müller stem cell morphology. Phase-contrast imaging of Müller stem cells cultured with and without ECM under control conditions (no treatment), in the presence of DMSO (vehicle), and in the presence of DAPT and bFGF. DAPT and bFGF treatment induced morphological changes, with the development of phase-bright nuclei and outgrowth of neurite-like structures (white arrow), suggestive of neural morphology. The combination of these two factors appeared to have a synergistic effect on neurite elongation. Freehand measurement of the cellular projections, using a calibrated image J scale enabled analysis of neurite length which was markedly increased in the presence of DAPT+bFGF in both the presence and absence of ECM. Scale bar=100µm

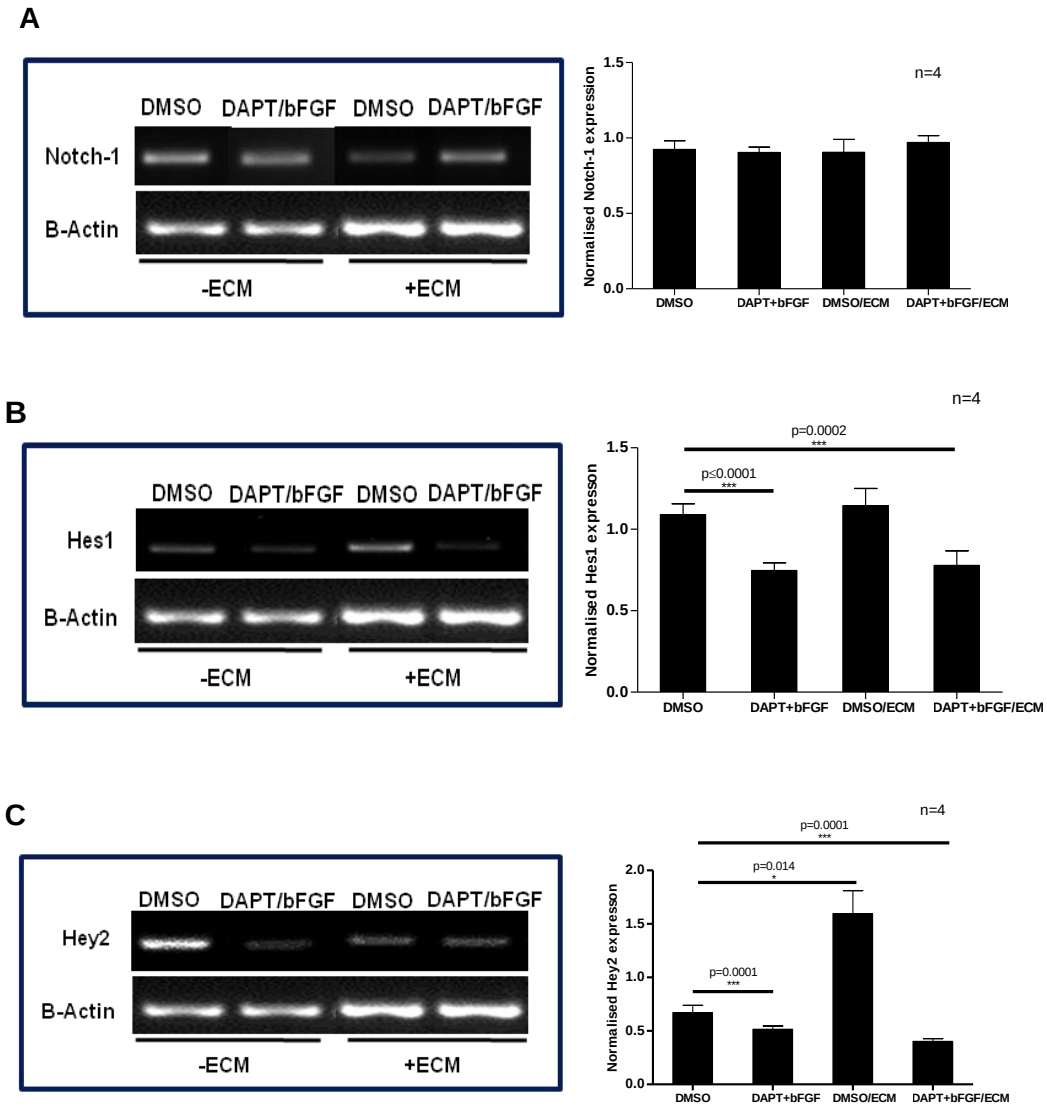

Figure 2.10: Transcription factors of neural development, following Notch inhibition in the presence of bFGF, in Müller stem cells. RT-PCR demonstrating the expression of genes involved in Notch signaling, specifically Notch-1, Hes1, and Hey2. This determined alterations in their expression profiling following Notch repression using DAPT and bFGF after 7 days culture, in the presence or absence of ECM coating. A) Notch-1 mRNA levels were not observed to change following cellular incubation with DAPT and bFGF, in the presence or absence of ECM. B) Hes1 was markedly reduced with DAPT and bFGF treatment in the presence and absence of ECM. C) Hey2 was also significantly reduced following treatment with DAPT and bFGF, with and without ECM. Beta actin was used as the housekeeping gene to normalise gene expression levels to. The results are the mean ± SEM of 4 experiments

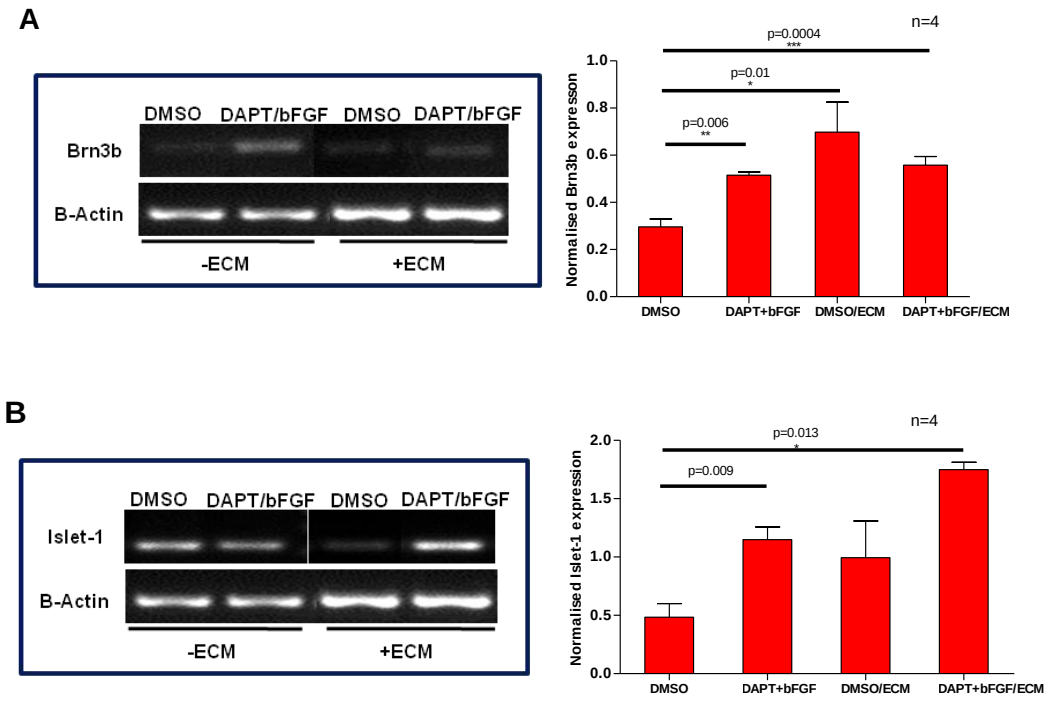

Figure 2.11: Markers of RGC precursors following Notch inhibition of Müller stem cells, cultured in the presence of bFGF. RT-PCR demonstrating the expression of genes associated with RGC precursor development, namely, Brn3b and Islet-1. Alteration in their expression was determined following Notch inhibition in the presence of bFGF after 7 days culture in the presence or absence of ECM. A) Treatment with DAPT and bFGF induced significant increase in Brn3b gene expression in the absence and presence of ECM. B) DAPT and bFGF also caused marked elevation in Islet-1 mRNA expression in both the absence and presence of ECM. Both markers showed increased expression with ECM coating alone, suggesting the importance of growth matrix for differentiation. Beta actin was used as the housekeeping gene to normalise gene expression levels

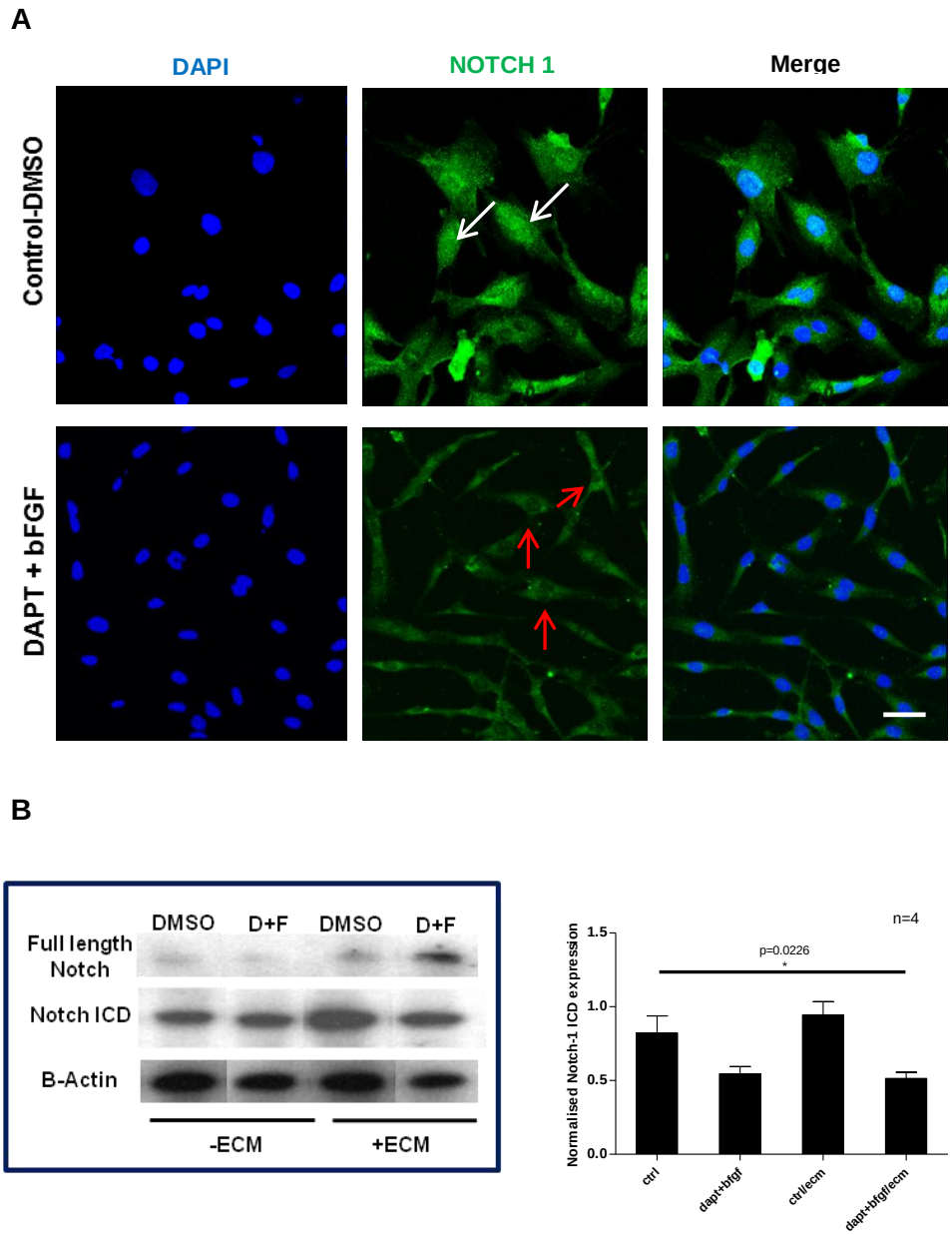

Figure 2.12: Expression of Notch-1 by Müller stem cells undergoing Notch signaling inhibition with DAPT, in the presence of bFGF. (A) Immunostaining of control (untreated cells) with Notch-1 antibody showed widespread intracellular localization within the cells. Staining was observed in both the nuclei (white arrows) and cytoplasm. However, staining of cells treated with DAPT and bFGF showed a decreased intracellular expression of this protein. Notch-1 expression within the perinuclear domains and nuclei diminished with treatment (red arrows). (B) Western blotting detected the presence of Notch ICD protein within control and treated cells, although a marginally lower quantity was found in cells treated with DAPT and bFGF, although not significant. However, a significant reduction in ICD expression was observed when cells were grown on ECM and DAPT+bFGF. The results are the mean ± SEM of 4 experiments.Scale bar=50um

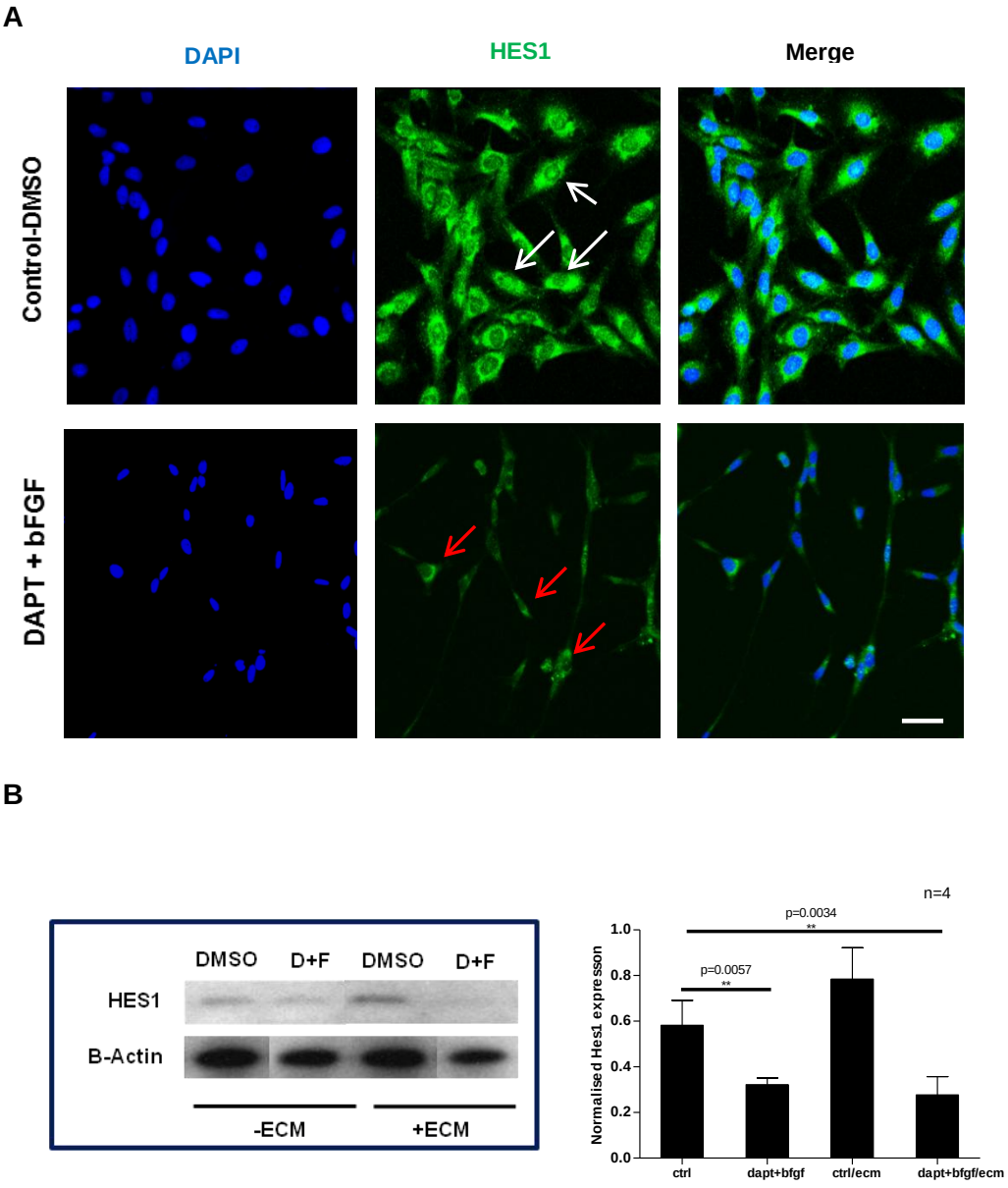

Figure 2.13: The effect of Notch inhibition on Hes1 protein expression by Müller stem cells undergoing Notch signaling repression in the presence of bFGF. (A) Immunostaining of untreated cells with Hes1 antibody demonstrated the localization of the Hes1 transcription factor within the perinuclear and nuclear domains of the cells (white arrow). However, staining of cells treated with DAPT and bFGF showed a decreased cellular expression of this factor. There was a marked decrease in nuclear and perinuclear staining (red arrows). (B) Western blotting confirmed depletion of Hes1 protein expression following Notch inhibition. A significant reduction in Hes1 expression was observed cells treated with DAPT and bFGF with or without ECM. The results are the mean ± SEM of 4 experiments. Scale bar=50µm

Immunocytochemical staining of DAPT and bFGF treated cells showed that the localisation of Notch was prominent in the cytosol (Figure 2.12A). This suggests that the cleavage and subsequent translocation of the Notch ICD has been arrested by DAPT, promoting differentiation. The localisation of Hes1 also proved to be modified. It was predominantly found within the perinuclear regions of treated cells, compared to the nuclear presence in untreated cells (Figure 2.13A). These observations suggest that DAPT and bFGF treatment led to translational repression of the Notch pathway and the promotion of differentiation.

2.3.3. Validation of Notch inhibition and differentiation protocols in various human Müller Stem Cell lines

In order to further validate the ability of Müller stem cells to differentiate into RGC following Notch downregulation, different cell lines were examined. The Müller stem cell lines 6387, 6391 and 6426 were cultured for 7 days, in the presence of ECM and DAPT ± bFGF. Screening of the three cell lines under non-differentiated and differentiated conditions confirmed the changes in Notch associated targets, as well as the emergence of RGC development using the above differentiation protocols. Confocal microscopy of the Müller cell line 6387 (Figure 2.14) demonstrated reduced levels of Hes1 staining following Notch inhibition either with or without bFGF. I addition, treatment with DAPT alone or with the addition of bFGF resulted in depleted levels of Hes1 mRNA (Figure 2.15B). Levels of mRNA coding for Notch did not change in cells cultured with DAPT in the presence or absence of bFGF (Figure 2.15A). However, the RGC marker Brn3b increased with DAPT treatment in the absence of bFGF, in the presence of bFGF its expression was not modified (Figure 2.15C). Islet-1 increased with Notch inhibition in the absence of bFGF, although its expression was not altered in the presence of both DAPT and bFGF (Figure 2.15D). presence of bFGF, reduced nuclear expression of Hes1 was also observed

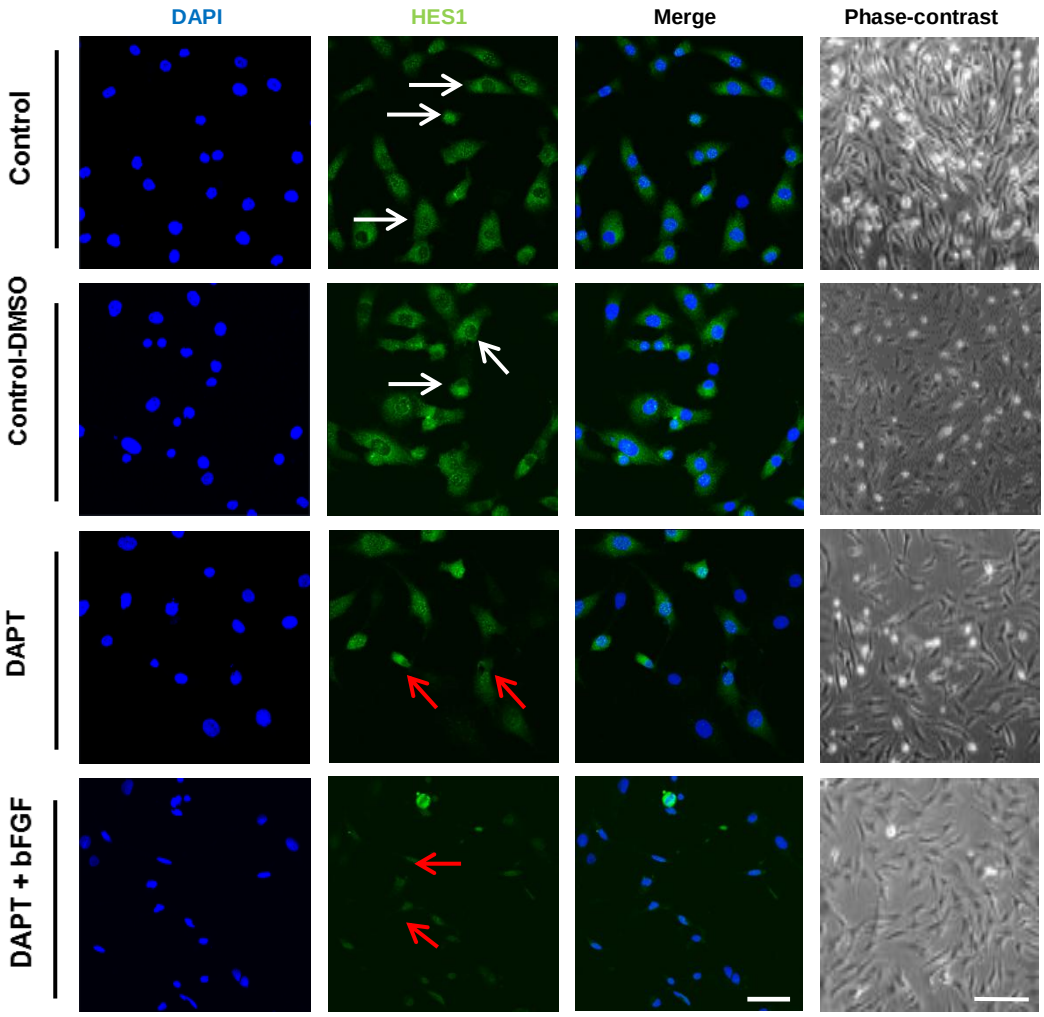

Figure 2.14: Effect of Notch inhibition upon Hes1 localisation in the 6387 Müller cell line. Confocal and phase-contrast imaging of the 6387 Müller cell line demonstrated changes in the morphological appearance and protein expression of Hes1. Following DAPT treatment in the presence and absence of bFGF phase-contrast showed morphological changes towards a neural phenotype. The extent of Notch activity is illustrated by a decrease in Hes1 staining of treated cells, although its presence remained located around and in the nucleus (confocal red arrows). Untreated cells had intense perinuclear and nuclear staining (confocal white arrows). Confocal scale bar=50µm. Phase-contrast scale bar=100µm

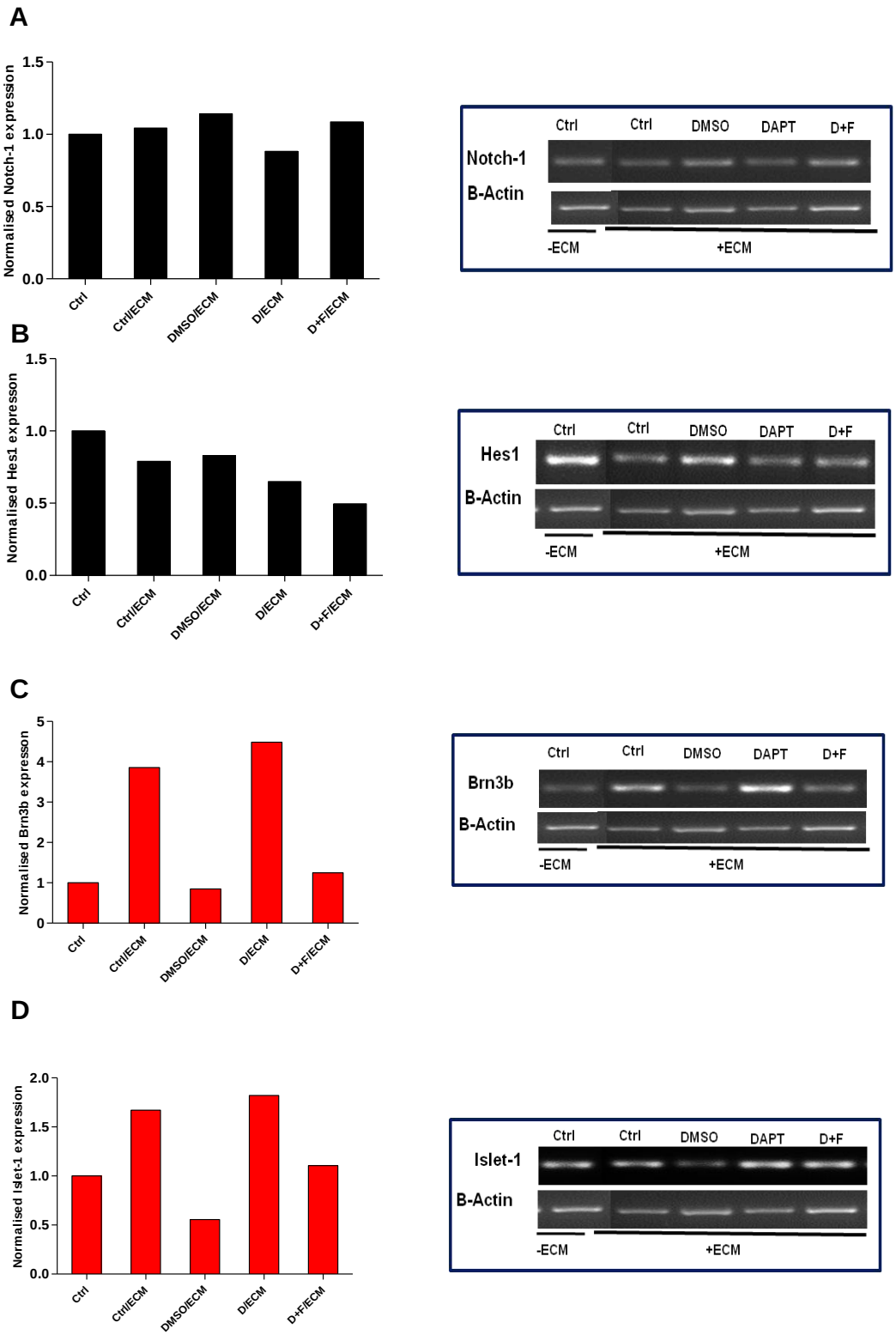

Figure 2.15: Notch inhibition in the 6387 Müller cell line cultured in the presence and absence of bFGF. RT-PCR was performed to examine the gene expression in the Muller cell line 6387 treated with DAPT in the presence and absence of bFGF, as compared with untreated cultures. A) Notch-1 expression was unaltered with treatment. B) Hes1 decreased marginally in cells cultured with DAPT in both the presence and absence of bFGF. C) Brn3b increased in cells treated with DAPT alone. D) Islet-1 expression increased following culture with DAPT alone. n=1

Immunocytochemical analysis of the Müller cell line 6391 showed reduced amounts of Hes1 in cells treated with DAPT in either the absence or presence of ECM (Figure 2.16). Cells cultured with DAPT either in the presence of bFGF showed a decrease in Notch mRNA, although DAPT alone did not alter the expression of Notch mRNA expression (Figure 2.17A). Similar to that seen with other cell lines, mRNA expression of Hes1 decreased with DAPT in presence or absence of bFGF (Figure 2.17B). The RGC maturation marker Brn3b increased in cells cultured on ECM under all culture conditions, however the addition of DAPT and bFGF did not change its expression, as compared to untreated cells (Figure 2.17C). Islet-1 expression remained unaltered with DAPT and bFGF treatment, however DAPT alone increased its expression (Figure 2.17D).

Finally, confocal imaging of the Müller cell line 6426 demonstrated reduced intensity of Hes1 antibody staining following treatment with DAPT in both the presence and absence of bFGF (Figure 2.18). Notch mRNA expression was diminished in the presence of DAPT alone (Figure 2.19A) whilst Hes1 expression remained unaltered with treatment with DAPT with bFGF (Figure 2.19B). The expression of Brn3b decreased with DAPT in the presence and absence of bFGF (Figure2.19C) and islet-1 decreased in cells treated with DAPT alone (Figure 2.19D). Validation of mature RGC gene expression was not found in this single experiment. Morphological alterations of neurite outgrowths were observed with Notch inhibition with DAPT and RGC protocols by confocal and phase-contrast imaging for all three cell lines.

2.3.4. MicroRNA Expression Profiles in Müller Stem Cells

Following the *in vitro* validation of RGC differentiation protocols, microarray analysis was conducted on total cellular RNA samples obtained from Müller stem cells cultured in the presence or absence of RGC differentiation factors. Agilent miRNA probe slides (two in total) were used to detect differences in miRNA profiles between Müller stem cells cultured under differentiating and

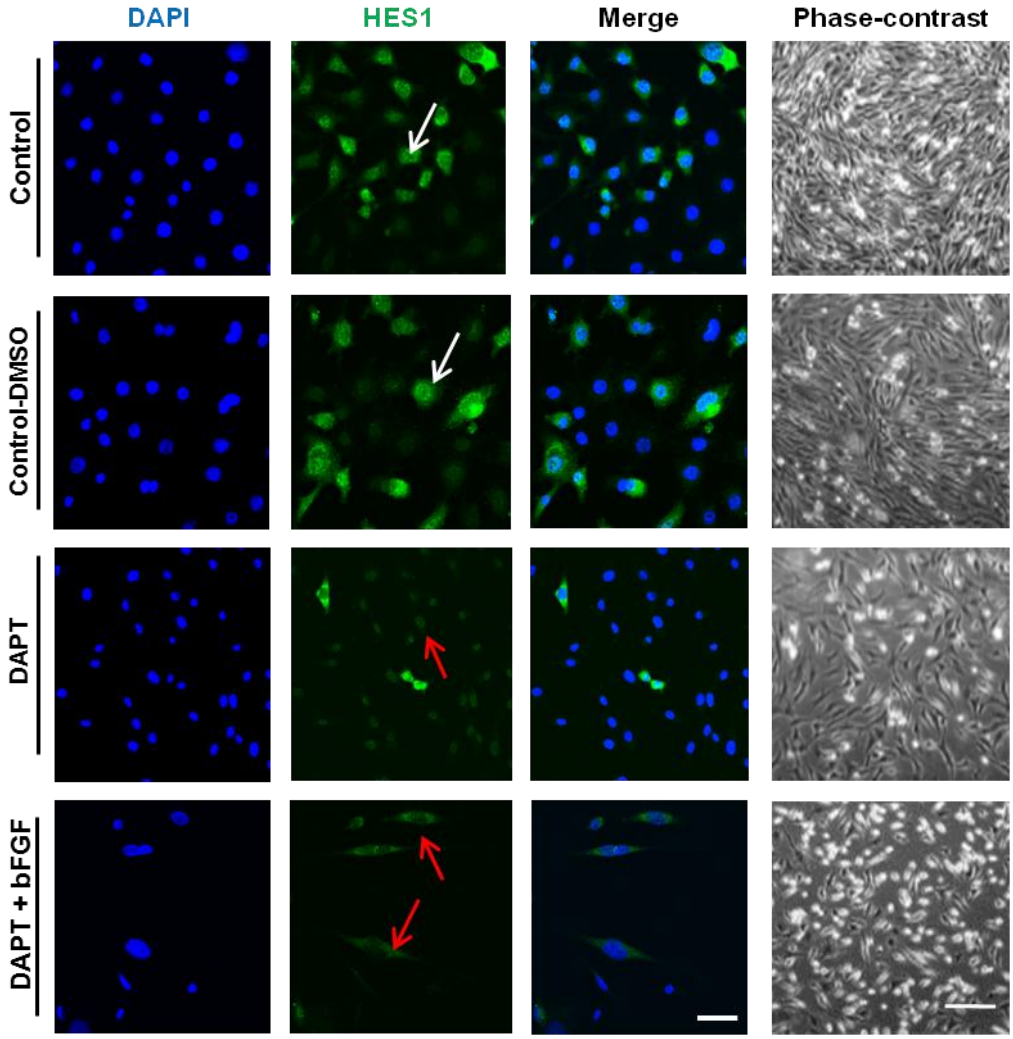

Figure 2.16: Effect of Notch inhibition upon Hes1 localisation in the 6391 Müller cell line. Confocal and phase-contrast imaging of the 6391 Müller cell line demonstrated changes in the morphological appearance and protein expression of Hes1. Following DAPT treatment in the presence and absence of bFGF phase-contrast showed morphological changes towards a neural phenotype. The extent of Notch activity is illustrated by a decrease in Hes1 staining of treated cells, although its presence remained located around and in the nucleus (confocal red arrows). Untreated cells had intense perinuclear and nuclear staining (confocal white arrows). Confocal scale bar=50µm, Phase-contrast scale bar=100µm

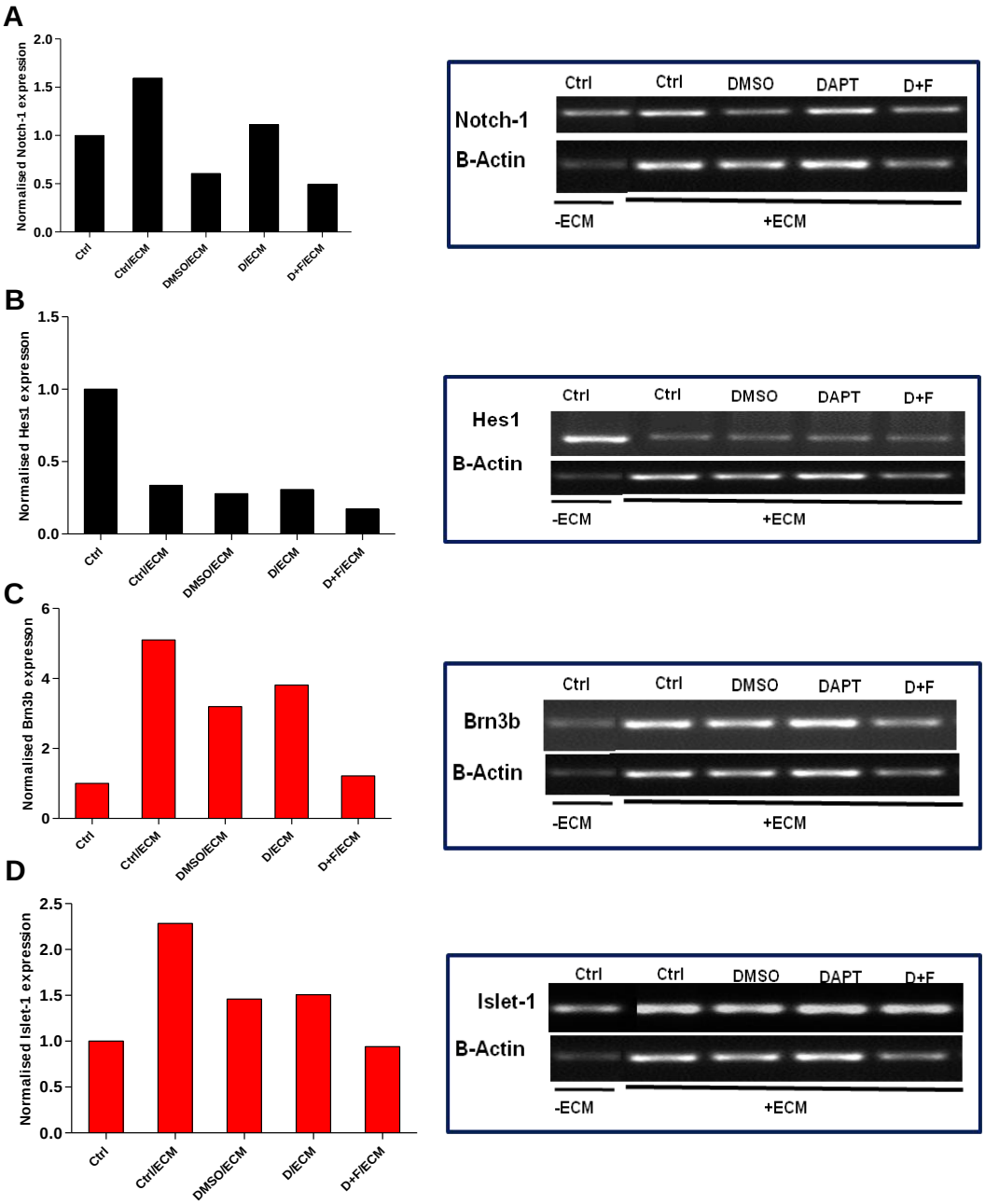

Figure 2.17: Notch inhibition in the 6391 Müller cell line cultured in the presence and absence of bFGF. RT-PCR was performed to examine the gene expression in the Muller cell line 6391 treated with DAPT in the presence and absence of bFGF, as compared with untreated cultures. A) Notch-1 expression decreased in cells treated with DAPT in the presence and absence of bFGF. B) Hes1 decreased with DAPT in both the presence and absence of bFGF, as well as with ECM alone. C) Brn3b expression increased with DAPT treatment alone. D) Islet-1 expression increased following culture with DAPT in the absence of bFGF. n=1

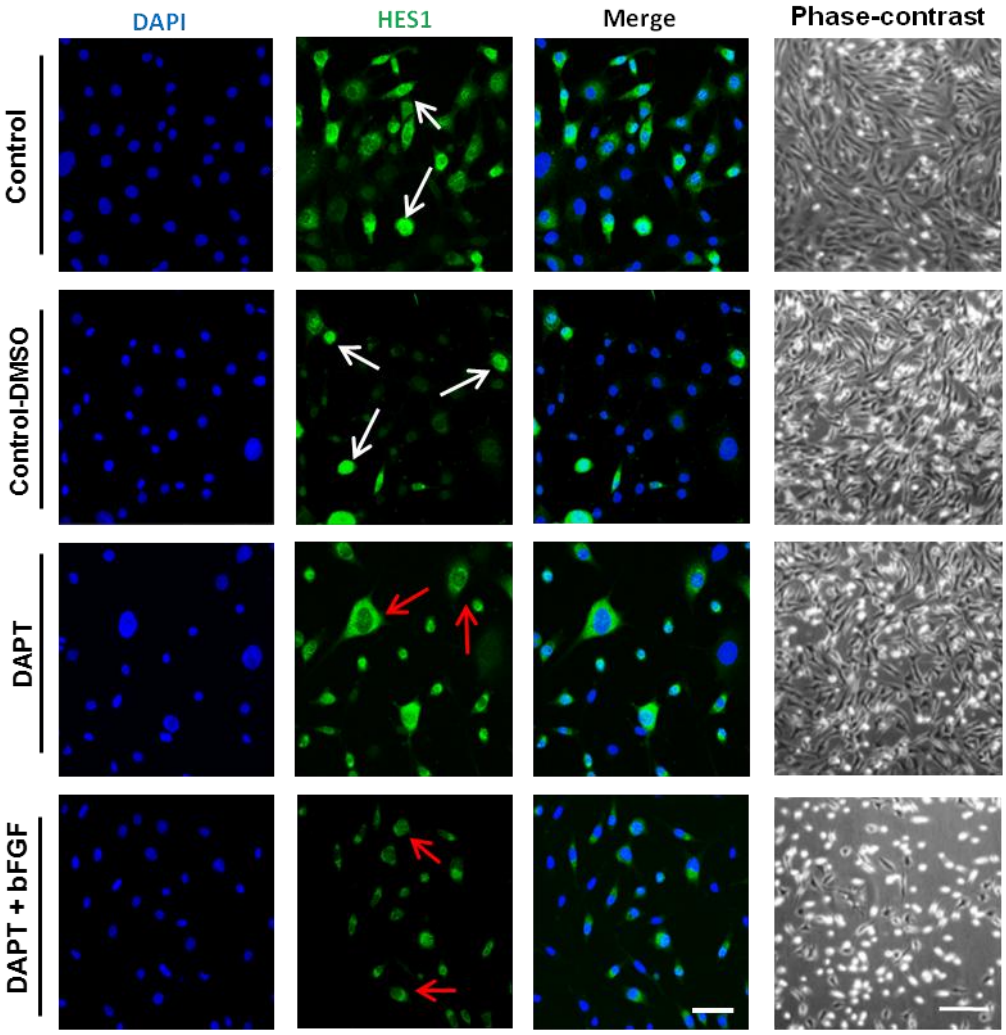

Figure 2.18: Effect of Notch inhibition upon Hes1 localisation in the 6426 Müller cell line. Confocal and phase-contrast imaging of the 6426 Müller cell line demonstrated changes in the morphological appearance and protein expression of Hes1. Following DAPT treatment in the presence and absence of bFGF phase-contrast showed morphological changes towards a neural phenotype. The extent of Notch activity is illustrated by a decrease in Hes1 staining of treated cells, although its presence remained located around and in the nucleus (confocal red arrows). Untreated cells had intense perinuclear and nuclear staining (confocal white arrows). Confocal scale bar=50µm, Phase-contrast scale bar=100µm

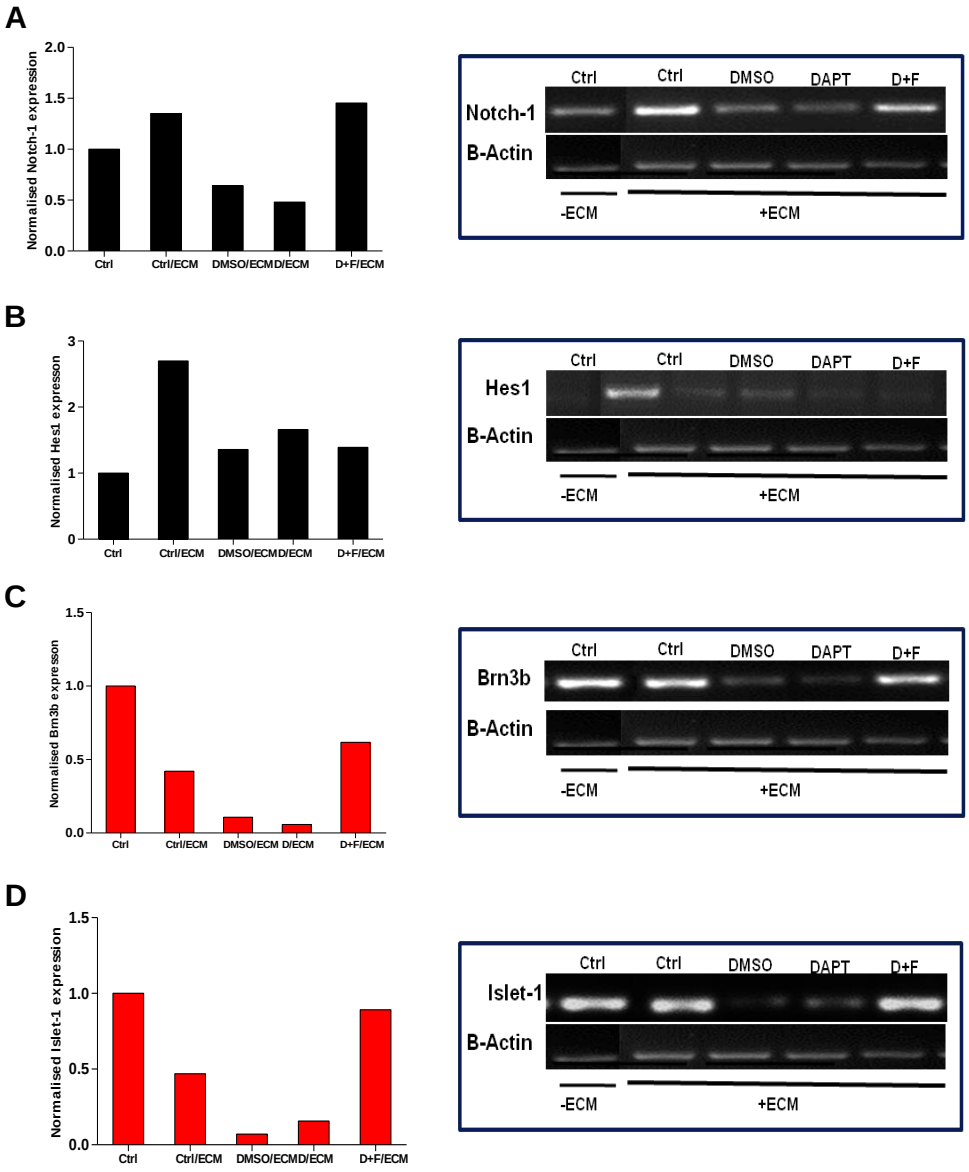

Figure 2.19: Notch inhibition in the 6426 Müller cell line cultured in the presence and absence of bFGF. RT-PCR was performed to examine the gene expression in the Müller cell line 6426 treated with DAPT in the presence and absence of bFGF, as compared with untreated cultures. A) Notch-1 expression decreased in cells treated with DAPT and marginally increased with the addition of bFGF. B) Hes1 increased with DAPT treatment in both the presence and absence of bFGF. C) Brn3b expression increased with DAPT treatment alone. D) Islet-1 expression increased following culture with DAPT in the presence of bFGF. n=1

untreated conditions. The quality of RNA samples collected and the robustness of the isolation process were assessed using an Agilent 2100 bioanalyzer (Agilent Technologies, UK) which gave a quality read out of 10/10 (Figure 2.20). The bioanalyser determined the degree of RNA degradation, summating and qualifying the different lengths of RNA. It distinguished the ribosomal, transfer, messenger and micro RNA amounts within the samples. This confirmed the quality of the miRNA within the samples and permitted yield efficient probing during the array analysis.

2.3.4.1. Expression of microRNA by Müller stem cells undergoing Notch inhibition in the absence of bFGF

The study involved comparing the expression of miRNA levels within Müller stem cell populations cultured on ECM in the presence of DAPT and untreated populations of Müller stem cells. The samples were studied for array quality to assure the array procedures produced comprehensive results, in order to infer from true representative data. A quality control heat map was produced to determine the robustness of the array procedure (Figure 2.21). The map shows details of the miRNA expression by cells cultured in the absence of ECM and in the presence of DMSO or on ECM in the presence of DAPT. The scale illustrates the relationship between the two separate treatments, red indicates a low level of correlation whilst yellow indicates a high level. The map demonstrates positive correlation between Müller populations cultured under the same treatment, whilst showing low levels of correlation within cultures grown under different conditions. This is indicative of the consistency of miRNA prevalence in the different culture groups, as well as the robustness of the processing procedures. The microarray heat map for the Müller populations gave an overview of the miRNAs upregulated following DAPT treatment (Figure 2.22). For each miRNA, the yellow colour indicates miRNAs with high expression; the blue

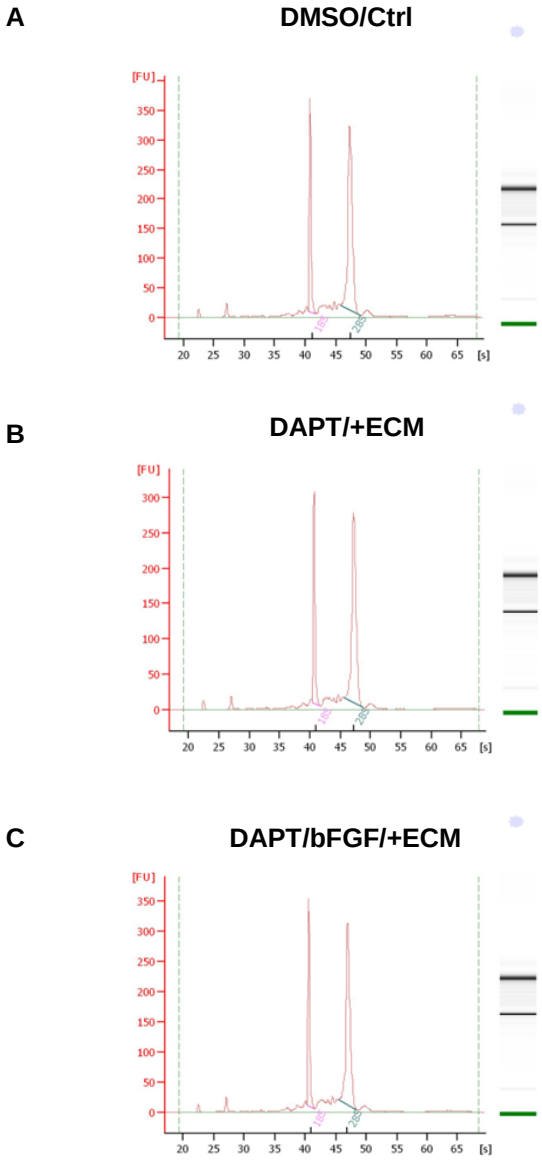

Figure 2.20: Quality Control of RNA samples: Examination of the total RNA was performed using the Agilent 2100 Bioanalyzer prior to labelling and hybridisation. The results of the analysis are displayed for the three experimental conditions, in the form of a gel image and electropherograms. Total RNA run on a denaturing agarose gel shows two distinct ribosomal peaks corresponding to the 18S (labelled pink) and 28S (labelled green) eukaryotic RNA. There are also smaller distinct peaks signifying the messenger and short sequence (micro) RNA. The Agilent 2100 expert software calculates a RNA Integrity Number (RIN). The readouts for (A) DMSO control, (B) DAPT and (C) DAPT with bFGF in the presence of ECM indicate stable RNA with high integrity, lacking molecular degradation. Samples were given RIN values of 10/10.

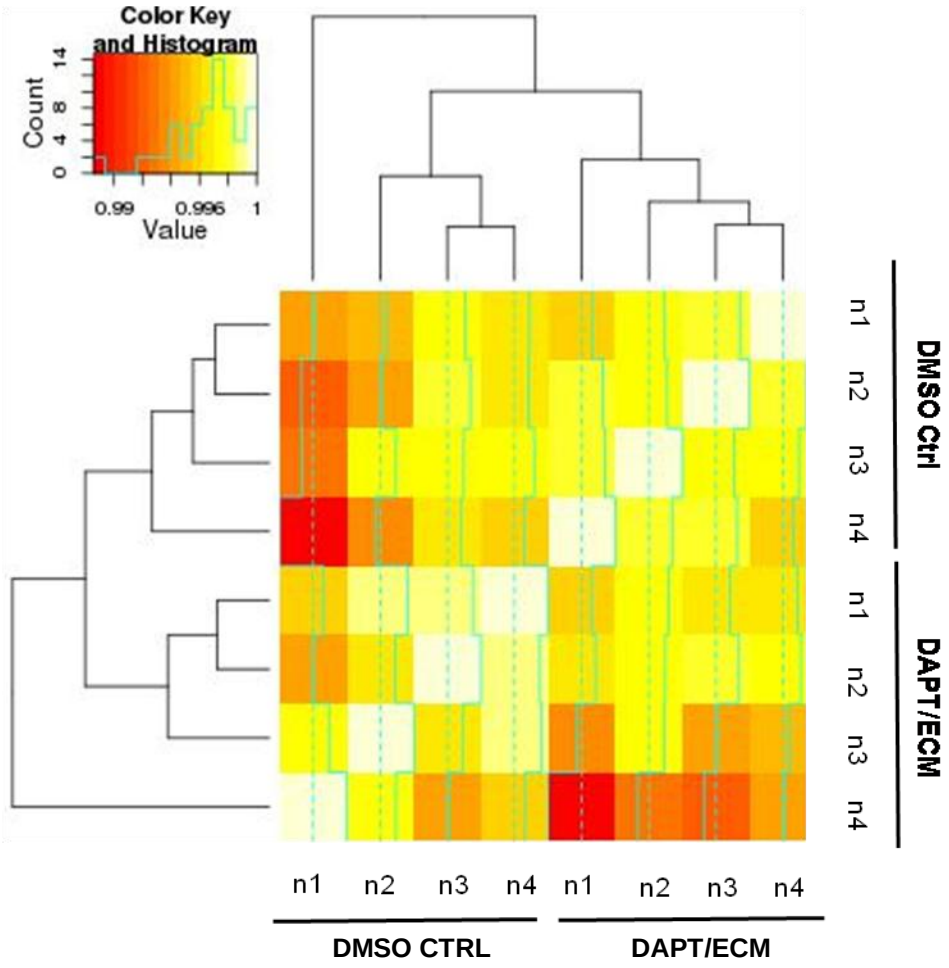

Figure 2.21: Quality control microarray heat map of Müller stem cells undergoing Notch inhibition. Each column represents microRNA isolated from Müller stem cells grown in the presence and absence of Notch inhibition. The map illustrates the association between treated and untreated control specimens, as well as the correlation between the two groups Yellow indicates strong correlation whilst red signifies a low correlation, n=4

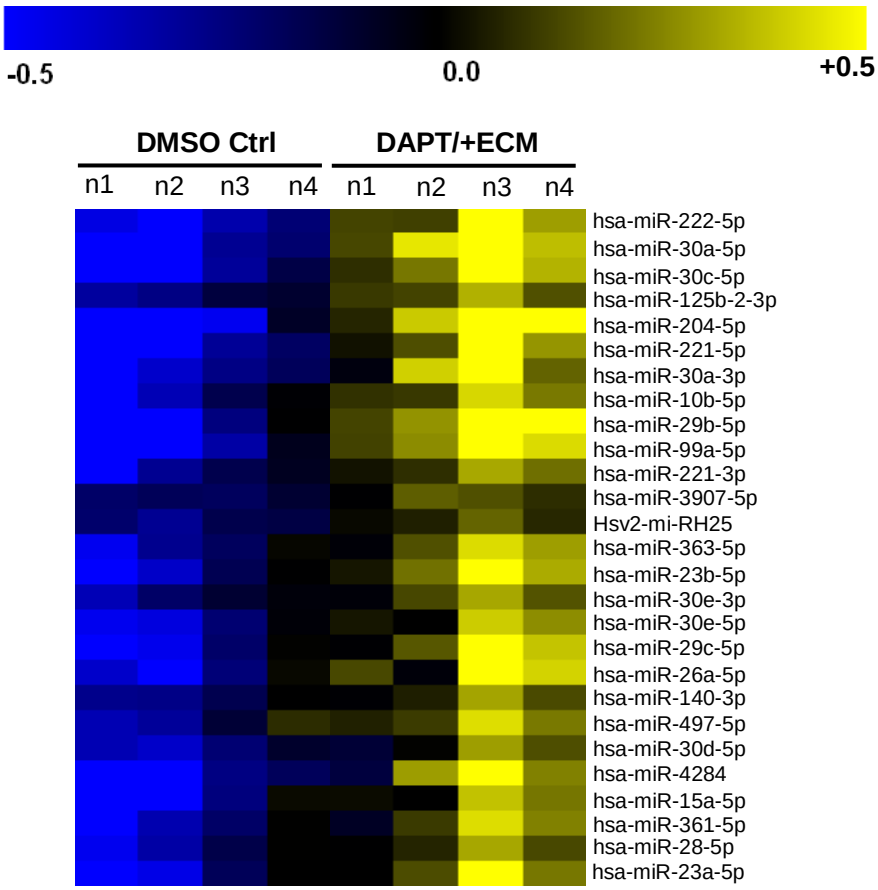

Figure 2.22: miRNA profiles of Müller stem cells undergoing Notch inhibition. Hierarchical clustering analysis was performed on miRNAs, isolated from Müller stem cells cultured in the presence or absence of ECM and DAPT. miRNAs are listed in abundance on the right hand side of the cluster, indicating the quantities of mature miRNA transcripts detected under both differentiating and untreated conditions. For each miRNA probe, data was median-centred, with the highest intensities in yellow. Scale= $\log_2$, n=4.

colour denotes miRNAs with low expression. Hierarchical clustering analysis identified the altered expression abundances of 27 different miRNAs following Notch inhibition. These miRNAs had significantly altered expression profiles between differentiating and untreated Müller populations. The data demonstrates large percentage increases that ranged from 21% to 107% (Table 2.1) following Notch inhibition with ECM treatment. The largest amplification induced by DAPT treatment was seen in the hsa-miR-204 and hsa-miR-30a levels, out of the all miRNAs detected. Figure 2.23 illustrates the relationship between inhibition of the Notch pathway in the presence of ECM coating, and the significant upregulation of miRNAs. The graphical representation of the top 27 transcripts found highlights the percentage increments within the miRNAs screened.

2.3.4.2. Expression of microRNA by Müller stem cells undergoing Notch inhibition in the presence of bFGF

The miRNA profile following treatment with DAPT to induce Notch inhibition in the presence of bFGF and ECM was also determined by microarray analysis. Quality of the array was assessed and determined the robustness and consistency of the data gathered (Figure 2.24). The quality control heat map indicated a strong correlation between Müller stem cells treated under the same culture regimes, whilst low correlation was observed between different treatment populations, confirming the efficiency of the array procedure, as well as the consistency of the results collated. Hierarchal clustering was performed and identified the enriched miRNAs generated by RGC differentiated cells as compared with untreated populations. This study identified 22 altered miRNA expression profiles and provided an overview of the miRNAs elevated with differentiation treatment (Figure 2.25). Examination of the percentage change of miRNAs enriched following treatment showed that DAPT alone caused hsa-miR-204 to increase by

Ascension number	miRNA ID	Percentage Change (%)	P-value
MIMAT0000265	hsa-miR-204-5p	107.81	0.023843
MIMAT0000087	hsa-miR-30a-5p	89.35	0.023843
MI0015893	hsa-miR-4284	83.06	0.043483
MIMAT0004514	hsa-miR-29b-5p	77.51	0.025284
MIMAT0000097	hsa-miR-99a-5p	72.89	0.025284
MIMAT0000244	hsa-miR-30c-5p	72.37	0.023843
MIMAT0004568	hsa-miR-221-5p	67.59	0.024982
MIMAT0000088	hsa-miR-30a-3p	62.70	0.025284
MIMAT0004569	hsa-miR-222-5p	58.52	0.015346
MIMAT0004587	hsa-miR-23b-5p	57.62	0.035565
MIMAT0004673	hsa-miR-29c-5p	55.93	0.043295
MIMAT0004496	hsa-miR-23a-5p	55.53	0.048249
MIMAT0000082	hsa-miR-26a-5p	47.52	0.043295
MIMAT0000068	hsa-miR-15a-5p	43.74	0.043483
MIMAT0000254	hsa-miR-10b-5p	41.57	0.025284
MIMAT0000692	hsa-miR-30e-5p	38.81	0.039297
MIMAT0000703	hsa-miR-361-5p	37.74	0.043483
MIMAT0003385	hsa-miR-363-5p	37.32	0.035565
MIMAT0004568	hsa-miR-221-3p	35.10	0.027823
MIMAT0002820	hsa-miR-497-5p	31.05	0.043295
MIMAT0004603	hsa-miR-125b-2-3p	30.84	0.023843
MIMAT0000085	hsa-miR-28-5p	29.69	0.043483
MIMAT0000245	hsa-miR-30d-5p	28.51	0.043483
MIMAT0000693	hsa-miR-30e-3p	25.50	0.039297
MIMAT0000431	hsa-miR-140-3p	23.99	0.043295
MI0013907	hsv2-miR-H25	22.047	0.034151
MI0016410	hsa-miR-3907-5p	21.03	0.028681

Table 2.1: List of miRNAs upregulated in Müller stem cells undergoing Notch inhibition. Expression is presented as percentage change in cells treated with DAPT, compared to control cultures. miRNAs are listed in ascending order, accession numbers taken from www.miRBase.org, n=4.

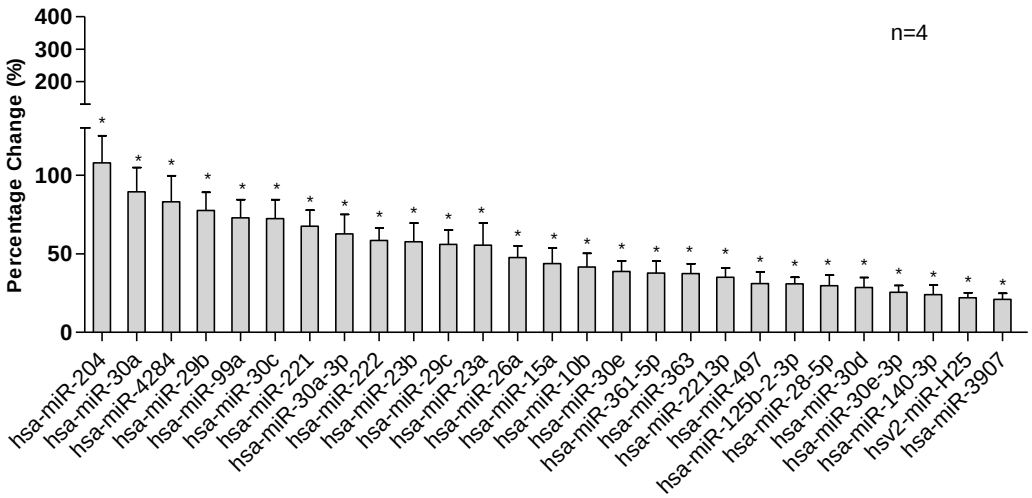

Figure 2.23: The miRNA expression levels in Müller stem cells undergoing Notch inhibition in the presence of ECM, as determined by microarray analysis. Graphical depiction of the significantly upregulated miRNAs compared to untreated Müller stem cell cultures, following Notch inhibition with DAPT with comparison to control cell culture. miRNAs are organised in ascending order, left to right. n=4 ***p<0.001 **p<0.01; *p<0.05

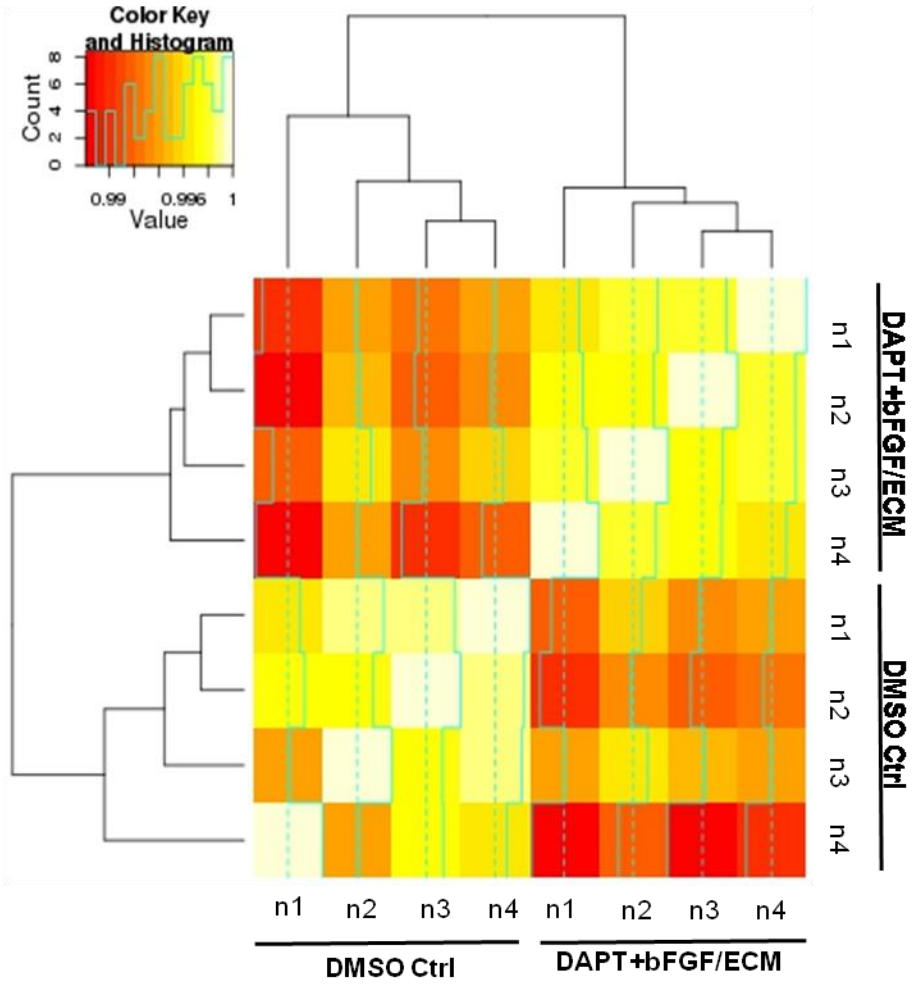

Figure 2.24: Quality control microarray heat map of Müller stem cells undergoing Notch inhibition in the presence of bFGF. Each column represents microRNA isolated from Müller stem cells grown in the presence or absence of Notch inhibitor with bFGF. The map illustrates the association between treated and untreated control specimens, as well as the correlation within the two groups. Yellow indicates strong correlation whilst red signifies low correlation. n=4

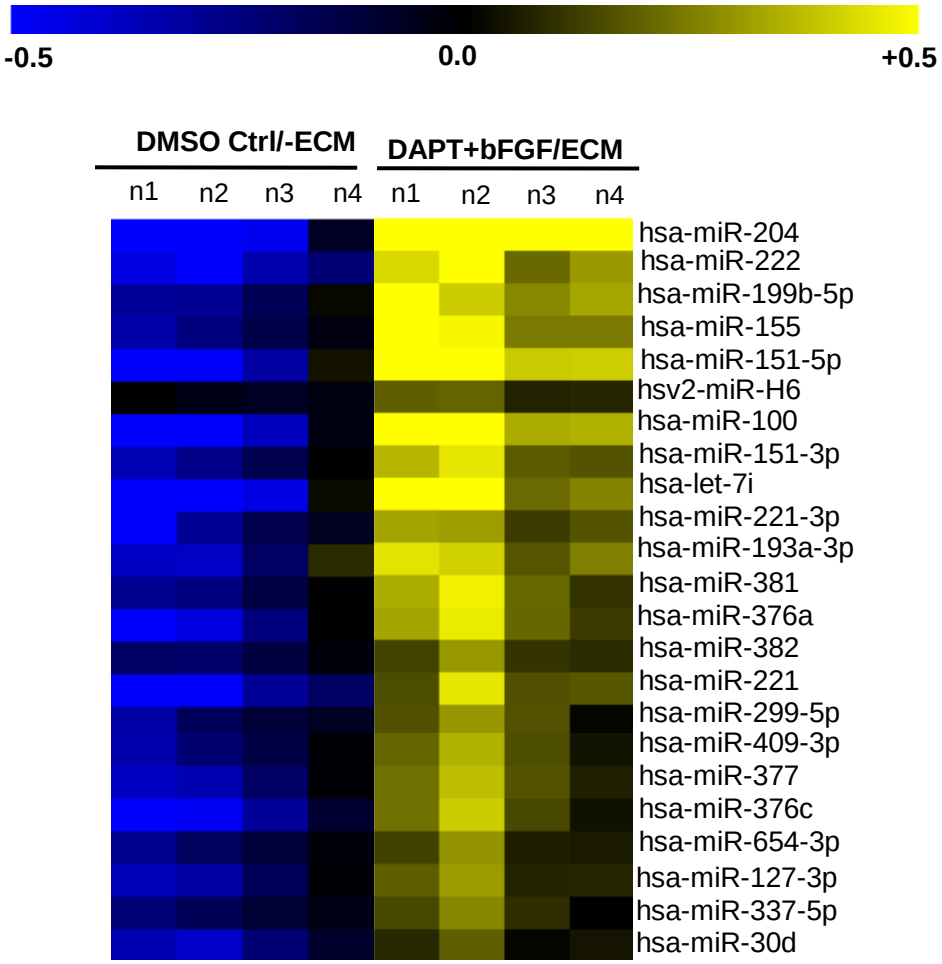

Figure 2.25: miRNA profiles of Müller stem cells following Notch inhibition. Hierarchical clustering analysis was performed on miRNAs, isolated from Müller stem cells cultured in the presence and absence of DAPT and bFGF. microRNAs are listed in abundance on the right hand side of the cluster, indicating the quantities of mature miRNA transcripts detected under both treated and untreated conditions. For each miRNA probe, data was median-centred, with the highest intensities in yellow. Scale= log2, n=4.

Ascension number	miRNA ID	Percentage Change (%)	P-value
MIMAT0000265	hsa-miR-204-5p	274.13	0.000287
MIMAT0000098	hsa-miR-100-5p	114.99	0.0053273
MI0000434	hsa-let-7i	106.45	0.0092618
MIMAT0004697	hsa-miR-151-5p	106.24	0.0037050
MIMAT0004569	hsa-miR-222-5p	70.14	0.0018665
MIMAT0004568	hsa-miR-221-5p	66.37	0.0164166
MIMAT0022861	hsa-miR-376c-5p	55.43	0.0289856
MIMAT0000646	hsa-miR-155-5p	55.32	0.003705
MIMAT0000263	hsa-miR-199b-5p	54.77	0.0023067
MIMAT0003386	hsa-miR-376a-5p	53.81	0.0142089
MIMAT0000459	hsa-miR-193a-3p	48.37	0.0108388
MIMAT0004568	hsa-miR-221-3p	42.72	0.0108083
MIMAT0000757	hsa-miR-151-3p	41.84	0.0078666
MIMAT0022862	hsa-miR-381-5p	38.13	0.0117819
MIMAT0004689	hsa-miR-377-5p	38.03	0.0249183
MIMAT0000446	hsa-miR-127-3p	31.52	0.0307239
MIMAT0001639	hsa-miR-409-3p	30.11	0.0234527
MIMAT0000245	hsa-miR-30d-5p	28.01	0.0473656
MIMAT0002890	hsa-miR-299-5p	26.41	0.0222157
MIMAT0000737	hsa-miR-382-5p	23.28	0.0142089
MIMAT0004814	hsa-miR-654-3p	22.63	0.0297285
MIMAT0004695	hsa-miR-337-5p	20.58	0.0473656
MI0013907	Hsv2-miR-H25	12.763	0.034151

Table 2.2: List of miRNAupregulated in Müller stem cells undergoing Notch inhibition in the presence of bFGF. Expression is presented as percentage changes in cells treated with DAPT and bFGF, compared to untreated DMSO cultures. miRNAs are listed in ascending order alongside their respective p values. Accession numbers were taken from miRBase.org, n=4.

107%, whilst the addition of bFGF increased the levels of hsa-miR-204 by 257% (Table 2.2). Illustration of the percentage changes, graphically, demonstrates the alteration within the miRNA profiles when ganglion maturation is favoured (Figure 2.26). These results have highlighted some potential targets that may contribute to developing protocols for RGC maturation of adult Müller stem cells, both *in vitro* and *in vivo*. The miRNAs enhanced using the RGC differentiation protocol included five miRNAs that were significantly upregulated in both conditions (Figure 2.27). These miRNAs included hsa-miR-204, hsa-miR-221, has-miR-222, hsa-221* and hsa-30d.

Notably these were highly expressed under both conditions, their differences between the treatment with DAPT in the presence or absence of bFGF was not significant and demonstrated only a marginal decline with the addition of bFGF, with exception to hsa-miR-204 which doubled in its expression (Figure 2.28).

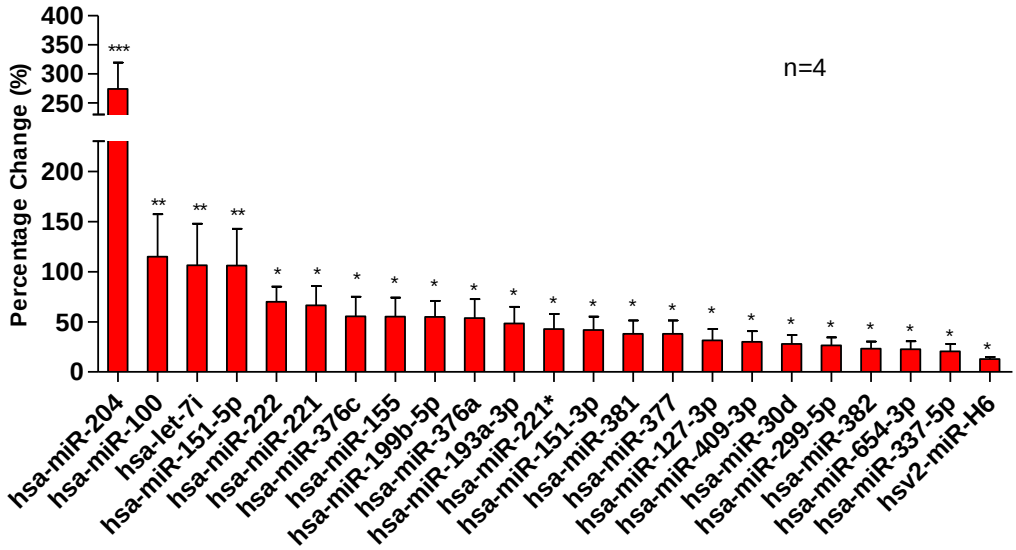

Figure 2.26: The miRNA expression levels in Müller stem cells undergoing Notch inhibition, following microarray analysis. Graphical depiction of the miRNAs that elevated significantly as compared with untreated Müller stem cells, following Notch inhibition with DAPT in the presence of bFGF. In ascending order, left to right. n=4 ***p<0.001 **p<0.01; *p<0.05

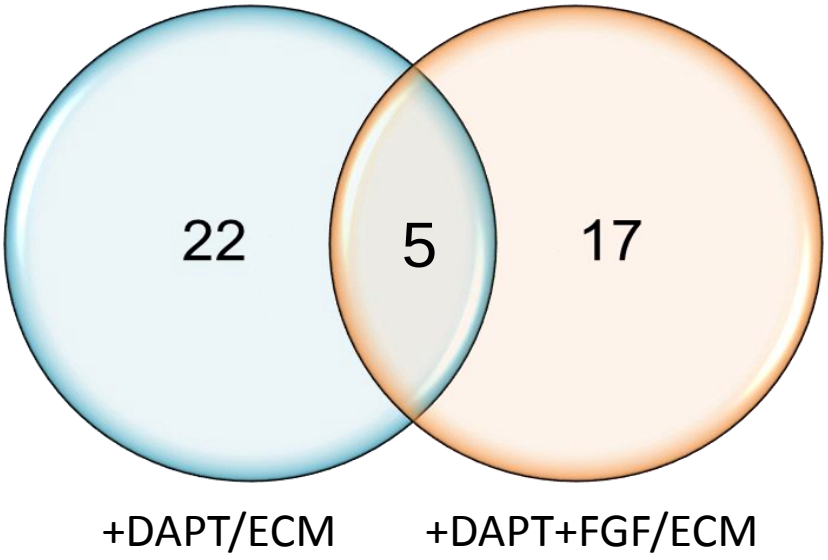

Figure 2.27: miRNA screen in Müller stem cells following Notch inhibition in the presence or absence of bFGF. Venn diagram showing the number of differentially expressed miRNAs between Müller stem cells cultured with DAPT in the presence or absence of bFGF. Five miRNAs overlap in significance between the two treatment regimens and include, hsa-miR-204, hsa-miR-221, hsa-miR-222, hsa-221-3p and hsa-30d. n=4

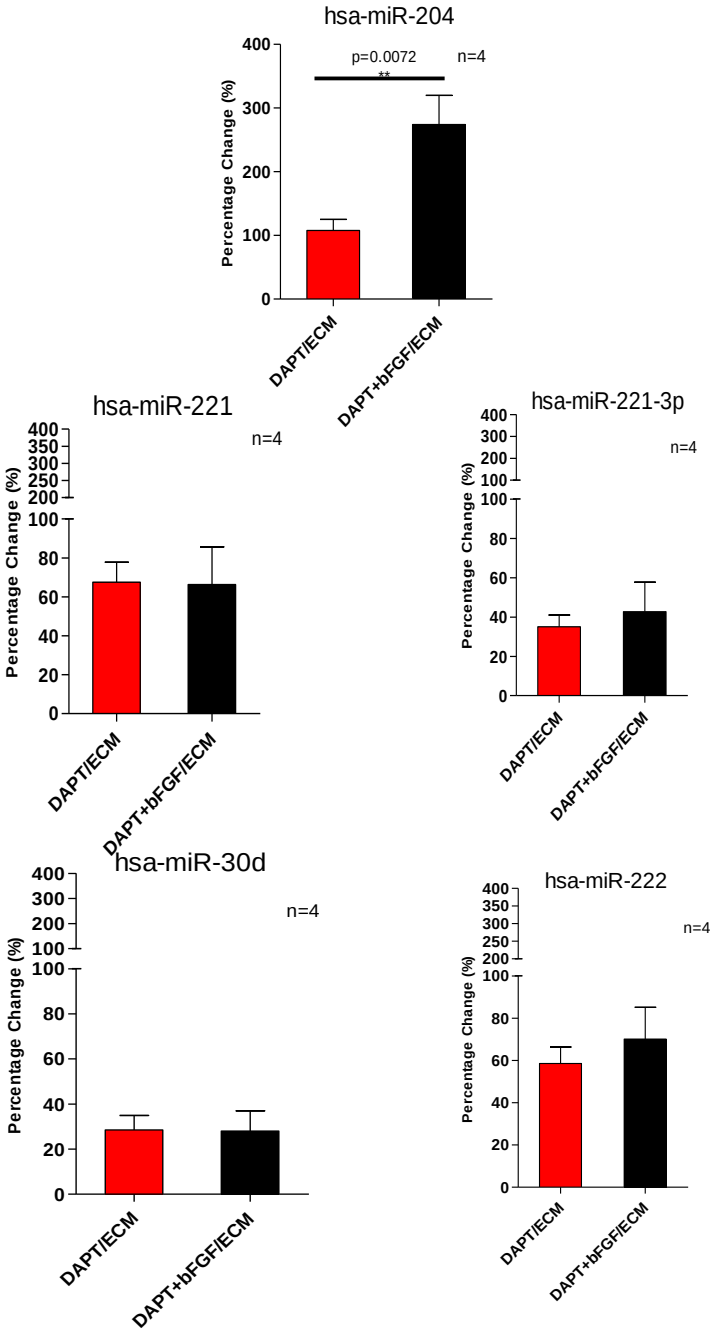

Figure 2.28: Comparison between miRNA prevalence in Müller stem cells undergoing Notch inhibition in the presence and absence of bFGF. hsa-miR-204, hsa-miR-221, hsa-miR-222, hsa-221-3p and hsa-30d overlap in their expression between the different treatment groups however, only hsa-miR-204 is markedly altered following Notch inhibition in the presence of bFGF. DAPT=red, DAPT and bFGF=black. n=4

2.4. Discussion

The principal objective of this chapter was to investigate molecular mechanisms involved in RGC differentiation of Müller stem cells, following Notch inhibition with the γ-secretase inhibitor DAPT (Hayes et al., 2007) and the addition of bFGF to cultured cells.

The initial results demonstrated the regulatory activity of Notch1 on Müller stem cells, where its baseline expression was relatively high. Notch was detected at the protein level and was found in and around the nucleus indicative of the stem cell character of the Müller glia cell lines examined. The results also suggested that, similar to that seen in ESCs and other progenitor populations, Müller stem cells are under the control of Notch signalling. This was inferred by observations that downregulation by DAPT led to decreased expression of Hes1 at both the mRNA transcript and protein levels. Brn3b, an early marker of RGC development, was also markedly upregulated following Notch inhibition, suggesting phenotypic alterations leading to expression of RGC markers. This effect was also seen with the addition of bFGF. Iselt-1 mRNA was also increased with DAPT treatment, providing further evidence of RGC differentiation. Neurite outgrowth was also seen upon Notch inhibition indicative of the morphological impact that DAPT treatment had on cellular cultures by promoting neurogenesis.

Following initial experiments, the array data highlighted numerous miRNAs whose expression profiles had altered following Notch inhibition. The significant upregulation of miRNAs in DAPT treated Müller stem cells suggest the emergence of novel targets under the direction of the Notch pathway. A number of miRNAs were identified, and are discussed below in relation to the Notch pathway and their potential roles in Müller stem cell progenicity.

hsa-miR-204, a tumor suppressor miRNA, has been reported to play a pivotal role in the differentiation of human cardiomyoyte progenitors, as it has

been shown to coordinate the beating action of mature cardiomyocytes. These cells, like human Müller stem cells, are unable to regenerate their native tissue *in vivo* following injury infarction of the myocardium. Forced inhibition of miR-204 in cardiac progenitors in culture promoted proliferation instead of differentiation. This suggests that miR-204 is a driving regulator of differentiation and proliferation in progenitor cells. The study also showed that activating the transcription factor 2 (ATF-2), a member of the CREB family and a basic leucine zipper, promotes proliferation of cardiomyocyte progenitors. One role of miR-204 was to target ATF-2, subsequently preventing cell cycling of cariomyocyte progenitors (Xiao et al., 2012).

In the medaka fish miR-204 has been shown to regulate various aspects of ocular development. Inhibition of miR-204 during development resulted in microphthalmia, as well as irregular dorso-ventral retinal patterning. Studies also demonstrated that miR-204 targets Meis2 and indirectly Pax6, which are upregulated when miR-204 is ablated. This miRNA has also demonstrated its expression in mature RPE, cilliary body, lens and neural retina (Conte et al., 2010).These studies suggest that miR-204 is an important differentiating factor in ocular development, with a similar role in cardio progenitors, and may provide a clue for its possible role within differentiating Müller stem cells. The relationship between Notch and miR-204 may stem from the possible involvement of ATF-2. Kalinichenko et al reported that haplo-insufficiency ((+/-) morphants) of the fork head box f1 transcription factor (Foxf1) in embryonic mice led to depleted expression of Notch-2 and its downstream target Hes1 in pulmonary tissue. Moreover, other transcription factors were also diminished in these morphants including SP-3, B lymphoma Mo-MLV insertion region 1 homolog (BMI-1) and ATF-2.These all act on cell cycling factors which promote the inhibition of self-renewal, and have been shown to prevent ageing in neurons, as well as other tissue types, specifically acting on p53 and p21Cip1 (Chatoo et al., 2009). The action of Foxf1 appears to trigger and enrich the transcription of Notch2. It directly binds to the murine

Notch-2 promoter, which in turn maintains ATF-2 levels to promote an undifferentiated and proliferative state. However, this study poses the question of whether miR-204 mediates the convergence of the Notch pathway and ATF-2 transcription and hence its activity on cell cycling in Müller stem cells.

Array analysis of lens epithelial cells found in opacified human posterior lens capsules identified mothers against decapentaplegic-4 (SMAD4) expression as a target for repression by hsa-204-5p. This miRNA also prevents transduction of the transformation growth factor-beta (TGF-β)/SMAD signalling pathway (Wang et al., 2013). This suppressive action prevented the progression of TGF-β induced epithelial-mesenchymal transition (EMT) and restoration of E-cadherin expression favouring an adherent and differentiated phenotype. This repressive molecule may impact on both signalling pathways to differentiate its role in different tissues.

Five members of the miR-30 family were enriched in Müller stem cell cultures following Notch inhibition, specifically hsa-miR-30a, hsa-miR-30c, hsa-miR-30e and hsa-miR-30d. The miR-30 family has been implicated in tumourogenesis and the progression of EMT in a number of cancers, and during development. The majority of research has found that this miRNA family is down regulated, permitting the expression of characteristic EMT factors including, Snail1, N-cadherin, vimentin and Beta-catenin. EMT within human pancreatic epithelial cells (Joglekar et al., 2009) and murine hepatocytes (Zhang et al., 2012) is mediated by different components of the miR-30 family. Hepatocyte TGF-β-1 induced EMT is prevented by the targeting of Snail1 by miR-30b. This suppression supports the expression of E-cadherin, promoting adherent and differentiated phenotypes. Alongside restoration of E-cadherin expression, mesenchymal bHLH transcription factors are repressed, and include Twist and Zinc finger E-box-binding homeobox (ZEB) 1 and ZEB2 factors. ZEB1 has been implicated in the

Notch pathway by mediating the transcription of mastermind-like proteins (MamL) and subsequent transduction of Notch ICD in pancreatic adenocarcinoma (Brabletz et al., 2011). The miR30 family also appears to modulate Notch via the Delta-like 4 (DLL4) ligand in lymphatic endothelial cells, inhibiting neovascularisation in sarcomas (Bridge et al., 2012). In this study, miR-30d was significantly elevated following DAPT treatment in the absence and presence of bFGF, suggesting that Müller stem cell differentiation into RGC may be controlled by 30d. This is further supported by a report that determined that miR-30d is upregulated through the repression of the PI3K/Akt pathway in renal cell carcinoma cells, and suggests that Notch inhibition is followed by suppression of this proliferative pathway (Wu et al., 2013).

The miR-30 family is also closely associated with the miR-29 family which appears to regulate cellular senescence through their targeting of B-Myb, blocking its translation to Myb-related protein B2 (MYBL2). B-Myb is an oncogene, positively promoting proliferation and upregulating the expression of c-Myc. Senescence progresses at the G0/G1 boundary by repressing E2F binding to the promoter of B-Myb (Bennett et al., 1996). Its mRNA transcript is also disrupted by miR-29 and miR-30, hindering its translation (Martinez et al., 2011). These groups of miRNAs may therefore play a role in cell cycling in Müller stem cells and may be under the regulation of Notch. A possible association between these families and Notch may involve the Retinoblastoma-like protein 1 (p107).This factor is involved in the prevention of B-Myb transcription, through its association with E2F-4. p107 determines the number of proliferative neuron progenitors in the mouse brain. *In vitro* assessment of p107-null murine brain populations demonstrated elevated amounts of Notch-1 and exhibited an enhanced capacity to form neurospheres (Vanderluit et al., 2004). Inhibiting Notch signalling effectors in Müller stem cells may enhance mi-R-30 and miR-29 by mediating the production of p107.

The upregulation of both hsa-miR-99a and hsa-miR-125b in Müller stem cells undergoing Notch inhibition presents a novel chromosome cluster that may be under the regulation of the Notch cascade. The miR-125b cluster on chromosome 21 includes miR-125b, miR-99a and miR-letc. miR-125b was upregulated in differentiating B lymphocytes that were actively dividing within germinal centres. Furthermore, ectopic miR-125b expression prevented the terminal differentiation of B lymphocytes (Gururajan et al., 2010). This suggests that this miRNA is involved in diversification rather than differentiation, and may play a similar role in the maturation of Müller stem cells towards a ganglion fate.

Like miR-204 and the miR-30 family, miR-99a is another miRNA upregulated in Müller stem cells following DAPT treatment, and appears to be related to EMT and TGF-β in cancer development. miR-99a acts in murine mammary cells promoting EMT and TGF- β expression. This miRNA has been also shown to prevent cell cycling in human glioblastomas *in vitro* and *in vivo*. Its action inhibits the PI3k/Akt pathway arresting cell growth. This increased expression leads to apoptosis, suggesting that it has an anti-tumourgenic role in these cells (Chakrabarti et al., 2013).

miR-99a has shown to inhibit proliferation in endometrioid cell carcinoma by negatively regulating the expression of mammalian target of rapamycin (mTOR) kinase. This factor acts to induce cell division but can lead to cancer if deregulated. miR-99a alongside miR-100 and miR-199b were downregulated in these cancer tissues, with miR-100 being identified as a biomarker for this type of malignancy (Torres et al., 2012). Moreover, miR-99a/100 caused apoptosis in oesophageal squamous cell carcinoma by also targets mTOR (Sun et al., 2013). Upregulation of miR-99a was not enhanced by DAPT treatment in the presence of bFGF. However, miR-100 and miR-199b were upregulated. It is therefore suggested that miR99a is initially promoted by Notch deregulation arresting cell cycling, although miR-100 and

miR-199b may be required for further mTOR ablation to provide a cell state suitable for Müller stem cell differentiation.

miR-100 is another tumour suppressive factor which reduces cell proliferation in a number of human cancers including ovarian (Peng et al., 2012), bladder (Oliveira et al., 2011) and acute myoleid leukemia (Zheng et al., 2012). The targets of this miRNA are predominantly factors involved in mitosis and one such agent is polo-like kinase 1 (PLK1) which is a serine/threonine kinase that controls the checkpoints in the cycling process. Though a regulatory role of Notch has yet to be demonstrated by miR-100, it can be suggested that the role of this miRNAs in Müller stem cells is one of Notch pathway inhibition serving to reduce cell proliferation.

Unlike some of the previous miRNAs, miR-199b-5p has been shown to negatively regulate Hes1 and the Notch signalling pathway by attenuating its activity in MB cells. It acts by suppressing their mitotic ability as well as their capacity to anchor together to promote paracrinal growth (Garzia et al., 2009). Therefore the presence of high levels of this miRNA in Müller stem cells undergoing Notch inhibition supports the assumption that differentiation occurred and that Müller stem cells do in fact maintain their potency via the Notch pathway.

miR-222 was enriched in Müller stem cells following Notch inhibition in the presence and absence of bFGF. This miRNA contributes to neural regeneration of dorsol root ganglia (DRG) neurons following injury and permits neurite branching and outgrowth by targeting the phosphatase and tensin homolog deleted on chromosome 10 (PTEN). It has been postulated, by the same study, that miR-222 may regulate the phosphorylation of the cAMP response element binding protein (CREB) through PTEN and c-Jun activation, which may enhance miR-222 expression and therefore disruption of PTEN lead to DRG regeneration (Zhou et al., 2012). The association between the Notch pathway and this miRNA may converge on the activity

between Notch-1 and PTEN. It has been reported that in murine thymocytes Notch-1 is able to regulate PTEN via the induction of Hes1 (Wong et al., 2012). PTEN appears to prevent neural regeneration which is reversed by miR-222 action. However, Hes1 also prevents PTEN activity in thymocytes promoting proliferation rather than differentiation. This may suggest the activity of miR-222 within the Müller stem cell population following Notch downregulation, and therefore Hes1 may behave independently on PTEN from Notch. Downregulation of Notch and Hes1 may allow PTEN to repress the PI3K/Akt pathway in Müller stem cells. This could alter the cellular progenicity, favouring a non-proliferative state. Further investigations into the expression of PTEN and CREB by Müller stem cells following Notch repression, may identify novel pathways involved in Müller stem cell cycling and differentiation in humans.

hsa-miR-100, hsa-miR-221, hsa-miR-222 and hsa-let-7i have been shown to be enriched in human umbilical vein endothelial cells (HUVECs) undergoing senescence, indicative of their potential role in maintaining an anti-proliferative, differentiated state of these cells (Dellago et al., 2013). These miRNAs were consistently upreguated in Müller stem cells following treatment with DAPT. Depending on the tissue the miR-221 family appears to have an opposite activity on proliferation in different forms of cancer. Prostate cancer cells have reduced levels of cell cycling with elevated miR-221 expression (Schaefer et al., 2010), while miR-221 acts by promoting cellular cycling in neck cancers (Nurul-Syakima et al., 2011). The importance of miR-221 in angiogenesis in zebrafish has been shown by its targeting of cyclin dependent kinase inhibitor 1b (CDKN1b) and phosphoinositide-3-kiase regulatory subunit-1 (pik33r1). It was also shown that Notch had a suppressive role on miR-221 activity during controlled angiogenic maturation in this species (Nicoli et al., 2012). The repressive action of Notch suggests that its inactivation would increase miR-221 presence, although its exact role in Müller stem cell differentiation is questionable. However it could be

suggested that its role may involve regulation of cell cycling and in this instance prevent proliferation.

Another interesting miRNA that increased following Notch inhibition is hsa-miR-23a. This miRNA has been found to target Hes1 and has demonstrated a high complementarity to the mRNA sequence upstream of the Hes1 STOP codon. This suppressive action in human NT2 cells leads to neural differentiation upon the addition of retinoic acid (Kawasaki and Taira, 2003). This activity may be important for the induction of Müller stem cells differentiation following Notch inhibition.

Profiling miRNAs of Müller stem cells that have undergone standardised RGC differentiation by Notch downregulation and bFGF showed significant elevations for hsa-miR-204, hsa-miR-100, hsa-miR-151-5p, hsa-miR199b-5p and let-7i when compared to untreated Müller populations. Although the majority of the miRNAs enriched with this treatment are similar to DAPT expression levels, their amounts are considerably higher. The overlapping miRNAs expression levels between the two treatments are miRNAs involved in regulating proliferation. Crucially the induced increase of let-7i expression in Müller stem cells is indicative of RGC development, which has been reported to be present within mature murine RGC populations *in vivo* (Loscher et al., 2007).

hsa-miR-151-5p has been investigated as a potential biomarker for metastatic form of breast cancer, where low expression signifies a reduction in metastatic ability (Krell et al., 2012). Treatment with DAPT in the presence of bFGF increased miR-151 expression in Müller stem cells. This suggests that its role in RGC maturation is negatively regulated by Notch, which may normally act to suppress its anti-proliferative action, similar to its role in breast cancer.

The addition bFGF did not increase the level of Notch activity as had been suggested by Faux et al, where bFGF encouraged Notch activity in neuroepithelium (Faux et al., 2001). This did not apply to Müller stem cells and in fact, at the mRNA and protein levels of Hes1 depletes while miRNAs associated with anti-proliferate roles are substantially upregulated with treatments involving bFGF. The role of bF6F on miRNAs and expression is not well understood and current research has been addressed to vascular development, in which it has been observed that bFGF elevation is followed by the subsequent promotion of mature miR-16 and miR-424 in endothelial cells (Chamorro-Jorganes et al., 2011).

In conclusion, a number of miRNAs have been shown to be elevated following Notch inhibition. A number of these miRNAs are reported to be related to inhibition of proliferation in oncogenic cells. They may represent a novel cohort of RNA molecules which are regulated by Notch or converge on its signalling pathway at different points. This is represented in a schematic diagram suggesting the possible role of various miRNAs on the differentiation and/or maintenance of progenicity of Müller stem cells (Figure 2.29).

Further studies are warranted to determine the possible targets of the miRNAs and their relationship to Müller stem cell plasticity to confirm their function within this population. This will aid their capacity to differentiate towards a ganglion cell fate. Investigations would involve ectopically expressing selective miRNAs, or downregulating these to study the phenotypic alterations induced. Evaluation of miRNAs contained within undifferentiated and differentiated Müller stem cells may also provide novel safer strategies for allographic transplantation. These molecules have the potential to alter the *in vivo* senescent state of Müller stem cells and to promote neural differentiation and retinal regeneration following damage.

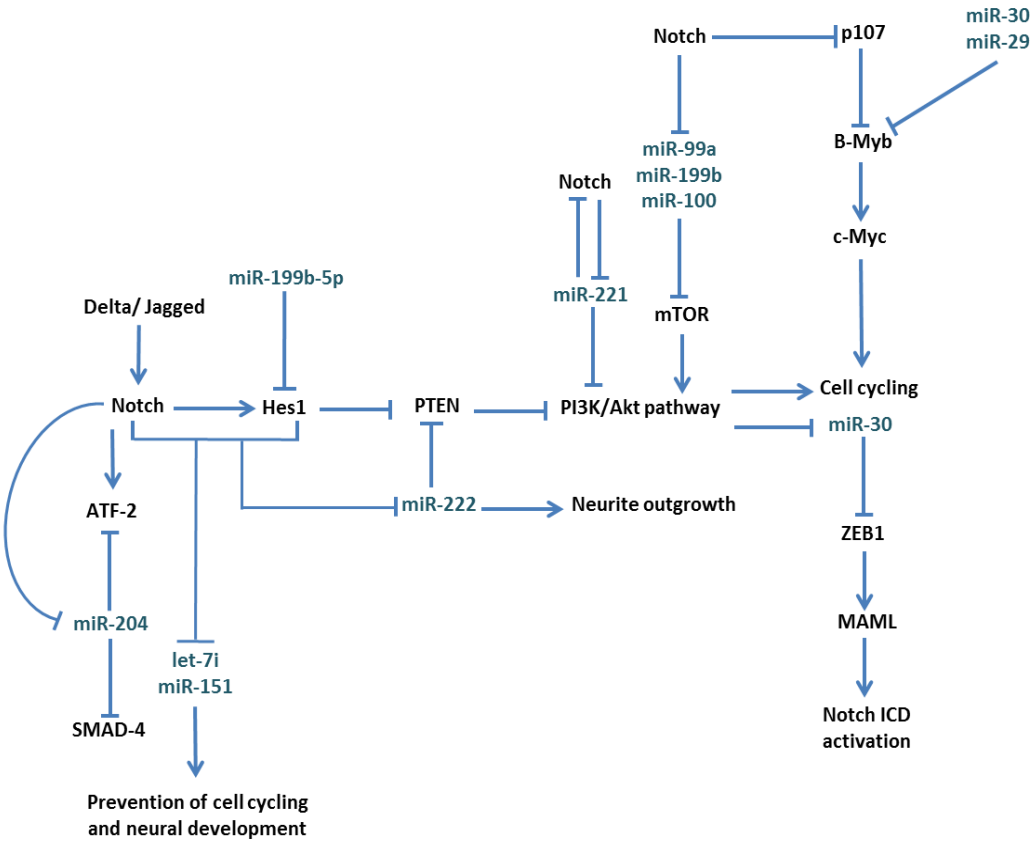

Figure 2.29: Proposed association of the Notch signaling pathway and upregulated miRNAs in Müller stem cells, following Notch inhibition in the presence and absence of bFGF. A schematic illustration of Notch targeting by miRNAs, identified by microarray analysis of differentiated Müller stem cells, based on the current literature.

Chapter 3: Biomaterials and their Potential Application for Retinal Cell Transplantation

3.1. Introduction

Biomaterials are defined as substances that interact with any biological matter. The science of biomaterials has developed rapidly and embodies a multidisciplinary field, which at present involves the interplay between biology, chemistry and medicine. Biomaterials can be sourced from nature or synthesised substances using a number of laboratory-based processes, and are frequently adapted for clinical use. Within the remit of medical research, biomaterials are often used for tissue engineering which aims to enhance or maintain the physiological function of cellular populations or tissue (Kumbar et al., 2006). In order to fulfil their regenerative role, biomaterials need to be completely biocompatible for their use within a clinical setting. Currently biomaterials are used to deliver drugs for internal therapeutic release into the body, prolonging their bioactivity (Ariga et al., 2006, Chavanpatil et al., 2006, Gunatillake et al., 2006).

Research into the scope of biomaterial applications has led to identification of their potential use as transplantable materials, supporting the delivery of grafted cells into a large variety of tissues. Engineered biomaterials can also be made to support cells to enhance their growth, and in the case of stem cells their maturation *in vitro*. Both these supportive roles centre on the ability of biomaterials to mimic the native extracellular matrix (ECM). Understanding the nature of native cell-matrix interactions, equips bioengineers with clues as to how to design and process appropriate materials for cellular grafting approaches. The main focus of research in this field has been to model the innate ECM of different tissues, and to identify substances that permit the highest degree of synergy with the local tissue, yet remain immunologically inert (Morais et al., 2010). The biomaterials designed for such tasks include, decellularised ECMs, biohybrid blends and completely synthetic-based materials, all of which need to be tailored to ensure cellular homeostasis (Lutolf and Blau, 2009, Place et al., 2009).

Regeneration of ocular tissues would benefit from the use of biomaterials that are engineered to improve the function of residual dystrophic cells or to replace damaged cells. The loss of functional RGCs during glaucoma progression highlights a retinal dysfunction that would gain from the use of suitable materials for cell replacement. Based on the anatomy of the retina and the surrounding tissues, a scaffold to support grafted cells would facilitate their delivery uniformly across the inner retina, which cannot be achieved by injections of cellular suspensions.

3.1.1. Types of Biomaterials

3.1.1.1. Natural biomaterials

Natural biomaterials have immense potential for biomedical application as they are sourced from natural materials and interact with cells *in vitro* in a similar manner as that occurring *in vivo*. Reconstituted ECM proteins have been used as 2D protein coats on culturing surfaces, and include collagens, fibronectin, laminin and Matrigel (Nojehdehian et al., 2010). These proteins are able to provide biocompatible artificial environments, supporting adherence, cellular growth and survival *in vitro*. However, in order to provide conditions for cellular grafting, these natural biomaterials need to be adapted into 3D topologies.

Natural hydrogels for culture have been developed from ECM derivatives including, collagen, fibrin (Eyrich et al., 2007), hyaluronic acid (Masters et al., 2004), Matrigel, chitosan, silk and alginate (Barralet et al., 2005). Some natural-based materials have been used to build scaffolds and include xenogenic proteins such as silk fibroin, chitosan, aliginate, cellulose and agarose (Prewitz et al., 2012). The commonality between these natural-based materials is that they are similar to the native ECM, in structure and can be induced to form different structures, ranging from hydrogels to fibrous scaffolds.

Hydrogels of type I collagen appear to retain vital features attributed to the native structure of this molecule, and demonstrates the capacity to support the delivery of aortic interstitial cells (Saha et al., 2007, Butcher and Nerem, 2004). Collagen hydrogels are also used regularly in wound healing studies and have shown their ability to support fibroblast survival and proliferation. Under culture conditions, fibroblasts have shown to remodel and adapt their 3D collagen matrix, analogous to their *in vivo* action (Hadjipanayi et al., 2009, Sethi et al., 2002). In addition, collagen-based hydrogels have been used to model different body environments in order to assess various treatments on cellular function. To that end fibroblasts embedded in collagen hydrogels have been examined for their ability to contract gels under different culture stimuli, including the presence of mitogens, drugs or other ECM additives (Nguyen and West, 2002).

Natural biomaterials have also been used in electrospinning processes to produce 3D matrices. Materials used for this purpose have included collagen (Matthews et al., 2002), gelatine (Salifu et al., 2011), elastin (Buttafoco et al., 2006), fibrinogen (McManus et al., 2006) and silk (Min et al., 2004). Silk fibroin has also been shown to possess some positive biomedical traits when electrospun, and has been found to promote cellular adhesion and proliferation (Wang, 2004, Venugopal et al., 2008), indicative of its potential for clinical use.

Cellulose acetate (Zhang and Hsieh, 2008) and Hyaluronic acid (Ji et al., 2006), are polysaccharides that can be electrospun to yield fibres for cellular scaffolds. Hyaluronic acid (HA) has been widely used in biomedical therapies including ophthalmology, surgery and drug delivery. HA has a very large volume to surface ratio making it ideal for incorporating therapeutic agents into its framework.

3.1.2. Collagen scaffolds

Choosing an appropriate biomaterial to engineer cellular scaffolds for regenerative medicine requires the material to be readily available, easy to process and suitable for transplantation to human subjects. Collagens have been suggested to be suitable proteins to fulfil this strategy. Due to the good knowledge of their synthesis and function within the body, collagens constitute an excellent material for the manufacture of 3D scaffolds. They represent a group of naturally occurring proteins that impart support and mechanical strength to all cells and tissues in the body and are essential components of the connective tissue, to which cells adhere. The word collagen derives from the Greek word meaning glue, which is a suitable description for both its form and function (Bhattacharjee and Bansal, 2005).

Collectively, collagens have a very complex molecular structure. Fibrillar collagens exhibit distinct hierarchical levels of amino acid organisation and association. These are similar in molecular structure although their configuration determines their ultimate structure and function. Type I, II, III, V and XI collagens are fibrillar in their arrangement and can assemble into fibrils based on their basic, primary structure. Fibrillar collagen structures are based on different combinations of 10 polypeptide chains; known as α-chains. These chains fold, first into transient tight left-handed secondary α-helices and finally into its triple helical tertiary structure, when secreted into the mature ECM (Ottani et al., 2002). The native structure of type I when extracted from tissue retains its tensile strength and has the ability to be remodelled *ex vivo.* Type I collagen therefore represents an attractive natural biomaterial to consider when investigating scaffold development for therapeutic cell delivery.

Collagens within tendons form long string-like structures that provide tensile strength, collagens contained within the skin give elastic and mechanical strength, and collagen fibrils found in bone aid the calcification and

maintenance of this tissue. To date, 28 types of collagens have been characterised, each with distinct molecular similarities and diversities, containing 42 different sub-types of polypeptide chains (Gordon and Hahn, 2010, Hulmes, 1992).

Type I Collagen is the most ubiquitous form of collagen present in the human body and can be found in almost all tissue types. It constitutes the predominate ECM protein in tendons, bone, and dermis, illustrating the range of tissues and formations type I collagen undertakes within the human body (Di Lullo et al., 2002). In experimental *in vitro* studies, type I collagen is commonly used as a protein coating for culture flasks to promote cellular adhesion. It is also used in hydrogel form to support the formation of cell-cell interactions *in vitro* (Franke et al., 2007, Salchert et al., 2005).

Collagen can be purified from various tissues types by means of enzymatic or acidic treatments. These agents act by removing the covalent crosslinks between collagen fibrils within the mature ECM. Purified forms of collagen may be remodelled into diverse forms with different properties, such as sponges, nanofibres and hydrogels, or can be blended with other polymers, either natural or synthetic (Rajan et al., 2006). Purified collagen can provide cellular support which allows collagen matrices to act as structural cellular scaffolds.

The method of extraction and source of type I collagen, and collagens as a whole can influence the mode of processing. This can also modify the ultimate structure produced which can play a key role in the biocompatibility of the structure made.

Collagen can be solubilised in acid (Kuznetsova and Leikin, 1999), neutral salt (Gross et al., 1955) or by proteolytic solutions (Abou Neel et al., 2013). These extraction methods alter the molecular structure of collagen in different ways. Proteolytic extraction cleaves the terminal peptides of the collagen fibrils, which modifies the rate at which fibrils form *in vitro*, however

this method does not remove the capacity for fibrils to form. In contrast, acid solubilisation does not cleave the terminal peptides from collagen fibrils, this ensures that stable covalent crosslinks are able to form *in vitro*, with better structural and mechanical integrity as compared to proteolytic extraction.

All extraction methods of collagen break the bonds between the complex networks of fibrils within native tissue. Although some alter its structure differently, they all destroy the innate structure which prevents the remodelling *in vitro* to be completely comparable to native collagen and is in fact collagen in the form of gelatine. The self-assembly of reconstituted collagen can influence the morphology of the fibrils produced and in turn the hierarchy of fibrillular structure. Reconstituted collagen in solution is unlike the collagen found in tissue, which is completely insoluble. Where this chapter describes collagen in solution, the protein described is collagen in its soluble form (gelatine).

3.1.3. Electrospinning

Electrospinning has become a useful tool for manufacture cellular scaffolds and has been employed to remodel type I collagen fibres. This process has been used to enhance the functionality of various biomaterials through the addition of bioactive agents, either within or outside the fibrous network. Bioactive agents are aimed to facilitate cellular adhesion, maturation, proliferation and neurite outgrowth (Hodgkinson et al., 2007). Electrospinning involves the application of a strong external electrical field to a charged polymer solution, which is then fed to a grounded collecting target via a needle tip (Figure 3.1A) (Matthews et al., 2002). Electrospinning is widely used in tissue engineering and can be refined to produce fibres of diameters

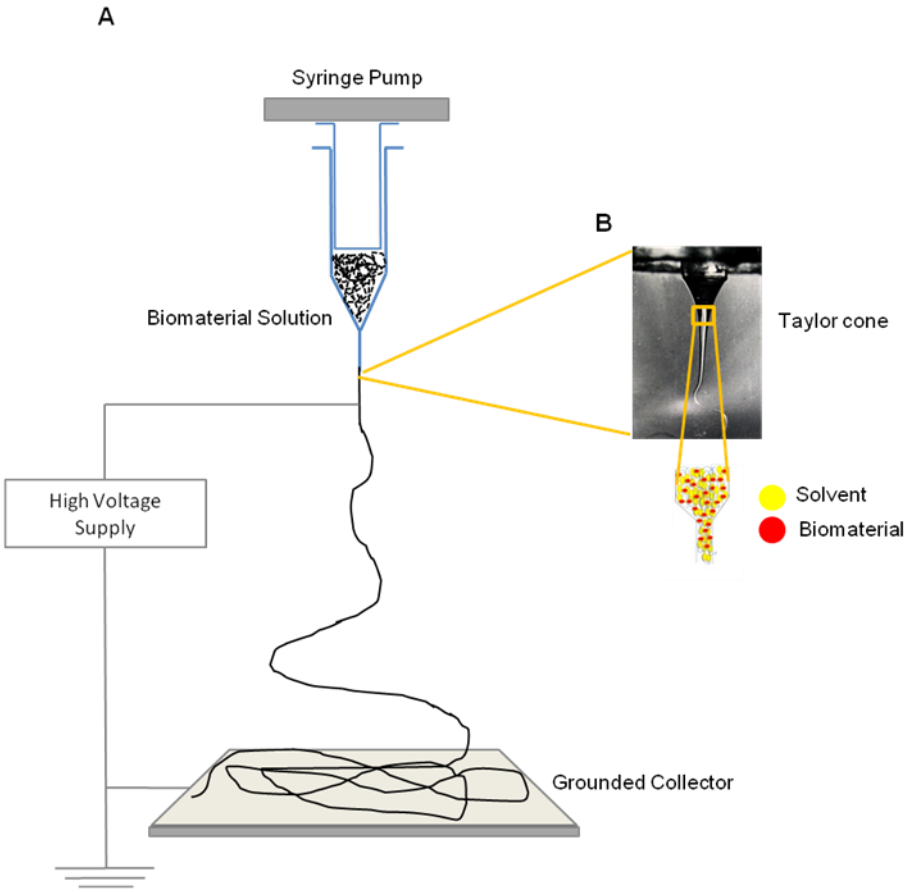

Figure 3.1: The Electrospinning process A) Diagrammatic representation of the rig used for the electrospinning process illustrating the set up of the equipment where the polymer solution is drawn by a high voltage device, (HPV) to a grounded target. **B)** A slow-capture image of a Taylor cone jetted from a needle tip at the initiation of electrospinning, and an illustration of the entanglement phenomenon which enables fibres to be drawn onto a surface.

100nm or less (nanospinning), which can enhance its application in cell therapies to treat different tissue degenerations. Scaffolds developed by electrospinning have demonstrated a great potential in biomedical applications such as wound dressing, drug delivery and enzyme immobilisation (Sill and von Recum, 2008).

During the spinning process, a stable electrospinning jet is formed at the tip of the needle and is termed Taylor cone (Figure 3.1B). The Taylor cone and subsequent fibre formation is driven by the application of a high electrical potential between the polymer solution and the grounded collector. This process was first described by Sir Geoffrey Taylor in his 1964 paper entitled 'Disintegration of Water Droplets' in an Electric Field. The jet emerges from the charged surface of the needle and accelerates through the electrical field toward the grounded target. The fibres are bent whilst being drawn from the needle tip creating a web-like non-woven structure on the surface of the grounded collector. Deposition of fibres also relies on the rapid evaporation of solvent to enable the polymer to solidify efficiently (SL Shenoy, 2005). This network mimics a number of native visceral ECMs that have the potential to promote cell adherence and proliferation. The ECM supporting the nervous system ranges in dimensions depending on the tissue, however the retina contains fibres of 100-1000nm in width.

Scaffolds built by electrospinning techniques can have different properties that result in a range of fibre thicknesses and morphologies. The structure and final thickness of fibres produced by this method is determined by several factors. The main parameters include the properties of the polymer solution, such as viscosity, elasticity, and the degree of surface tension. Additionally external factors can impose constraints on the spinning process and include the external electrical field strength, voltage, temperature and humidity. Collagen electrospinning creates a meshwork that resembles the physical structure of the innate ECM. The final structure of product, however,

can be influenced by extrinsic factors such as solvents and fixatives used to develop fibrous scaffolds.

Often studies focused on the production of collagen scaffolds for medical application have involved the development of gels or solid constructs such as powders or films, but these have failed to mimic the native *in vivo* properties of the ECM.

3.1.3.1. Factors influencing the structure of collagen fibres produced by electrospinning

Acetic and formic acid can be used as solvents for electrospinning collagen, although acidic environments can permanently destroy the topology of collagen fibres. Moreover, the slow evaporation rates of the acids and their strong affinity for collagen leads to the formation of wet, fused fibres which can eliminate the fibril structure impacting on its bioactivity. It is essential for some cell types to interact with matrices containing collagen fibre diameters akin to the native protein fibrils (20– 100nm in diameter) (Matthews et al., 2002), to ensure adhesive cell-matrix properties.

Collagen is also soluble in the chemical 1, 1, 1, 3, 3, 3 hexafluoro-2-isopropanol (HFIP) which can be used for electrospinning under similar parameters used with acid solvents. HFIP is extremely volatile and has a low affinity for collagen (J. A. Matthews, 2003), hence it is a suitable electrospinning solvent. Though very cytotoxic, cells have been shown to proliferate on scaffolds spun with HFIP and have been approved by the United States Food and Drug Administration (FDA). HFIP acts by partially denaturing the triple helix of native collagen but does not destroy its structure. HFIP itself, like collagen, has both highly hydrophobic and hydrophillic regions. It is thought that HFIP binds directly to collagen via hydrophobic and hydrophilic interactions, which act to support and divide the triple helices whilst in solution. HFIP dissolves the crystalline structures

contained within the triple collagen helixes, and stabilises the collagen fibrillar structure (Doillon et al., 1997). This ultimately facilitates cellular affinity to the scaffold matrix.

Naturally sourced biomaterials, including collagen, require stabilisation following spinning. This involves the formation of crosslinks between fibres to improve mechanical integrity. Collagen crosslinking occurs between two lysine residues, and can be induced by chemical or natural protein crosslinkers.

Chemical crosslinking agents are widely used to cross link type I collagen are themselves very cytotoxic. This feature can lead to extensive inflammation within tissues, preventing the survival of grafted cells. Chemical agents used to crosslink collagen include aldehydes, epoxy compounds and isocyanates. They covalently couple neighbouring fibrils and target reactive moieties of collagen side chains. The bonds formed may incorporate or retain derivatives of the agent used, for which degradation of the scaffolds may then lead to the release of agents that can be severely cytotoxic (Rothamel et al., 2005).

Natural crosslinking agents have offered an alternative strategy for crosslinking collagen. Plant derived genipin and nordihydroguaiaretic acid are natural products that can be used as crosslinkers, and could pose no major concerns of inflammation, compared to other chemicals. Catalysts have also been explored as protein crosslinkers. An example of such an agent is 1-Ethyl-3-(3-dimethylaminopropyl) carbodiimide (EDC), which associate with protein carboxylic groups to form o-isoacylurea structures. This results in the activated intermediate being attacked by a nucleophilic primary amino-group to form an amide crosslink. Isourea derivative of the applied carbodiimide is then eliminated and can be washed out (Everaerts et al., 2008). If washed sufficiently, carbodiimide-fixed scaffolds are non-cytotoxic and are entirely permissive to cell attachment and survival.

Biomaterials crosslinked with carbodiimide are in general significantly more biocompatible than those crosslinked with agents such as glutaraldehyde (GTA).

3.1.4. Plastic Compression

Understanding and mimicking the spatial organisation of the native ECM is the ultimate aim of bioengineers when fabricating materials for potential transplantation. Hydrogels composed of type I collagen constitute a possible candidate for use in tissue regeneration techniques. However, in its gelatinous state they contain a large amount of water, making its use difficult in regenerative medicine. Whilst collagen gels do provide a meshwork of randomised fibrils, it lacks the essential tight packing of the fibres, making them inherently weak (Brown et al., 2005). Furthermore, cells grown within gels may react differently when compared to their native counterparts under *in vivo* conditions, and due to the stringent extraction processes, type I collagen can lose its native characteristics and form weaker and less extensive interactions with cells *in vitro*. Though modifications of 3D scaffolds have been made for culturing systems, they do not totally parallel the features of the original ECM (Tibbitt and Anseth, 2009).

A novel method of hydrogel compression has been developed to overcome the above problems, which has been shown to improve the mechanical integrity and biomimicry of collagen. This process involves excluding the entire aqueous component of collagenous hydrogels. This results in the formation of randomised-tightly packed collagen fibrils reminiscent of the *in vivo* ECM. This process has been termed Plastic compression (PC) (Brown et al., 2005) (Figure 3.2). It involves applying a known weight to a collagen gel for a short period of time to remove aqueous components and avoiding the use of chemicals for crosslinking. The extent of crosslinking can be altered depending on the collagen concentration of the hydrogel. This protocol can be modified by creating a gradient between the mass applied,

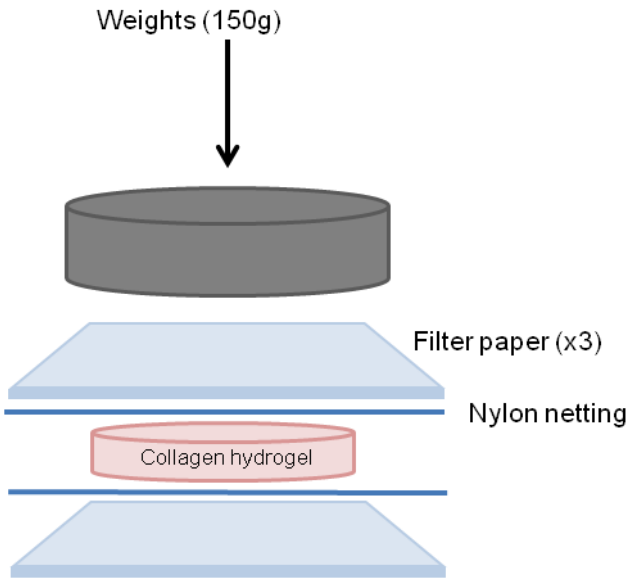

Figure 3.2: Plastic compression of Collagen hydrogels. Following polymerisation of collagen hydrogels, 150g weight is applied to remove the aqueous component. This results in an extensive network of crosslinks between collagen fibres. The dehydration process involved collecting the gel between two nylon sheets supported on filter paper, and applying the mass onto the rat tail (RTT) type I collagen hydrogel for 5 minutes.

time for compression and the collagen concentration (Kureshi et al., 2010). This results in the formation of scaffolds with different properties that can be used for different applications.

Factors affecting the PC process can alter the fibres created. The volume and spatial dynamics of the hydrogel at the start of polymerisation can change the density of collagen fibres within the final network. In addition, the temperature at the time of neutralisation can disrupt the rate of fibril polymerisation and lead to incomplete crosslinking. Compression weightsand time creates a dynamic gradient between scaffold elasticity and tensile strength. Specifically, longer periods and higher weight increase the number of crosslinks between collagen fibrils. Chemical factors influence the internal features of the hydrogel prior to neutralisation and centre on the concentration and the type of solvent used to dissolve the collagen. Acidic solutions of collagen can be made with acetic and hydrochloric acids which elicit different polymerisation features, and can ultimately alter the efficiency of neutralisation. Furthermore, the concentrations of collagen within the solutions also impact on the degree of polymerisation during neutralisation and crosslinking during compression procedures. Resulting fibres can be either extensively crosslinked, or weaker, with less stabilised fibrils, which can be appropriately adapted to target specific tissues.

These modified collagen hydrogels have been widely used in translational research as platforms for cell or therapeutic agent delivery, tissue scaffolds for repair, and as *in vitro* models of disease. Compressed collagen gels have been used to culture human bladder smooth muscle cells within its structure whilst supporting urothelial cells on their surface (Engelhardt et al., 2010). The cell populations were able to thrive and form densely packed cell layers, suggesting that PC collagen is an adequate substrate for these cells and that it has potential for cell replacement therapy of diseased bladders. Furthermore, PC collagen structures have been used to culture corneal cell

populations. To date, limbal epithelial stem cells, taken from human corneal biopsies have been expanded on PC collagen substrates, where feeder fibroblasts have been directly seeded within the matrix (Levis et al., 2010). The compressed scaffolds are able to retain the population of fibroblasts and create a feeder layer of cells which is suitable for transplantation. This study revealed that collagen was able to support both types of cells whilst also developing the tissue architecture of the native cornea.

3.2. Objectives and Experimental outline

This project aimed to determine the feasibility of constructing cellular substrates to deliver Müller stem cell-derived RGC precursors onto the inner retina. To create a biomaterial-based substrate for intraocular cell delivery, the scaffold would need to be able to withstand surgical manipulation, support migration of grafted cells to the site of degeneration, and allow cell integration and long-term survival. Lack of these features could heavily impact on the efficiency of successful transplantation. Furthermore understanding the development of cell-matrix synergy is key to develop suitable cellular scaffolds, and requires knowledge of the ultrastructural conformation of the matrix. This information can be used to determine the methods to prepare scaffolds using different biomaterials, enhancing the success of cell transplantation. On this basis, the following objectives were formulated:

1. To develop protocols for constructing electrospun type I rat tail collagen scaffolds and to examine their physical properties.
2. To develop protocols for constructing compressed type I rat tail collagen scaffolds and to explore their physical features.
3. To compare the biological properties of electrospun and compressed collagen scaffolds.
4. To compare the physical properties of electrospun and compressed scaffolds to facilitate *in vivo* transplantation.

To fulfil the above objectives, the following experiments were performed:

1. Investigation of the physical and chemical parameters needed for adequate formation of electrospun collagen scaffolds. This involved the use of different solvents, voltages, air gap distances and the use of different protein crosslinking agents.

2. Investigation of the physical and chemical parameters needed for adequate formation of compressed collagen scaffolds. This involved the use of different concentrations of collagen, volumes, and compression parameters.
3. Assessment of the ability of electrospun and compressed collagen scaffolds to support cell adhesion, growth and differentiation *in vitro*. These experiments involved the investigation of scaffolds to promote cell viability, as determined by hexosaminidase assays, and by inducing RGC differentiation upon Notch inhibition and growth factor stimulation.
4. Examination of the mechanical handling of scaffolds for transplantation purposes. These studies involved the physical handling of scaffolds, as well as the ability to pass them through a cannula for transplantation.

3.3. Results

3.3.1. Effect of different solvents on the formation of collagen fibres prepared by electrospinning methods

Rat tail type I collagen was dissolved in either acetic acid or HFIP at a concentrations of 50mg/ml. The voltage used to draw fibres was standardised to ensure a continuous fibre was draw and collected. It was found that the voltage needed for this application ranged between 12-12.5kV, with an air gap distance to the grounded target of 15cm for the collagen solutions. The feed rate used for the electrospinning process of collagen ranged between 2 and 5 ml/hr.

Under the above voltage conditions, fibres drawn from the solution containing acetic acid showed bleb formation (Figure 3.3). Fibres were drawn continuously and the ribbons formed were smooth, although large blebs were observed on the surface of the scaffolds, making them inappropriate for cell adherence. In contrast, collagen solutions made in HFIP, when electrospun under the same conditions used for spinning acetic acid solutions, produced smooth fibres without irregular blebbing on the scaffolds surface (Figure 3.3).

3.3.2. Effect of Different Crosslinking Agents on the Maintenance of the Ultrastructure of Electrospun Collagen Fibres

Crosslinking procedures were used to induce and maintain structural integrity of electrospun matrices. This investigation examined both physical and chemical methods of collagen crosslinking. Glutaraldehyde (GTA) vapour was used to chemically crosslink electrospun micro fibrils of collagen for 72 hours in a sealed environment. Samples crosslinked with GTA vapour (Figure 3.4A ii) and EDC/NHS (Figure 3.64A iii) did alter in appearance, turning to a straw yellow colour from an initial brilliant white colour (Figure 3.4A i), indicative of the fixative action of the

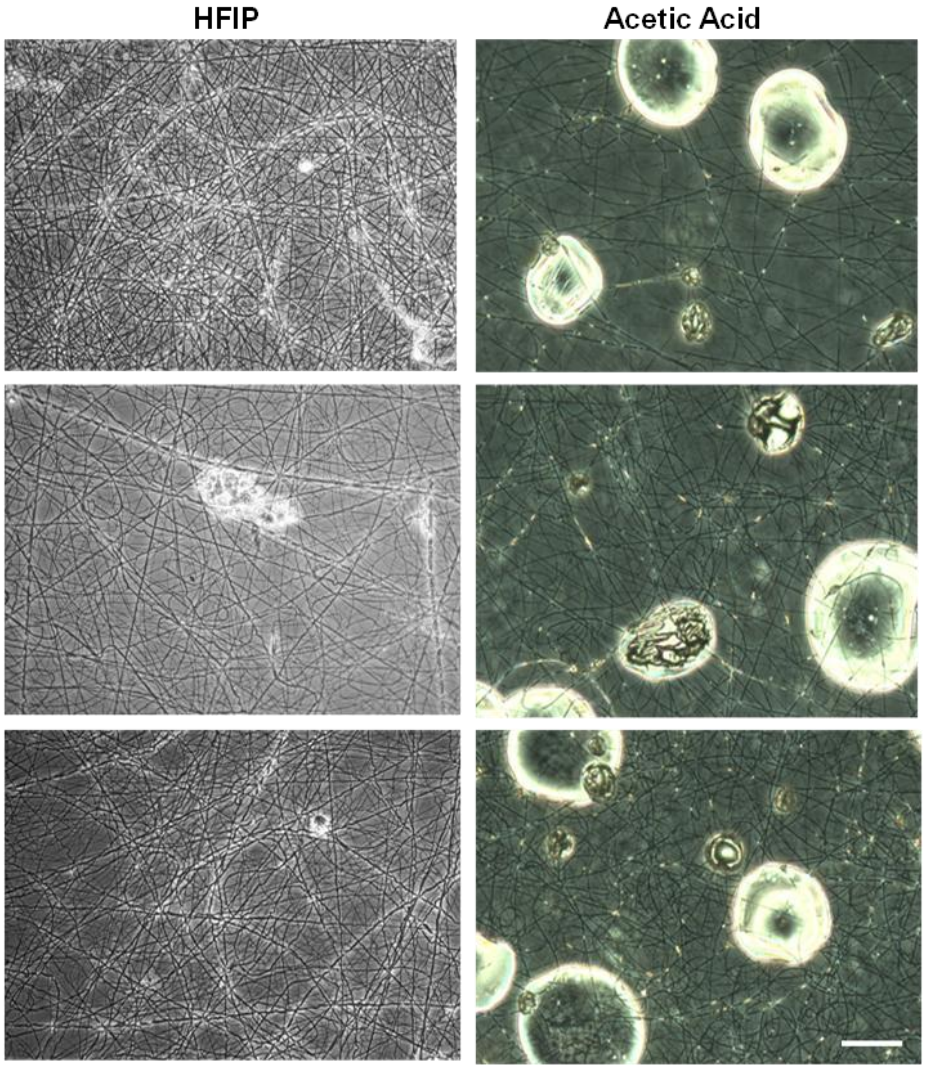

Figure 3.3: Morphology of Electronspun collagen fibres using various solvents. Triplicate phase-contrast images of rat tail type I collagen fibres electrospun from solutions containing 50mg/ml of collagen dissolved in either HFIP or acetic acid. The electrospinning parameters were 12kV and a 15cm air gap distance. Fibres drawn from a 22G needle for 1hr, HFIP solutions were continuous and smooth, whereas fibres produced from acetic acid solutions were irregular in morphology. Acetic acid also promoted bleb formation on the fibrillar surface possibly due to its slow evaporation rate, following fibre deposition on the grounded target. Scale bar= 50µm.

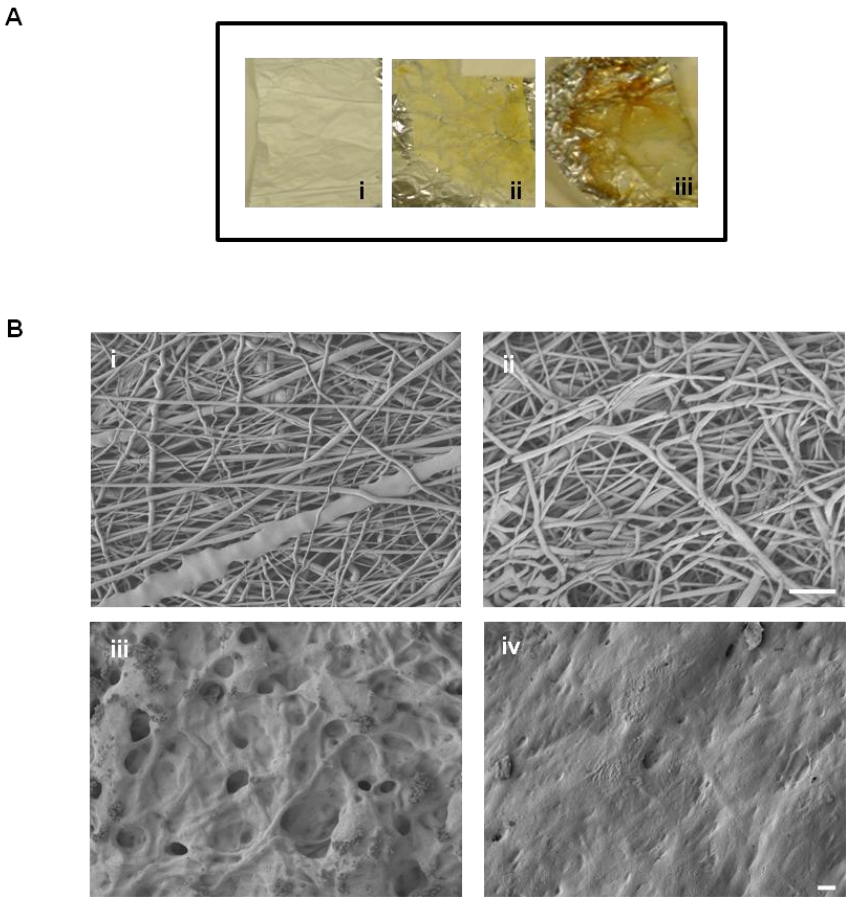

Figure 3.4: Effect of Crosslinkers on Electrospun collagen fibres: Scanning electron microscopy was used to examine the morphological structure of constructs produced by electrospinning. The micro-structures resulting from these crosslinking methods showed distinct fibre morphologies. **A)** Photographic images of the macroscopic features of electrospun collagen i) non-crosslinked ii) 15% GTA crosslinked and iii) EDC-NHS crosslinked collagen scaffolds. The fixation process with the different crosslinkers generated characteristic colour change in electrospun scaffolds. Scaffolds change from white (non-crossliked) to yellow (GTA) or yellow-brown (EDC-NHS). This alteration in colour is typical of protein crosslinking and structural modification. **B)** Scanning electron micrographs of the microstructure of electrospun collagen matrices i) non-crosslinked, or crosslinked with ii) 15% GTA, iii) EDC and iv) EDC-NHS. GTA crosslinked collagen produced matrices with well-defined fibres, similar to those observed prior to crosslinking. However, EDC crosslinking treatments produced fibres that lacked porosity. EDC alone created matrices without well-defined fibrils, compared to non-crosslinked and GTA treated collagen scaffolds. Fibres appeared to be fused when treated with EDC in both the presence and absence of NHS. Scale bar= 10µm.

crosslinkers. Electron microscopic examination of the fibres obtained following GTA crosslinking indicated that on average, the fibres had a diameter of 1.03± 0.026µm and a thickness of approximately 128 microns (Figure 3.4B).

The chemical 1-Ethyl-3-(3-dimethylaminopropyl) carbodiimide (EDC) was used as a non-toxic substitute for GTA vapour. It acts as a benign catalyst and is generally used in combination with N-hydroxysuccinimide (NHS). This acts as an "amine-group" giving substrate and provides a reservoir of amine-groups ($-NH_3$) for protein crosslinking. However, use of EDC either alone or in combination with NHS caused solubilisation of collagen fibres when hydrated (Figure 3.4B iii and iv). Whilst with EDC alone some fibrous and porous structure remained (Figure 3.4B iii), addition of NHS caused total loss of the fibrous architecture (Figure 3.4B iv). This observation prevented the progression of this work onto scaled up culturing of Müller stem cell-derived RGCs for transplantation.

3.3.3. Standardisation of methods to develop compressed collagen scaffolds

Ultra-thin collagen scaffolds were produced by compression of collagen hydrogels. Acidic solutions of collagen were neutralised with sodium hydroxide. Neutralisation was performed at room temperature and was indicated by colorimetric alteration of the acidic solution, from straw yellow to indigo-pink with the addition of sodium hydroxide (Figure 3.5A). After neutralisation, hydrogels were poured into titanium moulds and incubated at 37°C for 30 minutes to polymerise. Collagen hydrogels were then subjected to compression for 5 minutes under 150g/collagen hydrogel to remove their aqueous components. Scaffolds were then floated into PBS. To design suitable scaffolds for retinal transplantation, it was necessary to take into account various parameters required for safe and practical injection of cellular scaffolds into the eye. Delivery of ocular transplants would require

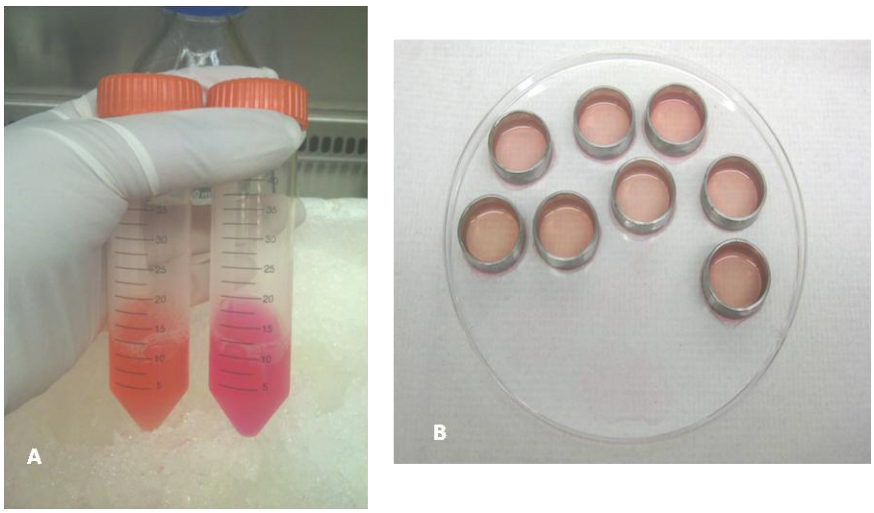

Figure 3.5: Physical appearance of collagen hydrogels. The figures illustrate the distinctive appearance of collagen hydrogels prior to compression A) collagen suspensions following neutralisation with sodium hydroxide; acidic suspension (left) and alkaline suspension (right) as visualised with phenol red. B) polymerised hydrogels following incubation of neutralised solutions at 37ºC for 30 mins. Titanium rings were used to cast collagen hydrogels.

transplantation through conventional sclerotomies formed during vitreoretinal surgery, no larger than 18G in size (lumen size of 0.64mm). Parameters used to produce compressed collagen scaffolds were set in order to achieve their passage through an 18G cannula. These included the use of hydrogel volumes of 300µl, cast in 1 cm moulds and concentrations ranging from 0.75mg/ml-2mg/ml. Both excessive and moderate neutralisation prevented polymerisation of hydrogels, giving the appearance of stable hydrogels. However, these hydrogels were structurally weak and rapidly lost stability when physically manipulated. It was therefore determined that a reduced amount of stable crosslinks had been formed between the collagen molecules. Compression of these gels resulted in thinner mats with larger diameters, suggesting low quantities of collagen fibres per unit of area of scaffold.

The surface of the scaffolds observed under low magnification phase-contrast microscopy showed the meso-structure with an imprint of the compression materials (Figure 3.6A). Microscopic examination using high magnification showed an ultrastructure composed of a closely packed network of collagen fibres (Figure 3.6B). Fibres produced by PC are on the nano-scale and exhibit native dimensions with an average diameter of 0.75±0.042µm. Thicknesses of collagen fibres produced by compression of Hydrogels prepared at different collagen concentrations resulted in consistent widths of approximately 20µm (Figure 3.6B).

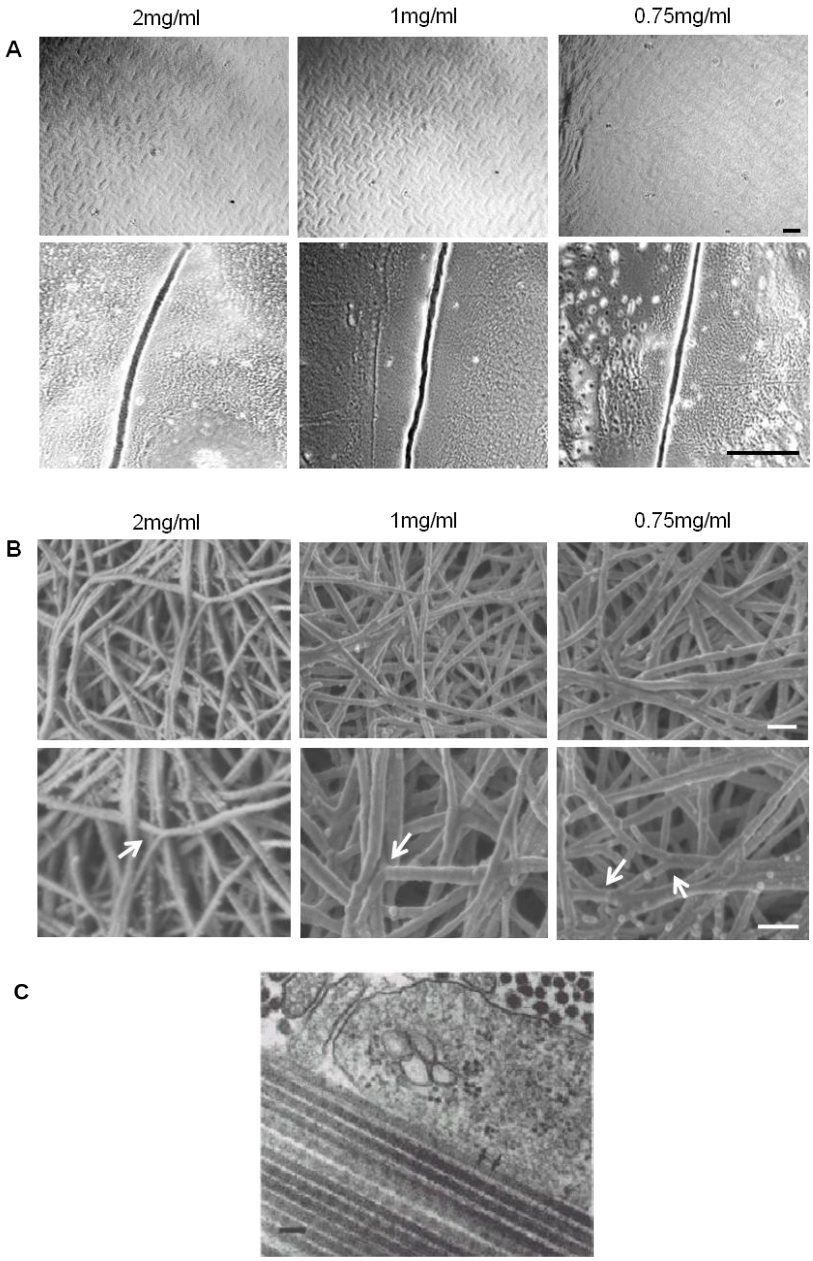

Figure 3.6: The Macrostructure and Ultrastructure of Plastic Compressed (PC) Rat tail type I Collagen hydrogels. The structure of the collagen hydrogels following compression recorded under **A)** phase-contrast illumination in PBS, for three concentrations of collagen, with an aerial perspective (top three images) and cross sections of scaffolds embedded in OCT (20 micron transverse sections) (bottom 3 images). Scale bar= 100µm. **B)** Scanning electron micrographs of decreasing, left to right, collagen concentrations depicting the ultrastructure within PC collagen constructs and the crosslinks formed between fibrils (white arrows). Scale bar 200nm. **C)** Transmission electrograph of native type I collagen, scale bar= 100run (taken from Bruns R et al, 2010).

3.3.4. Comparison between the Light Absorbent Properties and Porosity of Electrospun and Compressed Collagen Scaffolds

Collagen fibres produced by either compression or electrospinning were studied for porosity or area fraction of the pores, and optical density. These features may help to establish the physiological functionally of the scaffolds. Scaffolds were examined for their suitability for cell adhesion, whilst determination of their optical density was used to assess light absorbance and their ability to facilitate light passage onto the retina. The porosities measured using threshold set (binary black and white) SEM images in imageJ, indicated a significant difference between EDC-based methods and GTA vapour (Figure 3.7 A-C) with none or very few pores being identifiable in EDC scaffolds, whilst GTA crosslinked scaffolds had an average pore size of 4.75µm (Figure 3.7 E). Whilst EDC produces matrices that are able to undergo culturing systems, it may be assumed the degree of cellular affinity would be lower in these systems. The degree of porosity observed in compressed scaffolds was on average 50% of the surface area, with pore size averaging 475nm signifying the degree of mesoporosity and the size of pores being markedly smaller and higher in occurrence compared to electrospun scaffolds (Figure 3.7 E and F). Scaffolds that are suitable for eventual transplantation into the eye ideally should be transparent. To this end, the optical density of the scaffolds was determined within a range of 350nm-750nm using a spectrophotometer. The extent of visual light absorbance by the different scaffolds was negligible, indicating no hindrance of visual light transmission. No significant difference was observed between the different scaffolds (Figure 3.8 A and B). This finding suggests that both processes are able to create scaffolds which allow transmission of light and would promote light passage onto the retina, following transplantation.

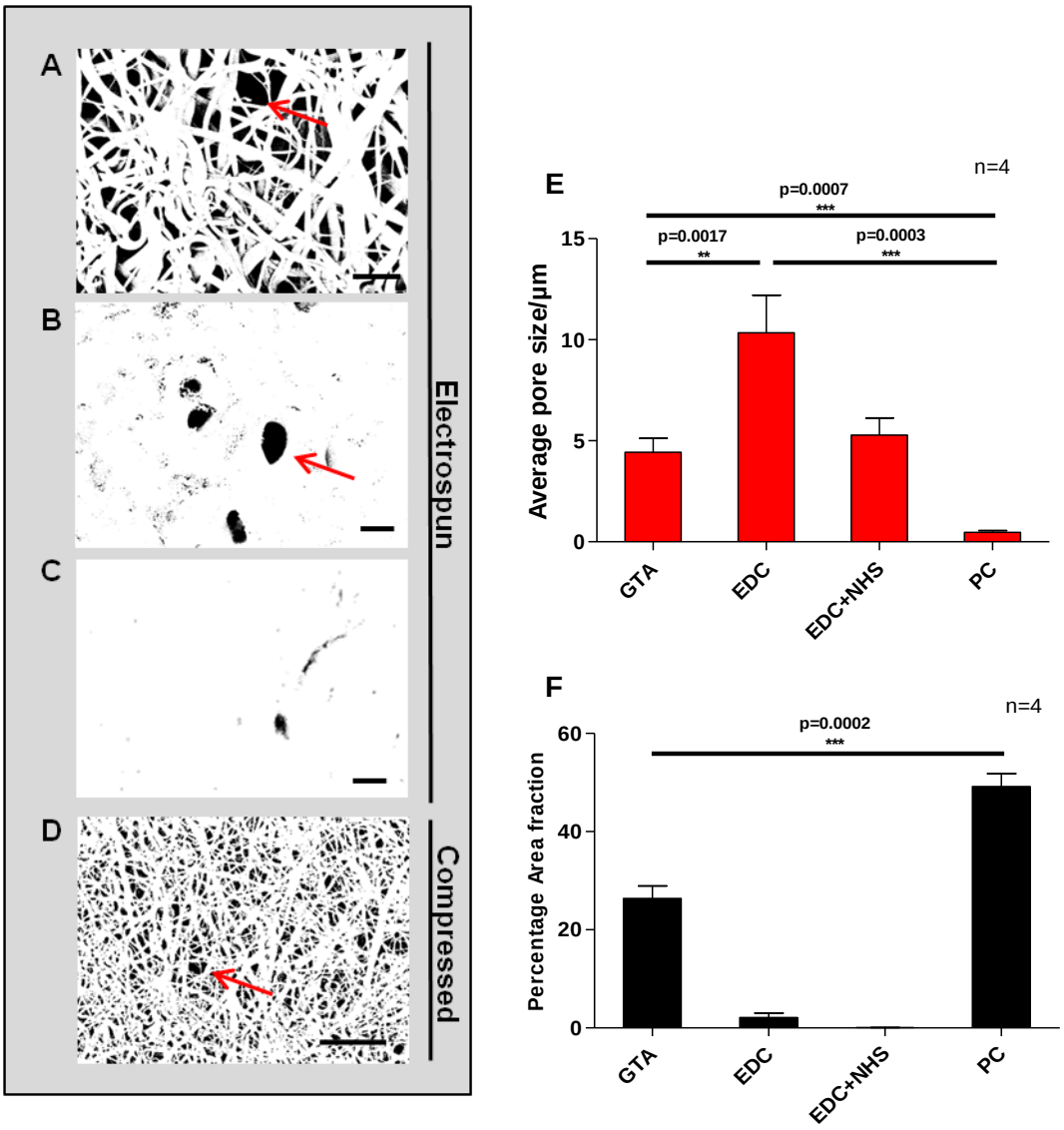

Figure 3.7: Physical Properties of Electrospun and Compressed collagen fibres. Constructs that are suitable for eventual transplantation into the eye, need to allow cell adhesion, influenced by porosity and pore size (red arrow), as well as permitting the passage of light. Porosity was measured from electron micrographs and imageJ software, where average pore size and area fraction was determined over the whole surface area, through the conversion of SEM images to black and white binary figures. Porosity levels were measured for **A)** 15% GTA, **B)** EDC, **C)** EDC+NHS electrospun scaffolds and **D)** compressed collagen scaffolds. Pore numbers were sparse for scaffolds processed with EDC treatments. Analysis of pore **E)** number and **F)** volume showed that the size when present was greater in EDC matrices than GTA crosslinked scaffolds and compressed scaffolds. This suggests that the original distance between the fibres may have been large, prior to fusion. GTA and compressed collagen scaffolds generated small pores with high frequencies. However, compressed collagen matrices had markedly higher pore density, as well as smaller sizes. (Scale bar=10µl)

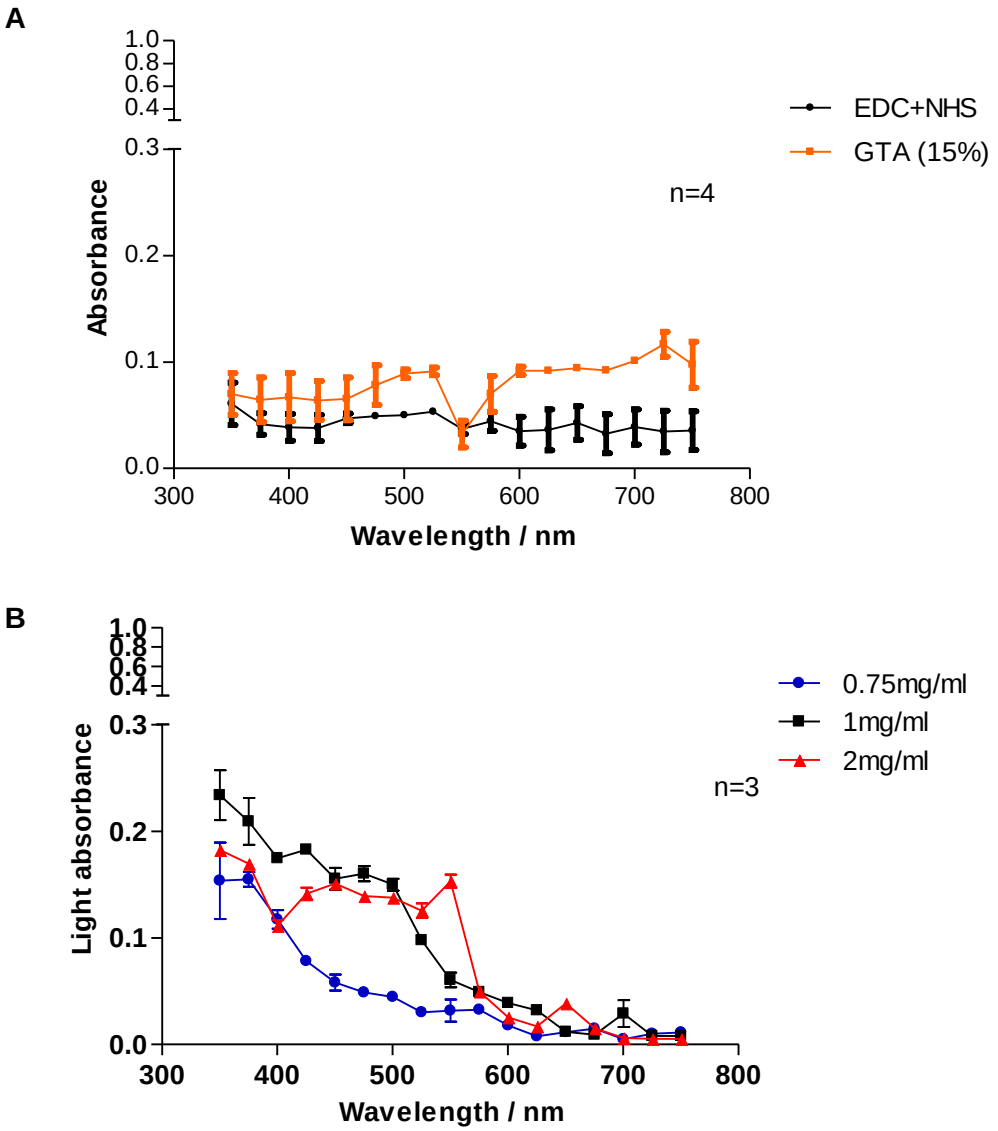

Figure 3.8: Optical Properties of Electrospun and Compressed collagen fibres. Constructs that are suitable for eventual transplantation into the eye, need to permit the passage of light through, for which we assessed optical density as an indicator of this function. The optical density of the various collagen scaffolds was determined over a range of 350nm-750nm using a spectrophotometer. The extent of visual light absorbance by **A)** electrospun scaffolds was negligible, indicating no significant hindrance of visual light absorbance. However, the degree of absorbance observed by **B)** compressed collagen fibres did demonstrate an increased level of absorbance within the shorter wave lengths (between 350-575nm)which indicates some absorption in the blue-green range of the visible spectrum.

3.3.5. Ability of Collagen Scaffolds to Support Cell Adhesion, Growth and Differentiation

Following examination of their physical characteristics, scaffolds were studied for their ability to support cells adhesion, growth and differentiation. Initially the extent of cellular adhesion on collagen scaffolds were examined by light microscopy for electrospun (Figure 3.9) and compressed (Figure 3.10) collagen scaffolds, over a 7 day culture period. Phase-contrast microscopy showed the biological capabilities of the cellular scaffolds, as indicated by their ability to support cell adhesion. Larger numbers of cells were shown to adhere onto scaffolds prepared by electrospinning collagen for 2hours, as compared with 1 hour. This indicates that cell adherence is dependent on the number of fibres within the scaffolds structure (Figure 3.9). Distinct focal adhesions were observed under SEM by both electrospun (Figure 3.11 A and B) and compressed collagen scaffolds (Figure 3.11 C, D, c and d), where they appeared to form long processes along the fibres. The close matrix-cell relationship established by the different scaffolds suggests that collagen is a suitable material for cellular scaffolds as it promotes cell adhesion and growth. Both electrospun and compressed collagen scaffolds were then examined for their ability to support Müller stem cells differentiation into RGCs. For this purpose cells were cultured in the presence the Notch1 inhibitor DAPT and bFGF for one week. These conditions had been previously shown to induce RGC differentiation and had been refined in initial experiments presented in this thesis in our laboratory (Singhal et al., 2012). Cells cultured with DAPT and bFGF adhered to collagen scaffolds; with SEM illustrating the capacity of the different fibres assisting in the formation and maintenance of neurite projections (Figure 3.11A, C and c). The adaptation to a neural morphology

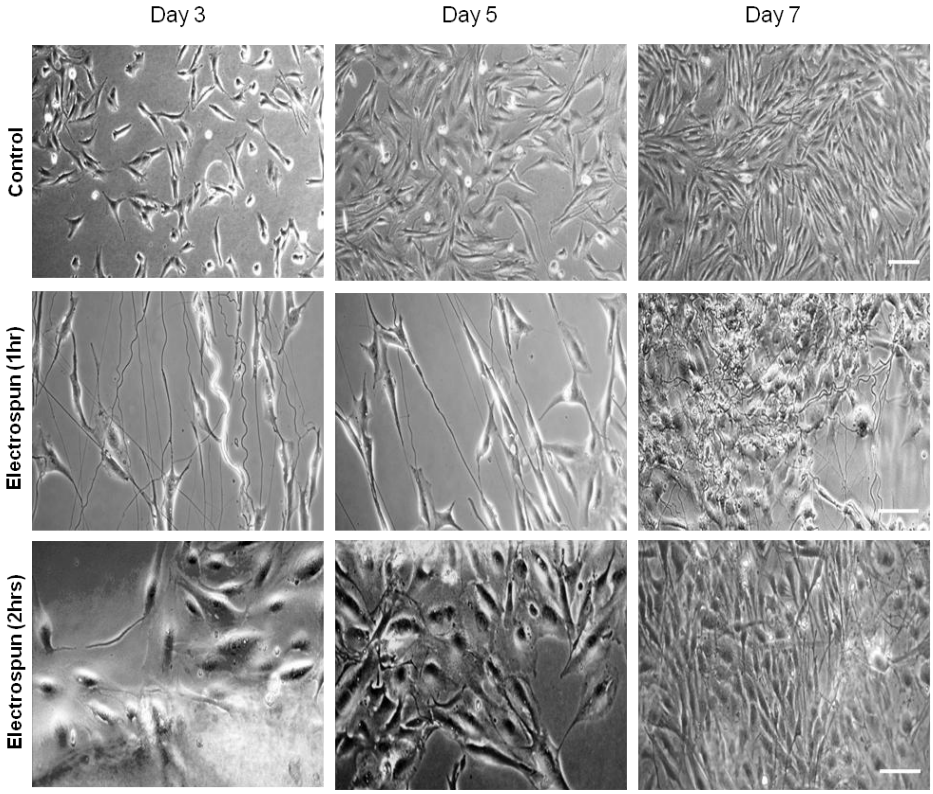

Figure 3.9: Light microscopy appearance of Müller stem cells grown on electrospun collagen fibres. Cells adhered to collagen scaffolds, with fibres assisting in the cell adhesion, viability and maintenance of cellular viability, over the course of 7 days culture. Phase contrast images under light microscopy of cells cultured in the absence of collagen matrices. Phase contrast image under light microscopy of cells cultured in the presence of collagen fibres, electrospun for 1 hour. Phase contrast image of cells cultured in the presence of collagen fibres, electrospun for 2 hours. Scale bar= 100µm

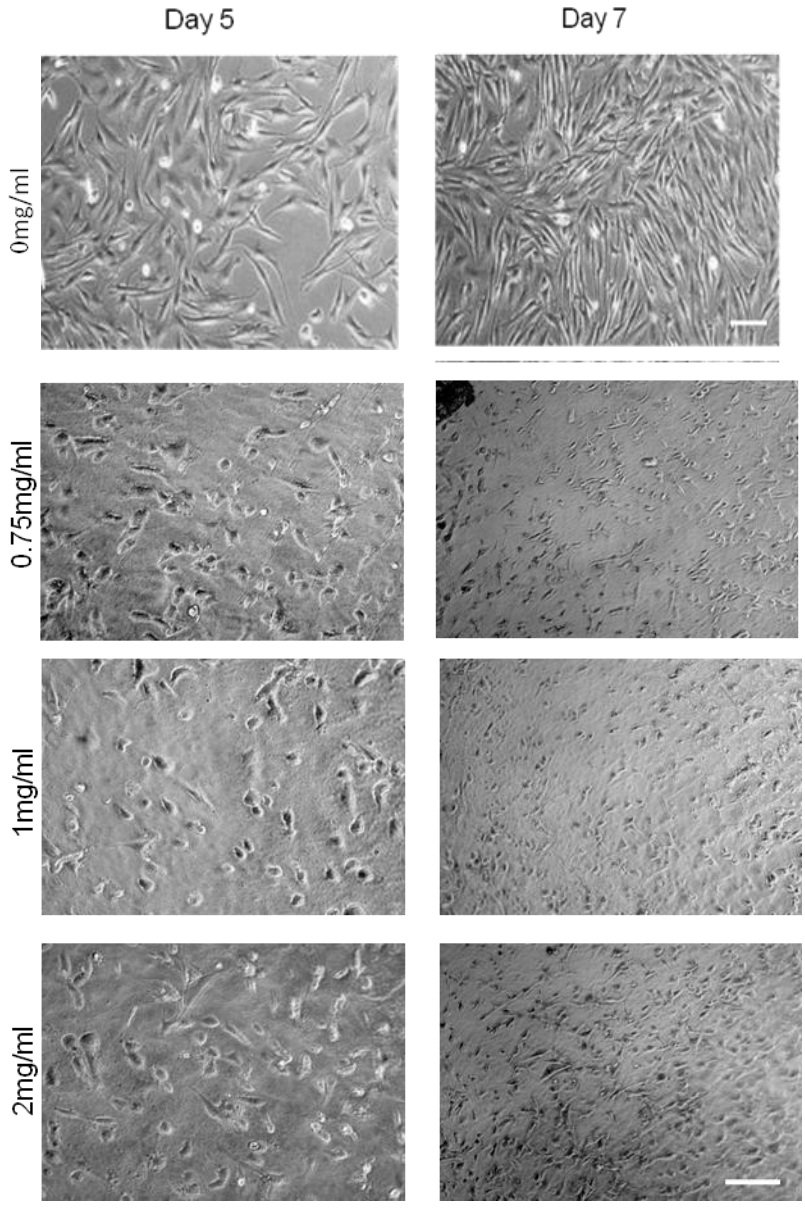

Figure 3.10: Culturing of Müller stem cells on Compressed Collagen scaffolds over 7 days. Kholer illumination showed that cells were able to adhere to PC collagen constructs over a 7 day period coupled with a decreasing collagen concentration, under control treatments. Cells cultured on 0.75mg/ml collagen, on 1mg/ml and cultured on 2mg/ml collagen scaffolds. Cells firmly adhered to the collagen constructs, with a flattened morphology and maintained growth over the 7 day culture period. Scale bar =100µm

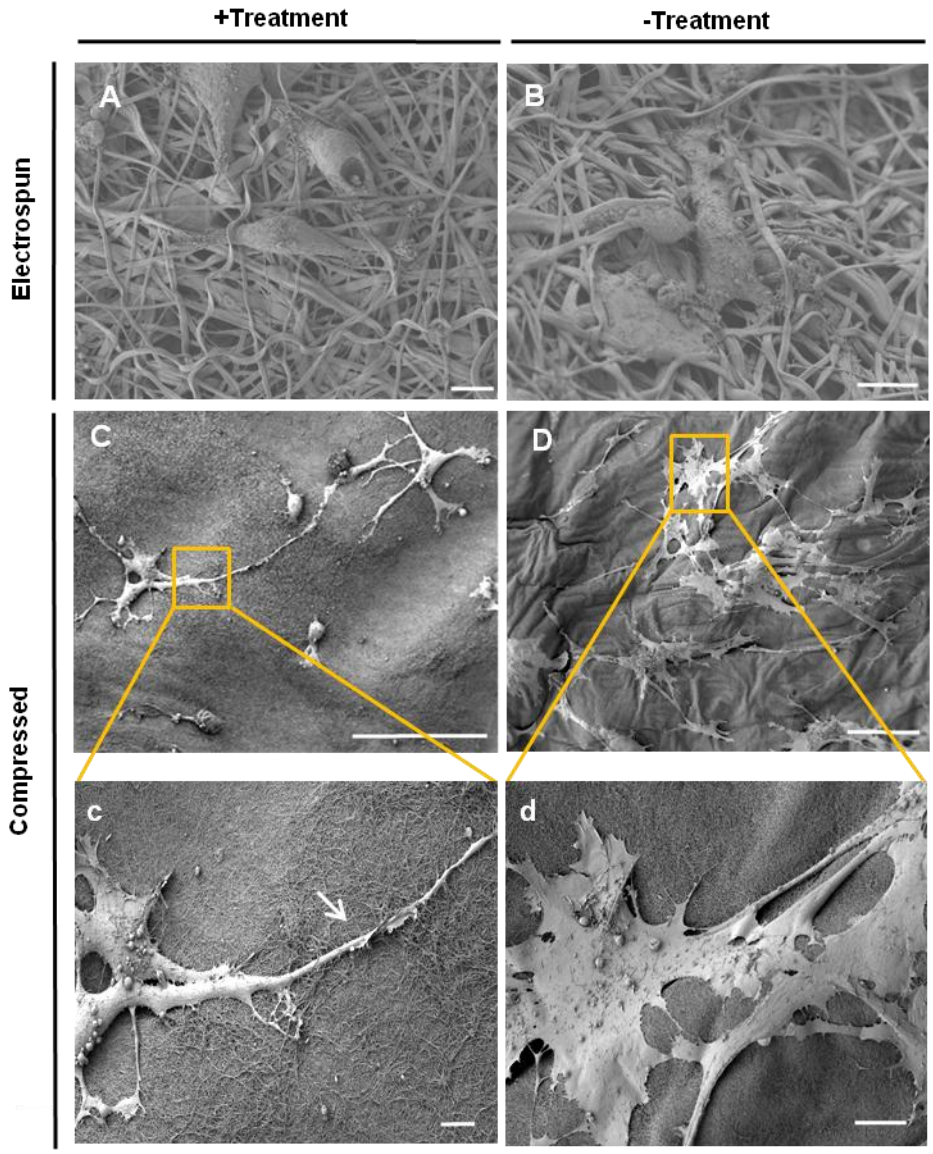

Figure 3.11: Matrix-cellular interaction between Müller stem cells and type I collagen scaffolds. Scanning electron-microscopy showed that cells developed long processes resembling axonal processes and neurites, which firmly attached to the collagen scaffolds cultured for 5 days. Cells cultured in the presence of DAPT and bFGF formed long cellular projections resembling axons and neurites, indicated by white arrows. In the absence of DAPT and bFGF, cells firmly adhered to the collagen constructs, but their morphology showed a characteristic flattened morphology (Figs B,D,d). A and B illustrate electrospun scaffolds crosslinked with 15% GTA. C,D,c and d illustrate compressed scaffolds. Figs c and d are magnifications of Figs C and D respectively to show adhesion details. Scale bar =A-B: 100µm: C-D:100µm; c and d:10µm

by the Müller stem cells is shown by the formation of long axonal processes into and along the fibres of compressed and electrospun scaffolds.

Acquisition of neural morphology by Müller stem cells cultured on type I collagen scaffolds was also shown by immunocytochemistry (Figure 3.12-3.16). GFP labelled Müller stem cells transfected with the lenti-viral GFP vector were seeded onto the scaffolds and cultured for 7 days (Figure 3.12). Cells were shown to adhere and form long cytoplasmic projections on electrospun collagen. Staining enabled labelled cells to be examined for any changes in morphology and phenotype. Müller stem cells cultured for 7 days on compressed and electrospun collagen scaffolds acquired neural-like morphologies, judged by their adoption of discrete and defined axonal projections. To determine whether cells cultured on the scaffolds differentiated into RGCs, they were stained with antibodies with mature RGC markers including HUD, ISLET-1, BRN3B and RT97.

Whilst GFP labelled cells showed morphological changes characteristic of neural development (Figure 3.12). It was not possible to determine whether It was not possible to identify the expression of RGC markers by Müller stem cells cultured on electrospun collagen scaffolds in the presence of DAPT and bFGF due to the intense autofluorescence observed in these scaffolds (Figure 3.13). This was ascribed to the non-specific binding of antibodies to the electrospun scaffolds, combined with their underlying autofluorescence (Figure 3.13B). Moreover, collagen itself is autoflourescent and it is ionically charged, which causes binding of antibodies in a non-specific manner. The intensity of fluorescence observed in electrospun scaffolds could also be attributed to the chemical crosslinking agent GTA. A protocol was used to quench this autoflorecence, where scaffolds were crosslinked with the minimum concentration of GTA vapour possible (15%), followed by vigorous washing with deionised water for 24 hours to remove excess GTA. Glycine (0.1M) and sodium borohydride were then added to remove autoflorescence.

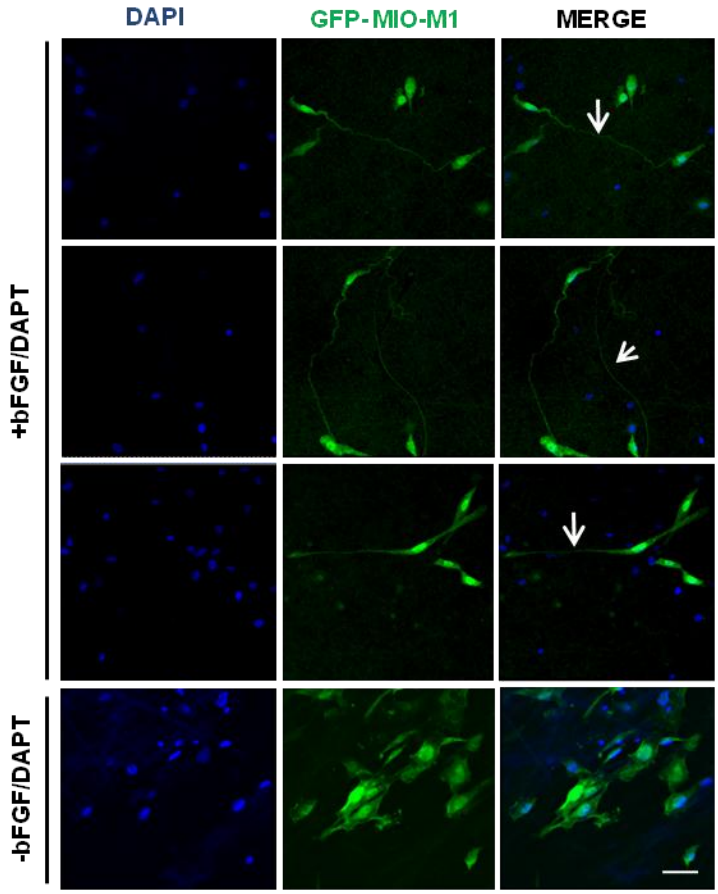

Figure 3.12: Morphological changes of Müller stem cells cultured on 15% GTA crosslinked electrospun collagen matrices in the presence of DAPT and bFGF. Acquisition of neural morphology by Müller stem cells cultured on type-I collagen scaffolds was shown by immunofluorescence analysis of GFP labelled Müller cells (green) seeded onto the scaffolds. Cells adhered and formed long cytoplasmic projections in the presence of bFGF (20ng/ml) and the Notch inhibitor DAPT (50ng/ml). DAPI staining (blue) positively identified the nuclei of florescent cells, whilst the green fluorescence showed the neuronal morphology of differentiated cells (white arrows). Scale bar=75µm

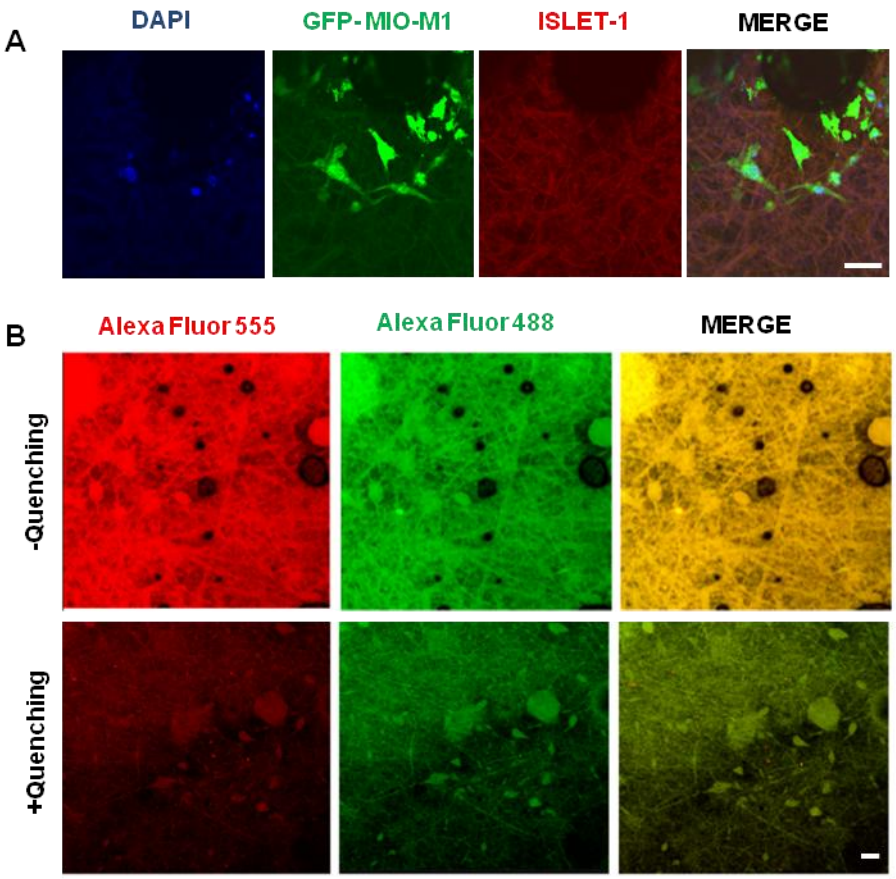

Figure 3.13: Immunofluorescence analysis of Müller stem cells cultured on electrospun collagen matrices in the presence of DAPT and bFGF. A) Müller stem cells cultured on electrospun collagen and stained for the RGC marker; Islet-1, wihich was not identified within cellular populations. Electrospun collagen crosslinked with 15% GTA exhibited non-specific secondary antibody binding. Identification of Müller stem cell differentiation into RGCs was not possible on these substrates due to autofluorescence. **B)** Sodium borohydride was used to quench the non-specific fluorescence observed by electrospun scaffolds. Glycine was used before quenching to bind any charged collagen molecules to prevent non-specific antibody binding. Quenching protocols had no significant effect. Scale bar= 100µm

However, this process only partially quenched the fluorescence but did not allow visualisation of specfic staining. Hence, to specifically show cellular expression of any protein marker in these scaffolds, the background of autofluorescence needs to be significantly reduced.

In contrast to electrospun collagen scaffolds, Müller stem cells cultured on compressed collagen in the presence of DAPT and bFGF, showed significant morphological changes. GFP labelled Müller stem cells were cultured in the absence of PC collagen scaffolds, as well as in the absence of differentiation factors (DAPT and bFGF) (Figure 3.14). These controls enable the comparsion between the expression of cells cultured in the presence of collagen and differentiation conditions. They also made possible the identification of phenotypic changes. Differentiated cells showed positive staining for markers of RGC precursors, when compared to untreated controls in the presence of compressed collgen (Figure 3.15A). Confocal microscopy demonstrated the expression of RGC markers expressed by Müller stem cells cultured on 0.75mg/ml PC collagen in the presence of DAPT and bFGF. Müller stem cells transfected with a lenti virus GFP adhered to collagen substrates in the presence or absence of DAPT and bFGF. Differentiation of cells into RGCs was confirmed by their co-expression of GFP and mature RGC markers HUD and ISLET-1 and the RGC precursor marker BRN3B. Staining for BRN3B, HUD and ISLET-1 was localised to the nuclei of the cells (Figure 3.15B). Cells were also counted for RGC marker expression compared to controls without DAPT+bFGF and compressed collagen scaffolds (Figure 3.16).All the RGC markers were significantly increased compare to controls. β-3-TUBULLIN and RT97 staining was localised within the cytosol along the length of the neurite outgrowth. Cellular projections were coupled with the enriched expression of both neural filament makers, signifying the development of axons. This suggests that compressed collagen substrates are able to support and maintain axonal growth and Müller stem cell differentiation (Figure 3.17).

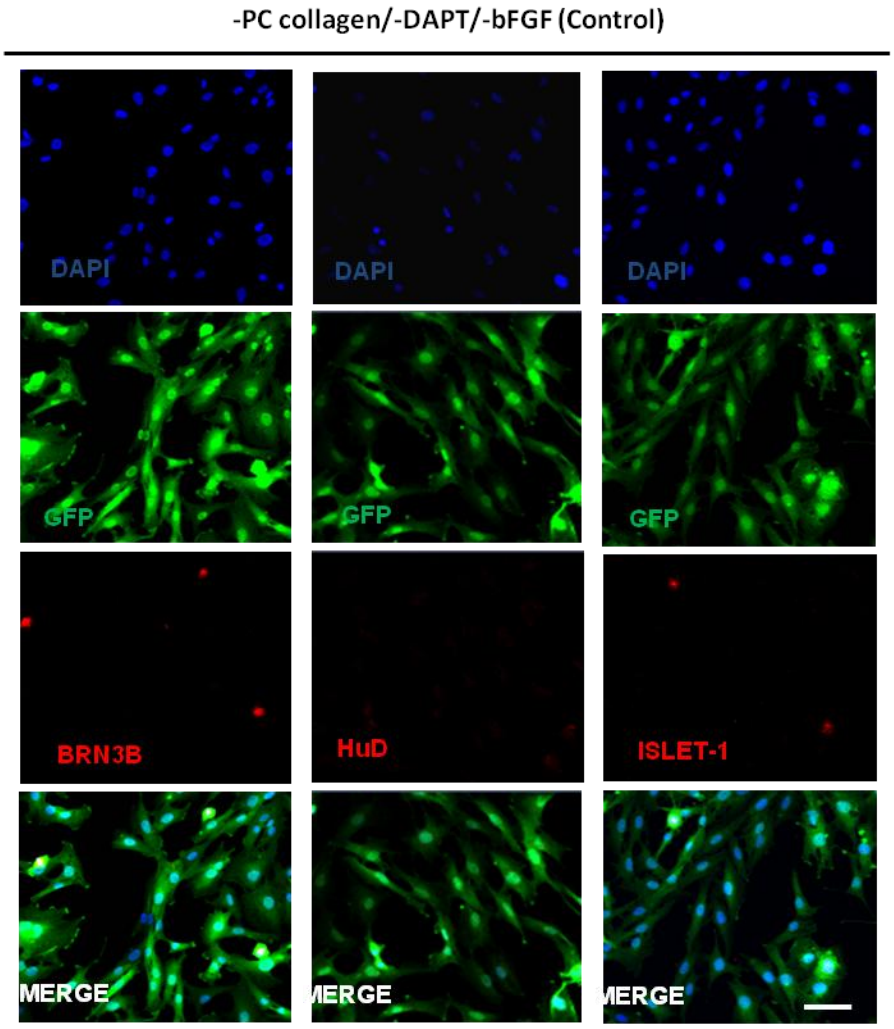

Figure 3.14: Müller stem cell expression of RGC markers in the absence of PC collagen constructs. Confocal microscopy demonstrated the expression of RGC markers expressed by Müller stem cells cultured under control conditions for 7 days. Human Müller stem cells (hMSC) transfected with a lentivirus GFP (green) grew in the absence of DAPT/ bFGF and PC collagen. Control conditions were compared to differentiation of cells into RGC, in order to determine the extent of RGC maturation using the markers ISLET-1, HuD and the RGC precursor marker BRN3B. Scale bar=50µm.

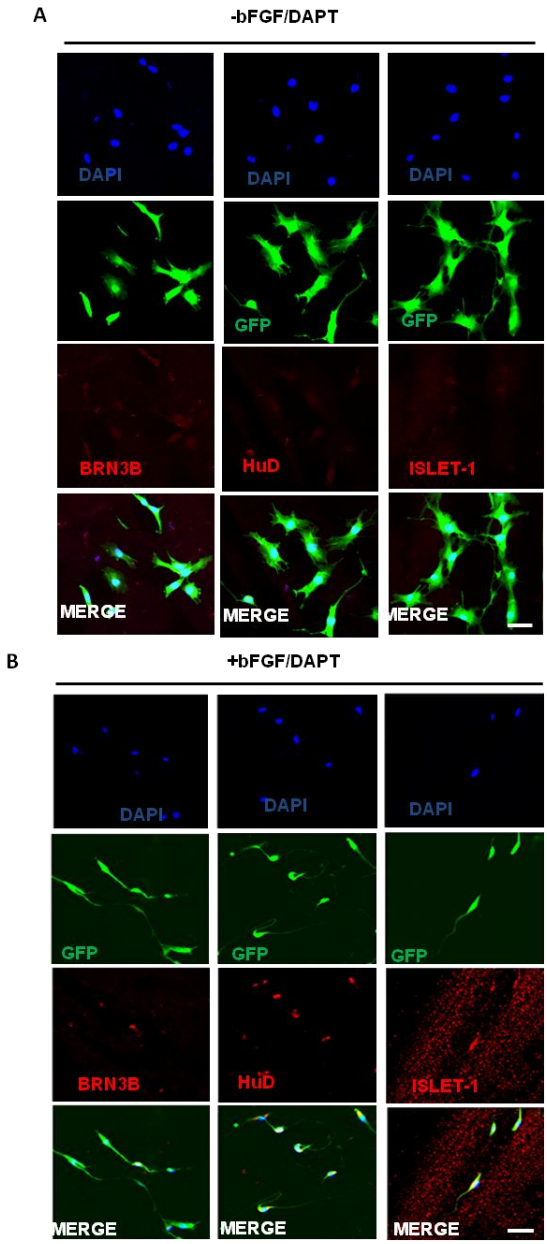

Figure 3.15: Müller stem cell differentiation and expression of RGC markers on PC collagen constructs. Confocal microscopy demonstrated the expression of RGC markers expressed by Müller stem cells cultured on 0.75mg/ml PC collagen in the presence of DAPT+bFGF for 7 days. Human Müller stem cells (hMSC) transfected with a lentivirus GFP (green) readily adhered to collagen substrates in the presence or absence of DAPT and bFGF. Differentiation of cells into RGC was confirmed by their co-expression of GFP, mature RGC markers HUD and ISLET-1 and the RGC precursor marker BRN3B when compared to controls. **A)** Müller stem cells cultured with bFGF and DAPT on compressed collagen constructs. **B)** Müller stem cells cultured in medium alone, without differentiation factors. Scale bar=50µm.

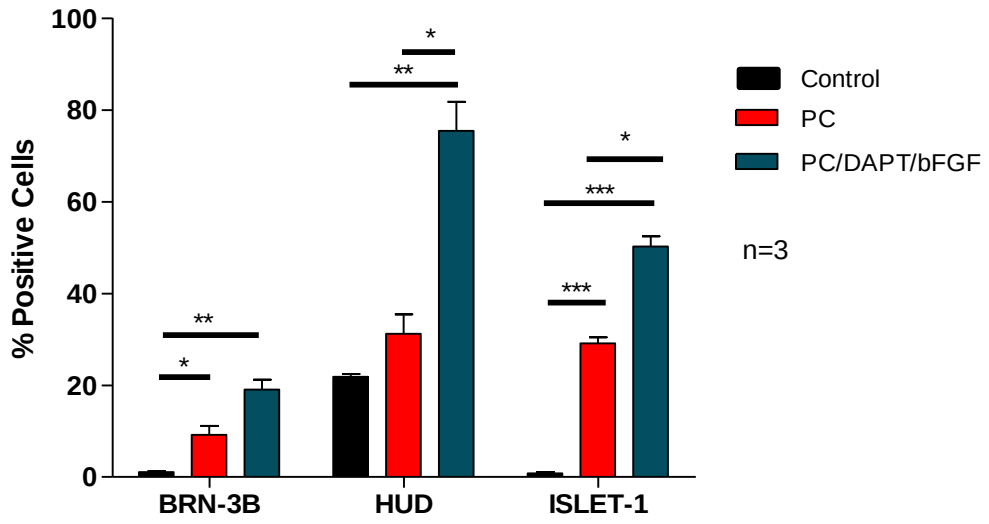

Figure 3.16: Graphic representation of Müller stem cell differentiation and expression of RGC markers on PC collagen constructs. The confocal microscopy demonstrated the expression of RGC markers expressed by Müller stem cells cultured on 0.75mg/ml PC collagen in the presence of DAPT+bFGF for 7 days. Differentiation of cells into RGCs was confirmed by their co-expression of GFP, mature RGC markers HUD and ISLET-1 and the RGC precursor marker BRN3B when compared to controls. Cells which positively expressed the RGC markers were counted, in the presence of PC collagen with or without differentiating factors. Comparison to no treatment and absence of PC collagen RGC marker expression was markedly increased in the presence of PC collagen either in the presence or absence of DAPT+bFGF.

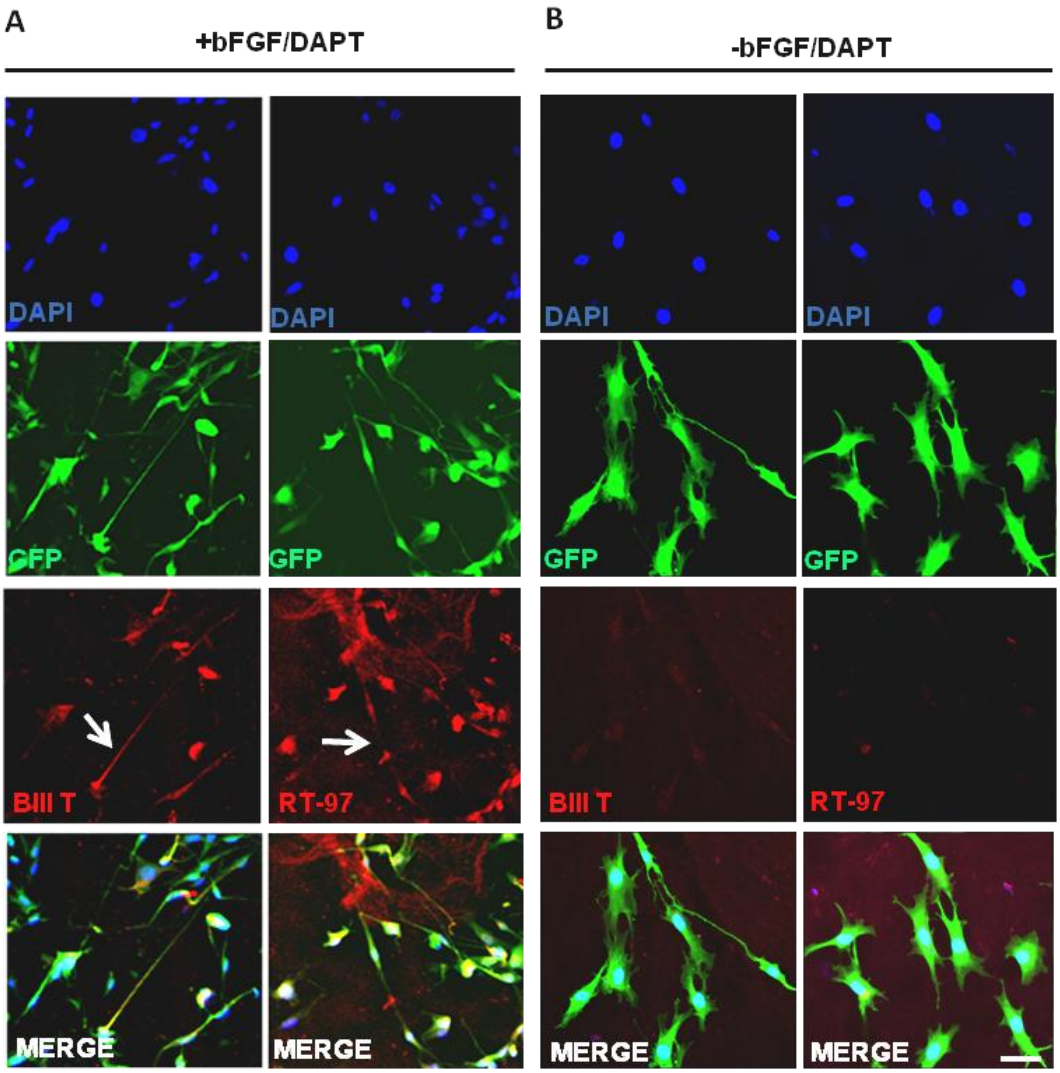

Figure 3.17: Müller stem cell differentiation and expression of neural markers upon culture on PC collagen scaffolds in the presence of DAPT and bFGF. Confocal microscopy demonstrated the upregulation in Müller stem cells of neural filament markers (ß-III Tubulin and RT-97), associated with axonal development. **A)** GFP labelled Müller stem cells (green) cultured for 7 days, in the presence of compressed collagen scaffolds (0.75mg/ml) and DAPT+bFGF developed neurite outgrowths (white arrows), stemming from pronounced cell bodies. Cellular projections were coupled with the enriched expression of both neural filament makers, signifying the development of axons. This suggests that compressed collagen substrates are able to support and maintain axonal growth and Müller stem cell differentiation. These were compared to **B)** controls, which lacked pronounced cytoplasmic outgrowths and did not express ß-III Tubulin or stain for RT97. Scale bar=50µm.

These observations indicate that collagen scaffolds can support and help guide cellular differentiation and behaviour of Müller stem cells.

Cellular toxicity of collagen scaffolds was examined over a seven day period. Cells were cultured on collagen scaffolds prepared under different protocols. These included electrospun scaffolds crosslinked by three different methods. Different concentrations of GTA vapours were used to crosslink the collagen microfibres for 72 hours, followed by thorough rinses with deionised water prior to seeding cells. A measure of cellular viability was obtained for each concentration of GTA using the Hexosaminidase assay to assess cell viability following collagen digestion.

There were no significant differences in cell viability between cells cultured on scaffolds crosslinked with low GTA concentrations (5-10%) and cells cultured on ECM or non-ECM coated plates (no matrix controls) (Figure 3.18A). This suggests that electrospun collagen scaffolds supports growth and viability of Müller stem cells. In contrast, cells grown on 25% GTA crosslinked scaffolds showed a marked decrease in cell viability as determined by Hexosaminidase assays readings. This suggests that GTA induces cell toxicity in Müller stem cells at concentrations above 10%. GTA has been repeatedly reported to be a toxic agent and deemed unsuitable for biomedical applications, including crosslinking proteins. On this basis, the study investigated other methods of collagen crosslinking. EDC in combination with NHS was assessed for their affect on cellular viability. The Hexosaminidase assay was again used to examine the amount of viable cells in the presence of EDC crosslinked collagen matrices (Figure 3.18B), where no differences were recorded. This data indicates that use of EDC does not modify cell growth and viability, suggesting that these agents are non-toxic to Müller stem cells in culture. Examination of cellular viability on collagen compressed scaffolds demonstrated a lack of toxicity indicating

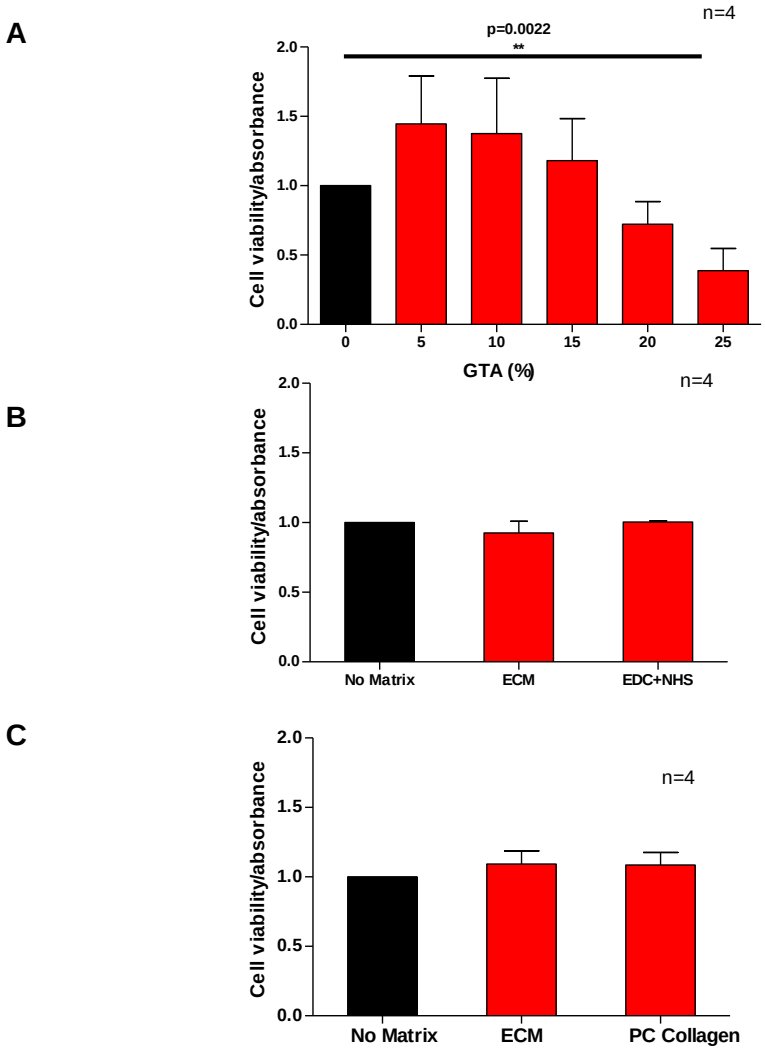

Figure 3.18: Müller stem cell viability following culture on collagen-based scaffolds. Müller stem cells were cultured on **A)** GTA cross-linked scaffolds, **B)** EDC+NHS crosslinked scaffolds and **C)** compressed collagen scaffolds for one week. Viability was assessed using the Hexosaminidase assay, based on the uptake of the enzymatic substrate by the lysosomes of living cells. Absorbance readings were normalised to no matrix controls and ECM (extracellular matrix). Different concentrations of GTA vapours were used to cross-link the collagen fibres. A significant decrease in cellular viability was observed with cells cultured on 25% GTA crosslinked collagen when compared to cells grown on no matrix controls following collagen degradation with collagenase D. Significant changes in cell viability were not detected in Müller stem cells cultured on 0.75mg/ml compressed collagen or electrospun EDC crosslinked collagen scaffolds.

these scaffolds support Müller stem cells for transplantation (Figure 3.18C). This study indicated that there was no alteration to cellular proliferation.

3.3.6. Comparison between the Mechanical Handling of Electrospun and Compressed Collagen Scaffolds

To ensure delivery of scaffolds, aimed at cell transplantation into the eye, scaffolds must be able to exhibit plasticity, to endure physical manipulation through cannulas used for retinal surgery. The relatively easy handling of GTA crosslinked scaffolds were shown to be comparable to human retinal explants. However, depending on the thickness of the collagen scaffolds resulting from different periods of electrospinning (up to 2 hours), scaffolds demonstrated different strengths when handled. Thin electrospun scaffolds did not withstand handling and were unable to pass through the lumen of an 18G cannula. These were fragile and became damaged by gentle mechanical manipulation. Moreover, the rigidity possessed by GTA crosslinked scaffolds made passage through an 18G cannula inconsistent and resulted in damage of the scaffold's structure (Figure 3.19).

EDC crosslinked electropspun scaffolds altered their macroscopic features when hydrated. They acquired a gelatinous consistency that changed their structural integrity. This gelatinous structure made cell culturing as wells as manipulation impossible and therefore they could not be considered as a tool for retinal transplantation.

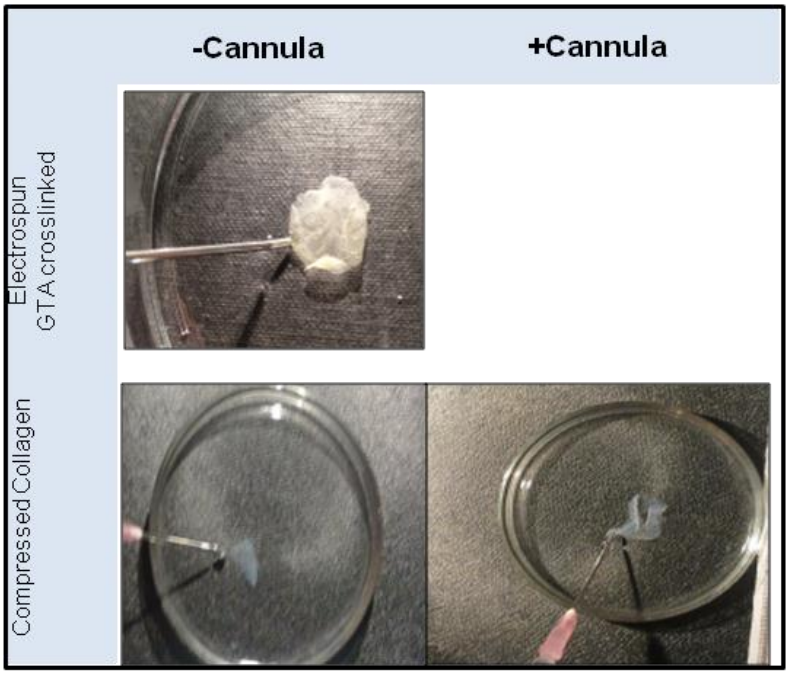

Figure 3.19: Mechanical properties of collagen-based scaffolds. Vitrectomy surgeries were performed via 20G ports where PC collagen scaffolds require entry into the eye via 18G cannulas. Both compressed and GTA crosslinked electrospun scaffolds were examined for their ability to enter the lumen of an 18G cannula. GTA crosslinked scaffolds failed to enter the lumen, whilst 0.75mg/ml compressed collagen scaffolds were able to withstand entry and expulsion from the lumen. Compressed collagen matrices of 0.75mg/ml, were shown to endure physical manipulation through an 18G cannula.

3.3.7. Ability of compressed collagen scaffolds to retain adherent cells for transplantation following passage through an 18G cannula

Compressed collagen scaffolds retained their shape and structural integrity through handling (Figure 3.20). Compressed collagen scaffolds demonstrated a suitable strength that can be modified in size, and were sufficiently elastic to return to its original shape following mechanical manipulation. This finding suggested that compressed collagen was a suitable candidate for *in vivo* cell transplantation on the inner retinal layer.

3.4. Discussion

The primary objective of this study was to examine the suitability of collagen-based scaffolds for transplantation of Müller stem cell-derived RGC precursors onto the inner retina. The study involved the examination of the physical and biological attributes of the collagen scaffolds produced. Engineering tissues to support cells either within or on biocompatible matrices is currently being applied to design regenerative treatments for pathologies affecting a wide range of tissues. The use of natural proteins to mimic such tissues emphasises the importance not only of restoring tissue architecture but also function, and therefore the arrangement of cellular frameworks may help to guide cell behaviour. Topological variations between different mature ECM networks centre on the cellular population that it contains. It is therefore important to consider the native organisation of tissues in need of repair. It has been reported that fibre alignment, topology and hierarchical arrangement of fabricated biomaterials is distinctly related to cell attachment and growth (Kureshi et al., 2010). Since the level of function by a protein is defined at the molecular level, the understanding of collagen scaffold structure and plasticity were important for this study. Evaluation of the physical attributes of the collagen scaffolds designed demonstrated different properties imparted by electrospininning and crosslinking agents, as

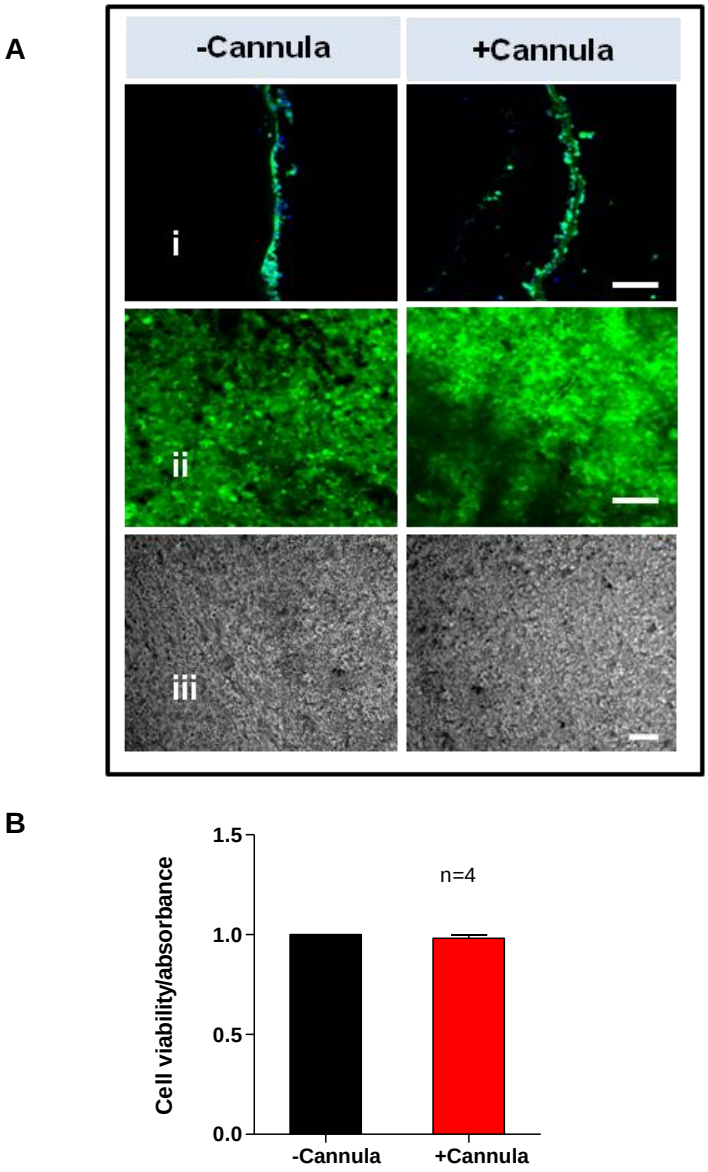

Figure 3.20: Cell numbers following *in vitro* manipulation with an 18G cannula. Vitrectomy surgeries were performed via 20G ports where PC collagen scaffolds require entry into the eye via 18G cannulas. **A)** 20,000 GFP labelled Muller stem cells, were seeded onto 0.75mg/ml compressed collagen matrices (0.5cm diameter) for 2 hours. Compressed collagen scaffolds were examined for topology and cell presence under confocal microscopy i) transverse sections ii) and iii) whole mount preparations. Phase contrast was also used to assess cell numbers and scaffold topology prior to and following manipulation. **B)** The Hexosaminidase Assay was used to examine the extent of cell loss following mechanical manipulation. There was no significant difference in cell viability between the scaffolds that underwent manipulation and those that did not.

well as plastic compression. GTA crosslinking procedures, as well as compression rendered the collagen fibrils insoluble in water, facilitating culturing regimes and manipulation *in vitro*.

The electrospinning process used in this study showed to be an easy method for preparation of collagen scaffolds for retinal cell transplantation. Relatively high voltages were required to overcome the surface tension created by the high viscosity of the biomaterial solutions. To overcome blebbing and irregular surfaces on the electrospun fibres, HFIP was identified as the most appropriate solvent for electrospinning collagen. It is possible that acetic acid used to suspend collagen lead to destabilisation of the triple helix structure. Damage to this structure may have therefore changed the spinning properties needed for producing suitable fibres. HFIP did not appear to denature collagen from its native form, but instead stabilise its conformation in solution, hence preserving the natural fibrillar structure of the collagen molecules whilst being stretched, favouring a uniform, fluid stream of fibres (Figure 3.3). The parameters used to electrospin rat tail type I collagen in HFIP were consistently reproducible. This enables fibres to be continuously fabricated to exhibit similar physical dimensions, unlike collagen solutions made with acetic acid. This provided the important initial step in the standardisation of electrospun collagen fibre production.

Following electrospinning, fibres required crosslinking to ensure their integrity upon hydration. Crosslinking acts to strengthen electrospun collagen fibres and facilitates the design of artificial 3D collagen matrices, suitable for maintaining cells *in vitro* and *in vivo*. For this study GTA was used as a crosslinking agent. This is a well-known fixative that produces insoluble crosslinked protein aggregates (Khadka and Haynie, 2010). It acts by creating cross bridges between protein molecules rather than producing weaker intramolecular (hydrogen) bonds, between the carboxyl groups of reactive side lysine residues. EDC was also examined for its crosslinking

efficiency either alone or in combination with NHS. However, subsequent generation of scaffolds using this agent proved inconsistent, as sufficient crosslinking was not always observed. Although EDC and NHS catalysed the formation of crosslinks within collagen scaffolds, the mechanism involved in this form of catalytic crosslinking is not fully understood. The links created originate from the catalytic activity of EDC, and its ability to crosslink free amine groups on proteins, specifically lysines, arginines and hydroxylysines. The lack of robustness observed with this crosslinker may be due to its limited interactions with the internal collagen fibrils of the scaffold. The initial incubation of spun fibres with EDC may have led to the crosslinking and fusion of fibrils on the surfaces of electrospun scaffolds. This may have created sealed matrices and prevented sufficient penetration of these agents, rendering scaffolds structurally weak. These crosslinked scaffolds may appear to have been sufficiently stable under dry conditions, however hydration lead to loss of fibre structure. Further work may be performed to crosslink fibrils with EDC as they are being drawn (Beachley, 2009). This could involve direct fibre submersion into an EDC solution, alongside the electrospinning process. Thinner scaffolds may also limit the generation of sealed scaffolds, which could compromise structural integrity and difficulty in handling the constructs for ocular implantation.

Compression of collagen hydrogels allows formation of high collagen density fibrils without compromising the macroscopic structure. Hydrogels are readily modified by cells (Eastwood et al., 1996) demonstrating their inherent weakness. Expulsion of water from collagen hydrogels led to randomised crosslinks between collagen fibrils, and constitutes an alternative method for rapid preparation of collagen scaffolds. Compressed collagen scaffolds supported *in vitro* culture of Müller stem cells (Figure 3.9 and 3.10) as well as facilitated mechanical manipulation for transplantation (Figure 3.19). The physical crosslinks between polymerised fibrils following compression generated tightly packed fibres (Figure 3.6). The process created collagen

networks resembling the native ECMs, and revealed hierarchy of fibrillar organisation.

The porosity of the collagen scaffolds varied between methods used for their production. The physical porosity of electrospun scaffolds was dependent on the crosslinker used (Figure 3.7). EDC protocols reduced the amount and size of the pores on the electrospun scaffolds. The apparent low number and size of pores may be ascribed to the fusion of fibres on the surfaces of the scaffolds, which could impact on the adherence and survival of Müller stem cells during and after implantation. GTA crosslinked scaffolds conserved the porosity of the constructs suggesting that this is a suitable agent for retaining ECM-like structures that support cellular adhesion and proliferation. Pores have been shown to play a vital role in bioengineering, where specific cell populations tend to have increased affinities for porous scaffolds (Wray et al., 2011, Guldberg et al., 2008, Lai et al., 2012). This feature also impacts on the diffusion of nutrients into and out of the scaffold matrices. Moreover, porous structures would favour drug or bioactive reagent release, as well as cellular support within the internal matrix of a scaffold. Low concentrations of GTA (<10%) did not prevent cell growth, as determined by the hexosaminidase assay to assess cell viability (Figure 3.18). This suggests that the porosity of scaffolds is not a determining factor for Müller cell adhesion and survival. Although, matrices supported normative growth of the Müller populations, without significant differences, increasing GTA concentration caused a decrease in cell growth. This suggests that GTA scaffolds may encourage immunogenic and inflammatory responses following implantation. It is possible that hydrolytic degradation of collagen constructs crosslinked with GTA may lead to the eventual release of residual cytotoxic chemical derivatives. This would induce cell toxicity within the microenvironment whether *in situ* or *in vivo*.

Optical density of the constructs indicated that they allow the passage of visible light through their matrices (Figure 3.8A and B), suggesting that spun fibres would not prevent light reaching the retina following scaffold implantation. Therefore photoreceptors would be able to transduce their sensory information to the brain without disruption. This attribute of collagen scaffolds is important when considering implantation onto the light sensitive retina, and demonstrates that these scaffolds exhibit appropriate features for transplanting retinal cells.

Subsequently, the relationship between matrix and cellular populations was also analysed under SEM, which confirmed close matrix-cell interactions with GTA crosslinked and compressed collagen scaffolds. The ability of the collagen scaffolds to support cell growth and differentiation was determined by light (Figure 3.9 and 3.10), electron (Figure 3.11), confocal microscopy (Figure 3.12-3.17) and hexosaminidase assays (Figure 3.18). Both, GTA crosslinked and compressed collagen proved to promote adherence and growth, whereas RGC differentiation of Müller stem cells was well identified on compressed scaffolds. Compressed and GTA crosslinked collagen scaffolds facilitated the development of neurite outgrowths by Müller stem cells cultured under differentiating conditions. Long axonal processes were identified under SEM and confocal microscopy, with primary and secondary dendrites on these cells observed on the scaffolds (Figure 3.11).

To examine the differentiation of Müller stem cells on collagen matrices, staining was performed. Confocal microscopy illustrated morphological changes as compared with untreated populations, as well as the expression of RGC markers. Proteins typical of RGCs were enriched in cultures undergoing Notch inhibition in the presence of bFGF on compressed substrates. In contrast the determination of RGC maturation of Müller cells grown on GTA matrices was not possible due to the autofluorescence exhibited by these scaffolds. Singhal et al designed a Brn3b reporter to

indicate the differentiation of Müller stem cell derived RGCs both *in vitro* and post transplantation in rodent ocular tissue (Singhal et al., 2012). This method could be used in the future to identify differentiation of Müller stem cells on GTA crosslinked scaffolds by highlighting cells that expressed Brn3b and had undergone neural differentiation.

Collagenase D was used to fully degrade the collagen scaffolds to allow cell release for examination of viability. This study suggested that compressed collagen scaffolds supported cell adhesion for transplantation of Müller stem cells or neurons derived from these cells. The number of cells obtained after collagen digestion, were comparable to cultures on tissue plates. However, there is a need to examine the degradation rate of these types of collagen constructs *in vivo* in the absence of ECM degrading agents. The scaffolds prepared are therefore useful for differentiation of Müller stem cells and may potentially be used as temporary *in vivo* supports until grafted cells have migrated into the RGC layer.

Thin GTA crosslinked scaffolds, prepared with low spinning times were fragile and did not achieve physical properties to allow mechanical handling, unlike their thicker equivalent samples. Furthermore, to assess their capacity for surgical handling, scaffolds were drawn into 18G cannulas. GTA crosslinked scaffolds failed to pass through the lumen of the cannula, possibly due to their rigidity and thickness. This would ultimately prevent the use of GTA crosslinked collagen scaffolds for surgical implantation.

Further studies into the potential use of electrospun scaffolds may need polymeric enhancement of collagen prior to electrospinning. This may be potentially achieved by blending of collagen with other biomaterials to avoid the use of harsh crosslinking and prevent the formation of rigid scaffolds.

Polyesters have been used to improve structural integrity of collagen scaffolds for tissue engineering. They come in many forms, some of which

are biodegradable such as poly (glycolic acid) PGA, poly(lactic acid) PLA and the co-polymer poly (lactic-co-glycolcolic) PLGA. The most common method of producing hybrid scaffolds is either to electrospin or freeze-dry a synthetic polymer and immerse it in a highly concentrated acidic solution of collagen to allow the deposition of the protein. An alternative method is to electrospin the collagen and polyester in a common solvent, usually with a low synthetic polymer concentration, to produce a matrix based on the molecular structure previously outlined.

Natural polymers have also been used extensively to improve collagen scaffolds. Collagen has been spun with denatured collagen (gelatine) (Salifu et al., 2011), elastin (Buttafoco et al., 2006) and glycosaminoglycan (GAG) (Spilker et al., 2001), (O'Brien et al., 2004), which improve the *in vitro* cell-matrix interactions, vital for *in vivo* therapies. However they require stabilisation through crosslinking which is a potential limitation as evidenced by the effects of GTA and EDC in this study.

Our research entails cellular delivery supported on collagen-based scaffolds. However, the majority of research within this field is committed to producing tissue substitutes where the formulated tissue is incorporated into the body of an organ (Prewitz et al., 2012). Whilst we need to simply provide a substrate that can support cells for retinal delivery, ultimately the physical and biological features of the scaffolds used need to facilitate delivery, and support grafted cells temporarily. Scaffolds also need to be biocompatible, to remove any potential for long term immune reactivity (Ekdahl et al., 2011), which can cause damage to the retina. Degradation of matrices under *in vitro* conditions would not necessarily mimic *in vivo* degradation, which may alter the choice of substrate. In this instance short term stability would be favoured over long term durability.

Collagen is an attractive candidate for the design of scaffolds for retinal transplantation, as it is a natural polymer with potentially low immunogenicity

as compared to other polymers. Collagen scaffolds can be potentially designed to comply with different mechanical requirements needed for cell replacement therapies. Macromolecules and other possible therapeutic agents such as chondroitinase ABC (ChABC) used to facilitate cell migration into the retina, and the precursors themselves can be included within the scaffold construct.

In summary, compressed collagen scaffolds yielded a mechanically strong construct without the need for toxic crosslinking chemicals and facilitated cell proliferation. They are comparatively inexpensive and rapid to produce.

Chapter 4: Transplantation of RGC Precursors *ex vivo* and *in vivo* using Compressed Collagen Scaffolds

4.1. Introduction

When considering the development of cell-based therapies for glaucoma, the aim of such research would be to restore and maintain vision by promoting the survival of partially damaged RGCs or replacing irreversibly damaged RGCs. However, it should be noted that prolonged raised IOP can not only damage RGCs leading to the clinical observation of optic disc cupping, but may also cause degeneration of other cell populations within the neural retina, primarily amacrine cells. (Kerrigan-Baumrind et al., 2000, Hernandez et al., 2009). Patients with advanced glaucoma that have not responded to conventional treatments may be suitable candidates for such cell-based therapies. The aim of this chapter was to study the ability to deliver Müller stem cell-derived RGCs onto the retina using compressed collagen scaffolds. This would enable assessment of the feasibility of translating such a therapeutic approach to a larger mammalian eye similar in size to that of humans.

The majority of research undertaken for the development of stem cells into novel treatments for retinal disease has been focused upon identifying appropriate cell niches for transplantation and developing protocols to aid the differentiation of such cells. The majority of research in this field has concentrated on replacing photoreceptors and retinal pigment epithelial (RPE) cells, but very little work has been performed to treat RGC loss. Experimental studies have led to variable outcomes and further research is required before such therapies may be developed further for human application.

4.1.1. Stem Cell populations used for sourcing RGCs for retinal transplantation

Protocols have been refined for several stem cell populations to induce RGC differentiation, with different degrees of differentiation achieved. The stage of differentiation has widely been assessed using the phenotypic expression profiles of RGCs as well as their functional outcomes evaluating their response to various stimuli.

Murine ESCs have been cultured under a regime involving extrinsic factors which lead to elevated expression of RGC markers, including Ath5, Brn3b Thy-1 and Isl-1 (Jagatha et al., 2009). Human ESCs have an innate ability to spontaneously form neurons, which has facilitated the refinement of differentiating protocols. Neuronal precursors derived from such populations have been used in various animal models of retinal neuropathies (Aoki et al., 2009). Intravitreal and sub-retinal injections of these cells in mice have shown that neural cells are able to integrate into the host retina and express photoreceptor markers over a prolonged period of time (Banin et al., 2006). Transplantation of human ESCs with neuronal morphology have been transplanted into murine models of NMDA depleted RGCs. Cells were observed to migrate and maintain ganglion cell expression profiles whilst residing within the host tissue (Aoki et al., 2008). Co-culture systems comprising explanted foetal rodent retina with the addition of adult rodent hippocampal progenitors have been used to promote the differentiation of these progenitors towards a retinal cell fate. These cells, when transplanted into the RGC depleted rat retina, successfully integrated into the host retina, where cells aligned along the RGC layer and sent out projections into the inner plexiform layer (Mellough et al., 2007).

Cells have been isolated from mammalian adult tissues and re-programmed to create populations of iPS cells, forcing these to constitutively express stem cell markers. Cells isolated and re-programmed from mice somatic cells have

been induced to develop into retinal neurons *in vitro,* mainly of the RGCs and photoreceptors cell lineages (Parameswaran et al., 2010). This suggests that they may be used to develop stem cell approaches for treatments of retinal degenerative conditions.

4.1.2. Experimental Models of Glaucoma used to Assess the Effect of RGC Transplantation

Intravitreal transplantation of human mesenchymal stem cells into rodent models of optic nerve damage showed little evidence of cellular integration into the host tissue and demonstrated lack of RGC maturation of the transplanted cells (Hill et al., 2009). Bull et al studied the intravitreal transplantation of undifferentiated human Müller stem cells into the laser model of rodent glaucoma, which showed a lack of integration within host tissue as well as marked activation of microglia (Bull et al., 2008). However our laboratory has recently developed a robust protocol for differentiating adult human Müller stem cells, into RGC precursors, which have been used for transplantation. Differentiated cells exhibit an RGC phenotype, and adopt a characteristic neuronal morphology (Singhal et al., 2012). Following transplantation into a rodent model of NMDA induced RGC depletion, RGCs derived from human Müller stem cells integrated into host tissue and demonstrated functionality, as judged by improvement of the negative component of scotopic threshold response (nSTR) of the electroretinogram (ERG). The nSTR is an indicator of RGC function and measures responsiveness to low light intensity below visual thresholds. These observations are to date the only evidence where transplantation of stem cells for glaucoma has been successful in achieving integration into host tissue whilst aligning within the target cell layer, as well as improving RGC function of the host animal. Research undertaken by MacLaren et al revealed that in order to achieve optimal integration *in vivo*; stem cells to be used for photoreceptor replacement require differentiation to a specific ontogenetic

stage prior to transplantation (MacLaren et al., 2006). The restoration of ganglion cell function following RGC-derived Müller stem cell transplantation further highlights the importance of differentiating stem cells prior to implantation.

The anatomy of the retina also poses difficulties when transplanting cells onto the inner retinal surface. In order to facilitate integration into the RGC layer, it will be necessary to ensure widespread distribution of cells across the whole retina. In addition, the environment needs to be permissive for cell integration and be able to support development of neural connections with the transplanted cells (Bull and Martin, 2007). Like other neural replacement therapies, functional RGC replacement would entail the formation of numerous synapses between host and grafted cells, converging to direct new neurite outgrowths to the optic nerve. Therefore it is important to define efficient cellular differentiation protocols (MacLaren et al., 2006) prior to transplantation, and protocols to maintain cell survival and integration following transplantation.

4.1.3. Barriers for Retinal Stem Cell Migration and Integration following Transplantation

Trauma and progressive degeneration of nerve tissue initiates a cascade of events within the site of injury, and can be rapid (spinal cord injury (SCI)), or slow (glaucoma). All of these events involve elements of necrosis, apoptosis and scarring, leading to functional loss. Gliosis causes the formation of a glial scar embodying reactive glia and astrocytes, which upregulate their production of chondroitin sulphate proteoglycans (CSPGs) (Fawcett and Asher, 1999). This is of important relevance to cell transplantation, as CSPGs have been shown to inhibit migration of transplanted cells and formation of new synapses (Silver and Miller, 2004). Transplantation of stem cell based therapies for inner retinal degeneration in humans will face many

natural barriers, including the larger sized vitreous cavity and the presence of abnormal extracellular matrix within damaged retina.

Chondroitin sulphate proteoglycans (CSPGs) belong to the aggrecan family of proteins (Yamaguchi, 2000). They regulate the development of the neural tube and associated neural crest cells by directing their out-growth patterns. The concentration of CSPGs around neurons is thought to underpin the loss of progenicity over time within the progenitor population, due to steric hindrance (Sharma et al., 2012). These molecules contribute to the lack of permissiveness of the neural ECM to respond to the regenerative plasticity of resident adult neurons and transplanted cells.

Gliosis and neurodegeneration cause rapid CSPG up-regulation in reactive glia and astrocytes, and deposition within the site of neural damage (McKeon et al., 1995). Microglia are the resident inflammatory cells of the retina and also produce ECM molecules, specifically the regenerative inhibitors CSPG during retinal degeneration (Uhlin-Hansen and Kolset, 1988, Jones et al., 2002, Ng and Streilein, 2001). CSPGs play a key role in suppressing axonal extension and regeneration of apoptotic cells within the site of injury (Silver and Miller, 2004, Smith-Thomas et al., 1995), suggesting that inhibition of these molecules may aid neural recovery and facilitate integration of grafted cells.

Targeting CSPGs has mainly involved the cleavage of their reactive GAG, moieties, preventing their binding and anchorage to other components of cells and matrices. Digesting the GAG side chains into simple disaccharides promotes their catabolism and ECM permissiveness to regeneration. Chrondroitinase ABC (ChABC) is the main enzyme used to cleave GAG. Its application to repair spinal cord injury (SCI) (Bradbury et al., 2002) and similar CNS injuries have been examined using *in vitro* and *in vivo* models of neural damage. Such experiments demonstrated re-growth of damaged neurites within corticospinal, reticulospinal and nigrostriatal populations

following ChABC digestion (Garcia-Alias and Fawcett, 2012). Moreover studies assessing the migration of transplanted cells demonstrated that axonal integration was enhanced when the peripheral regions of the spinal ECM were treated with ChABC (Fouad et al., 2005, Karimi-Abdolrezaee et al., 2010, Tom et al., 2009, Garcia-Alias and Fawcett, 2012). Determining whether this regeneration was solely due to the breakdown of the ECM or to the activation of growth within healthy and damaged axons, was achieved by monitoring the regeneration of complete and semi-transected spinal cords (Fouad et al., 2005, Tom et al., 2009). Partially severed cords owed their regeneration to both transplanted and host cell populations, whilst complete transected spinal cords underwent rejuvenation by the regeneration of damaged axons. These tests were indicative of the importance of enhancing CNS regeneration by creating an environment free of inhibitory molecules.

Studies of adult rat retina have also been carried out by Tropea et al, which involved partial denervation of the superior colliculus. Subsequent treatment with ChABC to the superior colliculus restored some damage caused to the RGC population (Tropea et al., 2003). Addition of brain-derived neurotrophic factor (BDNF) further enhanced sprouting of damaged RGCs. This evidence illustrates the synergistic interaction between these two agents, where the trophic factor has an improved effect in combination with the degradation of CSPGs.

Inhibiting abnormal production of CSPGs within the degenerate retina may enable this tissue to become permissive to integration of transplanted Müller stem cells. Treatment with ChABC may also facilitate neural interactions between both undamaged and partially damaged ganglion cells *in situ*.

4.1.4. Vitrectomy as a tool for surgical delivery of cellular scaffolds onto the retina

Methods used for intravitreal injection of therapeutic agents, including cells, into small rodent eyes may not be appropriate for the human eye due to differences in anatomical features amongst species. The lens contained within rodent eyes occupies over 70% of the spatial capacity of the optic cavity (Powers and Green, 1978). This feature means that when cells are injected into the vitreous, the lens may serve as a scaffold to facilitate cell migration into the host retina. Higher order mammals such as rabbits, primates and cats have dimensions closer to that of the human eye, where the nature of tissue arrangement is significantly different to that of rodents. Higher mammals have evolved to have smaller lenses occupying only 10-20% of the spatial capacity (Coleman, 1979) (Figure 4.1). The lack of a large lens means that transplantation of cells into the vitreous of a higher mammal would lead to their dispersion and/or pooling within the inferior part of the vitreous. There is therefore a need to develop methods to deliver cells to the inner retina in higher mammals with this anatomical configuration.

The design of a scaffold for cell transplantation is determined by the anatomical structure and accessibility of the tissues undergoing transplantation. In order to provide sufficient cellular integration into the inner retina, the implant must align along the inner retinal surface. However to facilitate this process, the vitreous would require removal. Vitrectomy, a procedure routinely undertaken for treatment of retinal detachment in human patients, therefore constitutes a feasible option for implantation of cellular scaffolds onto the retina.

The human eye contains 3.5-4ml of vitreous humour (Coleman, 1979), the translucent gelatinous mass that fills the eye cavity. Vitreous is primarily composed of water, with a loosely compact network of type II collagen

associated with proteins such as hyaluronic acid and glycosaminoglycans (Swann, 1980, Itakura et al., 2009).

The vitreous is loosely attached to the neural retina except at the peripheral vitreous base and optic nerve head. The vitreous body functions to maintain the structure of the eye whilst also contributing to maintaining a stable intraocular pressure.

A

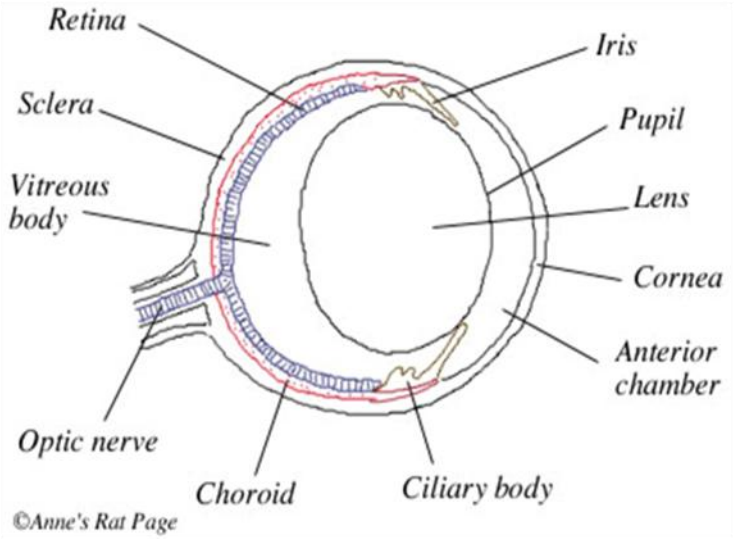

B

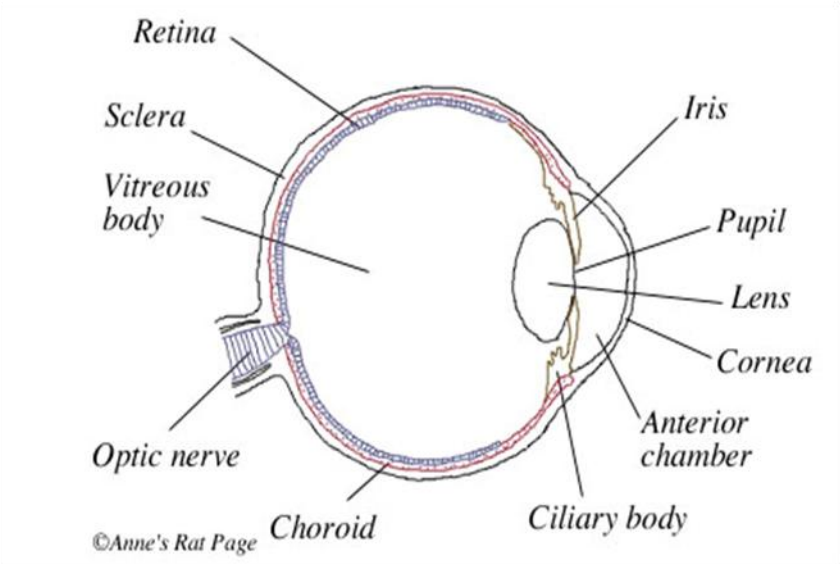

Figure 4.1: Anatomical drawings of A) rat and B) human illustrating the major differences in the geometric dimensions of these two mammalian ocular structures. Images taken from http://www.ratbehavior.org/Eyes.htm

Pars plana vitrectomy involves the partial or total removal of the vitreous and has been developed over the last 35 years (Aguni et al., 2009, Wallenten et al., 2008). A 20 or 23 gauge MVR blade is then used to create three pars plana sclerotomies (Aguni et al., 2009, Wimpissinger and Binder, 2007), avoiding injuring the neural retina, as well as avoiding touching the lens in phakic patients (Figure 4.2). One port is for a suture infusion line to maintain globe pressure during the operation and the other two ports allow instrumentation to facilitate the removal of the vitreous and manipulation of the retina under fluid, followed by fluid-air exchange at the end of the procedure.

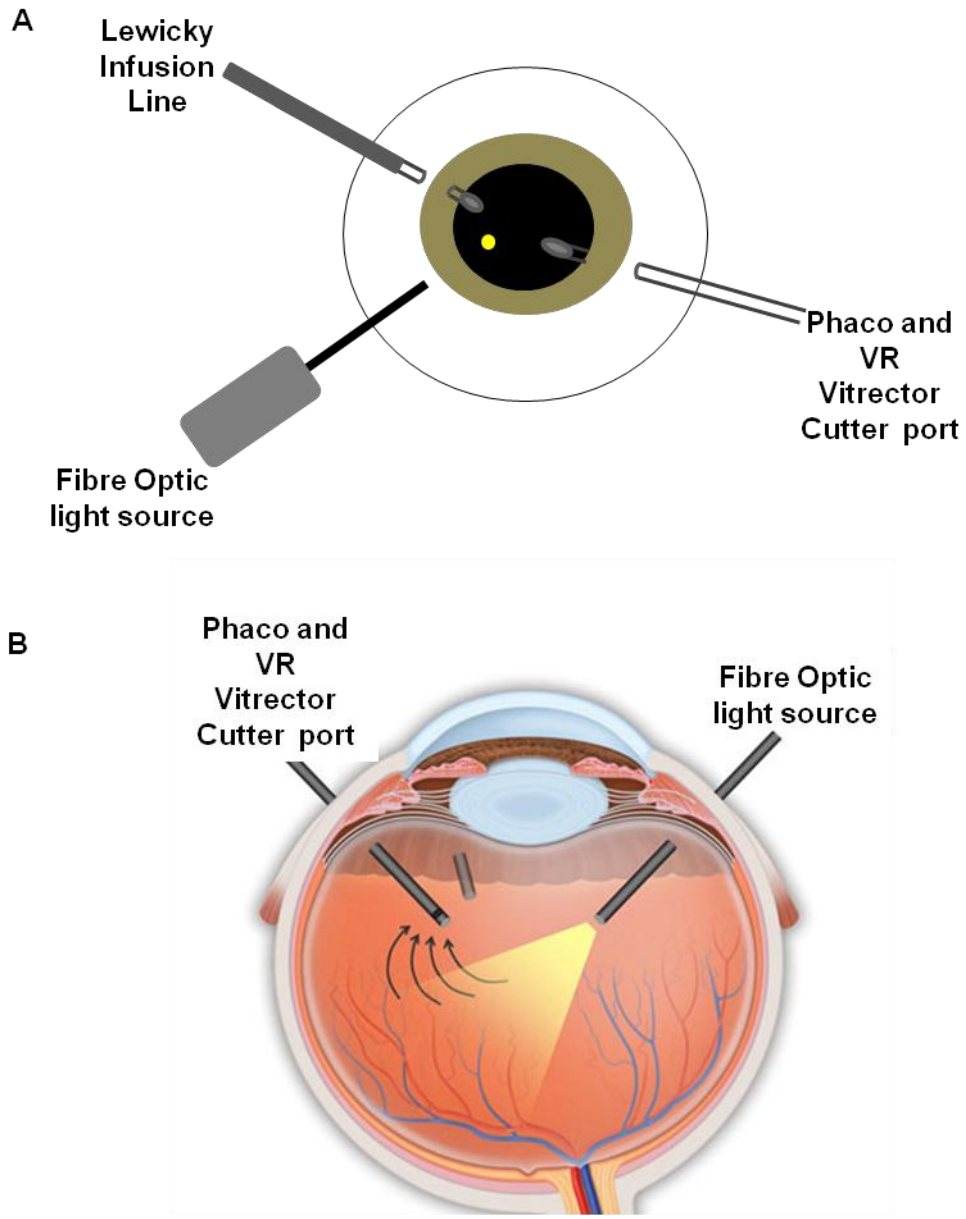

Figure 4.2: Illustration of Vitrectomy surgery. A) Image of vitreous removal following port creation via MVR blade. B) Cross sectional representation of instrument placement during vitrectomy, adapted from http://www.valleyretina.com/info-surg/info-surg-pars.html

4.2. Objectives and Experimental Outline

Having previously developed protocols to obtain RGCs derived from human Müller stem cells, as well as to produce suitable compressed collagen scaffolds to support cell delivery, it was a natural progression for research to transplant cellular scaffolds onto the retina *in vivo.* The aim of this chapter was therefore to investigate the ability of cellular scaffolds prepared with compressed collagen type I to support migration of transplanted cells onto the retina *ex vivo* and *in vivo*.

The general objectives of this chapter were:

1. To examine the ability of cellular scaffolds to support migration and integration of RGC precursors onto the RGC layer of explanted human retina *ex vivo.*
2. To determine the ability of cellular scaffolds to support migration and integration of RGC precursors into the RGC layer of rabbit retina *in vivo*.

The experiments performed to achieve these objectives were as follows:

1. Cadaveric human retina obtained from Moorfields eye bank, was explanted *in vitro* and transplanted with RGC-derived Müller stem cells attached to compressed collagen scaffolds. This was facilitated by incubation with ChABC. Following fixation, retinal tissue was analysed for transplanted cell integration into the inner retina.
2. For the *in vivo* studies, transplantation was performed in vitrectomised eyes of female pigmented Chinchilla bastard rabbits. Efficiency of cell delivery from collagen scaffolds was examined using immunohistological techniques 2-3 weeks post transplantation.

To assess the efficiency of cell delivery using scaffolds, Müller stem cells were induced to differentiate into RGCs by culturing with DAPT and bFGF for one week, akin to previous studies performed in rat by our laboratory. Enriched RGC populations derived from Müller stem cells were prepared for transplantation onto explanted human retina, as well as for surgical implantation into 2.5-3kg female Chinchilla rabbits, in the presence of ChABC (see below). Explanted retinas from the adult human eye were cultured for a maximum of 7 days, following *in vitro* transplantation of cellular scaffolds. Rabbit eyes were analysed after 2-3 weeks post transplantation. Specimens were analysed for survival and migration of grafted cells into the retina using confocal microscopy.

Vitreoretinal surgery was undertaken by two surgeons from Moorfields Eye Hospital, collaborating in this study, Mr DG Charteris and Mr H Jayaram. During this investigation I was responsible for the preparation of cellular scaffolds and therapeutic agents (ChABC), animal husbandry, sterilisation and preparation of surgical instruments, as well as providing technical assistance with vitrectomy equipment during surgery. The rabbit eye has an axial length of 18-21mm comparable to the adult human eye of 22-23mm, indicating that the dimensions of the globe in both species are similar (Hughes, 1972). However, the equatorial length of the human lens is 16mm with a depth value between 4-5mm (Taylor et al., 1996), 18% of the spatial cavity. In contrast, the rabbit contains a relative large lens of 5-7mm depth in adults which accounts for 28% of the ocular cavity (Hughes, 1972). The rabbit eye has a lower volume of vitreous (2ml) compared to the human (4ml) due to the larger lens and smaller outer radius and axial length (Friedrich et al., 1997a, Friedrich et al., 1997b). Rabbits have been used extensively to study the mode of systemic drug delivery and release within the eye for human models of ocular degenerations (Heller, 2005). The rabbit eye has more similar anatomical features to the human eye compared to rodents, which makes the rabbit an attractive model to examine the feasibility of

cellular scaffold transplantation. In this study, this mode of transplantation aimed to achieve direct contact between the scaffold and the RGC layer, following vitrectomy.

4.2.1. Transplantation protocol

Compressed type I rat tail collagen scaffolds were prepared as follows: 300µl of 0.75mg/ml collagen were cast in 1cm diameter rings, followed by compression under 150g weight for 5 minutes. Human Müller stem cells stably transfected with the human immunodeficiency virus type 1 (HIV-1 based lentiviral vector) expressing human recombinant GFP were used for this study to determine the localisation of transplanted cells within the host tissue. GFP transfected Müller stem cells were differentiate in RGCs by culture on ECM in the presence of bFGF and DAPT. Cells were then dissociated from culture surfaces and assessed for their viability. Harvested cells were then added to prepared collagen scaffolds at a concentration of $4x10^5$ per scaffold side. Cellular scaffolds were incubated at 37°C for a maximum of 2 hours per side, in DMEM containing 10% FCS, to aid adhesion. Scaffolds loaded with cells were then rinsed and washed 3 times for 10 minutes in sterile PBS, to remove serum. Scaffolds were stored in PBS at room temperature for up to 1 hour prior transplantation. Prior *to in vitro* transplantation, 0.4U/10µl of ChABC were placed onto the retina and incubated at 37°C for 10 minutes. When applied onto the retina *in vivo*, the enzyme was left for 5 minutes, prior to implantation of cellular scaffolds.

Following removal of the lens by phacoemulsification (Figure 4.2) the vitreous body was removed using a high frequency pneumatic cutter which was inserted into the posterior segment through the pars plana sclerotomy. Delivery of both ChABC and cellular scaffolds was achieved using a 18G cannula directed towards the medullary raphe. Following scaffold implantation local injections of gentamicin and triamcinolone (washed and reconstituted in sterile water to 80µg/ml) were given subconjunctivally to

prevent post-operative infection and to reduce post-operative inflammation. Furthermore, in order to reduce the risk of the xenogeneic transplanted cells being rejected by the host, animals were orally immunosuppressed daily with cyclosporine (0.15mg/kg/day), three days prior to and following transplantation throughout the duration of the experiment, to prevent xenographic rejection of the transplanted cells. To control inflammation, operated eyes also were given topical drops of dexamethasone 0.1% and chloramphenicol daily following surgery until sacrifice.

4.3. Results

4.3.1. Transplantation of RGCs onto explanted human retina using compressed collagen scaffolds

Müller stem cell-derived RGCs were obtained by standardised protocols, and were seeded onto one side of compressed collagen scaffolds and incubated for 1-2 hours to allow cell attachment. Cellular scaffolds were placed onto explanted cadaveric human retina and cultured up to 7 days at 37ºC. The cellular scaffolds did not align onto the explanted retina, possibly due to the lack of pressure on the construct, permitting it to float. However, in the absence of Chondroitinase ABC, cells were observed to detach from the scaffolds but did not migrate onto the retina (Figure: 4.3). Following incubation in the presence of Chondroitinase ABC, although scaffolds did not attach to the retina, cells detached from the scaffolds migrated into the retina, possibly aided by this enzyme. This indicates that scaffolds can be used as a tool for cellular delivery onto the retina (Figure 4.3B).

4.3.2. Delivery of RGCs using compressed collagen scaffolds onto the inner rabbit retina

4.3.2.1. Histological assessment of rabbit transplantation without lens removal

Haematoxylin and eosin (H&E) staining, as well as confocal microscopy was used to determine the histological features of transplanted rabbit eyes. This assessment confirmed that cellular scaffolds were located adjacent to the posterior retina. However, microscopic imaging of transplanted retina in rabbits where the crystalline lens was left in place, demonstrated severe disruption of the retinal architecture when compared to normal non-transplanted eyes (Figure 4.5). It was thought that the damage caused to the retina was induced during surgery for scaffold implantation, due to breaks caused at port placement.

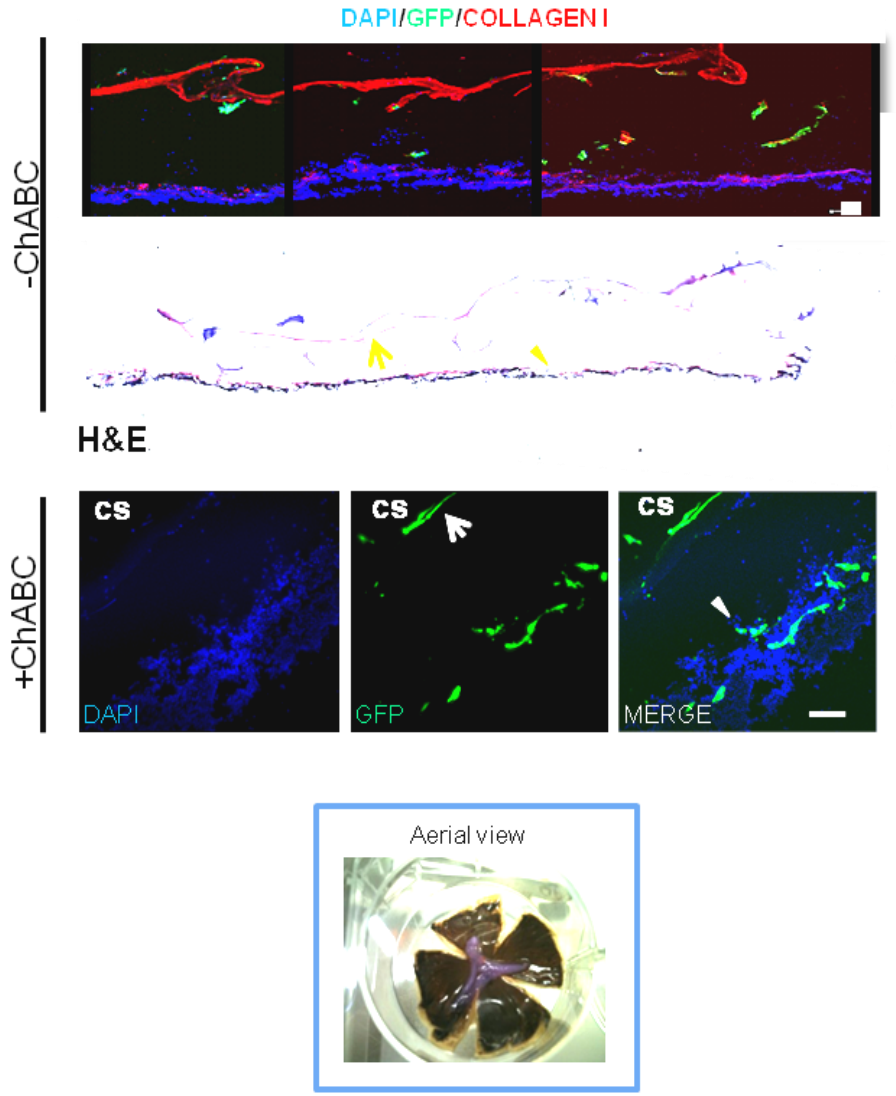

Figure 4.3: *In vitro* transplantation onto human retinal explants. GFP-labelled Muller stem cell-derived RGCs were differentiated for 7 days prior to *in vitro* transplantation. Cellular scaffolds were incubated for 2 hours at 37ºC, to aid cell adhesion. Confocal images and H&E image of cryosections of retina transplanted *in vitro* with collagen constructs supporting GFP-labelled Müller-derived RGCs, incubated with and without ChABC prior to transplantation. The upper image represents the migration of GFP-labeled cells onto retinal explant in the absence of Chondroitinase ABC (-ChABC). The lower image represents incubation of retinal explants with ChABC (+ChABC) prior to transplantation. Imaging with the addition of ChABC shows migration of cells from the cellular scaffold (cs) (open arrow) into or onto the retina (arrowhead). H & E. Yellow arrows correspond to the cs (open arrow) and retina (arrowhead). Scale bar=50µm.

Ports were introduced at the posterior pars plana to minimise the risk of lens touch and retinal breaks. However sclerotomies created in this region were associated with retinal detachment and widespread bleeding (Figure 4.5).This made implantation of the cellular scaffolds onto the medullary raphe difficult (Figure 4.6). Due to this complication, a new approach was undertaken to perform a lensectomy (surgical lens removal) to allow the port entry sites to be placed more anteriorly within the pars plana.

4.3.2.2. Macroscopic features of the *in vivo* transplanted rabbit with lens removal

Macroscopic imaging using an inverted florescent microscope, of transplanted rabbit eyes, revealed that transplantation of scaffolds onto lensectomised and vitrectomised eye resulted in cell delivery onto the retinal macula. This was determined by the presence of GFP-positive cells in this region (Figure 4.7). Following 14 days after transplantation, scaffolds appeared to remain posteriorly in direct contact with the neural retina, within regions adjacent to the original delivery site.

4.3.2.3. Histological examination of the rabbit retina following *in vivo* transplantation

Initial investigations for transplantation of cellular scaffolds were undertaken without lens removal, following the surgical complications lenses were removed and examined by Haematoxylin and eosin (H&E) staining and confocal microscopy. Cellular scaffolds were found within anterior regions of the eye, adjacent to the ciliary body and port site (Figure 4.8). This suggests that there are other components involved in the delivery of cellular scaffolds, distinct from lens removal and port site location. This also indicated that delivery of scaffolds to the anterior part of the eye did not allow scaffold alignment along the neural retina preventing cells from attaching and migrating into the inner retina.

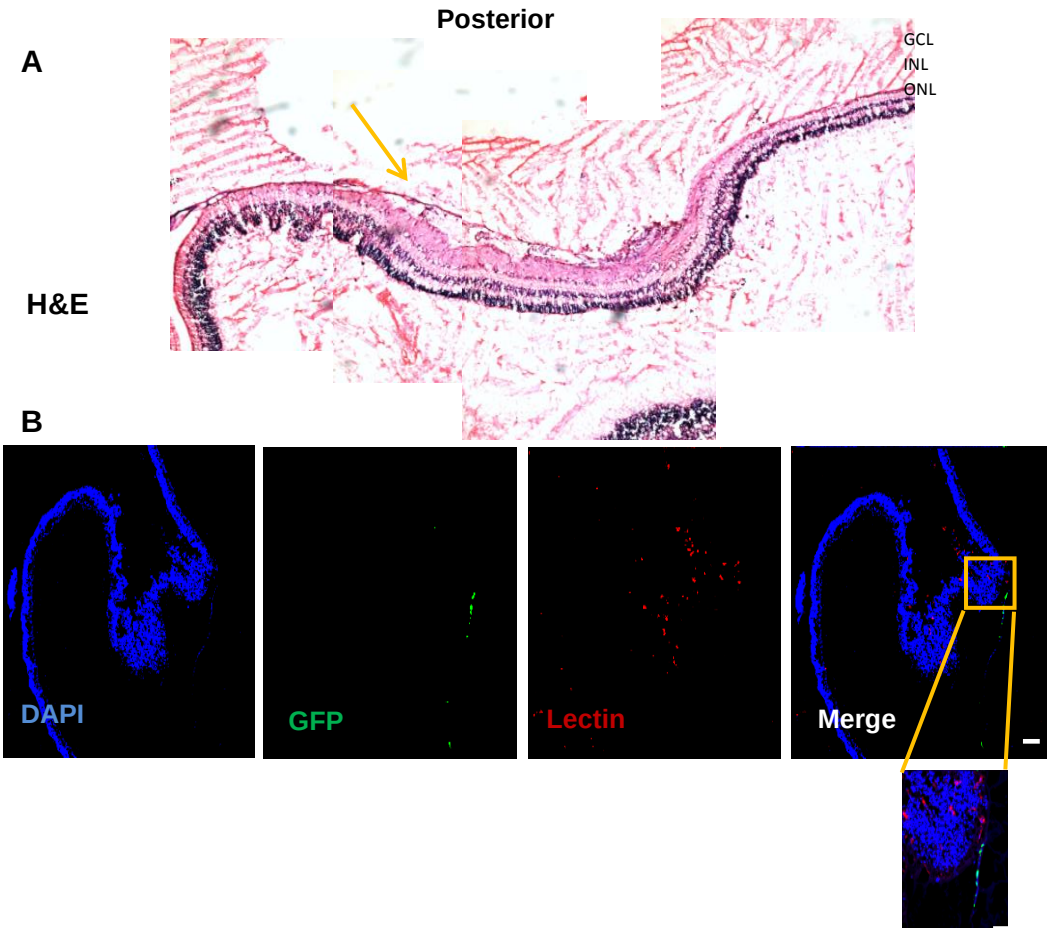

Figure 4.5: Histological examination of vitrectomised rabbit eyes, following *in vivo* transplantation of compressed collagen scaffolds without lens removal. Cryosections of a vitrectomy transplanted eye 14 days post surgery, showed retinal detachment within the posterior region of the eye and the onset of choroidial and vascular bleeding. A) H&E staining of the posterior region of the rabbit eye, proximal to the compressed collagen scaffold (yellow arrow). B) Confocal imaging identified a minimal amount of GFP-labelled cells within the sites of retinal detachment Confocal showed expression of the microglia marker lectin (red), within the regions of detached retina. Scale bar=100µm.

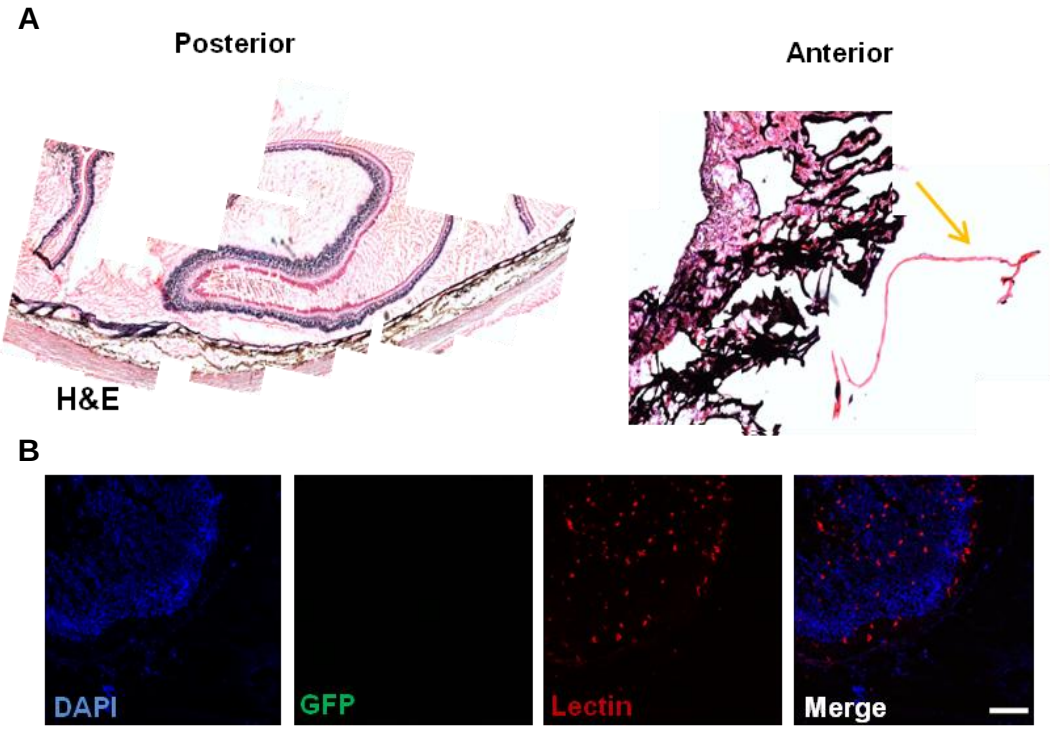

Figure 4.6: Histological examination of vitrectomised rabbit eyes, following *in vivo* transplantation of compressed collagen scaffolds without lens removal. Cryosections of a vitrectomy transplanted eye 14 days post-surgery demonstrated retinal detachment within the posterior region of the eye and the onset of choroidal and vascular bleeding. B) H&E staining of the posterior and anterior regions of a rabbit eye, as well as B) confocal microscopy of the posterior retina. H&E staining identified the presence of the cellular scaffold within the anterior segment of the eye, adjacent to the iris (yellow arrow). Confocal analysis of a posterior section, showed elevated expression of the microglia marker lectin (red), within the retina. Scale bar=100µm.

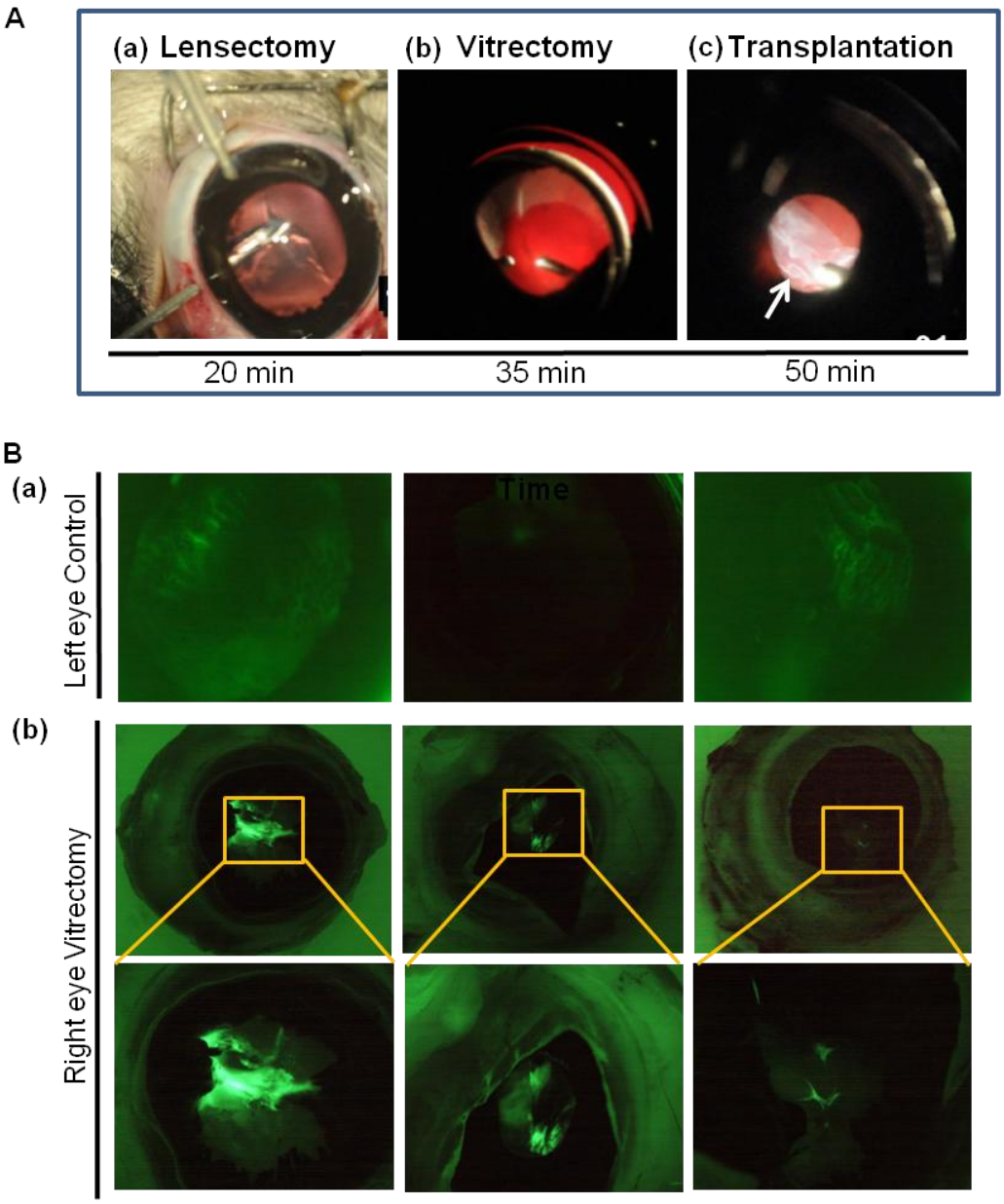

Figure 4.7: Macroscopic imaging of *In vivo* transplantation of PC cellular scaffolds into lensectomised and vitrectomised rabbit eyes. A) Images depicting the vitrectomy stages for cellular scaffold transplantation: a) lensectomy b) vitrectomy c) insertion of cellular scaffold by cannula injection (white arrow). B) fundus imaging of (a) control eyes and eyes (b) transplanted with cellular scaffolds to which GFP-labelled Müller stem cell-derived RGCs had been adhered. Images were taken under FITC illumination with cornea and lens removed (control eyes only) to identify GFP presence within the transplanted eyes. Imaging confirmed the presence of GFP in the posterior portion of the eye.

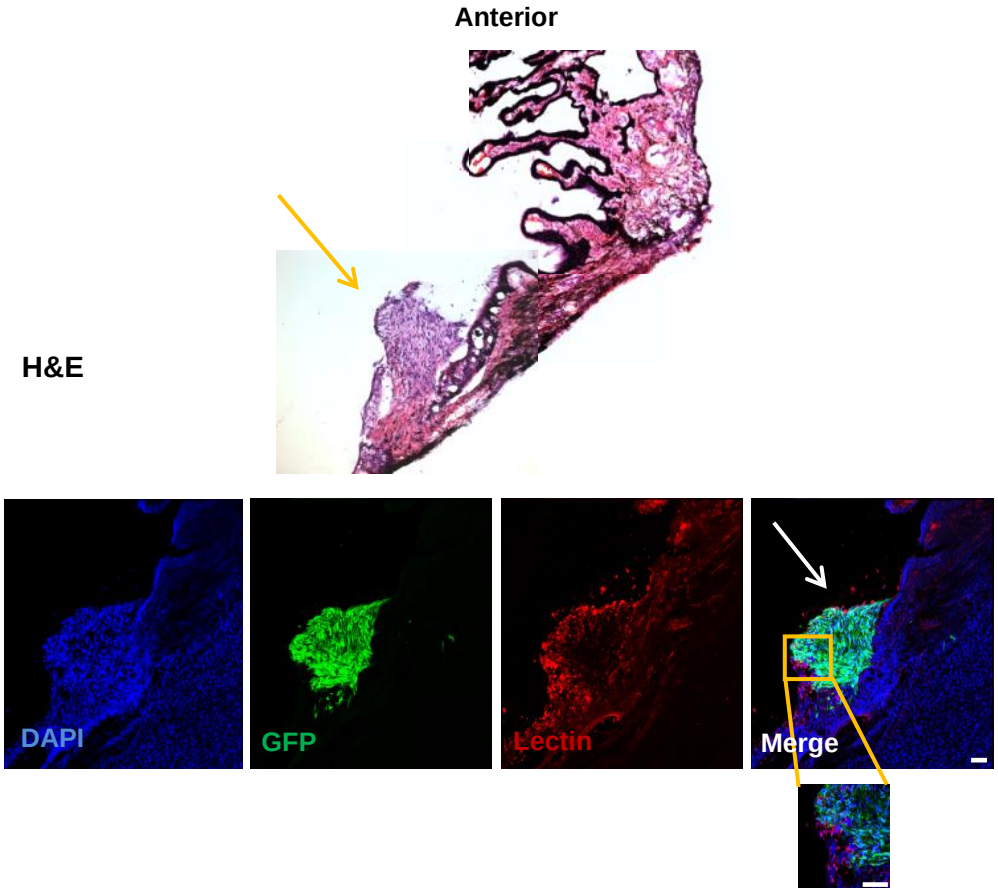

Figure 4.8: Histological examination of vitrectomised rabbit eyes, following *in vivo* transplantation of compressed collagen scaffolds following lensectomy. Globes of transplanted rabbit eyes were removed and sectioned 14 days post surgery. Cryosectioning and staining demonstrated aggregation of cellular scaffolds adjacent and proximal to the vitrectomy port sites. H&E showed the macroscsopic location of the cellular mass. Whilst confocal microscopy identified the mass as GFP-labelled Müller stem cells, which was also coupled with microglial mobilisation to the site of aggregation. Microglia was identified by lectin staining (red). Scale bar=100µm.

Conversely, there was evidence that cellular scaffolds place on the medullary raphe allowed migration of cells onto the retina (Figure 4.9). Although, cellular scaffolds were observed adjacent to the neural retina, GFP-positive cells were not found to have integrated into host retina within this region. However, cells were seen to have migrated into host retina in regions located close to the scaffold, where the scaffolds had not attached.

There was no evidence, in any of the experiments, of conventional RGC morphology adopted by transplanted cells. There was a lack of synaptic connections made with host cells, as well as a lack of neurite outgrowth observed by transplanted cells.

4.3.3. Examination of the rabbit inflammatory response following cellular scaffold transplantation

Determination of the inflammatory response in rabbit ocular tissues following scaffold transplantation was achieved by examining the presence of microglia. Immunohistochemistry was carried out by staining histological sections of rabbit retinae with the protein lectin. Microscopy of retinal tissue revealed that transplanted eyes had accumulation of cells staining for lectin at the site of the transplant (Figures 4.5, 4.6, 4.8 and 4.9). Similar accumulation of microglia was observed in all retinae, where cellular scaffolds had been delivered either posteriorly or anteriorly. Activation of microglia within host tissue was also evident when retinal detachment and haemorrhaging occurred, even in the absence of grafted cells (4.5 and 4.6).

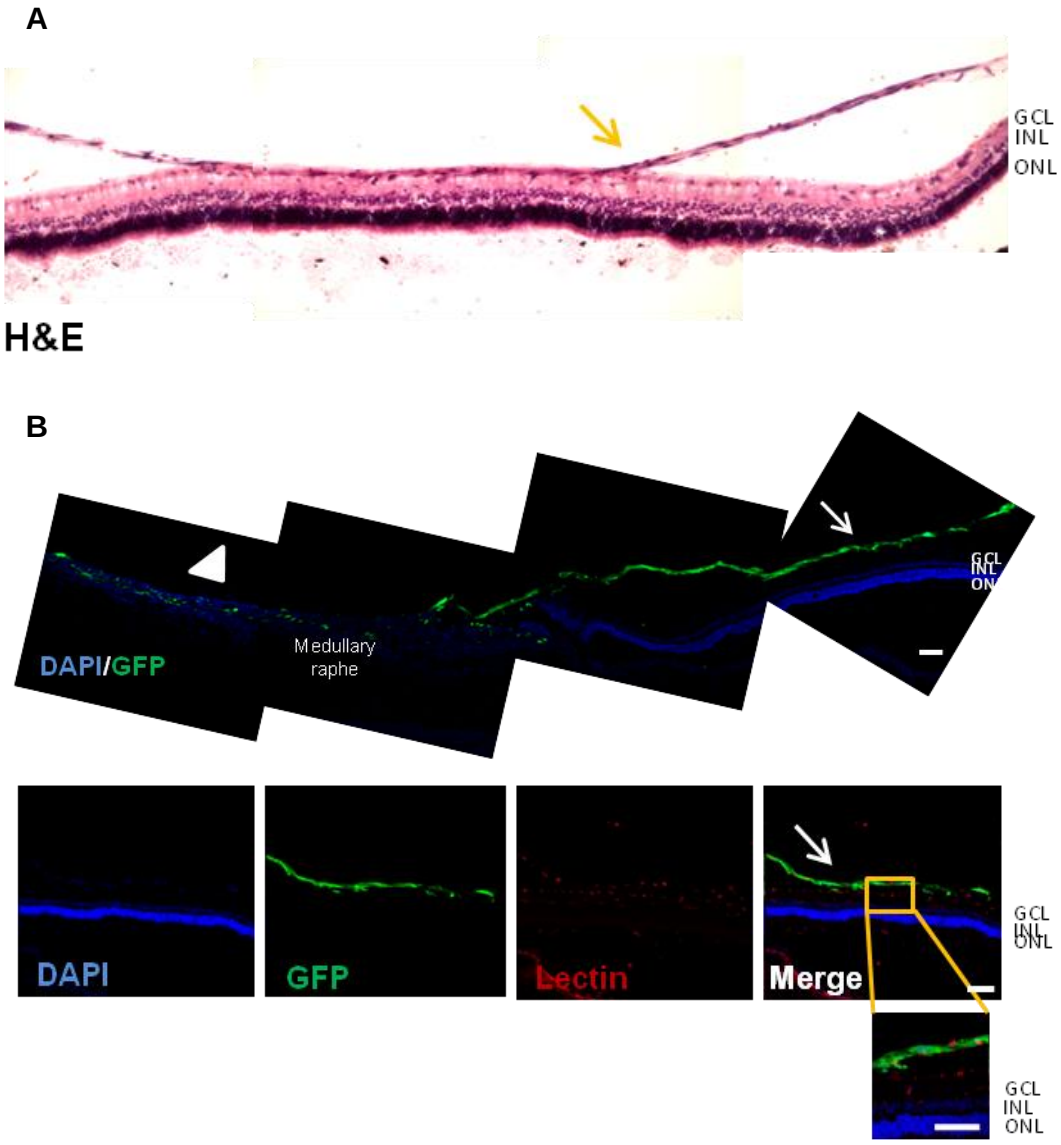

Figure 4.9: Histological examination of vitrectomised rabbit eyes, following *in vivo* transplantation of compressed collagen scaffolds following lensectomy. A) H&E stained cryosections of a rabbit eye transplanted with a cellular scaffold. This showed the scaffold in the posterior retina (yellow arrow). The cellular scaffold appears to attach to the retina at some points without disrupting the retinal morphology. B) Confocal imaging of cryosections of the vitrectomised and transplanted eye showed migration of cells from the scaffold (open arrow) onto the retinal tissue (medullary raphe; arrowhead). Adjacent sections were also stained for lectin to identify microglia activity within the transplanted globe, and confirmed activation of microglia in the ganglion layer proximal to the GFP-labelled cells, highlighted by enhanced view (yellow box). Scale bar=100µm.

4.4. Discussion

Observations from these experiments illustrate the need for vitrectomy surgery for adequate cellular scaffold delivery into a large eye. The study aimed to transplant appropriately differentiated Müller stem cells supported on compressed collagen scaffolds onto the inner retina. This process was clearly facilitated by having direct access to the inner retinal surface.

Previous work by our laboratory has demonstrated the migratory capabilities of Müller stem cells. Their ability to migrate into dystrophic RCS rat retina has been shown, as well as their ability to integrate into the RGC layer. This was facilitated by breakdown of the inner limiting membrane (ILM) with Chondroitinase ABC and anti-inflammatory treatment with Triamcinolone (Singhal et al., 2008, Singhal et al., 2012). Moreover, further work carried out within our lab demonstrated the migratory ability of Müller stem cell-derived photoreceptors when transplanted into the sub-retinal space of dystrophic rats. However, transplantation of differentiated Müller stem cell-derived photoreceptors displayed the capacity to orientate themselves within the photoreceptor lamina whilst maintaining their expression profiles of photoreceptors (Jayaram et al, submitted). Importantly, transplantation of RGCs and photoreceptors-derived from Müller stem cells also resulted in functional improvement *in vivo*, using experimental models of retinal degeneration.

These findings highlighted the fact that integration within the correct retinal laminations cause functional improvement. Integration into respective retinal layers centred on appropriate differentiation protocols, in addition to creating permissive retinal environments for cells to migrate. Secretion of CSPGs following neural degeneration is an inhibitory factor for regeneration of nervous tissue. These molecules prevent the re-growth of damaged axons and the integration of grafted cells (Bradbury et al., 2002, Diaz-Martinez and Velasco, 2009). Activation and proliferation of microglia has been found in

degenerated RCS rat retina and this is an important cause of damage to grafted cells (de Kozak et al., 1997, Roque et al., 1996, Thanos and Richter, 1993).

The current study aimed to develop protocols for Müller stem cell derived RGCs transplantation into the larger eye, analogous to that of humans, to examine if similar Müller stem cell migratory capacities were evident. Scaffold development aimed to encourage uniform distribution of grafted cells onto the retina, preventing their aggregation on the inferior retina. Uniformity of grafted cell migration into rodent retinae was aided by the small vitreous cavity, allowing direct placement and cell support by the large lens in this species. Differentiated RGCs were seen to attach well to compressed scaffolds and endured invasive surgical manipulation via an 18 gauge cannula (Chapter 3).

Delivery of cellular scaffolds appeared to be dependent on the surgical procedures used. Procedures that did not include removal of the lens demonstrated widespread retinal trauma, including detachments alongside extensive choroidal and retinal bleeding (Figure 4.5 and 4.6). Cellular scaffolds were found within the anterior (Figure 4.5) or posterior (Figure 4.6) regions of the retina. Removal of lens prior to transplantation permitted revision of port entry sites which prevented the trauma observed in procedures without lensectomy. Although the dimensions of the human and rabbit eyes are similar, the difference is lens morphology necessitated the use of surgical lensectomy which would most likely be unnecessary in human subjects. The rabbit lens created a physical barrier for appropriate port placement and since the pars plana is smaller in the rabbit, ports were subsequently positioned more anteriorly, following lensectomy. As with previous surgeries, the delivery sites of the cellular scaffolds varied in location following lensectomy. Cellular scaffolds were found within anterior (Figure 4.8) and posterior (Figure 4.9) regions of the eye. This suggests that

apart from port sites and lens geometry other physical factors are involved in surgical delivery. Angulation of cannulas within the ports may have contributed to the aggregation of cellular scaffolds within the anterior regions adjacent to the entry at the neural retinal-ciliary body junction. Steeper angles of the cannulas may promote directed placement of scaffolds onto the retina. The rate and/or force used to eject scaffolds from cannulas may have also determined the final site of delivery. Visualisation of original scaffold delivery positions were not always determined during surgery, but it is likely that they remain in the same position throughout the experiment.

Cellular scaffold transplantation into rabbit eyes, when delivered onto the inner retinal surface were subsequently held in place against the retina, enabling proximal attachment (Figure 4.9). Attachments between host tissue and scaffolds failed to induce migration of RGC precursors into host tissue, possibly due to the lack of breakdown of the ECM by insufficient levels of ChABC. Limited integration faced in these studies could be improved by efficient sustained ChABC release to prolong its activity. *In vitro* human retinal explants demonstrated cell integration by scaffold transplantation of RGCs following incubation with ChABC (Figure 4.3). Lack of ChABC presence failed to support cellular migration and appeared to induce cellular dispersion into the local media, suggesting that ChABC is vital for cellular integration (Figure 4.3). The *in vivo* state of degenerated retina would be vastly different to normal *ex vivo* tissues and *in vivo* eyes. Dystrophic and glaucomatous eyes would contain abnormal amounts of CSPG molecules, as well as cellular debris due to retinal degeneration (Zhang et al., 2003). Hence the modulation of the normal retinal ECM is a key factor to consider for cellular transplantation into degenerated retina. CSPG rich matrices treated with active ChABC have been shown to improve integration of transplanted photoreceptors (Inatani and Tanihara, 2002). Experiments carried out during this study have positively identified cellular migration onto host retina, although in many cases these regions were not proximal to the

scaffolds. This may indicate that temporary support by cellular scaffolds is sufficient for migration onto the retina.

Where migration was observed, classical axonal organisation was not adopted by transplanted cells. The extension of neurite and dendritic outgrowths within the RGC population embodies a feature where the orientation and direction of axons converge collectively towards the optic nerve. In some cases axons do not synapse until they extend into the visual cortex. This feature, to date has not been observed following transplantation of other stem cells. However, our lab has shown that synapses can form between transplanted Müller stem cell-derived RGCs and their local rat host neurons (Singhal et al., 2012). This transplantation caused functional recovery of a RGC depleted population, suggesting that limited integration may be sufficient to improve retinal function rather than having to completely replace and mimic the native retinal ganglion cell layer.

In summary, this chapter demonstrates that Müller stem cell derived RGC can be delivered into larger eyes via compressed scaffolds. However, the mechanical process of surgery needs to be standardised for further investigations. The physical manipulations during operative procedures need to comply with stringent parameters for the rabbit. Barriers to surgical transplantation include the presence of the lens, cannula angulation and port placement. Biological barriers were also highlighted by this investigation. Promotion of cellular integration into host tissue requires adequate modulation of the adjacent retinal environment using ChABC (Singhal et al., 2012). Stabilisation and prolonged activity of ChABC would provide a permissive retinal microenvironment amenable to cellular integration. At present, frequent and numerous injection of the enzyme is the most common mode of delivery (Coumans et al., 2001), which can be a lengthy and invasive process. Thermal instability and leeching limits the activity of ChABC. There is a need to improve the delivery of ChABC by generating a

slow-release mechanism that is able to maintain therapeutic dosage of ChABC in the retina. Fabricated matrices have been designed to incorporate ChABC as well as other agents which aid neural regeneration. Hydrogels consisting of fibrin (Taylor and Sakiyama-Elbert, 2006, Hyatt et al., 2010) and agarose (Lee et al., 2010) have been used to assess *in vivo* use and delivery of ChABC, and they merit investigation into their suitability for retinal delivery. Electrospun collagen has also been nominated as a suitable substrate by impregnation with NT-3 and ChABC via microbial transglutaminase (Liu et al., 2012). Further investigations would determine the feasibility of sustaining ChABC delivery by collagen-based scaffolds for ocular use. Stabilising ChABC could improve the integration and survival of transplanted cells over an extended period.

Further determination of compressed cellular scaffolds suitability would involve studies in larger mammalian glaucomatous eyes such as hereditary animal models, including Siamese cats with primary congenital glaucoma (Sigle et al., 2011).

Chapter 5: General Discussion

5.1. Introduction

Müller stem cells within the retina of zebrafish and *Xenopus* have the innate capacity to regenerate retina throughout life. Early post natal chicks have also shown limited retinal regeneration ascribed to the unique abilities possessed by Müller stem cells (Fischer and Reh, 2001). The human retina also contains a population of Müller glia with stem cell characteristics. These cells express markers of multipotency (Lawrence et al., 2007) specifically restricted to retinal neurons. However, unlike zebrafish and amphibians these cells are unable to repopulate neural cells endogenously following damage. Müller glia like other glial cells can re-enter the cell cycle in order to proliferate, forming glial scars and propagating within the spaces of apoptotic cells and disconnected synapses (Lewis et al., 2010). This feature to de-differentiate and proliferate is harboured by all Müller glia of different species, which therefore represent a cellular source to generate new neurons. Isolating this population from human retina has led to the emergence of stem cell research for human retinal diseases and the development of cell-based therapies.

Degeneration within the retinal ganglion cell population is one of the pathological features of glaucoma which accounts for 15% of all registered blind in England (Bunce et al., 2010). Current therapies to treat glaucoma involve either pharmacological such as *Lumican* or surgical interventions, such as filtration surgery, to reduce ocular pressure by improving the drainage of excess aqueous. These aim to delay the onset of neuronal and eventual visual loss. Glaucoma, as well as other retinal dystrophies, may benefit from Müller stem cell transplantation. These cells can be easily isolated from cadaveric tissue and can be grown extensively for allogeneic transplantation. Moreover, understanding the pathways involved in the differentiation processes of Müller stem cells would enhance the technology of cell-based therapies. Patients would also benefit by developing regimes

that involve activating the regenerative capabilities of endogenous Müller stem cells, possibly via small molecule or gene therapies.

The main objectives of this thesis were to further study the potential use of Müller stem cell-based therapies to treat glaucoma. The present study therefore investigated the molecular aspects of Notch signalling in the differentiation of Müller stem cells into RGCs. This involved assessing RGC markers and miRNA expression of cells undergoing differentiation. This study also aimed to examine practical transplantation of Müller stem cell-derived RGCs onto the retina by determining the suitability of type I collagen to engineer a transplantable cellular scaffold.

5.2. miRNA regulation of RGC development in Müller stem cells

Studies into the molecular regulation of the Notch pathway in human Müller stem cells involved the examination of the presence of mature microRNAs. The Notch pathway appears to control the development of RGCs derived from human Müller stem cells (Singhal et al., 2012). Inhibition of the Notch pathway with a gamma secretase inhibitor (DAPT) prevents the translocation of the Notch intracellular domain (ICD) to the nucleus. This prevents the transcription of bHLH genes which operate to prevent differentiation and promote progenicity of neural stem cells (Kageyama et al., 2005)**.**

Microarray data highlighted the presence of several upregulated miRNAs in Müller stem cells following Notch inhibition in the presence and absence of bFGF. These findings suggest the emergence of novel targets of the Notch pathway, which may promote neural development within Müller stem cell populations.

Treatment with DAPT alone in Müller stem cells generated significant upregulation of miRNAs involved in cell cycling, with some being linked to

Notch signalling. Others have also been shown to enhance differentiation or establish a cellular state which is needed to promote diversification prior to terminal differentiation.

Interestingly, the miR-30 family of miRNAs was enriched in DAPT treated Müller stem cells. This family has been implicated in the repression of the bHLH transcription factors involved in epithelial-mesenchymal transition (EMT), and indirectly on the Notch pathway. One of these targets has been linked to Notch, preventing the binding of its intracellular domain to nuclear targets. ZEB1 has been reported as a target of miR30, which prevents ZEB1 promoting the transcription of MamL and the transduction of the Notch-ICD (Brabletz et al., 2011). miR-30 members also appear to mediate the triggering of Notch by repressing DLL4 in sarcomas, preventing cell cycling (Bridge et al., 2012). A closely related family to miR-30 also demonstrated elevated expression in treated Müller stem cells, and is involved in cell cycling. The miR-29 family was also upregulated and presents a new target of the Notch pathway and may converge on its action on p107 in the proliferation of neurons (Vanderluit et al., 2004).

The mTOR kinase proliferative action was highlighted in this study by the markedly enriched expression of miR-99a in Müller stem cells undergoing Notch inhibition. This factor is deregulated in oncogenic cells causing abnormal rapid proliferation, and may be repressed during Notch inhibition in Müller stem cells by miR-99a. Another proliferative cascade implicated by this study was the PI3K/Akt pathway. This can be inferred by the observation that miR-221 and miR-222 were elevated in cultures undergoing Notch inhibition, miR-222 has been associated with preventing cell cycling by repressing the expression of factors involved in PTEN, which in turn acts to prevent PI3K/Akt signalling (Wong et al., 2012, Zhou et al., 2012), and miR221 is known to act by preventing the phosphorylation of a PI3K subunit

(Nicoli et al., 2012). Therefore they may play a role in the activation of the PI3K/Akt pathway.

A cluster on chromosome 21 was enriched in DAPT treated Müller cell populations, namely the miR-125b cluster, which contains miRNAs that are involved in diversification rather than terminal differentiation (Gururajan et al., 2010). This suggests that Notch prevents this cluster from promoting this initial diversification step in Müller stem cell differentiation.

miRNAs profiles of Müller stem cells cultured with DAPT and bFGF showed enriched expression of hsa-miR-204, hsa-miR-100, hsa-miR-151-5p, hsa-miR199b-5p and let-7i. These RNA molecules are involved in proliferation, whilst miR-199b is linked to Hes1 regulation (Andolfo et al., 2012, Garzia et al., 2009) and let-7i indicates the development of RGC within Müller stem cell populations (Loscher et al., 2007).

Five miRNAs were found to be significantly upregulated in Müller populations, undergoing Notch inhibition in both the presence and absence of bFGF. Although miR-204-5p was significantly enriched following the addition of bFGF, this miRNA doubled in expression following DAPT treatment and constituted the highest elevation for the array. Subsequent addition of bFGF to cultures further enhanced the expression of miR-204-5p, which was the only miRNA that was common to both treatment groups. miR-204 in the eye appears to target Pax6 indirectly, impacting on the final size and organisation of the ocular tissue in the medaka fish (Conte et al., 2010). This miRNA is also expressed in the mature neural retina. The interplay between RGC development and Notch inhibition may converge mainly on miR-204 in Müller stem cells. This relationship presents a novel target of the Notch pathway, and possible involvement of miR-204 in the maturation of human RGCs derived for Müller stem cells.

In conclusion, miRNAs that appear to be under the regulation of the Notch pathway were upregulated following DAPT treatment of Müller stem cells. This not only demonstrates the impact of Notch inhibition in the development of RGCs, but also identifies targets that may be used to induce regeneration of the ganglion cell population by quiescent Müller stem cells *in vivo*.

5.3. Investigations into the potential use of Electrospun Collagen scaffolds as a tool for Müller stem cell transplantation

Investigations into scaffolds produced by electrospinning type I collagen suggested that the 3D matrices obtained were able to support cellular attachment and growth. However, the need for crosslinking with cytotoxic chemicals makes them unsuitable for translation to human therapies.

Culturing of Müller stem cells was possible on electrospun collagen, with the degree of cell recovery being dependent on the crosslinking process. Crosslinking involved using agents that propagated the formation of crosslinks between lysine groups of adjacent collagen fibres. Those agents were then washed from the scaffolds, resulting in a construct able to maintain its 3D structure under culture conditions. EDC coupled with the amine group donator NHS provided a catalyst for crosslinking, ensuring complete leaching of the chemicals following incubation. Cells were observed to adhere and proliferate at a normal rate when supported on these matrices although the degree of crosslinking was not consistently reproducible with the same experimental parameters. The use of glutaraldehyde vapour to crosslink proved to induce cell death at high concentrations, possibly due to remnants of the chemical remaining within the matrix network. GTA forms protein crosslinks through incorporation of its reactive moiety into the link. This creates a potential chemical reservoir that releases its contents when the matrix is either disrupted or remodelled. It was therefore expected that lower concentrations would provide culture

systems more conducive to maintain cell viability. However, very low concentrations of GTA led to a lack of crosslinks within the fibrillar framework resulting in instability and rapid structural deterioration when placed into culture media. GTA also prevented the identification of inherent and mature markers of both retinal stem cells and RGCs due to the high charge on the collagen surface; causing non-specific binding of secondary antibodies. Additional experiments using electrospun collagen could assess the use of alternative crosslinkers such as genipin or vitamin B. However, the extent of crosslinking by these agents has been reported as being insufficient for *in vivo* application. Further investigations could examine the use of different polymers; natural or synthetic, and their competencies for physical implantation into the body as well as their biocompatibility.

Synthetic polymers are currently being investigated by tissue engineers for dermal grafts as well as internal visceral enhancers or supports. Many of the proposed materials are easily produced within finite parameters and can be modelled under different conditions generating fibrous, gelatinous structures or sheets. An additional factor which limited the use of electrospun collagen scaffolds for transplantation was the lack of biodegradability under culture conditions. The removal of such cellular supports following transplantation would not be desirable in those patients with damaged retinal tissue. Further surgery may lead to increased risk of inflammation and damage to residual functional retina, hence it would be preferable to design a substrate which is able to degrade under physiological conditions.

Although the scaffolds produced by electrospinning were stable when crosslinked with GTA, the therapy proposed for cell transplantation using an engineered support is primarily dependent on the biocompatibility of the substrate. Collagen, being a natural polymer, would be suited to the physiological conditions of the human body, and would potentially be more appropriate than those scaffolds composed of synthetic materials. However,

chemical processing of the fabricated collagen is a limiting factor when designing an electrospun scaffold and would also be the limiting factor to produce cellular scaffolds for human application.

5.4. Plastic compressed collagen scaffolds as a potential tool for Müller stem cell transplantation

The present results indicated that Müller stem cells readily adhered to collagen substrates that had undergone crosslinking via plastic compression. Collagen is innately strong and is the main protein found in the body which provides a variety of cells with mechanical support. Collagen is sourced from dermal mammalian tissues and is extracted for *in vitro* culturing; being a naturally occurring polymer, the degree of biocompatibility of the protein is thought to be much greater than that of synthetic sources. The various extraction methods used denature the collagen, weakening the original framework of the proteins ultrastructure. Unlike other chemical measures taken to crosslink extracted collagen samples, plastic compression involves physical crosslinking by removing the water component of hydrogels (Brown et al., 2005).

Müller stem cells are able to firmly attach to compressed collagen substrates and are able to grow at normal rates when compared to no matrix controls. Müller stem cells subjected to differentiation protocols involving culture with DAPT and bFGF were also observed to adhere firmly to constructs. Examination of the presence of RGC markers in Müller cell-derived RGCs demonstrated that these cells positively stained for proteins of mature retinal ganglion cells and early neural precursors *in vitro*. Constructs were also stable when subjected to physical manipulation for surgical processing, although at low concentrations of the protein, constructs were easily damaged through handling.

Further studies on the preparation of these constructs would entail exploring the extent of their degradation under both *in vitro* and *in vivo* conditions. Like electrospun collagen, compressed substrates were not seen to degrade over extended periods of time (up to 3 months) at any concentration. The degree of protein breakdown could be determined by ELISA analysis in order to quantify the amount of collagen present within the supernatants. Furthermore, in order for the structure of the constructs to be suitable for transplantation the structure must be temporary. Although the scaffolds designed during this investigation were not found to biodegrade, future studies could be aimed at designing protocols to create a transplantable construct which can deliver cells and therapeutic agents to the ganglion layer and later degrade without releasing products that activate local microglia. Tailoring the structure of collagen constructs may aid their degradation by creating weak junctions within the collagens fibres. Blends of polymers; natural, synthetic or a mixture of both could also be employed to yield a construct suitable for *in vivo* use. The rationale behind blends is to merge favourable traits of the different materials that could potentially yield a biodegradeable and biocompatible scaffold for Müller stem cell transplantation. This may also help overcome the contraction processes imposed on the collagen substrates by cells. Further understanding of the extent of crosslinks created via physical compression could also lead to possible modifications of the constructs.

The evidence presented in this study suggests that compressed collagen creates matrices support Müller stem cells in culture as well as their differentiation towards a retinal ganglion cell fate. Following modifications of these constructs, they may constitute a potential tool for cell transplantation onto the inner retina.

5.5. Transplantation of RGC precursors *ex vivo* and *in vivo* using compressed collagen scaffolds

Vitrectomy followed by intraocular transplantation of human Müller stem cell derived RGCs led to delivery of cells onto the inner retinal surface. Although alignment of scaffolds was observed within some subjects, aggregation was also observed within anterior segments of the ocular cavity, adjacent to port entry sites.

Supporting Müller stem cells on compressed collagen for transplantation aimed to prevent cell aggregation following a single bolus injection. While Müller stem cells were supported on PC scaffolds, the extent of uniform migration onto the retina was dependent on surgical parameters, as well as modulation of the local retinal ECM. Transplantation of stem cells for cell-based therapies encounter many barriers, where the mode of transplantation, locality of the region undergoing transplantation and the source of cells used are all relevant to the choice and design of cellular scaffolds. However, one major limitation of functional integration of stem cells into host tissue is the microenvironment condition, created by abnormal deposition of ECM and the presence of inflammatory microglia (Gehrmann et al., 1995, Singhal et al., 2008).

Cellular scaffolds delivered directly onto the inner retinal surface, were seen to facilitate alignment of cells uniformly along the inner retina. However, integration into host tissue was not observed. The lack of migration observed in regions of close contact between the scaffold and retina may be ascribed to insufficient delivery of ChABC. This enzyme acts by targeting the neural ECM which acts to direct neural tissue during development, and is present within adult tissue. Following neurodegeneration in the CNS, including the retina, these proteins are known to accumulate (Steinmetz et al., 2005, Zhang et al., 2003). ChABC digests the reactive glycosaminoglycan (GAG) side chains into simple disaccharides, from their

CSPG core. The application of ChABC to treat spinal cord injury (Bradbury et al., 2002) and similar CNS injuries have been extensively examined both *in vitro* and *in vivo*, and have been shown to have a positive impact upon the extent of axonal regeneration. Such experiments demonstrated re-growth of damaged neurites within corticospinal, reticulospinal and nigrostriatal populations following ChABC treatment (Garcia-Alias and Fawcett, 2012). Moreover, studies assessing the migration of transplanted cells illustrated that generation of axons was enhanced when the peripheral regions of the spinal ECM, interfacing the graft, had undergone treatment with ChABC (Fouad et al., 2005, Karimi-Abdolrezaee et al., 2010, Tom et al., 2009, Garcia-Alias and Fawcett, 2012).

Therefore, and as previously described (Singhal et al., 2012, Singhal et al., 2008), injection of ChABC onto retinal tissue prior to transplantation is important for providing optimal conditions for integration of transplanted Müller stem cell derived RGCs into the retinal ganglion cell layer.

Entry sites made for surgical instruments and the infusion line were directed into the pars plana which is the junction between the neural retina and ciliary body. This region measures between 2-3mm in humans, but the rabbit equivalent is smaller and more vascular in nature. In addition, the rabbit eye also houses a larger lens within the anterior chamber. These anatomical differences required modification of the surgical technique. Therefore, rabbits underwent lensectomy (lens removal) in order to correct the limitation of spatial placement of portals. However, cellular scaffolds were observed to remain proximal to the site of entry. This localisation of scaffolds may have been due to their insufficient expulsion from the cannula or due to the angulation and depth of the cannula which may have contributed to cellular aggregation, cell death, changing the properties of the original scaffolds. To that end, extensive repopulation of the ganglion layer was not observed. Cells tended to integrate within the region close to the

scaffolds if aligned along the retina. Extensive microglial mobilisation was also seen within regions of cellular aggregation, indicating a local immune response to grafted cells. This could be prevented in future studies by ensuring administration of sufficient anti-inflammatory drugs prior and throughout the experiment.

The application of Müller stem cell derived RGCs for human glaucoma therapies would require implantation into degenerated retina where the structure and microenvironment would be abnormal, posing difficulties for cells to integrate into the retina. Future studies would need to identify whether transplanted Müller stem cells are able to integrate into diseased tissue where the architecture is deteriorated. This would entail creating a model of retinal ganglion depletion or glaucoma in a large mammal. Furthermore, functional assessment by ERGs, alongside histological analysis would determine the extent of retinal repair by these cells. The degree of migration and cell replacement is likely to be coupled with the efficiency of ILM and local ECM modulation achieved by ChABC, hence effective delivery would entail stabilising this proteolytic enzyme.

5.6. Conclusions

This work demonstrated that miRNA profiles alter following Notch inhibition in Müller stem cells, suggesting that the maturation of RGCs *in vitro* can be modulated by small molecules. This work also demonstrated that although it is possible to generate collagen-based scaffolds that support cell growth and adhesion, there are still many factors that need to be assessed for appropriate fabrication and delivery. Preparation of cellular scaffolds for retinal transplantation require emphasis upon their structural integrity and the biocompatibility of the biomaterials used. Müller stem cells could be cultured *in vitro* with type I collagen, however plastic compressed collagen scaffolds generated the most suitable constructs for transplantation. Implantation of these scaffolds demonstrated that Müller stem cells could be

supported during the grafting process, and could be positioned in close proximity to the retina during surgery. Therefore, it can be proposed that PC collagen scaffolds may constitute a viable source of material to support inner retinal cell grafting, but further studies are needed to evaluate and refine the optimal conditions and modifications required to produce biodegradable and non-contractile scaffolds. A final limitation to cellular integration *in vivo* following scaffold delivery is the efficiency of modulation to the local retinal ECM. In order to restore function to the ganglion layer, grafted cells need to migrate and synapse with host neurons to promote residual cell survival or cell replacement, and appropriate degradation of the ECM *in vivo* by ChABC needs to be established.

Müller stem cells from human retina constitute a potential source of cells that may be used to produce RGCs *in vitro*, for delivery onto the inner retina *in vivo*. However, the alterations of miRNAs following Notch inhibition suggest that these cells house intrinsic regulatory molecules for RGC maturation and have the potential to be modified *in vivo*. This would remove the financial and regulatory implications of stem cell transplantation, and merit further studies to induce their endogenous regeneration without the need for transplantation.

Chapter 6: Materials and Methods

6.1. Construction of type I collagen scaffolds using Electrospinning methods

Electrospinning was performed within an interlocked extraction cabinet. Rat tail type I collagen (First link UK) was dissolved in either acetic acid or hexafluoroisopropanol; HFIP, (Appollo scientific Ltd), at a concentration of 50mg/ml. Solutions were brought up to room temperature before transferring to a syringe attached to a 22 gage cannula. Under appropriate voltages ranging between 12kV-15kV, using a HPV power supply, collagen fibres were drawn onto a grounded target enclosed within aluminium foil. The grounded targets were set at a range of distances between 10cm-20cm. Fibres were drawn for a maximum of two hours. The infuse rates ranging between 2-5ml/hr were applied via a Harvard 4400 syringe pump.

6.1.1. Crosslinking of electrospun collagen scaffolds

6.1.1.1. Glutaraldehyde vapour crosslinking

Air dried non-crosslinked collagen scaffolds supported on foil were crosslinked within a sealed desiccator. Collagen scaffolds were placed onto a perforated ceramic tray within the desiccator and, exposed to glutaraldehyde (GTA) vapours (Sigma-Alrich). The presence of aqueous solutions of 5-25% glutaraldehyde within the desiccator, contained in a glass Petri dish under the perforated tray, ensured the release of glutaraldehyde fumes and the progression of chemical crosslinking. Collagen scaffolds were allowed to crosslink for 72 hours at room temperature, followed by washes over 24 hours with deionised water. Matrices were then air dried in a fume cupboard at room temperature.

6.1.1.2. EDC crosslinking

Collagen scaffolds were crosslinked within a sealed glass dish containing aqueous solutions of 1-Ethyl-3-(3-dimethylaminopropyl) carbodiimide (EDC) (Appollo Scientific), alone or supplemented with N-hydroxylsucinimide (NHS) (Sigma-Aldrich). A solution of 30wt% EDC alone or EDC in combination with NHS at a ratio of 1:1 (w/w), in a 9:1 (v/v) mixture of acetone and water was used to induce the crosslinking process. Scaffolds were fully immersed in the solutions for 2 hours at room temperature on a slow shaker. Collagen scaffolds were then air dried overnight in a fume cupboard and repeatedly rinsed and washed with deionised water several times, in order to remove any residual reagents.

6.2. Construction of type I collagen scaffolds by plastic compression

Rat tail type I collagen (FirstLink UK) solutions were made in 0.06% acetic acid at a stock concentration of 2mg/ml. Solutions were subsequently diluted to 1-0.75 mg/ml in 0.06% acetic acid. One part of Minimum essential medium 10x (Invitrogen Ltd, UK) was added to 8 parts of collagen solution to aid neutralisation. Under sterile culture conditions, solutions underwent neutralisation by the addition of 5M sodium hydroxide (Sigma-Aldrich, Dorset, UK) drop-wise, to ensure collagen polymerisation. This was monitored by colorimetric change from straw yellow to pale pink (neutral pH). The solutions were left on ice for 20 minutes to disperse bubbles formed during neutralisation. Volumes of these solutions, 300µl-1ml were then added to titanium circular moulds ranging from 0.5cm-2cm diameters and subsequently incubated at 37°C in 5% CO_2 for up to 30 minutes to induce fibrillogenesis. Hydrogels were removed from incubation and placed between two nylon meshes. Hydrogels were then compressed under 150g loads for 5 minutes. Compressed collagen scaffolds were floated off the nylon into Phosphate Buffered Saline (PBS) before cell culture procedures.

6.3. Cell culture

6.3.1. Müller Stem Cell Culture

Established Müller stem cell lines at the Institute of Ophthalmology were used in this study. To passage these cells, monolayers of cultured cells were dissociated using TryplE^{TM} x1 (Life technologies), followed by 5 minute incubation at 37°C, 5% CO_2. Dulbecco's Modified Eagle Medium (DMEM) supplemented with FCS (5mls per T-175) was added to the flasks to collect the dissociated the cells. Cell suspensions were centrifuged at 1400 rpm at 15°C for 5 minutes. Supernatants were aspirated, whilst cell pellets were resuspended in fresh media and added to new culture flasks. Fully confluent monolayers formed after 7 days and were maintained through passaging in a 1/5 dilution.

Cell stocks were maintained by cryopreservation of cultured cells and was performed by resuspending cell pellets from T-25 culture flasks in 1ml of freezing mix composed of; 40% FCS and 10% Dimethyl Sulfoxide (DMSO) (Sigma-Aldrich, UK) in DMEM. Cell suspensions were transferred to cryovials that were placed within an isopropanol freezing cassette at -80°C for 24 hours, this ensured controlled cryopreservation. Frozen suspensions were then transferred to -150°C for long term storage.

All cells were grown and passaged in DMEM containing L-Glutamax without pyruvate (PAA, UK), 10% FCS (Biosera), 5ml mixture of penicillin (2,000U/ml) and streptomycin (2,000µl/ml) (Life technologies) in 500mls of DMEM. Incubated at 37°C in 5% CO_2 air atmosphere.

6.3.2. Use of extracellular matrix substrates and growth factors to culture Müller stem cells

For differentiation Müller stem cells were cultured on polystyrene tissue culture plates or flasks (Nunc, Thermo Scientific) coated with ECM Gel from

Engelbreth-Holm-Swarm murine sarcoma (ECM) (cat no: E1270, Sigma-Aldrich, UK), reconstituted to stock concentrations as per company instructions and subsequently aliquoted and stored at -20°C. Aliquots were diluted in sodium bicarbonate buffer; 15mM Na_2CO_3, 35mM $NaHCO_3$, pH 9.6 to a working concentration of 50ng/ml. They were also stored at -20°C until use. To coat the surfaces of culture plastics, it was ensured that the matrix solution covered the entire area (a minimum of 1ml/ T-25 flask). Flasks or plates were incubated at 4°C overnight or at 37°C for 2 hours. Prior to cell culture, ECM solutions were fully aspirated and flasks were washed with sterile PBS.

Recombinant Human Fibroblast Growth Factor-2 (bFGF; cat no: F0291, Sigma-Aldrich, UK) and N-[N-(3,5-difluorophenacetyl)-l-alanyl]-S-phenylglycine t-butyl ester (DAPT; cat no: D5942, Sigma Aldrich, UK) were reconstituted according to the manufacturer's instructions and stored in aliquots at -20°C prior to use. bFGF was diluted in culture medium to yield a final concentration of 20ng/ml, whilst DAPT was diluted to a concentration of 50ng/ml. These factors and their concentrations were determined by previous studies performed in the laboratory (Singhal et al., 2012). There was no subsequent replenishment of factors during the progression of the experiments. For differentiation studies the FCS content of culture media was reduced to 5% in order to reduce Müller stem cell proliferation.

6.3.3. Use of collagen-based scaffolds for Müller Stem Cell Culture

Electrospun collagen scaffolds were sterilised by immersion in 70% ethanol for two hours at room temperature. Under cell culture conditions the ethanol solutions were removed and scaffolds were rinsed with sterile PBS. Scaffolds were then repeatedly washed three times for 10 minutes with sterile PBS. DMEM containing 10% FCS and Penicillin Streptomycin was added to scaffolds and incubated for 8hrs, or overnight, at 37°C in 5% CO_2. Media was then removed and cells seeded onto "wet" scaffolds. Compressed

collagen scaffolds were transferred from PBS into 2.5cm tissue culture dishes prior to DMEM and Müller stem cells addition.

100% GFP lenti-viral labelled MIO-M1 were grown to a confluent layer in a T-25 tissue culture flasks, using DMEM containing 10% FCS (as above). Once a confluent layer was formed, cells were detached by trypsinisation, following subsequent pelleting and resuspension cells were counted using a haematocytometer. Cell viability and number were determined by dilution with trypan blue (1:1 ratio, 10µl) and added to the haemotocytometer. Unstained viable cells were counted within the squares of the central grid; the inner and four corner squares. Following counting cells were suspended at a concentration of 12,500 cells/ml. 2ml of this suspension was added to scaffolds, which were incubated at 37ºC until a subconfluent layer was obtained after 7 days.

6.3.4. *In vitro* transplantation of cellular scaffolds onto explanted retina

Donor human eyes from Moorfields eye bank were obtained under ethical approval for *ex vivo* explant culture. Anterior portions of the globes were removed 4mm from the Limbus. The vitreal body was then gently removed and the globe dissected into quadrants down to the optic nerve head. The retina was carefully separated from the RPE layer by folding the retinal quadrants towards the centre; the optic nerve was then cut to detach the retina. Retinas were then placed on 0.4 µM pore PTFE hydrophilic cell culture insert 30 mm diameter filter (Millipore, USA) contained in a 6-well plate. Müller stem cell derived RGCs were placed onto 1cm, 300µl-0.75mg/ml compressed collagen scaffolds at a concentration of $11.25x10^4$ cells/ml for 2 hours prior to placing onto retinal explants. Explants were cultured for a maximum of 7 days. The culture medium comprised 48.5 ml Neurobasal A-Medium (cat no: 12349, Life Technologies, UK) and 1.5 ml mixture of media supplements (Wang et al., 2002). Supplements were made

of 500 µl of 2% B-27 (cat no: 17504-044, Life Technologies), 200 µl of 0.8mM L-Glutamine (cat no: 25-005-CI, Cellgro), 250 µl of 1% N-2 (cat no: 17502048, Life Technologies) and 500 µl of 100U/ml Penicillin/Streptomycin (cat no: 15140122, Life technologies). Ex vivo tissues were then prepared for cryosectioning and confocal microscopy.

6.4. Cell Viability Assay

Cell viability was assessed using the hexosaminidase assay which evaluates the number of living cells by colorimetric determination of hexosaminidase levels within lysomes. 96 well plates were seeded with 5,000 cells/well (in accordance with growth rate analysis) and cultured for 7 days at 37°C in 5% CO_2. Examination of hexosaminidase levels involved initial centrifugation of the plates at 1400rpm for 3 minutes. Culture media was subsequently removed from the plates and rinsed with PBS to remove residual serum. Plates were then centrifuged again prior to substrate addition. 60µl per of hexosaminidase substrate was transferred to each well and incubated at 37°C for 4 hours. The reaction was blocked by the addition of 90 µl of 0.1M glycine-sodium hydroxide buffer, pH 10.4. The absorbance was read at 405nm with a blank reading taken at 620nm. Control readings were also collected for substrate and buffer alone at the time of recording.

The hexosaminidase substrate was made by adding 200mg of p-nitrophenyl-N-acetyl-β-D-glucosaminide to 78ml of 0.1M Tris sodium citrate, adjusted to pH 5.0 and 78ml of 0.5% Triton X-100 in water.

6.5. Collagen digestion of scaffolds

Stock solutions of 0.5% collagenase D (Roche) in PBS containing calcium and magnesium were diluted 1:10(v/v) with PBS. Media was removed from the collagen scaffolds and 90µl of diluted collagenase D was added to each scaffold. The collagen scaffolds were then incubated for 30 minutes at 37°C.

The digestion system was disrupted at 10 minute intervals by severe pipetting. The plates were centrifuged at 9,000rpm for 5minutes to separate the cells and collagen from the enzyme solution. The collagenase D was then removed and the cell viability assessed by trypan blue exclusion and hexosaminidase assay.

6.6. Measurement of optical density of collagen scaffolds

Ocular densities of collagen scaffolds were analysed using absorption spectra and the Safire software. For the assay, collagen scaffolds were place onto the culture surfaces of 96 or 24 well plates (Nunc) in PBS and measured, without lids, for light absorption over the visual range (350nm-750nm) with 10 averaged readings taken per well.

6.7. Electron microscopy analysis of collagen scaffolds

The adhesion and cellular-matrix behaviour were assessed by scanning and transmission electron-microsopy (SEM and TEM) respectively. The collagen scaffolds were fixed in Karnovsky's fixative for 2 hours and then rinsed and washed with 0.1M sodium cacodylate at pH 7.4, 3 times for 10 minutes. Secondary fixation was achieved by submerging scaffolds in 1% (w/v) aqueous osmium tetroxide for 2 hours in the dark. The scaffolds were rinsed repeatedly with deionised water to remove excess secondary fix. The specimens were then dehydrated by ascending alcohol concentrations; 50%, 70%, 90% and 100% ethanol solutions, with 4 changes for each ethanol concentration. Specimens for SEM analysis were air dried for 8 hours and subsequently mounted onto carbon stubs. The specimens underwent vacuum gold coating before examination under scanning electron microscopy (JEOL JSM 5500 LV). ImageJ was used to measure the area fraction of SEM mcrographs to determine both the pore size and the number of pores per surface area.

6.8. Western Blotting

6.8.1. Protein Isolation from cultured cells

Following culture under varying conditions, whole cell lysates from dissociated monolayers of Müller stem cells were processed to study their protein expression profiles. Radio immunoprecipitation Assay Buffer (RIPA, Sigma-Aldrich) was used to isolate nuclear and cytoplasmic proteins. To 1ml of cold RIPA buffer; 10µl of protease inhibitor cocktail (P8340, Sigma-Aldrich, UK), 0.05mM Dithiothreitol (DTT), 1mM Phenylmethylsulphonyl Fluoride (PMSF) and 3mM Sodium Orthovanadate were added. Cells were detached by scraping, and washed with cold PBS to remove residual FCS. Subsequent to centrifugation, supernatants were removed and pellets were disrupted with cold RIPA containing protease inhibitors (100µl/ T75 pellet). Pellets were homeogenised, vortexed briefly and left on ice for 5 minutes for cells to complete lysis. Suspensions were then centrifuged at 9000rpm to remove cellular debris. The supernatants containing the cellular proteins were collected and placed at -20°C for short-term storage or -80°C for long-term storage.

Protein levels were measured using the Bio-Rad Protein Assay Dye Reagent (cat no: 500-0006, Bio-Rad Labs, UK) and the colorimetric Bradford Assay. The assay dye, consisting of coomassie brilliant blue G-20 was diluted 1 in 4 with 50µl of this reagent added to 2.5µl of protein sample. The mixture was vigorously pipetted and incubated at room temperature for 5 minutes. The dye binds to proteins altering the conformation of the dye's structure changing its colour from brown to blue. The absorbance was measured at 450nm to 595nm, against a blank reading consisting of the diluted reagent with 2.5µl of molecular grade water (Roche). Protein levels were determined by extrapolation of absorbance onto standard curves prepared with bovine serum albumin of known concentrations.

6.8.2. Protein Gel Electrophoresis

The NuPAGE system was used to perform gel electrophoresis (Life Technologies, UK). To detect proteins with molecular weights between 14-55kDa, 4-12% Bis-Tris gels were run with MES SDS running buffer (cat no: B0002, Life technologies, UK). For proteins larger than 55KDa, 12% Bis-Tris gels with MOPS SDS running buffer (cat no: NP0001, Life Technologies, UK) were used. The gels used contained 15 wells of 1.5mm size. Preparation of protein for gel loading involved denaturing the complex structures into linear conformations that could be resolved as separate bands and thus their molecular weights. The total volume run for each sample was 30µl. This was prepared by mixing 3µl of 10x reducing agent (cat no: NP0009, Life technologies, UK), 7.5µl of NuPAGE loading buffer (cat no: NP0007, Life Technologies, UK) and a maximum volume of 19.5µl of protein lysate. The volume 19.5µl for the protein was adjusted based on the lowest protein concentration yielded for each set of control and test samples and brought up to this volume with water. Samples were then heated for 10 minutes at 80°C to denature the proteins.

Gels were placed into the internal chambers of XCell Surelock Mini-Cell Gel Electrophoresis cassettes (cat no: EI0001, Life Technologies, UK) and 200ml of running buffer were added to this chamber (200ml containing 500µl of antioxidant) (cat no: NP0005, Life Technologies, UK). The external chamber was filled with water to keep the system cool during running. Gels combs were removed gently and loaded with protein sample solutions (15µl) and protein ladder (5µl, cat no: P7709L, Biolabs, UK) and run at 180V for 1 hour.

6.8.3. Protein transfer onto PVDF membranes

Polyvinylidene fluoride (PDVF) membranes (Immobilon-FL PVDF, 0.45 µm; cat no: IPFL00010, Millipore) were prepared for wet transfer and involved cutting membranes to size and submersion into methanol for 2 minutes,

washed in distilled water and placed into NuPAGE transfer buffer containing (cat no: NP0006-1, Life Technologies, UK) 15% methanol v/v for a minimum of 10 minutes. Wet transfer was conducted using the XCell Surelock Mini-Cell Gel Electrophoresis cassette at 35V for 90 minutes.

6.8.4. Protein immunodetection

Subsequent to protein transfer onto PDVF membranes, these were blocked at 37°C for 1 hour with 5% FCS in 1x TBS and containing 0.1% Tween20. Following blocking, relevant antibodies were diluted in the blocking solution, and added to the membranes, which were placed in plastic casing and sealed to avoid dehydration. Membranes were incubated overnight at 4°C on a slow shaker, then washed 3 times with 1x TBS and 0.1% Tween20 for an hour. The membranes were incubated at room temperature on a slow shaker with appropriate horseradish peroxidise secondary antibody (HRP) for 2 hours and washed again as previously described. These were X-rayed following rapid incubation (maximum of 5 minutes) with Pierce ECL Western Blotting Substrate (cat no: 32209, Thermo Scientific Intl) where substrate A and B were diluted at a ratio of 40:1 (v/v).

6.9. Reverse- transcription polymerase chain reaction

6.9.1. RNA Isolation

Müller stem cells cultured under various conditions were analysed for mRNA and miRNA expression levels. Cells were detached and centrifuged to obtain a cell pellet which was then washed with 1 ml of cold PBS and spun at 4000rpm for 5 minutes. Pellets were resuspended in QIAzol lysis Reagent to extract RNA in accordance with the manufacturer's instructions. Total RNA from T-75 cell monolayers was isolated using the miRNeasy Mini Kit (cat no: 217004, Qiagen). This enabled purification of total RNA using a column isolation system which includes RNA from 18 nucleotides (nt) upwards. Total RNA was eluted with 22µl of RNase free water and the concentrations

measured using a spectrophotometer (Nanodrop-1000, Thermo Scientific). Samples were stored at -80°C and thawed prior to use for both array analysis and RT-PCR processing.

6.9.2. Reverse Transcription (RT)

SuperScript III Reverse Transcriptase kit for RT-PCR (cat no: 18080-093, Life Technologies, UK) was used to generate cDNA from isolated RNA samples. Each RT preparation contained 500ng of RNA to ensure comparative results were obtained for the various conditions examined. A 20µl mixture was made as per manufacturer's instructions where RNA/water samples were made up to 11µl containing 500ng of RNA. Samples were initially incubated at 65°C for 5 minutes, with 25µM of oligo-d(T)^{20} primer and 10mM of dNTP$^{12\text{-}18}$. Following this initial incubation, the solution was then mixed with 4µl of 5x reaction buffer, 2µl of 0.1M Dithiothreitol (DTT), 2µl RNase Inhibitor (40U/µl) and 2µl SuperScript III reagent. The solution was vortexed and transferred to a gradient thermo cycler (Eppendorf, UK). The incubations were carried out at 25°C for 10 minutes, 42°C for 1 hour, 99°C for 5 minutes and then held at 4°C. The cDNA produced was stored at -20°C until processed for PCR.

6.9.3. Polymerase Chain reaction (PCR)

Gotaq x2 Master mix (Promega, UK) was used to process cDNA synthesised from RNA samples in order to perform PCR. A 25µl solution was prepared per PCR reaction over ice, using 1-2µl of cDNA according to the manufacturer's instructions. Solutions contained 13µl of GoTaq x2 Master Mix, forward and reverse primers of the genes of interest and molecular grade water. Primers were obtained in desalted forms from Life technologies Custom primer service and resuspended to a working dilution of 50µM in

molecular grade water. Final primer concentrations were adjusted at concentrations between 0.2-0.4µM/ml. PCR mixtures were then transferred to a thermocycler where they were subjected to an initial denaturation step at 94°C for 2 minutes, 94°C for 30 seconds, primer annealing temperature for 30 seconds, 72°C for extension for 1 minute. Steps 2-4 were then repeated between 28-35 cycles followed by a final extension at 72°C for 7 minutes and finally held at 4°C. PCR products were analysed by electrophoresis on a 2% agarose gel containing 1:15000 Gel Red nucleic acid gel stain. Each well was loaded with 10µl of PCR product. In each gel had at least one well was loaded with 1 kb DNA ladder (TrackIt, cat no: 10488-072, Life Technologies, UK) to enable band size identification for specific genes. Gels were cast and run at 110V for 45 minutes and subsequently imaged under UV light using the Genesnap Image Acquisition program. Densitometry measurements of autoexposed images were used to analyse the relative levels of gene expression using Image J software. All genes were normalised to the respective β-Actin levels.

6.9.4. microRNA Analysis

Total RNA was isolated as described previously. Each sample was eluted into 22µl of RNAse free water. A 2µl volume was examined for degradation using the Agilent 2100 Bioanalyzer RNA 6000 Nano LabChip Kit (Agilent Technologies, USA). The quality of each sample was assigned an arbitrary unit based on a graphical read-out of nucleotide size against fluorescence.

The RNA was then assessed for miRNA levels using Aligent miRNA Microarray system with miRNA Complete Labelling and Hyb kit (Agilent

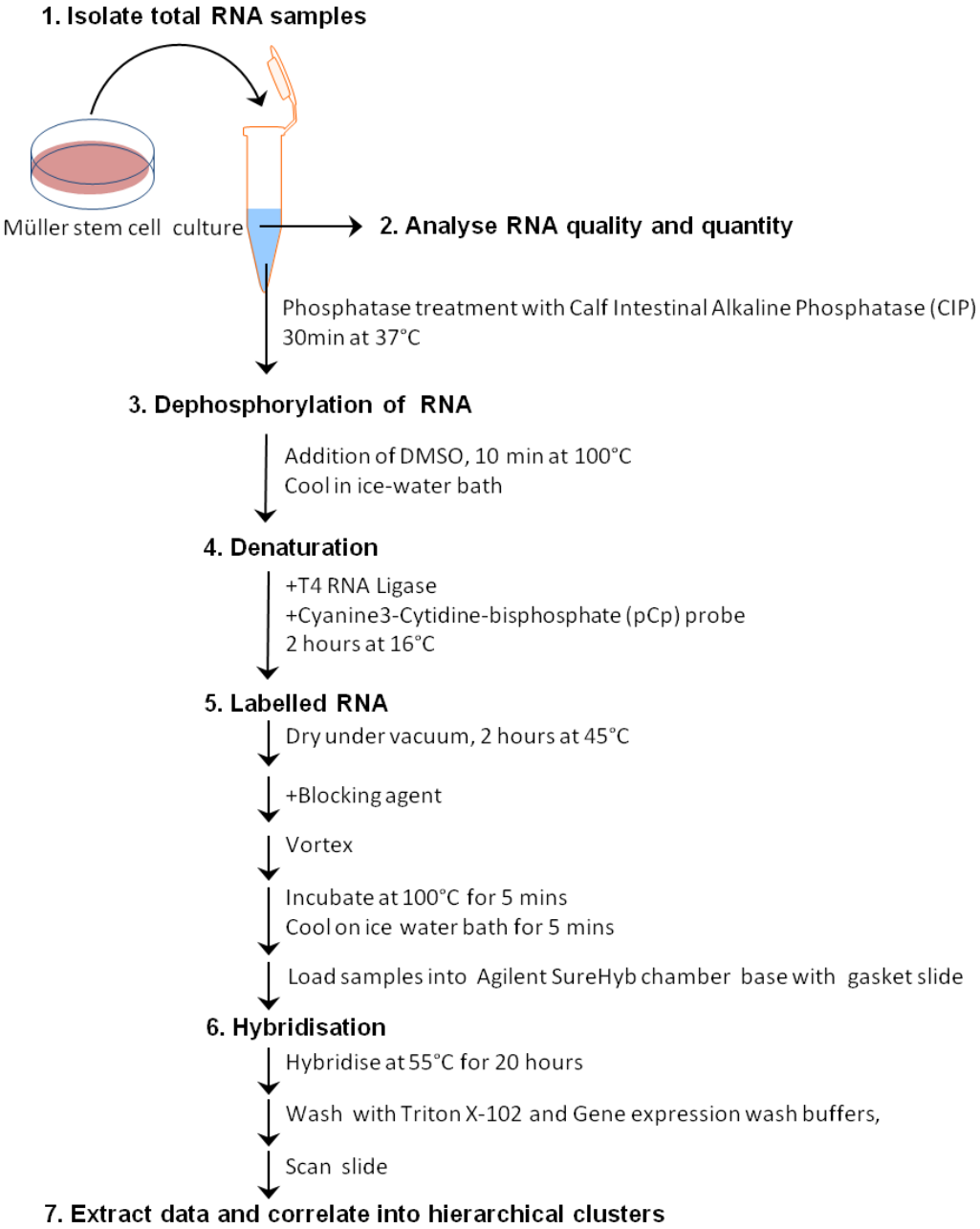

Figure 6.1: Microarray work flow. Total RNA samples were isolated from Müller stem cultures, after one week and processed for array analysis. Microarray analysis techniques enabled miRNA profiling of Müller stem cell cultures. Protocol follows the Agilent methods for miRNA detection.

Technologies, USA) (Figure 6.1), in which dephosphorylation of 100ng RNA was performed. Samples were then labelled with Cyanine3-pCp and incubated for 2 hours at 16°C. Labelled RNA was desalted and dried under vacuum for 3 hours at 55°C. RNA samples were then loaded onto a SureHyb 8-well chamber and hybridised for 20 hours at 55°C under agitation at 20rpm. Slides were scanned under FITC fluorescence and emission profiles recorded.

6.10. Immunostaining

6.10.1. Immunostainning of cells and retinae

Cells were cultured as described previously on 13 mm glass coverslips coated with ECM in 24 well plates for a maximum of 7 days, without factor or medium replenishment.

Following culture media was aspirated and cells fixed with 4% paraformaldehyde for 10 minutes. Wells were then rinsed and washed twice for 5 minutes, with PBS. Cryropreservation was achieved by incubating the wells with 30% sucrose for 10 minutes at room temperature, followed by removal of sucrose. Aired dried specimens were stored at -20°C for later use.

Blocking solution was prepared by adding 5% Donkey serum (cat no: 017-00-121, Jackson Labs) and 0.3% triton X-100 to 1xTBS. Cells were incubated for 1 hour at room temperature with freshly made blocking solution. Primary antibodies were diluted in the same solution and added to the wells overnight at 4°C or 2 hours at room temperature. Wells were subsequently washed three times with TBS for 5 minutes. Secondary antibodies labelled with Alexa Fluoros fluorescent dyes (Life Technologies, UK) were diluted 1:500 in block solution. Cells were then incubated in the dark for 2 hours at room temperature with the secondary antibodies. Wells were rinsed and washed with TBS as before. Nuclei were stained with 4,6-

diamidino-2-phenylindole, DAPI (Sigma-Aldrich) 5mg/ml, diluted 1 in 5000 in PBS for 1 minute at room temperature. Cells were rinsed again and washed once for 5 minutes with TBS. Buffer was then aspirated and coverslips were mounted on glass slides using Vectashield Mounting Medium (cat no: H-1000, Vector labs, USA). Edges were sealed with nail vanish, air dried under darkness and stored at 4°C prior to microscopical analysis.

Cryostat tissue sections were obtained between 15-20µm thickness and air dried overnight at room temperature before processing as described above, although tissues were fixed in 4% PFA, overnight at 4°C and placed in 30% sucrose for 48 hours at 4°C. Prior to sectioning tissue was embedded in OCT medium (cat no: SURG08609E, VWR, UK) over dry ice. Images were captured using a Zeiss LSM 710 confocal microscope and Zen Lite software.

6.10.2. Quenching auotofluorescence of glutaraldehyde crosslinked collagen scaffolds

To quench the autofluorescence of the chemically crosslinked constructs a 1% solution of sodium borohydride in PBS was added. The scaffolds were incubated in the actively bubbling solution for 40 minutes and then rinsed twice with PBS.

6.10.3. Wholemount Immunostaining of Müller stem cells on collagen scaffolds

Scaffolds were incubated for 10min with 4% paraformaldehyde and washed with PBS for 5 minutes prior to staining. Scaffolds were then incubated with blocking solutions (0.3% triton X-100, 5% donkey serum and 2% BSA in TBS) for 1 hour at room temperature. 200µl of primary antibodies diluted in blocking solution were added, and incubated overnight at 4ºC. Primary antibodies were then removed and scaffolds were washed with TBS 3 times for 5 minutes. 500µl of Alexa-fluor secondary antibodies diluted 1:500 in

blocking solution were then added, and scaffolds were incubated for 1 hour at room temperature, covered in foil to preserve fluorescence. Scaffolds were washed as before, and stained with 4,6-diamidino-2-phenylindole, DAPI (Sigma-Aldrich) 5mg/ml, diluted 1:5000 in PBS for two minutes at room temperature. Finally they were washed as before, and rinsed with distilled water. Collagen scaffolds were gently removed, placed onto slides and left to dry at room temperature. Subsequently the scaffolds were mounted with vector shield (Vectalabs). Coverslips were placed over scaffolds and sealed with clear vanish. Slides were imaged using the Leica DM IRE2 confocal or the Zeiss LSM 710 microscope and images obtained by over-lay snapshots taken at different wavelengths. Images were analysed using the LSM Zeiss browser or Leica confocal software.

6.11. *In vivo* transplantation of cellular scaffolds onto the rabbit retina

6.11.1. Cellular and scaffold preparation

Müller stem cells were transfected with an immunodeficiency virus type 1 (HIV-1) based lentiviral vector which expresses low toxicity hrGFP (Yanez-Munoz et al., 2006). Transfection was undertaken by the molecular therapy laboratory at the Institute of Ophthalmology, where transfection efficiency was 90%. Cells were expanded and later stored at -150°C for future work. Preceding transplantation GFP-lentiviral transfected Müller stem cells were placed in culture and differentiated into RGC precursor for a maximum of 7 days. For the duration of the experiment cells were examined under light microscopy to observe morphology and viability. Prior to transplantation, compressed collagen scaffolds were made as follows: 0.75mg/ml collagen with a volume of 300µl were added to a 1cm diameter casting ring which underwent compression under 150g for 5 minutes. Scaffolds were removed from nylons and placed onto 1cm coverslips contained within 2.2cm diameter MaTek dishes and flattened. Cells were added dropwise onto the scaffolds at

a density of $4x10^5$/250µl per side and incubated at 37°C at for a maximum of 2 hours in DMEM containing 10% FCS to aid adhesion. Scaffolds loaded with cells were then rinsed and washed 3 times for 10 minutes with sterile PBS (PAA) to remove residual serum. Scaffolds were stored in PBS at room temperature prior to transplantation.

6.11.2. Rabbit Husbandry

Chinchilla bastard female rabbits between 2.5-3kg were maintained according to Home Office regulations for the care and use of laboratory-based animals in the UK (Scientific Procedures Act). This species was chosen to examine the applicability of collagen scaffolds for Müller stem cell derived RGC transplantation. Scaffold transplantation was made after surgical removal of the vitreous body via 18G Pars Plana vitrectomy performed by Mr David G Charteris and Mr Hari Jayaram, surgeons from Moorfields Eye Hospital.

Animals were immunosuppressed with oral Ciclosporin A (Sandimmun, Novartis, UK) administered orally once a day in water; 150ml/kg/day together with Prednisolone. The steroid Prednisolone was given for the duration of the experiment but dosages were lowered weekly as follows: week 1- 2.1mg/kg/day; week 2- 1.4mg/kg/day; and week 3- 0.7mg/kg/day. Rabbits were immunosuppressed 3 days prior to transplantation, and immunosuppression was continued for the duration of the study.

6.11.3. Vitrectomy

Rabbits were anaesthetised with an intramuscular injection of Ketamine; 50mg/kg (Ketaset, Fort Dodge Animal Health, UK) and 20mg/ml of Xylazine (Rompun, Bayer). The pupils of the eye to be vitrectomised were dilated with 15 tropicamide and 2.5% Phenylephrine (Chauvin Pharmaceuticals, UK). Following dilation, rabbits were placed under the surgical microscope. The

animals were then draped, leaving the operated eye exposed. The eye was then disinfected with povidone iodine eye drops (Moorfields Pharmaceuticals, UK). An adolescent speculum was placed within the ocular cavity to fix the globe in a firm position. The conjunctiva was then dissected equatorially down to the sclera for vitrectomy port entry. To maintain ocular pressure during surgery a Lewicky infusion line was placed anteriorly at the cornea-iris junction and screwed into the cornea. Two entry ports were made 2mm posteriorly from the limbus via 20G MVR blade. Port sites were located generally at 4 and 8 o'clock on the limbal circumference; inferotemporally. Bleeding at port entry sites was controlled using bipolar diathermy. Lensectomy was undertaken via one port with a phacoemulsification probe. Its action involved disrupting the lens structure using ultrasound, whilst simultaneously aspirating the debris. The second entry site was used to insert a subsidiary infusion line with saline, to maintain pressure within the eye. Upon completion of lensectomy, the probe was removed and a vitrectomy cutter inserted with the alternative port used for insertion of a fiberoptic instrument set to 100% illumination. This was to visualise the retina for the duration of the vitrectomy. This apparatus simultaneously cuts and aspirates the vitreous and was set at 750cpm (cuts per minute) with a maximum aspiration of 250mmHg. Total removal of the vitreous was conducted to ensure direct access to the retinal inner surface. Once achieved, the intraocular infusion was exchanged to air in order to remove the fluid contained within the posterior chamber of the eye, to maintain the ocular pressure. ChABC (0.4U/10µl) was injected prior to delivery of the scaffolds, via a 18G cannula and incubated at body temperature for 5 minutes. Prepared cellular scaffolds were then drawn up into an 18G cannula attached to 1ml syringe and inserted via an existing entry port. The cannula was angled down towards the medullary raphe and subsequently injected, delivering the cellular scaffolds supported onto the inner retinal surface.

Ports were sequentially sutured, with the conjunctiva being sewn back into place at the limbus. A subconjunctival injection of gentamicin and triamcinolone was given at the end of the procedure (washed and reconstituted in sterile water at a concentration of 80µg/ml); (Kenalog, Squibb Pharmaceuticals). Operated eyes were given topical drops of Dexamethasone 0.1% (Alcon Laboratories, UK) to control post-operative inflammation. Procedures lasted no more than 90 minutes.

6.11.4. Tissue Acquisition

Upon completion of *in vivo* studies, rabbits were sacrificed via ear cannulation and sodium pentobarbitone injection (1ml/kg), to achieve rapid terminal anaesthesia. Both eyes were then removed via excision of the distal ocular tissues and optic nerve. Globes were fixed overnight in 4% PFA at 4°C and transferred to 30% sucrose for 48 hours for cryopreservation. Eyes were embedded into OCT medium (cat no: SURG08609E, VWR, UK) over dry ice and subsequently sectioned and processed as outlined previously for immunohistochemistry.

Chapter 7: References

(2012) Japanese launch skin stem cell trials for dry AMD. *Optom Vis Sci,* 89**,** 117-8.

ABOU NEEL, E. A., BOZEC, L., KNOWLES, J. C., SYED, O., MUDERA, V., DAY, R. & HYUN, J. K. (2013) Collagen--emerging collagen based therapies hit the patient. *Adv Drug Deliv Rev,* 65**,** 429-56.

AGUNI, J. S., MEYER, C. H. & RODRIGUES, E. B. (2009) Transconjunctival 20-gauge vitrectomy: a pilot study. *Ophthalmologica,* 223**,** 12-6.

AL-DEWACHI, H. S., APPLETON, D. R., WATSON, A. J. & WRIGHT, N. A. (1979) Variation in the cell cycle time in the crypts of Lieberkuhn of the mouse. *Virchows Arch B Cell Pathol Incl Mol Pathol,* 31**,** 37-44.

ALWARD, W. L. M. (1999) *Glaucoma: The Requisites, 1e*, Mosby.

ANDOLFO, I., LIGUORI, L., DE ANTONELLIS, P., CUSANELLI, E., MARINARO, F., PISTOLLATO, F., GARZIA, L., DE VITA, G., PETROSINO, G., ACCORDI, B., MIGLIORATI, R., BASSO, G., IOLASCON, A., CINALLI, G. & ZOLLO, M. (2012) The micro-RNA 199b-5p regulatory circuit involves Hes1, CD15, and epigenetic modifications in medulloblastoma. *Neuro Oncol,* 14**,** 596-612.

ANDREAZZOLI, M. (2009) Molecular regulation of vertebrate retina cell fate. *Birth Defects Res C Embryo Today,* 87**,** 284-95.

AOKI, H., HARA, A., NIWA, M., MOTOHASHI, T., SUZUKI, T. & KUNISADA, T. (2008) Transplantation of cells from eye-like structures differentiated from embryonic stem cells in vitro and in vivo regeneration of retinal ganglion-like cells. *Graefes Arch Clin Exp Ophthalmol,* 246**,** 255-65.

AOKI, H., HARA, A., NIWA, M., YAMADA, Y. & KUNISADA, T. (2009) In vitro and in vivo differentiation of human embryonic stem cells into retina-like organs and comparison with that from mouse pluripotent epiblast stem cells. *Dev Dyn,* 238**,** 2266-79.

ARIGA, K., NAKANISHI, T. & MICHINOBU, T. (2006) Immobilization of biomaterials to nano-assembled films (self-assembled monolayers, Langmuir-Blodgett films, and layer-by-layer assemblies) and their related functions. *J Nanosci Nanotechnol,* 6**,** 2278-301.

BAI, F., PENG, H., ETLINGER, J. D. & ZEMAN, R. J. (2010) Partial functional recovery after complete spinal cord transection by combined chondroitinase and clenbuterol treatment. *Pflugers Arch,* 460**,** 657-66.

BANIN, E., OBOLENSKY, A., IDELSON, M., HEMO, I., REINHARDTZ, E., PIKARSKY, E., BEN-HUR, T. & REUBINOFF, B. (2006) Retinal incorporation and differentiation of neural precursors derived from human embryonic stem cells. *Stem Cells,* 24**,** 246-57.

BAO, B., WANG, Z., ALI, S., KONG, D., LI, Y., AHMAD, A., BANERJEE, S., AZMI, A. S., MIELE, L. & SARKAR, F. H. (2011) Notch-1 induces epithelial-mesenchymal transition consistent with cancer stem cell phenotype in pancreatic cancer cells. *Cancer Lett,* 307**,** 26-36.

BARRALET, J. E., WANG, L., LAWSON, M., TRIFFITT, J. T., COOPER, P. R. & SHELTON, R. M. (2005) Comparison of bone marrow cell growth on 2D and 3D alginate hydrogels. *J Mater Sci Mater Med,* 16**,** 515-9.

BAUCH, H., STIER, H. & SCHLOSSHAUER, B. (1998) Axonal versus dendritic outgrowth is differentially affected by radial glia in discrete layers of the retina. *J Neurosci,* 18**,** 1774-85.

BAUMANN, M. D., KANG, C. E., STANWICK, J. C., WANG, Y., KIM, H., LAPITSKY, Y. & SHOICHET, M. S. (2009) An injectable drug delivery platform for sustained combination therapy. *J Control Release,* 138**,** 205-13.

BAYE, L. M. & LINK, B. A. (2007) Interkinetic nuclear migration and the selection of neurogenic cell divisions during vertebrate retinogenesis. *J Neurosci,* 27**,** 10143-52.

BEACHLEY, V. W., X. (2009) Fabrication of nanofiber reinforced protein structures for tissue engineering. *Materials Science and Engineering C,* 29**,** 2448-2453.

BENNETT, J. D., FARLIE, P. G. & WATSON, R. J. (1996) E2F binding is required but not sufficient for repression of B-myb transcription in quiescent fibroblasts. *Oncogene,* 13**,** 1073-82.

BERNARDOS, R. L., BARTHEL, L. K., MEYERS, J. R. & RAYMOND, P. A. (2007) Late-stage neuronal progenitors in the retina are radial Müller glia that function as retinal stem cells. *J Neurosci,* 27**,** 7028-40.

BERSON, E. L. (2007) Long-term visual prognoses in patients with retinitis pigmentosa: the Ludwig von Sallmann lecture. *Exp Eye Res,* 85**,** 7-14.

BHATIA, B., JAYARAM, H., SINGHAL, S., JONES, M. F. & LIMB, G. A. (2011a) Differences between the neurogenic and proliferative abilities of Müller glia with stem cell characteristics and the ciliary epithelium from the adult human eye. *Exp Eye Res,* 93**,** 852-61.

BHATIA, B., SINGHAL, S., JAYARAM, H., KHAW, P. T. & LIMB, G. A. (2010) Adult retinal stem cells revisited. *Open Ophthalmol J,* 4**,** 30-8.

BHATIA, B., SINGHAL, S., LAWRENCE, J. M., KHAW, P. T. & LIMB, G. A. (2009) Distribution of Müller stem cells within the neural retina: evidence for the existence of a ciliary margin-like zone in the adult human eye. *Exp Eye Res,* 89**,** 373-82.

BHATIA, B., SINGHAL, S., TADMAN, D. N., KHAW, P. T. & LIMB, G. A. (2011b) SOX2 is required for adult human Müller stem cell survival and maintenance of progenicity in vitro. *Invest Ophthalmol Vis Sci,* 52**,** 136-45.

BHATTACHARJEE, A. & BANSAL, M. (2005) Collagen structure: the Madras triple helix and the current scenario. *IUBMB Life,* 57**,** 161-72.

BIBEL, M., RICHTER, J., SCHRENK, K., TUCKER, K. L., STAIGER, V., KORTE, M., GOETZ, M. & BARDE, Y. A. (2004) Differentiation of mouse embryonic stem cells into a defined neuronal lineage. *Nat Neurosci,* 7**,** 1003-9.

BLACKSHAW, S., HARPAVAT, S., TRIMARCHI, J., CAI, L., HUANG, H., KUO, W. P., WEBER, G., LEE, K., FRAIOLI, R. E., CHO, S. H., YUNG, R., ASCH, E., OHNO-MACHADO, L., WONG, W. H. & CEPKO, C. L. (2004) Genomic analysis of mouse retinal development. *PLoS Biol,* 2**,** E247.

BRABLETZ, S., BAJDAK, K., MEIDHOF, S., BURK, U., NIEDERMANN, G., FIRAT, E., WELLNER, U., DIMMLER, A., FALLER, G., SCHUBERT, J. & BRABLETZ, T. (2011) The ZEB1/miR-200 feedback loop controls Notch signalling in cancer cells. *EMBO J,* 30**,** 770-82.

BRADBURY, E. J., MOON, L. D., POPAT, R. J., KING, V. R., BENNETT, G. S., PATEL, P. N., FAWCETT, J. W. & MCMAHON, S. B. (2002) Chondroitinase ABC promotes functional recovery after spinal cord injury. *Nature,* 416**,** 636-40.

BRIDGE, G., MONTEIRO, R., HENDERSON, S., EMUSS, V., LAGOS, D., GEORGOPOULOU, D., PATIENT, R. & BOSHOFF, C. (2012) The microRNA-30 family targets DLL4 to modulate endothelial cell behavior during angiogenesis. *Blood,* 120**,** 5063-72.

BROWN, N. L., KANEKAR, S., VETTER, M. L., TUCKER, P. K., GEMZA, D. L. & GLASER, T. (1998) Math5 encodes a murine basic helix-loop-helix transcription factor expressed during early stages of retinal neurogenesis. *Development,* 125**,** 4821-33.

BROWN, R. A., WISEMAN, M., CHUO, C. B., CHEEMA, U. & NAZHAT, S. N. (2005) Ultrarapid Engineering of Biomimetic Materials and Tissues: Fabrication of Nano- and Microstructures by Plastic Compression. *Advanced Functional Materials,* 15**,** 1762-1770.

BULL, N. D., JOHNSON, T. V., WELSAPAR, G., DEKORVER, N. W., TOMAREV, S. I. & MARTIN, K. R. (2011) Use of an adult rat retinal explant model for screening of potential retinal ganglion cell neuroprotective therapies. *Invest Ophthalmol Vis Sci,* 52**,** 3309-20.

BULL, N. D., LIMB, G. A. & MARTIN, K. R. (2008) Human Müller stem cell (MIO-M1) transplantation in a rat model of glaucoma: survival, differentiation, and integration. *Invest Ophthalmol Vis Sci,* 49**,** 3449-56.

BULL, N. D. & MARTIN, K. R. (2007) Optic nerve restoration: new perspectives. *J Glaucoma,* 16**,** 506-11.

BUNCE, C., XING, W. & WORMALD, R. (2010) Causes of blind and partial sight certifications in England and Wales: April 2007-March 2008. *Eye (Lond),* 24**,** 1692-9.

BURK, U., SCHUBERT, J., WELLNER, U., SCHMALHOFER, O., VINCAN, E., SPADERNA, S. & BRABLETZ, T. (2008) A reciprocal repression between ZEB1 and members of the miR-200 family promotes EMT and invasion in cancer cells. *EMBO Rep,* 9**,** 582-9.

BUTCHER, J. T. & NEREM, R. M. (2004) Porcine aortic valve interstitial cells in three-dimensional culture: comparison of phenotype with aortic smooth muscle cells. *J Heart Valve Dis,* 13**,** 478-85; discussion 485-6.

BUTTAFOCO, L., KOLKMAN, N. G., ENGBERS-BUIJTENHUIJS, P., POOT, A. A., DIJKSTRA, P. J., VERMES, I. & FEIJEN, J. (2006) Electrospinning of collagen and elastin for tissue engineering applications. *Biomaterials,* 27**,** 724-34.

CARR, A. J., VUGLER, A. A., HIKITA, S. T., LAWRENCE, J. M., GIAS, C., CHEN, L. L., BUCHHOLZ, D. E., AHMADO, A., SEMO, M., SMART, M. J., HASAN, S., DA CRUZ, L., JOHNSON, L. V., CLEGG, D. O. & COFFEY, P. J. (2009) Protective effects of human iPS-derived retinal pigment epithelium cell transplantation in the retinal dystrophic rat. *PLoS One,* 4**,** e8152.

CHAKRABARTI, M., BANIK, N. L. & RAY, S. K. (2013) Photofrin based photodynamic therapy and miR-99a transfection inhibited FGFR3 and PI3K/Akt signaling mechanisms to control growth of human glioblastoma In vitro and in vivo. *PLoS One,* 8**,** e55652.

CHAMORRO-JORGANES, A., ARALDI, E., PENALVA, L. O., SANDHU, D., FERNANDEZ-HERNANDO, C. & SUAREZ, Y. (2011) MicroRNA-16 and microRNA-424 regulate cell-autonomous angiogenic functions in endothelial cells via targeting vascular endothelial growth factor receptor-2 and fibroblast growth factor receptor-1. *Arterioscler Thromb Vasc Biol,* 31**,** 2595-606.

CHATOO, W., ABDOUH, M., DAVID, J., CHAMPAGNE, M. P., FERREIRA, J., RODIER, F. & BERNIER, G. (2009) The polycomb group gene Bmi1 regulates antioxidant defenses in neurons by repressing p53 pro-oxidant activity. *J Neurosci,* 29**,** 529-42.

CHAVANPATIL, M. D., KHDAIR, A. & PANYAM, J. (2006) Nanoparticles for cellular drug delivery: mechanisms and factors influencing delivery. *J Nanosci Nanotechnol,* 6**,** 2651-63.

CHEN, C. C., LIAO, C. H., WANG, Y. H., HSU, Y. M., HUANG, S. H., CHANG, C. H. & FANG, H. W. (2012) Cartilage fragments from osteoarthritic knee promote chondrogenesis of mesenchymal stem cells without exogenous growth factor induction. *J Orthop Res,* 30**,** 393-400.

CHISTIAKOV, D. A. (2011) Diabetic retinopathy: Pathogenic mechanisms and current treatments. *Diabetes Metab Syndr,* 5**,** 165-72.

CHOW, R. L. & LANG, R. A. (2001) Early eye development in vertebrates. *Annu Rev Cell Dev Biol,* 17**,** 255-96.

COLEMAN, D. J. (1979) Ultrasonic measurement of eye dimensions. *Int Ophthalmol Clin,* 19**,** 225-36.

CONTE, I., CARRELLA, S., AVELLINO, R., KARALI, M., MARCO-FERRERES, R., BOVOLENTA, P. & BANFI, S. (2010) miR-204 is required for lens and retinal development via Meis2 targeting. *Proc Natl Acad Sci U S A,* 107**,** 15491-6.

COOKE, M. J., WANG, Y., MORSHEAD, C. M. & SHOICHET, M. S. (2011) Controlled epi-cortical delivery of epidermal growth factor for the stimulation of endogenous neural stem cell proliferation in stroke-injured brain. *Biomaterials,* 32**,** 5688-97.

COUMANS, J. V., LIN, T. T., DAI, H. N., MACARTHUR, L., MCATEE, M., NASH, C. & BREGMAN, B. S. (2001) Axonal regeneration and functional recovery after complete spinal cord transection in rats by delayed treatment with transplants and neurotrophins. *J Neurosci,* 21**,** 9334-44.

DAS, A. V., EDAKKOT, S., THORESON, W. B., JAMES, J., BHATTACHARYA, S. & AHMAD, I. (2005) Membrane properties of retinal stem cells/progenitors. *Prog Retin Eye Res,* 24**,** 663-81.

DAS, A. V., MALLYA, K. B., ZHAO, X., AHMAD, F., BHATTACHARYA, S., THORESON, W. B., HEGDE, G. V. & AHMAD, I. (2006) Neural stem cell properties of Müller glia in the mammalian retina: regulation by Notch and Wnt signaling. *Dev Biol,* 299**,** 283-302.

DE FEO, D., MERLINI, A., LATERZA, C. & MARTINO, G. (2012) Neural stem cell transplantation in central nervous system disorders: from cell replacement to neuroprotection. *Curr Opin Neurol,* 25**,** 322-33.

DE JONG, P. T. (2006) Age-related macular degeneration. *N Engl J Med,* 355**,** 1474-85.

DE KOZAK, Y., COTINET, A., GOUREAU, O., HICKS, D. & THILLAYE-GOLDENBERG, B. (1997) Tumor necrosis factor and nitric oxide production by resident retinal glial cells from rats presenting hereditary retinal degeneration. *Ocul Immunol Inflamm,* 5**,** 85-94.

DEL BENE, F., WEHMAN, A. M., LINK, B. A. & BAIER, H. (2008) Regulation of neurogenesis by interkinetic nuclear migration through an apical-basal notch gradient. *Cell,* 134**,** 1055-65.

DELAUNE, E., LEMAIRE, P. & KODJABACHIAN, L. (2005) Neural induction in Xenopus requires early FGF signalling in addition to BMP inhibition. *Development,* 132**,** 299-310.

DELLAGO, H., PRESCHITZ-KAMMERHOFER, B., TERLECKI-ZANIEWICZ, L., SCHREINER, C., FORTSCHEGGER, K., CHANG, M. W., HACKL, M., MONTEFORTE, R., KUHNEL, H., SCHOSSERER, M., GRUBER, F., TSCHACHLER, E., SCHEIDELER, M., GRILLARI-VOGLAUER, R., GRILLARI, J. & WIESER, M. (2013) High levels of oncomiR-21 contribute to the senescence induced growth arrest in normal human cells and its knock-down increases the replicative life span. *Aging Cell*.

DEREGOWSKI, V., GAZZERRO, E., PRIEST, L., RYDZIEL, S. & CANALIS, E. (2006) Role of the RAM domain and ankyrin repeats on notch signaling and activity in cells of osteoblastic lineage. *J Bone Miner Res,* 21**,** 1317-26.

DI LULLO, G. A., SWEENEY, S. M., KORKKO, J., ALA-KOKKO, L. & SAN ANTONIO, J. D. (2002) Mapping the ligand-binding sites and disease-associated mutations on the most abundant protein in the human, type I collagen. *J Biol Chem,* 277**,** 4223-31.

DIAZ-MARTINEZ, N. E. & VELASCO, I. (2009) [Axonal growth inhibition by chondroitin sulfate proteoglycans in the central nervous system]. *Rev Invest Clin,* 61**,** 140-9.

DIMOS, J. T., RODOLFA, K. T., NIAKAN, K. K., WEISENTHAL, L. M., MITSUMOTO, H., CHUNG, W., CROFT, G. F., SAPHIER, G., LEIBEL, R., GOLAND, R., WICHTERLE, H., HENDERSON, C. E. & EGGAN, K. (2008) Induced pluripotent stem cells generated from patients with ALS can be differentiated into motor neurons. *Science,* 321**,** 1218-21.

DOILLON, C. J., DROUIN, R., COTE, M. F., DALLAIRE, N., PAGEAU, J. F. & LAROCHE, G. (1997) Chemical inactivators as sterilization agents for bovine collagen materials. *J Biomed Mater Res,* 37**,** 212-21.

DORSKY, R. I., RAPAPORT, D. H. & HARRIS, W. A. (1995) Xotch inhibits cell differentiation in the Xenopus retina. *Neuron,* 14**,** 487-96.

DU, T. & ZAMORE, P. D. (2005) microPrimer: the biogenesis and function of microRNA. *Development,* 132**,** 4645-52.

DYER, M. A. & CEPKO, C. L. (2001) p27Kip1 and p57Kip2 regulate proliferation in distinct retinal progenitor cell populations. *J Neurosci,* 21**,** 4259-71.

EASTWOOD, M., PORTER, R., KHAN, U., MCGROUTHER, G. & BROWN, R. (1996) Quantitative analysis of collagen gel contractile forces generated by dermal fibroblasts and the relationship to cell morphology. *J Cell Physiol,* 166**,** 33-42.

EKDAHL, K. N., LAMBRIS, J. D., ELWING, H., RICKLIN, D., NILSSON, P. H., TERAMURA, Y., NICHOLLS, I. A. & NILSSON, B. (2011) Innate immunity activation on biomaterial surfaces: a mechanistic model and coping strategies. *Adv Drug Deliv Rev,* 63**,** 1042-50.

ENGELHARDT, E. M., STEGBERG, E., BROWN, R. A., HUBBELL, J. A., WURM, F. M., ADAM, M. & FREY, P. (2010) Compressed collagen gel: a novel scaffold for human bladder cells. *J Tissue Eng Regen Med,* 4**,** 123-30.

EVANS, M. J. & KAUFMAN, M. H. (1981) Establishment in culture of pluripotential cells from mouse embryos. *Nature,* 292**,** 154-6.

EVERAERTS, F., TORRIANNI, M., HENDRIKS, M. & FEIJEN, J. (2008) Biomechanical properties of carbodiimide crosslinked collagen: influence of the formation of ester crosslinks. *J Biomed Mater Res A,* 85**,** 547-55.

EYRICH, D., BRANDL, F., APPEL, B., WIESE, H., MAIER, G., WENZEL, M., STAUDENMAIER, R., GOEPFERICH, A. & BLUNK, T. (2007) Long-term stable fibrin gels for cartilage engineering. *Biomaterials,* 28**,** 55-65.

FAIGLE, R. & SONG, H. (2013) Signaling mechanisms regulating adult neural stem cells and neurogenesis. *Biochim Biophys Acta,* 1830**,** 2435-48.

FALKNER-RADLER, C. I., KREBS, I., GLITTENBERG, C., POVAZAY, B., DREXLER, W., GRAF, A. & BINDER, S. (2011) Human retinal pigment epithelium (RPE) transplantation: outcome after autologous RPE-choroid sheet and RPE cell-suspension in a randomised clinical study. *Br J Ophthalmol,* 95**,** 370-5.

FAUSETT, B. V. & GOLDMAN, D. (2006) A role for alpha1 tubulin-expressing Müller glia in regeneration of the injured zebrafish retina. *J Neurosci,* 26**,** 6303-13.

FAUSETT, B. V., GUMERSON, J. D. & GOLDMAN, D. (2008) The proneural basic helix-loop-helix gene ascl1a is required for retina regeneration. *J Neurosci,* 28**,** 1109-17.

FAUX, C. H., TURNLEY, A. M., EPA, R., CAPPAI, R. & BARTLETT, P. F. (2001) Interactions between fibroblast growth factors and Notch regulate neuronal differentiation. *J Neurosci,* 21**,** 5587-96.

FAWCETT, J. W. & ASHER, R. A. (1999) The glial scar and central nervous system repair. *Brain Res Bull,* 49**,** 377-91.

FISCHER, A. J., MCGUIRE, C. R., DIERKS, B. D. & REH, T. A. (2002) Insulin and fibroblast growth factor 2 activate a neurogenic program in Müller glia of the chicken retina. *J Neurosci,* 22**,** 9387-98.

FISCHER, A. J., OMAR, G., EUBANKS, J., MCGUIRE, C. R., DIERKS, B. D. & REH, T. A. (2004a) Different aspects of gliosis in retinal Müller glia can be induced by CNTF, insulin, and FGF2 in the absence of damage. *Mol Vis,* 10**,** 973-86.

FISCHER, A. J. & REH, T. A. (2000) Identification of a proliferating marginal zone of retinal progenitors in postnatal chickens. *Dev Biol,* 220**,** 197-210.

FISCHER, A. J. & REH, T. A. (2001) Müller glia are a potential source of neural regeneration in the postnatal chicken retina. *Nat Neurosci,* 4**,** 247-52.

FISCHER, A. J. & REH, T. A. (2003) Potential of Müller glia to become neurogenic retinal progenitor cells. *Glia,* 43**,** 70-6.

FISCHER, A. J., WANG, S. Z. & REH, T. A. (2004b) NeuroD induces the expression of visinin and calretinin by proliferating cells derived from toxin-damaged chicken retina. *Dev Dyn,* 229**,** 555-63.

FOUAD, K., SCHNELL, L., BUNGE, M. B., SCHWAB, M. E., LIEBSCHER, T. & PEARSE, D. D. (2005) Combining Schwann cell bridges and olfactory-ensheathing glia grafts with chondroitinase promotes locomotor recovery after complete transection of the spinal cord. *J Neurosci,* 25**,** 1169-78.

FRANKE, K., POMPE, T., BORNHAUSER, M. & WERNER, C. (2007) Engineered matrix coatings to modulate the adhesion of CD133+ human hematopoietic progenitor cells. *Biomaterials,* 28**,** 836-43.

FRIEDRICH, S., CHENG, Y. L. & SAVILLE, B. (1997a) Drug distribution in the vitreous humor of the human eye: the effects of intravitreal injection position and volume. *Curr Eye Res,* 16**,** 663-9.

FRIEDRICH, S., CHENG, Y. L. & SAVILLE, B. (1997b) Finite element modeling of drug distribution in the vitreous humor of the rabbit eye. *Ann Biomed Eng,* 25**,** 303-14.

FRISCH, S. M. & FRANCIS, H. (1994) Disruption of epithelial cell-matrix interactions induces apoptosis. *J Cell Biol,* 124**,** 619-26.

FRISCH, S. M. & SCREATON, R. A. (2001) Anoikis mechanisms. *Curr Opin Cell Biol,* 13**,** 555-62.

GAIANO, N., NYE, J. S. & FISHELL, G. (2000) Radial glial identity is promoted by Notch1 signaling in the murine forebrain. *Neuron,* 26**,** 395-404.

GAN, L., WANG, S. W., HUANG, Z. & KLEIN, W. H. (1999) POU domain factor Brn-3b is essential for retinal ganglion cell differentiation and survival but not for initial cell fate specification. *Dev Biol,* 210**,** 469-80.

GARCIA-ALIAS, G. & FAWCETT, J. W. (2012) Training and anti-CSPG combination therapy for spinal cord injury. *Exp Neurol,* 235**,** 26-32.

GARZIA, L., ANDOLFO, I., CUSANELLI, E., MARINO, N., PETROSINO, G., DE MARTINO, D., ESPOSITO, V., GALEONE, A., NAVAS, L., ESPOSITO, S., GARGIULO, S., FATTET, S., DONOFRIO, V., CINALLI, G., BRUNETTI, A., VECCHIO, L. D., NORTHCOTT, P. A., DELATTRE, O., TAYLOR, M. D., IOLASCON, A. & ZOLLO, M. (2009) MicroRNA-199b-5p impairs cancer stem cells through negative regulation of HES1 in medulloblastoma. *PLoS One,* 4**,** e4998.

GEHRMANN, J., MATSUMOTO, Y. & KREUTZBERG, G. W. (1995) Microglia: intrinsic immuneffector cell of the brain. *Brain Res Brain Res Rev,* 20**,** 269-87.

GORDON, M. K. & HAHN, R. A. (2010) Collagens. *Cell Tissue Res,* 339**,** 247-57.

GREGORY, P. A., BERT, A. G., PATERSON, E. L., BARRY, S. C., TSYKIN, A., FARSHID, G., VADAS, M. A., KHEW-GOODALL, Y. & GOODALL, G. J. (2008) The miR-200 family and miR-205 regulate epithelial to mesenchymal transition by targeting ZEB1 and SIP1. *Nat Cell Biol,* 10**,** 593-601.

GROSS, J., HIGHBERGER, J. H. & SCHMITT, F. O. (1955) EXTRACTION OF COLLAGEN FROM CONNECTIVE TISSUE BY NEUTRAL SALT SOLUTIONS. *Proc Natl Acad Sci U S A,* 41**,** 1-7.

GULDBERG, R. E., DUVALL, C. L., PEISTER, A., OEST, M. E., LIN, A. S., PALMER, A. W. & LEVENSTON, M. E. (2008) 3D imaging of tissue integration with porous biomaterials. *Biomaterials,* 29**,** 3757-61.

GUNATILLAKE, P., MAYADUNNE, R. & ADHIKARI, R. (2006) Recent developments in biodegradable synthetic polymers. *Biotechnol Annu Rev,* 12**,** 301-47.

GUO, H., INGOLIA, N. T., WEISSMAN, J. S. & BARTEL, D. P. (2010) Mammalian microRNAs predominantly act to decrease target mRNA levels. *Nature,* 466**,** 835-40.

GURURAJAN, M., HAGA, C. L., DAS, S., LEU, C. M., HODSON, D., JOSSON, S., TURNER, M. & COOPER, M. D. (2010) MicroRNA 125b inhibition of B cell differentiation in germinal centers. *Int Immunol,* 22**,** 583-92.

HADJIPANAYI, E., MUDERA, V. & BROWN, R. A. (2009) Guiding cell migration in 3D: a collagen matrix with graded directional stiffness. *Cell Motil Cytoskeleton,* 66**,** 121-8.

HATAKEYAMA, J., SAKAMOTO, S. & KAGEYAMA, R. (2006) Hes1 and Hes5 regulate the development of the cranial and spinal nerve systems. *Dev Neurosci,* 28**,** 92-101.

HAYES, S., NELSON, B. R., BUCKINGHAM, B. & REH, T. A. (2007) Notch signaling regulates regeneration in the avian retina. *Dev Biol,* 312**,** 300-11.

HELLER, J. (2005) Ocular delivery using poly(ortho esters). *Adv Drug Deliv Rev,* 57**,** 2053-62.

HENTZE, H., SOONG, P. L., WANG, S. T., PHILLIPS, B. W., PUTTI, T. C. & DUNN, N. R. (2009) Teratoma formation by human embryonic stem cells: evaluation of essential parameters for future safety studies. *Stem Cell Res,* 2**,** 198-210.

HERNANDEZ, M., RODRIGUEZ, F. D., SHARMA, S. C. & VECINO, E. (2009) Immunohistochemical changes in rat retinas at various time periods of elevated intraocular pressure. *Mol Vis,* 15**,** 2696-709.

HILL, A. J., ZWART, I., TAM, H. H., CHAN, J., NAVARRETE, C., JEN, L. S. & NAVARRETE, R. (2009) Human umbilical cord blood-derived mesenchymal stem cells do not differentiate into neural cell types or integrate into the retina after intravitreal grafting in neonatal rats. *Stem Cells Dev,* 18**,** 399-409.

HINDS, J. W. & HINDS, P. L. (1974) Early ganglion cell differentiation in the mouse retina: an electron microscopic analysis utilizing serial sections. *Dev Biol,* 37**,** 381-416.

HIRANO, M., YAMAMOTO, A., YOSHIMURA, N., TOKUNAGA, T., MOTOHASHI, T., ISHIZAKI, K., YOSHIDA, H., OKAZAKI, K., YAMAZAKI, H., HAYASHI, S. & KUNISADA, T. (2003) Generation of structures formed by lens and retinal cells differentiating from embryonic stem cells. *Dev Dyn,* 228**,** 664-71.

HODGKINSON, G. N., TRESCO, P. A. & HLADY, V. (2007) The differential influence of colocalized and segregated dual protein signals on neurite outgrowth on surfaces. *Biomaterials,* 28**,** 2590-602.

HU, M. & EASTER, S. S. (1999) Retinal neurogenesis: the formation of the initial central patch of postmitotic cells. *Dev Biol,* 207**,** 309-21.

HUANG, K. M., DENTCHEV, T. & STAMBOLIAN, D. (2008) MiRNA expression in the eye. *Mamm Genome,* 19**,** 510-6.

HUDSON, C. (1996) The clinical features and classification of diabetic retinopathy. *Ophthalmic Physiol Opt,* 16 Suppl 2**,** S43-8.

HUGHES, A. (1972) A schematic eye for the rabbit. *Vision Res,* 12**,** 123-38.

HUGHES, A. (1979) A schematic eye for the rat. *Vision Res,* 19**,** 569-88.

HULMES, D. J. (1992) The collagen superfamily--diverse structures and assemblies. *Essays Biochem,* 27**,** 49-67.

HYATT, A. J., WANG, D., KWOK, J. C., FAWCETT, J. W. & MARTIN, K. R. (2010) Controlled release of chondroitinase ABC from fibrin gel reduces the level of inhibitory glycosaminoglycan chains in lesioned spinal cord. *J Control Release,* 147**,** 24-9.

IDELSON, M., ALPER, R., OBOLENSKY, A., BEN-SHUSHAN, E., HEMO, I., YACHIMOVICH-COHEN, N., KHANER, H., SMITH, Y., WISER, O., GROPP, M., COHEN, M. A., EVEN-RAM, S., BERMAN-ZAKEN, Y., MATZRAFI, L., RECHAVI, G., BANIN, E. & REUBINOFF, B. (2009) Directed differentiation of human embryonic stem cells into functional retinal pigment epithelium cells. *Cell Stem Cell,* 5**,** 396-408.

INATANI, M. & TANIHARA, H. (2002) Proteoglycans in retina. *Prog Retin Eye Res,* 21**,** 429-47.

IORIO, M. V., VISONE, R., DI LEVA, G., DONATI, V., PETROCCA, F., CASALINI, P., TACCIOLI, C., VOLINIA, S., LIU, C. G., ALDER, H., CALIN, G. A., MENARD, S. & CROCE, C. M. (2007) MicroRNA signatures in human ovarian cancer. *Cancer Res,* 67**,** 8699-707.

ITAKURA, H., KISHI, S., KOTAJIMA, N. & MURAKAMI, M. (2009) Decreased vitreal hyaluronan levels with aging. *Ophthalmologica,* 223**,** 32-5.

IVEY, K. N., MUTH, A., ARNOLD, J., KING, F. W., YEH, R. F., FISH, J. E., HSIAO, E. C., SCHWARTZ, R. J., CONKLIN, B. R., BERNSTEIN, H. S. & SRIVASTAVA, D. (2008) MicroRNA regulation of cell lineages in mouse and human embryonic stem cells. *Cell Stem Cell,* 2**,** 219-29.

J. A. MATTHEWS, E. D. B., G. E. WNEK, D. G. SIMPSON, G. L. BOWLIN , J. (2003) Electrospinning of Collagen Type II: A Feasibility Study. *Bioactive and Compatible Polymers,* 18**,** 125.

JACOBS, W. B. & FEHLINGS, M. G. (2003) The molecular basis of neural regeneration. *Neurosurgery,* 53**,** 943-48; discussion 948-50.

JADHAV, A. P., CHO, S. H. & CEPKO, C. L. (2006) Notch activity permits retinal cells to progress through multiple progenitor states and acquire a stem cell property. *Proc Natl Acad Sci U S A,* 103**,** 18998-9003.

JAGATHA, B., DIVYA, M. S., SANALKUMAR, R., INDULEKHA, C. L., VIDYANAND, S., DIVYA, T. S., DAS, A. V. & JAMES, J. (2009) In vitro differentiation of retinal ganglion-like cells from embryonic stem cell derived neural progenitors. *Biochem Biophys Res Commun,* 380**,** 230-5.

JANG, S., CHO, H. H., CHO, Y. B., PARK, J. S. & JEONG, H. S. (2010) Functional neural differentiation of human adipose tissue-derived stem cells using bFGF and forskolin. *BMC Cell Biol,* 11**,** 25.

JI, Q., HAO, X., MENG, Y., ZHANG, M., DESANO, J., FAN, D. & XU, L. (2008) Restoration of tumor suppressor miR-34 inhibits human p53-mutant gastric cancer tumorspheres. *BMC Cancer,* 8**,** 266.

JI, Q., HAO, X., ZHANG, M., TANG, W., YANG, M., LI, L., XIANG, D., DESANO, J. T., BOMMER, G. T., FAN, D., FEARON, E. R., LAWRENCE, T. S. & XU, L. (2009) MicroRNA miR-34 inhibits human pancreatic cancer tumor-initiating cells. *PLoS One,* 4**,** e6816.

JI, Y., GHOSH, K., SHU, X. Z., LI, B., SOKOLOV, J. C., PRESTWICH, G. D., CLARK, R. A. & RAFAILOVICH, M. H. (2006) Electrospun three-dimensional hyaluronic acid nanofibrous scaffolds. *Biomaterials,* 27**,** 3782-92.

JOGLEKAR, M. V., PATIL, D., JOGLEKAR, V. M., RAO, G. V., REDDY, D. N., MITNALA, S., SHOUCHE, Y. & HARDIKAR, A. A. (2009) The miR-30 family microRNAs confer epithelial phenotype to human pancreatic cells. *Islets,* 1**,** 137-47.

JOHL, S. S. & BURGETT, R. A. (2006) Dermal filler agents: a practical review. *Curr Opin Ophthalmol,* 17**,** 471-9.

JOHNSON, T. V., BULL, N. D., HUNT, D. P., MARINA, N., TOMAREV, S. I. & MARTIN, K. R. (2010) Neuroprotective effects of intravitreal mesenchymal stem cell transplantation in experimental glaucoma. *Invest Ophthalmol Vis Sci,* 51**,** 2051-9.

JOHNSON, T. V., BULL, N. D. & MARTIN, K. R. (2009) Transplantation prospects for the inner retina. *Eye (Lond),* 23**,** 1980-4.

JONES, L. L., YAMAGUCHI, Y., STALLCUP, W. B. & TUSZYNSKI, M. H. (2002) NG2 is a major chondroitin sulfate proteoglycan produced after spinal cord injury and is expressed by macrophages and oligodendrocyte progenitors. *J Neurosci,* 22**,** 2792-803.

JULIAN, D., ENNIS, K. & KORENBROT, J. I. (1998) Birth and fate of proliferative cells in the inner nuclear layer of the mature fish retina. *J Comp Neurol,* 394**,** 271-82.

KAGEYAMA, R., OHTSUKA, T., HATAKEYAMA, J. & OHSAWA, R. (2005) Roles of bHLH genes in neural stem cell differentiation. *Exp Cell Res,* 306**,** 343-8.

KANEKAR, S., PERRON, M., DORSKY, R., HARRIS, W. A., JAN, L. Y., JAN, Y. N. & VETTER, M. L. (1997) Xath5 participates in a network of bHLH genes in the developing Xenopus retina. *Neuron,* 19**,** 981-94.

KANG, C. E., POON, P. C., TATOR, C. H. & SHOICHET, M. S. (2009) A new paradigm for local and sustained release of therapeutic molecules to the injured spinal cord for neuroprotection and tissue repair. *Tissue Eng Part A,* 15**,** 595-604.

KAPADIA, O. D. S. (2000) Stargardt's macular dystrophy. *Clin Eye Vis Care,* 12**,** 71-78.

KARALI, M., PELUSO, I., MARIGO, V. & BANFI, S. (2007) Identification and characterization of microRNAs expressed in the mouse eye. *Invest Ophthalmol Vis Sci,* 48**,** 509-15.

KARIMI-ABDOLREZAEE, S., EFTEKHARPOUR, E., WANG, J., SCHUT, D. & FEHLINGS, M. G. (2010) Synergistic effects of transplanted adult neural stem/progenitor cells, chondroitinase, and growth factors promote functional repair and plasticity of the chronically injured spinal cord. *J Neurosci,* 30**,** 1657-76.

KASSEN, S. C., THUMMEL, R., BURKET, C. T., CAMPOCHIARO, L. A., HARDING, M. J. & HYDE, D. R. (2008) The Tg(ccnb1:EGFP) transgenic zebrafish line labels proliferating cells during retinal development and regeneration. *Mol Vis,* 14**,** 951-63.

KAWASAKI, H. & TAIRA, K. (2003) Hes1 is a target of microRNA-23 during retinoic-acid-induced neuronal differentiation of NT2 cells. *Nature,* 423**,** 838-42.

KAY, J. N., FINGER-BAIER, K. C., ROESER, T., STAUB, W. & BAIER, H. (2001) Retinal ganglion cell genesis requires lakritz, a Zebrafish atonal Homolog. *Neuron,* 30**,** 725-36.

KERRIGAN-BAUMRIND, L. A., QUIGLEY, H. A., PEASE, M. E., KERRIGAN, D. F. & MITCHELL, R. S. (2000) Number of ganglion cells in glaucoma eyes compared with threshold visual field tests in the same persons. *Invest Ophthalmol Vis Sci,* 41**,** 741-8.

KHADKA, D. B. & HAYNIE, D. T. (2010) Insoluble synthetic polypeptide mats from aqueous solution by electrospinning. *ACS Appl Mater Interfaces,* 2**,** 2728-32.

KHLUSOV, I. A., KHLUSOVA, M. Y., ZAITSEV, K. V., KOLOKOL'TSOVA, T. D., SHARKEEV, Y. P., PICHUGIN, V. F., LEGOSTAEVA, E. V., TROFIMOVA, I. E., KLIMOV, A. S. & ZHDANOVA, A. I. (2011) Pilot in vitro study of the parameters of artificial niche for osteogenic differentiation of human stromal stem cell pool. *Bull Exp Biol Med,* 150**,** 535-42.

KHVOROVA, A., REYNOLDS, A. & JAYASENA, S. D. (2003) Functional siRNAs and miRNAs exhibit strand bias. *Cell,* 115**,** 209-16.

KLASSEN, H., ZIAEIAN, B., KIROV, II, YOUNG, M. J. & SCHWARTZ, P. H. (2004) Isolation of retinal progenitor cells from post-mortem human tissue and comparison with autologous brain progenitors. *J Neurosci Res,* 77**,** 334-43.

KONG, D., BANERJEE, S., AHMAD, A., LI, Y., WANG, Z., SETHI, S. & SARKAR, F. H. (2010) Epithelial to mesenchymal transition is mechanistically linked with stem cell signatures in prostate cancer cells. *PLoS One,* 5**,** e12445.

KORPAL, M., LEE, E. S., HU, G. & KANG, Y. (2008) The miR-200 family inhibits epithelial-mesenchymal transition and cancer cell migration by direct targeting of E-cadherin transcriptional repressors ZEB1 and ZEB2. *J Biol Chem,* 283**,** 14910-4.

KRELL, J., FRAMPTON, A. E., JACOB, J., PELLEGRINO, L., ROCA-ALONSO, L., ZELOOF, D., ALIFRANGIS, C., LEWIS, J. S., JIAO, L. R., STEBBING, J. & CASTELLANO, L. (2012) The clinico-pathologic role of microRNAs miR-9 and miR-151-5p in breast cancer metastasis. *Mol Diagn Ther,* 16**,** 167-72.

KRICHEVSKY, A. M., KING, K. S., DONAHUE, C. P., KHRAPKO, K. & KOSIK, K. S. (2003) A microRNA array reveals extensive regulation of microRNAs during brain development. *RNA,* 9**,** 1274-81.

KRICHEVSKY, A. M., SONNTAG, K. C., ISACSON, O. & KOSIK, K. S. (2006) Specific microRNAs modulate embryonic stem cell-derived neurogenesis. *Stem Cells,* 24**,** 857-64.

KUMBAR, S. G., NAIR, L. S., BHATTACHARYYA, S. & LAURENCIN, C. T. (2006) Polymeric nanofibers as novel carriers for the delivery of therapeutic molecules. *J Nanosci Nanotechnol,* 6**,** 2591-607.

KURESHI, A., CHEEMA, U., ALEKSEEVA, T., CAMBREY, A. & BROWN, R. (2010) Alignment hierarchies: engineering architecture from the nanometre to the micrometre scale. *J R Soc Interface,* 7 Suppl 6**,** S707-16.

KUZNETSOVA, N. & LEIKIN, S. (1999) Does the triple helical domain of type I collagen encode molecular recognition and fiber assembly while telopeptides serve as catalytic domains? Effect of proteolytic cleavage on fibrillogenesis and on collagen-collagen interaction in fibers. *J Biol Chem,* 274**,** 36083-8.

KWON, C., HAN, Z., OLSON, E. N. & SRIVASTAVA, D. (2005) MicroRNA1 influences cardiac differentiation in Drosophila and regulates Notch signaling. *Proc Natl Acad Sci U S A,* 102**,** 18986-91.

LAGOS-QUINTANA, M., RAUHUT, R., MEYER, J., BORKHARDT, A. & TUSCHL, T. (2003) New microRNAs from mouse and human. *RNA,* 9**,** 175-9.

LAI, J. Y., LI, Y. T., CHO, C. H. & YU, T. C. (2012) Nanoscale modification of porous gelatin scaffolds with chondroitin sulfate for corneal stromal tissue engineering. *Int J Nanomedicine,* 7**,** 1101-14.

LAMBA, D. A., GUST, J. & REH, T. A. (2009) Transplantation of human embryonic stem cell-derived photoreceptors restores some visual function in Crx-deficient mice. *Cell Stem Cell,* 4**,** 73-9.

LAPCIK, L., JR., LAPCIK, L., DE SMEDT, S., DEMEESTER, J. & CHABRECEK, P. (1998) Hyaluronan: Preparation, Structure, Properties, and Applications. *Chem Rev,* 98**,** 2663-2684.

LAVAIL, M. M., FAKTOROVICH, E. G., HEPLER, J. M., PEARSON, K. L., YASUMURA, D., MATTHES, M. T. & STEINBERG, R. H. (1991) Basic fibroblast growth factor protects photoreceptors from light-induced degeneration in albino rats. *Ann N Y Acad Sci,* 638**,** 341-7.

LAWRENCE, J. M., SINGHAL, S., BHATIA, B., KEEGAN, D. J., REH, T. A., LUTHERT, P. J., KHAW, P. T. & LIMB, G. A. (2007) MIO-M1 cells and similar Müller glial cell lines derived from adult human retina exhibit neural stem cell characteristics. *Stem Cells,* 25**,** 2033-43.

LEE, H., MCKEON, R. J. & BELLAMKONDA, R. V. (2010) Sustained delivery of thermostabilized chABC enhances axonal sprouting and functional recovery after spinal cord injury. *Proc Natl Acad Sci U S A,* 107**,** 3340-5.

LEVIN, L. A. (2005) Pathophysiology of the progressive optic neuropathy of glaucoma. *Ophthalmol Clin North Am,* 18**,** 355-64, v.

LEVIS, H. J., BROWN, R. A. & DANIELS, J. T. (2010) Plastic compressed collagen as a biomimetic substrate for human limbal epithelial cell culture. *Biomaterials,* 31**,** 7726-37.

LEVKOVITCH-VERBIN, H., SADAN, O., VANDER, S., ROSNER, M., BARHUM, Y., MELAMED, E., OFFEN, D. & MELAMED, S. (2010) Intravitreal injections of neurotrophic factors secreting mesenchymal stem cells are neuroprotective in rat eyes following optic nerve transection. *Invest Ophthalmol Vis Sci,* 51**,** 6394-400.

LEWIS, G. P., CHAPIN, E. A., LUNA, G., LINBERG, K. A. & FISHER, S. K. (2010) The fate of Müller's glia following experimental retinal detachment: nuclear migration, cell division, and subretinal glial scar formation. *Mol Vis,* 16**,** 1361-72.

LI, Y., SAUVE, Y., LI, D., LUND, R. D. & RAISMAN, G. (2003) Transplanted olfactory ensheathing cells promote regeneration of cut adult rat optic nerve axons. *J Neurosci,* 23**,** 7783-8.

LI, Y., VANDENBOOM, T. G., 2ND, KONG, D., WANG, Z., ALI, S., PHILIP, P. A. & SARKAR, F. H. (2009) Up-regulation of miR-200 and let-7 by natural agents leads to the reversal of epithelial-to-mesenchymal transition in gemcitabine-resistant pancreatic cancer cells. *Cancer Res,* 69**,** 6704-12.

LIU, N., OKAMURA, K., TYLER, D. M., PHILLIPS, M. D., CHUNG, W. J. & LAI, E. C. (2008) The evolution and functional diversification of animal microRNA genes. *Cell Res,* 18**,** 985-96.

LIU, T., XU, J., CHAN, B. P. & CHEW, S. Y. (2012) Sustained release of neurotrophin-3 and chondroitinase ABC from electrospun collagen nanofiber scaffold for spinal cord injury repair. *J Biomed Mater Res A,* 100**,** 236-42.

LIU, W., KHARE, S. L., LIANG, X., PETERS, M. A., LIU, X., CEPKO, C. L. & XIANG, M. (2000) All Brn3 genes can promote retinal ganglion cell differentiation in the chick. *Development,* 127**,** 3237-47.

LIU, W., MO, Z. & XIANG, M. (2001) The Ath5 proneural genes function upstream of Brn3 POU domain transcription factor genes to promote retinal ganglion cell development. *Proc Natl Acad Sci U S A,* 98**,** 1649-54.

LIU, X. S., CHOPP, M., ZHANG, R. L., TAO, T., WANG, X. L., KASSIS, H., HOZESKA-SOLGOT, A., ZHANG, L., CHEN, C. & ZHANG, Z. G. (2011) MicroRNA profiling in subventricular zone after stroke: MiR-124a regulates proliferation of neural progenitor cells through Notch signaling pathway. *PLoS One,* 6**,** e23461.

LIVESEY, F. J. & CEPKO, C. L. (2001) Vertebrate neural cell-fate determination: lessons from the retina. *Nat Rev Neurosci,* 2**,** 109-18.

LOSCHER, C. J., HOKAMP, K., KENNA, P. F., IVENS, A. C., HUMPHRIES, P., PALFI, A. & FARRAR, G. J. (2007) Altered retinal microRNA expression profile in a mouse model of retinitis pigmentosa. *Genome Biol,* 8**,** R248.

LOUVI, A. & ARTAVANIS-TSAKONAS, S. (2006) Notch signalling in vertebrate neural development. *Nat Rev Neurosci,* 7**,** 93-102.

LUTOLF, M. P. & BLAU, H. M. (2009) Artificial stem cell niches. *Adv Mater,* 21**,** 3255-68.

MACAYA, D. & SPECTOR, M. (2012) Injectable hydrogel materials for spinal cord regeneration: a review. *Biomed Mater,* 7**,** 012001.

MACK, A. F., GERMER, A., JANKE, C. & REICHENBACH, A. (1998) Müller (glial) cells in the teleost retina: consequences of continuous growth. *Glia,* 22**,** 306-13.

MACLAREN, R. E., PEARSON, R. A., MACNEIL, A., DOUGLAS, R. H., SALT, T. E., AKIMOTO, M., SWAROOP, A., SOWDEN, J. C. & ALI, R. R. (2006) Retinal repair by transplantation of photoreceptor precursors. *Nature,* 444**,** 203-7.

MAGUIRE, A. M., SIMONELLI, F., PIERCE, E. A., PUGH, E. N., JR., MINGOZZI, F., BENNICELLI, J., BANFI, S., MARSHALL, K. A., TESTA, F., SURACE, E. M., ROSSI, S., LYUBARSKY, A., ARRUDA, V. R., KONKLE, B., STONE, E., SUN, J., JACOBS, J., DELL'OSSO, L., HERTLE, R., MA, J. X., REDMOND, T. M., ZHU, X., HAUCK, B., ZELENAIA, O., SHINDLER, K. S., MAGUIRE, M. G., WRIGHT, J. F., VOLPE, N. J., MCDONNELL, J. W., AURICCHIO, A.,

HIGH, K. A. & BENNETT, J. (2008) Safety and efficacy of gene transfer for Leber's congenital amaurosis. *N Engl J Med,* 358**,** 2240-8.

MARQUARDT, T., ASHERY-PADAN, R., ANDREJEWSKI, N., SCARDIGLI, R., GUILLEMOT, F. & GRUSS, P. (2001) Pax6 is required for the multipotent state of retinal progenitor cells. *Cell,* 105**,** 43-55.

MARQUARDT, T. & GRUSS, P. (2002) Generating neuronal diversity in the retina: one for nearly all. *Trends Neurosci,* 25**,** 32-8.

MARTINEZ, I., CAZALLA, D., ALMSTEAD, L. L., STEITZ, J. A. & DIMAIO, D. (2011) miR-29 and miR-30 regulate B-Myb expression during cellular senescence. *Proc Natl Acad Sci U S A,* 108**,** 522-7.

MASON, C. & DUNNILL, P. (2008) A brief definition of regenerative medicine. *Regen Med,* 3**,** 1-5.

MASTERS, K. S., SHAH, D. N., WALKER, G., LEINWAND, L. A. & ANSETH, K. S. (2004) Designing scaffolds for valvular interstitial cells: cell adhesion and function on naturally derived materials. *J Biomed Mater Res A,* 71**,** 172-80.

MATTHEWS, J. A., WNEK, G. E., SIMPSON, D. G. & BOWLIN, G. L. (2002) Electrospinning of collagen nanofibers. *Biomacromolecules,* 3**,** 232-8.

MCKEON, R. J., HOKE, A. & SILVER, J. (1995) Injury-induced proteoglycans inhibit the potential for laminin-mediated axon growth on astrocytic scars. *Exp Neurol,* 136**,** 32-43.

MCMANUS, M. C., BOLAND, E. D., KOO, H. P., BARNES, C. P., PAWLOWSKI, K. J., WNEK, G. E., SIMPSON, D. G. & BOWLIN, G. L. (2006) Mechanical properties of electrospun fibrinogen structures. *Acta Biomater,* 2**,** 19-28.

MELLER, K. & TETZLAFF, W. (1976) Scanning electron microscopic studies on the development of the chick retina. *Cell Tissue Res,* 170**,** 145-59.

MELLOUGH, C. B., CUI, Q. & HARVEY, A. R. (2007) Treatment of adult neural progenitor cells prior to transplantation affects graft survival and integration in a neonatal and adult rat model of selective retinal ganglion cell depletion. *Restor Neurol Neurosci,* 25**,** 177-90.

MERKLE, F. T., TRAMONTIN, A. D., GARCIA-VERDUGO, J. M. & ALVAREZ-BUYLLA, A. (2004) Radial glia give rise to adult neural stem cells in the subventricular zone. *Proc Natl Acad Sci U S A,* 101**,** 17528-32.

MIELE, L., GOLDE, T. & OSBORNE, B. (2006a) Notch signaling in cancer. *Curr Mol Med,* 6**,** 905-18.

MIELE, L., MIAO, H. & NICKOLOFF, B. J. (2006b) NOTCH signaling as a novel cancer therapeutic target. *Curr Cancer Drug Targets,* 6**,** 313-23.

MIELE, L. & OSBORNE, B. (1999) Arbiter of differentiation and death: Notch signaling meets apoptosis. *J Cell Physiol,* 181**,** 393-409.

MIN, B. M., LEE, G., KIM, S. H., NAM, Y. S., LEE, T. S. & PARK, W. H. (2004) Electrospinning of silk fibroin nanofibers and its effect on the adhesion and spreading of normal human keratinocytes and fibroblasts in vitro. *Biomaterials,* 25**,** 1289-97.

MORAIS, J. M., PAPADIMITRAKOPOULOS, F. & BURGESS, D. J. (2010) Biomaterials/tissue interactions: possible solutions to overcome foreign body response. *AAPS J,* 12**,** 188-96.

MORRIS, A. C., SCHOLZ, T. & FADOOL, J. M. (2008) Rod progenitor cells in the mature zebrafish retina. *Adv Exp Med Biol,* 613**,** 361-8.

MOSS, E. G., LEE, R. C. & AMBROS, V. (1997) The cold shock domain protein LIN-28 controls developmental timing in C. elegans and is regulated by the lin-4 RNA. *Cell,* 88**,** 637-46.

MU, X., FU, X., BEREMAND, P. D., THOMAS, T. L. & KLEIN, W. H. (2008) Gene regulation logic in retinal ganglion cell development: Isl1 defines a critical branch distinct from but overlapping with Pou4f2. *Proc Natl Acad Sci U S A,* 105**,** 6942-7.

MU, X. & KLEIN, W. H. (2004) A gene regulatory hierarchy for retinal ganglion cell specification and differentiation. *Semin Cell Dev Biol,* 15**,** 115-23.

MURAKAMI, Y., YASUDA, T., SAIGO, K., URASHIMA, T., TOYODA, H., OKANOUE, T. & SHIMOTOHNO, K. (2006) Comprehensive analysis of microRNA expression patterns in hepatocellular carcinoma and non-tumorous tissues. *Oncogene,* 25**,** 2537-45.

NAGEL, A. C. & PREISS, A. (2011) Fine tuning of Notch signaling by differential co-repressor recruitment during eye development of Drosophila. *Hereditas,* 148**,** 77-84.

NAKAGAWA, M., KOYANAGI, M., TANABE, K., TAKAHASHI, K., ICHISAKA, T., AOI, T., OKITA, K., MOCHIDUKI, Y., TAKIZAWA, N. & YAMANAKA, S. (2008) Generation of induced pluripotent stem cells without Myc from mouse and human fibroblasts. *Nat Biotechnol,* 26**,** 101-6.

NEELEY, W. L., REDENTI, S., KLASSEN, H., TAO, S., DESAI, T., YOUNG, M. J. & LANGER, R. (2008) A microfabricated scaffold for retinal progenitor cell grafting. *Biomaterials,* 29**,** 418-26.

NELSON, B. R., UEKI, Y., REARDON, S., KARL, M. O., GEORGI, S., HARTMAN, B. H., LAMBA, D. A. & REH, T. A. (2011) Genome-wide analysis of Müller glial differentiation reveals a requirement for Notch signaling in postmitotic cells to maintain the glial fate. *PLoS One,* 6**,** e22817.

NELSON, C. M. & HYDE, D. R. (2012) Müller glia as a source of neuronal progenitor cells to regenerate the damaged zebrafish retina. *Adv Exp Med Biol,* 723**,** 425-30.

NG, T. F. & STREILEIN, J. W. (2001) Light-induced migration of retinal microglia into the subretinal space. *Invest Ophthalmol Vis Sci,* 42**,** 3301-10.

NGUYEN, K. T. & WEST, J. L. (2002) Photopolymerizable hydrogels for tissue engineering applications. *Biomaterials,* 23**,** 4307-14.

NICOLI, S., KNYPHAUSEN, C. P., ZHU, L. J., LAKSHMANAN, A. & LAWSON, N. D. (2012) miR-221 is required for endothelial tip cell behaviors during vascular development. *Dev Cell,* 22**,** 418-29.

NOJEHDEHIAN, H., MOZTARZADEH, F., BAHARVAND, H., MEHRJERDI, N. Z., NAZARIAN, H. & TAHRIRI, M. (2010) Effect of poly-L-lysine coating on retinoic acid-loaded PLGA microspheres in the differentiation of carcinoma stem cells into neural cells. *Int J Artif Organs,* 33**,** 721-30.

NURUL-SYAKIMA, A. M., YOKE-KQUEEN, C., SABARIAH, A. R., SHIRAN, M. S., SINGH, A. & LEARN-HAN, L. (2011) Differential microRNA expression and identification of putative miRNA targets and pathways in head and neck cancers. *Int J Mol Med,* 28**,** 327-36.

O'BRIEN, F. J., HARLEY, B. A., YANNAS, I. V. & GIBSON, L. (2004) Influence of freezing rate on pore structure in freeze-dried collagen-GAG scaffolds. *Biomaterials,* 25**,** 1077-86.

OHSAWA, R. & KAGEYAMA, R. (2008) Regulation of retinal cell fate specification by multiple transcription factors. *Brain Res,* 1192**,** 90-8.

OKAMURA, K., CHUNG, W. J. & LAI, E. C. (2008a) The long and short of inverted repeat genes in animals: microRNAs, mirtrons and hairpin RNAs. *Cell Cycle,* 7**,** 2840-5.

OKAMURA, K., PHILLIPS, M. D., TYLER, D. M., DUAN, H., CHOU, Y. T. & LAI, E. C. (2008b) The regulatory activity of microRNA* species has substantial influence on microRNA and 3' UTR evolution. *Nat Struct Mol Biol,* 15**,** 354-63.

OKITA, K., ICHISAKA, T. & YAMANAKA, S. (2007) Generation of germline-competent induced pluripotent stem cells. *Nature,* 448**,** 313-7.

OKITA, K., NAKAGAWA, M., HYENJONG, H., ICHISAKA, T. & YAMANAKA, S. (2008) Generation of mouse induced pluripotent stem cells without viral vectors. *Science,* 322**,** 949-53.

OKUYAMA, R., TAGAMI, H. & AIBA, S. (2008) Notch signaling: its role in epidermal homeostasis and in the pathogenesis of skin diseases. *J Dermatol Sci,* 49**,** 187-94.

OLIVEIRA, J. C., BRASSESCO, M. S., MORALES, A. G., PEZUK, J. A., FEDATTO, P. F., DA SILVA, G. N., SCRIDELI, C. A. & TONE, L. G. (2011) MicroRNA-100 acts as a tumor suppressor in human bladder carcinoma 5637 cells. *Asian Pac J Cancer Prev,* 12**,** 3001-4.

ONG, J. M. & DA CRUZ, L. (2012) A review and update on the current status of stem cell therapy and the retina. *Br Med Bull,* 102**,** 133-46.

OOTO, S., AKAGI, T., KAGEYAMA, R., AKITA, J., MANDAI, M., HONDA, Y. & TAKAHASHI, M. (2004) Potential for neural regeneration after neurotoxic injury in the adult mammalian retina. *Proc Natl Acad Sci U S A,* 101**,** 13654-9.

OSAKADA, F., OOTO, S., AKAGI, T., MANDAI, M., AKAIKE, A. & TAKAHASHI, M. (2007) Wnt signaling promotes regeneration in the retina of adult mammals. *J Neurosci,* 27**,** 4210-9.

OTTANI, V., MARTINI, D., FRANCHI, M., RUGGERI, A. & RASPANTI, M. (2002) Hierarchical structures in fibrillar collagens. *Micron,* 33**,** 587-96.

OTTESON, D. C. & HITCHCOCK, P. F. (2003) Stem cells in the teleost retina: persistent neurogenesis and injury-induced regeneration. *Vision Res,* 43**,** 927-36.

PAKULSKA, M. M., BALLIOS, B. G. & SHOICHET, M. S. (2012) Injectable hydrogels for central nervous system therapy. *Biomed Mater,* 7**,** 024101.

PARAMESWARAN, S., BALASUBRAMANIAN, S., BABAI, N., QIU, F., EUDY, J. D., THORESON, W. B. & AHMAD, I. (2010) Induced pluripotent stem cells generate both retinal ganglion cells and photoreceptors: therapeutic implications in degenerative changes in glaucoma and age-related macular degeneration. *Stem Cells,* 28**,** 695-703.

PARK, S. M., GAUR, A. B., LENGYEL, E. & PETER, M. E. (2008) The miR-200 family determines the epithelial phenotype of cancer cells by targeting the E-cadherin repressors ZEB1 and ZEB2. *Genes Dev,* 22**,** 894-907.

PARKER, J. S. & BARFORD, D. (2006) Argonaute: A scaffold for the function of short regulatory RNAs. *Trends Biochem Sci,* 31**,** 622-30.

PASCOLINI, D. & MARIOTTI, S. P. (2012) Global estimates of visual impairment: 2010. *Br J Ophthalmol,* 96**,** 614-8.

PENG, D. X., LUO, M., QIU, L. W., HE, Y. L. & WANG, X. F. (2012) Prognostic implications of microRNA-100 and its functional roles in human epithelial ovarian cancer. *Oncol Rep,* 27**,** 1238-44.

PENNESI, M. E., CHO, J. H., YANG, Z., WU, S. H., ZHANG, J., WU, S. M. & TSAI, M. J. (2003) BETA2/NeuroD1 null mice: a new model for transcription factor-dependent photoreceptor degeneration. *J Neurosci,* 23**,** 453-61.

PERA, E. M., WESSELY, O., LI, S. Y. & DE ROBERTIS, E. M. (2001) Neural and head induction by insulin-like growth factor signals. *Dev Cell,* 1**,** 655-65.

PIANTINO, J., BURDICK, J. A., GOLDBERG, D., LANGER, R. & BENOWITZ, L. I. (2006) An injectable, biodegradable hydrogel for trophic factor delivery enhances axonal rewiring and improves performance after spinal cord injury. *Exp Neurol,* 201**,** 359-67.

PLACE, E. S., EVANS, N. D. & STEVENS, M. M. (2009) Complexity in biomaterials for tissue engineering. *Nat Mater,* 8**,** 457-70.

POWERS, M. K. & GREEN, D. G. (1978) Single retinal ganglion cell responses in the dark-reared rat: grating acuity, contrast sensitivity, and defocusing. *Vision Res,* 18**,** 1533-9.

PREWITZ, M., SEIB, F. P., POMPE, T. & WERNER, C. (2012) Polymeric biomaterials for stem cell bioengineering. *Macromol Rapid Commun,* 33**,** 1420-31.

RAJAN, N., HABERMEHL, J., COTE, M. F., DOILLON, C. J. & MANTOVANI, D. (2006) Preparation of ready-to-use, storable and reconstituted type I collagen from rat tail tendon for tissue engineering applications. *Nat Protoc,* 1**,** 2753-8.

RAYMOND, P. A. (1991) Retinal regeneration in teleost fish. *Ciba Found Symp,* 160**,** 171-86; discussion 186-91.

REH, T. A. & FISCHER, A. J. (2001) Stem cells in the vertebrate retina. *Brain Behav Evol,* 58**,** 296-305.

REH, T. A. & LEVINE, E. M. (1998) Multipotential stem cells and progenitors in the vertebrate retina. *J Neurobiol,* 36**,** 206-20.

REICHENBACH, A., KASPER, M., SCHNITZER, J., OSBORNE, N. N. & PRITZ-HOHMEIER, S. (1994a) A set of early-born neurons is distinctly labeled by several defined antibodies in the adult rabbit retina. *J Hirnforsch,* 35**,** 391-5.

REICHENBACH, A., ZIEGERT, M., SCHNITZER, J., PRITZ-HOHMEIER, S., SCHAAF, P., SCHOBER, W. & SCHNEIDER, H. (1994b) Development of the rabbit retina. V. The question of 'columnar units'. *Brain Res Dev Brain Res,* 79**,** 72-84.

REMBOLD, M., LOOSLI, F., ADAMS, R. J. & WITTBRODT, J. (2006) Individual cell migration serves as the driving force for optic vesicle evagination. *Science,* 313**,** 1130-4.

RODRIGUEZ, A., GRIFFITHS-JONES, S., ASHURST, J. L. & BRADLEY, A. (2004) Identification of mammalian microRNA host genes and transcription units. *Genome Res,* 14**,** 1902-10.

ROESCH, K., JADHAV, A. P., TRIMARCHI, J. M., STADLER, M. B., ROSKA, B., SUN, B. B. & CEPKO, C. L. (2008) The transcriptome of retinal Müller glial cells. *J Comp Neurol,* 509**,** 225-38.

RONCHINI, C. & CAPOBIANCO, A. J. (2001) Induction of cyclin D1 transcription and CDK2 activity by Notch(ic): implication for cell cycle disruption in transformation by Notch(ic). *Mol Cell Biol,* 21**,** 5925-34.

ROQUE, R. S., IMPERIAL, C. J. & CALDWELL, R. B. (1996) Microglial cells invade the outer retina as photoreceptors degenerate in Royal College of Surgeons rats. *Invest Ophthalmol Vis Sci,* 37**,** 196-203.

ROTHAMEL, D., SCHWARZ, F., SAGER, M., HERTEN, M., SCULEAN, A. & BECKER, J. (2005) Biodegradation of differently cross-linked collagen membranes: an experimental study in the rat. *Clin Oral Implants Res,* 16**,** 369-78.

ROWAN, S. & CEPKO, C. L. (2004) Genetic analysis of the homeodomain transcription factor Chx10 in the retina using a novel multifunctional BAC transgenic mouse reporter. *Dev Biol,* 271**,** 388-402.

RYAN, D. G., OLIVEIRA-FERNANDES, M. & LAVKER, R. M. (2006) MicroRNAs of the mammalian eye display distinct and overlapping tissue specificity. *Mol Vis,* 12**,** 1175-84.

SAHA, K., POLLOCK, J. F., SCHAFFER, D. V. & HEALY, K. E. (2007) Designing synthetic materials to control stem cell phenotype. *Curr Opin Chem Biol,* 11**,** 381-7.

SALCHERT, K., OSWALD, J., STRELLER, U., GRIMMER, M., HEROLD, N. & WERNER, C. (2005) Fibrillar collagen assembled in the presence of glycosaminoglycans to constitute bioartificial stem cell niches in vitro. *J Mater Sci Mater Med,* 16**,** 581-5.

SALIFU, A. A., NURY, B. D. & LEKAKOU, C. (2011) Electrospinning of nanocomposite fibrillar tubular and flat scaffolds with controlled fiber orientation. *Ann Biomed Eng,* 39**,** 2510-20.

SCHAEFER, A., JUNG, M., MOLLENKOPF, H. J., WAGNER, I., STEPHAN, C., JENTZMIK, F., MILLER, K., LEIN, M., KRISTIANSEN, G. & JUNG, K. (2010) Diagnostic and prognostic implications of microRNA profiling in prostate carcinoma. *Int J Cancer,* 126**,** 1166-76.

SCHWARZ, D. S., HUTVAGNER, G., DU, T., XU, Z., ARONIN, N. & ZAMORE, P. D. (2003) Asymmetry in the assembly of the RNAi enzyme complex. *Cell,* 115**,** 199-208.

SEIGEL, G. M., MUTCHLER, A. L. & IMPERATO, E. L. (1996) Expression of glial markers in a retinal precursor cell line. *Mol Vis,* 2**,** 2.

SETHI, K. K., YANNAS, I. V., MUDERA, V., EASTWOOD, M., MCFARLAND, C. & BROWN, R. A. (2002) Evidence for sequential utilization of fibronectin, vitronectin, and collagen during fibroblast-mediated collagen contraction. *Wound Repair Regen,* 10**,** 397-408.

SHAKHBAZAU, A. V., PETYOVKA, N. V., KOSMACHEVA, S. M. & POTAPNEV, M. P. (2011) Neurogenic induction of human mesenchymal stem cells in fibrin 3D matrix. *Bull Exp Biol Med,* 150**,** 547-50.

SHARMA, K., SELZER, M. E. & LI, S. (2012) Scar-mediated inhibition and CSPG receptors in the CNS. *Exp Neurol,* 237**,** 370-8.

SIGLE, K. J., CAMANO-GARCIA, G., CARRIQUIRY, A. L., BETTS, D. M., KUEHN, M. H. & MCLELLAN, G. J. (2011) The effect of dorzolamide 2% on circadian intraocular pressure in cats with primary congenital glaucoma. *Vet Ophthalmol,* 14 Suppl 1**,** 48-53.

SILL, T. J. & VON RECUM, H. A. (2008) Electrospinning: applications in drug delivery and tissue engineering. *Biomaterials,* 29**,** 1989-2006.

SILVER, J. & MILLER, J. H. (2004) Regeneration beyond the glial scar. *Nat Rev Neurosci,* 5**,** 146-56.

SINGH, A. (2005) Medical therapy of glaucoma. *Ophthalmol Clin North Am,* 18**,** 397-408, vi.

SINGHAL, S., BHATIA, B., JAYARAM, H., BECKER, S., JONES, M. F., COTTRILL, P. B., KHAW, P. T., SALT, T. E. & LIMB, G. A. (2012) Human Müller Glia with Stem Cell Characteristics Differentiate into Retinal Ganglion Cell (RGC) Precursors In Vitro and Partially Restore RGC Function In Vivo Following Transplantation. *Stem Cells Transl Med,* 1**,** 188-99.

SINGHAL, S., LAWRENCE, J. M., BHATIA, B., ELLIS, J. S., KWAN, A. S., MACNEIL, A., LUTHERT, P. J., FAWCETT, J. W., PEREZ, M. T., KHAW, P. T. & LIMB, G. A. (2008) Chondroitin sulfate proteoglycans and microglia

prevent migration and integration of grafted Müller stem cells into degenerating retina. *Stem Cells,* 26**,** 1074-82.

SL SHENOY, W. B., HL FRISCH, GE WNEK (2005) Role of Chain Entanglements on fibre Formation during Electrospinning of Polymer Solutions: Good solvent, Non-specific Polymer-Polymer Interaction Limit. *Polymer,* 46**,** 8990.

SLACK, F. J., BASSON, M., LIU, Z., AMBROS, V., HORVITZ, H. R. & RUVKUN, G. (2000) The lin-41 RBCC gene acts in the C. elegans heterochronic pathway between the let-7 regulatory RNA and the LIN-29 transcription factor. *Mol Cell,* 5**,** 659-69.

SMIRNOVA, L., GRAFE, A., SEILER, A., SCHUMACHER, S., NITSCH, R. & WULCZYN, F. G. (2005) Regulation of miRNA expression during neural cell specification. *Eur J Neurosci,* 21**,** 1469-77.

SMITH-THOMAS, L. C., STEVENS, J., FOK-SEANG, J., FAISSNER, A., ROGERS, J. H. & FAWCETT, J. W. (1995) Increased axon regeneration in astrocytes grown in the presence of proteoglycan synthesis inhibitors. *J Cell Sci,* 108 (Pt 3)**,** 1307-15.

SODHA, S., WALL, K., REDENTI, S., KLASSEN, H., YOUNG, M. J. & TAO, S. L. (2011) Microfabrication of a three-dimensional polycaprolactone thin-film scaffold for retinal progenitor cell encapsulation. *J Biomater Sci Polym Ed,* 22**,** 443-56.

SOTTILE, V., LI, M. & SCOTTING, P. J. (2006) Stem cell marker expression in the Bergmann glia population of the adult mouse brain. *Brain Res,* 1099**,** 8-17.

SPILKER, M. H., ASANO, K., YANNAS, I. V. & SPECTOR, M. (2001) Contraction of collagen-glycosaminoglycan matrices by peripheral nerve cells in vitro. *Biomaterials,* 22**,** 1085-93.

STEINMETZ, M. P., HORN, K. P., TOM, V. J., MILLER, J. H., BUSCH, S. A., NAIR, D., SILVER, D. J. & SILVER, J. (2005) Chronic enhancement of the intrinsic growth capacity of sensory neurons combined with the degradation of inhibitory proteoglycans allows functional regeneration of sensory axons through the dorsal root entry zone in the mammalian spinal cord. *J Neurosci,* 25**,** 8066-76.

STERN, J. H. & TEMPLE, S. (2011) Stem cells for retinal replacement therapy. *Neurotherapeutics,* 8**,** 736-43.

STUMP, G., DURRER, A., KLEIN, A. L., LUTOLF, S., SUTER, U. & TAYLOR, V. (2002) Notch1 and its ligands Delta-like and Jagged are expressed and active in distinct cell populations in the postnatal mouse brain. *Mech Dev,* 114**,** 153-9.

SUN, J., CHEN, Z., TAN, X., ZHOU, F., TAN, F., GAO, Y., SUN, N., XU, X., SHAO, K. & HE, J. (2013) MicroRNA-99a/100 promotes apoptosis by targeting mTOR in human esophageal squamous cell carcinoma. *Med Oncol,* 30**,** 411.

SWANN, D. A. (1980) Chemistry and biology of the vitreous body. *Int Rev Exp Pathol,* 22**,** 1-64.

TAKADA, S. & ASAHARA, H. (2012) Current strategies for microRNA research. *Mod Rheumatol,* 22**,** 645-53.

TAKAHASHI, K. & YAMANAKA, S. (2006) Induction of pluripotent stem cells from mouse embryonic and adult fibroblast cultures by defined factors. *Cell,* 126**,** 663-76.

TARANOVA, O. V., MAGNESS, S. T., FAGAN, B. M., WU, Y., SURZENKO, N., HUTTON, S. R. & PEVNY, L. H. (2006) SOX2 is a dose-dependent regulator of retinal neural progenitor competence. *Genes Dev,* 20**,** 1187-202.

TAYLOR, S. J. & SAKIYAMA-ELBERT, S. E. (2006) Effect of controlled delivery of neurotrophin-3 from fibrin on spinal cord injury in a long term model. *J Control Release,* 116**,** 204-10.

TAYLOR, V. L., AL-GHOUL, K. J., LANE, C. W., DAVIS, V. A., KUSZAK, J. R. & COSTELLO, M. J. (1996) Morphology of the normal human lens. *Invest Ophthalmol Vis Sci,* 37**,** 1396-410.

THANOS, S. & RICHTER, W. (1993) The migratory potential of vitally labelled microglial cells within the retina of rats with hereditary photoreceptor dystrophy. *Int J Dev Neurosci,* 11**,** 671-80.

THOFT, R. A., WILEY, L. A. & SUNDARRAJ, N. (1989) The multipotential cells of the limbus. *Eye (Lond),* 3 (Pt 2)**,** 109-13.

TIBBETTS, M. D., SAMUEL, M. A., CHANG, T. S. & HO, A. C. (2012) Stem cell therapy for retinal disease. *Curr Opin Ophthalmol,* 23**,** 226-34.

TIBBITT, M. W. & ANSETH, K. S. (2009) Hydrogels as extracellular matrix mimics for 3D cell culture. *Biotechnol Bioeng,* 103**,** 655-63.

TOKUMOTO, Y., OGAWA, S., NAGAMUNE, T. & MIYAKE, J. (2010) Comparison of efficiency of terminal differentiation of oligodendrocytes from induced pluripotent stem cells versus embryonic stem cells in vitro. *J Biosci Bioeng,* 109**,** 622-8.

TOM, V. J., SANDROW-FEINBERG, H. R., MILLER, K., SANTI, L., CONNORS, T., LEMAY, M. A. & HOULE, J. D. (2009) Combining peripheral nerve grafts and chondroitinase promotes functional axonal regeneration in the chronically injured spinal cord. *J Neurosci,* 29**,** 14881-90.

TOMITA, M., LAVIK, E., KLASSEN, H., ZAHIR, T., LANGER, R. & YOUNG, M. J. (2005) Biodegradable polymer composite grafts promote the survival and differentiation of retinal progenitor cells. *Stem Cells,* 23**,** 1579-88.

TORRES, A., TORRES, K., PESCI, A., CECCARONI, M., PASZKOWSKI, T., CASSANDRINI, P., ZAMBONI, G. & MACIEJEWSKI, R. (2012) Deregulation of miR-100, miR-99a and miR-199b in tissues and plasma coexists with increased expression of mTOR kinase in endometrioid endometrial carcinoma. *BMC Cancer,* 12**,** 369.

TRABUCCHI, M., BRIATA, P., GARCIA-MAYORAL, M., HAASE, A. D., FILIPOWICZ, W., RAMOS, A., GHERZI, R. & ROSENFELD, M. G. (2009) The RNA-binding protein KSRP promotes the biogenesis of a subset of microRNAs. *Nature,* 459**,** 1010-4.

TROPEA, D., CALEO, M. & MAFFEI, L. (2003) Synergistic effects of brain-derived neurotrophic factor and chondroitinase ABC on retinal fiber sprouting after denervation of the superior colliculus in adult rats. *J Neurosci,* 23**,** 7034-44.

TROPEPE, V., COLES, B. L., CHIASSON, B. J., HORSFORD, D. J., ELIA, A. J., MCINNES, R. R. & VAN DER KOOY, D. (2000) Retinal stem cells in the adult mammalian eye. *Science,* 287**,** 2032-6.

UHLIN-HANSEN, L. & KOLSET, S. O. (1988) Cell density-dependent expression of chondroitin sulfate proteoglycan in cultured human monocytes. *J Biol Chem,* 263**,** 2526-31.

UMINO, Y. & SAITO, T. (2002) Spatial and temporal patterns of distribution of the gap junctional protein connexin43 during retinal regeneration of adult newt. *J Comp Neurol,* 454**,** 255-62.

VADIVELU, S., BECKER, D. & MCDONALD, J. W. (2005) Generating chimeric spinal cord: a novel model for transplantable oligodendrocyte progenitors derived from embryonic stem cells. *Neurosurg Focus,* 19**,** E3.

VANDERLUIT, J. L., FERGUSON, K. L., NIKOLETOPOULOU, V., PARKER, M., RUZHYNSKY, V., ALEXSON, T., MCNAMARA, S. M., PARK, D. S., RUDNICKI, M. & SLACK, R. S. (2004) p107 regulates neural precursor cells in the mammalian brain. *J Cell Biol,* 166**,** 853-63.

VENUGOPAL, J., LOW, S., CHOON, A. T. & RAMAKRISHNA, S. (2008) Interaction of cells and nanofiber scaffolds in tissue engineering. *J Biomed Mater Res B Appl Biomater,* 84**,** 34-48.

VERNENGO, J., FUSSELL, G. W., SMITH, N. G. & LOWMAN, A. M. (2008) Evaluation of novel injectable hydrogels for nucleus pulposus replacement. *J Biomed Mater Res B Appl Biomater,* 84**,** 64-9.

WALCOTT, J. C. & PROVIS, J. M. (2003) Müller cells express the neuronal progenitor cell marker nestin in both differentiated and undifferentiated human foetal retina. *Clin Experiment Ophthalmol,* 31**,** 246-9.

WALLENTEN, K. G., ANDREASSON, S. & GHOSH, F. (2008) Retinal function after vitrectomy. *Retina,* 28**,** 558-63.

WANG, S. W., KIM, B. S., DING, K., WANG, H., SUN, D., JOHNSON, R. L., KLEIN, W. H. & GAN, L. (2001) Requirement for math5 in the development of retinal ganglion cells. *Genes Dev,* 15**,** 24-9.

WANG, S. W., MU, X., BOWERS, W. J. & KLEIN, W. H. (2002) Retinal ganglion cell differentiation in cultured mouse retinal explants. *Methods,* 28**,** 448-56.

WANG, X. E. A. (2004) Electrostatic Assembly of Conjugated Polymer Thin Layers on Electrospun Nanofibrous Membranes for Biosensors. *Nano Letters* 4**,** 331-334.

WANG, Y., LI, W., ZANG, X., CHEN, N., LIU, T., TSONIS, P. A. & HUANG, Y. (2013) MicroRNA-204-5p regulates epithelial-to-mesenchymal transition

during human posterior capsule opacification by targeting SMAD4. *Invest Ophthalmol Vis Sci,* 54**,** 323-32.

WATT, A. J. & FORRESTER, L. M. (2006) Deriving and identifying hepatocytes from embryonic stem cells. *Stem Cell Rev,* 2**,** 19-22.

WIENHOLDS, E., KLOOSTERMAN, W. P., MISKA, E., ALVAREZ-SAAVEDRA, E., BEREZIKOV, E., DE BRUIJN, E., HORVITZ, H. R., KAUPPINEN, S. & PLASTERK, R. H. (2005) MicroRNA expression in zebrafish embryonic development. *Science,* 309**,** 310-1.

WILKINSON, C. P., FERRIS, F. L., 3RD, KLEIN, R. E., LEE, P. P., AGARDH, C. D., DAVIS, M., DILLS, D., KAMPIK, A., PARARAJASEGARAM, R. & VERDAGUER, J. T. (2003) Proposed international clinical diabetic retinopathy and diabetic macular edema disease severity scales. *Ophthalmology,* 110**,** 1677-82.

WIMPISSINGER, B. & BINDER, S. (2007) Entry-site-related retinal detachment after pars plana vitrectomy. *Acta Ophthalmol Scand,* 85**,** 782-5.

WONG, G. W., KNOWLES, G. C., MAK, T. W., FERRANDO, A. A. & ZUNIGA-PFLUCKER, J. C. (2012) HES1 opposes a PTEN-dependent check on survival, differentiation, and proliferation of TCRbeta-selected mouse thymocytes. *Blood,* 120**,** 1439-48.

WRAY, L. S., HU, X., GALLEGO, J., GEORGAKOUDI, I., OMENETTO, F. G., SCHMIDT, D. & KAPLAN, D. L. (2011) Effect of processing on silk-based biomaterials: reproducibility and biocompatibility. *J Biomed Mater Res B Appl Biomater,* 99**,** 89-101.

WU, C., JIN, B., CHEN, L., ZHUO, D., ZHANG, Z., GONG, K. & MAO, Z. (2013) MiR-30d induces apoptosis and is regulated by the Akt/FOXO pathway in renal cell carcinoma. *Cell Signal,* 25**,** 1212-21.

WULCZYN, F. G., SMIRNOVA, L., RYBAK, A., BRANDT, C., KWIDZINSKI, E., NINNEMANN, O., STREHLE, M., SEILER, A., SCHUMACHER, S. & NITSCH, R. (2007) Post-transcriptional regulation of the let-7 microRNA during neural cell specification. *FASEB J,* 21**,** 415-26.

XIAO, J., LIANG, D., ZHANG, H., LIU, Y., ZHANG, D., PAN, L., CHEN, X., DOEVENDANS, P. A., SUN, Y., LIANG, X., SLUIJTER, J. P. & CHEN, Y. H.

(2012) MicroRNA-204 is required for differentiation of human-derived cardiomyocyte progenitor cells. *J Mol Cell Cardiol,* 53**,** 751-9.

XU, S., SUNDERLAND, M. E., COLES, B. L., KAM, A., HOLOWACZ, T., ASHERY-PADAN, R., MARQUARDT, T., MCINNES, R. R. & VAN DER KOOY, D. (2007) The proliferation and expansion of retinal stem cells require functional Pax6. *Dev Biol,* 304**,** 713-21.

YAMAGUCHI, Y. (2000) Lecticans: organizers of the brain extracellular matrix. *Cell Mol Life Sci,* 57**,** 276-89.

YANEZ-MUNOZ, R. J., BALAGGAN, K. S., MACNEIL, A., HOWE, S. J., SCHMIDT, M., SMITH, A. J., BUCH, P., MACLAREN, R. E., ANDERSON, P. N., BARKER, S. E., DURAN, Y., BARTHOLOMAE, C., VON KALLE, C., HECKENLIVELY, J. R., KINNON, C., ALI, R. R. & THRASHER, A. J. (2006) Effective gene therapy with nonintegrating lentiviral vectors. *Nat Med,* 12**,** 348-53.

YANG, Z., QIAO, H. & LI, X. (2010) Effects of the CNTF-collagen gel-controlled delivery system on rat neural stem/progenitor cells behavior. *Sci China Life Sci,* 53**,** 504-10.

YI, R., DOEHLE, B. P., QIN, Y., MACARA, I. G. & CULLEN, B. R. (2005) Overexpression of exportin 5 enhances RNA interference mediated by short hairpin RNAs and microRNAs. *RNA,* 11**,** 220-6.

YOUNG, R. W. (1985) Cell differentiation in the retina of the mouse. *Anat Rec,* 212**,** 199-205.

YU, X., ZOU, J., YE, Z., HAMMOND, H., CHEN, G., TOKUNAGA, A., MALI, P., LI, Y. M., CIVIN, C., GAIANO, N. & CHENG, L. (2008) Notch signaling activation in human embryonic stem cells is required for embryonic, but not trophoblastic, lineage commitment. *Cell Stem Cell,* 2**,** 461-71.

YURCO, P. & CAMERON, D. A. (2005) Responses of Müller glia to retinal injury in adult zebrafish. *Vision Res,* 45**,** 991-1002.

ZHANG, J., ZHANG, H., LIU, J., TU, X., ZANG, Y., ZHU, J., CHEN, J. & DONG, L. (2012) miR-30 inhibits TGF-beta1-induced epithelial-to-mesenchymal transition in hepatocyte by targeting Snail1. *Biochem Biophys Res Commun,* 417**,** 1100-5.

ZHANG, L. & HSIEH, Y. L. (2008) Ultrafine cellulose acetate fibers with nanoscale structural features. *J Nanosci Nanotechnol,* 8**,** 4461-9.

ZHANG, X., GRAVES, P. R. & ZENG, Y. (2009) Stable Argonaute2 overexpression differentially regulates microRNA production. *Biochim Biophys Acta,* 1789**,** 153-9.

ZHANG, X. & ZENG, Y. (2010) Regulation of mammalian microRNA expression. *J Cardiovasc Transl Res,* 3**,** 197-203.

ZHANG, X. M. & YANG, X. J. (2001) Regulation of retinal ganglion cell production by Sonic hedgehog. *Development,* 128**,** 943-57.

ZHANG, Y., RAUCH, U. & PEREZ, M. T. (2003) Accumulation of neurocan, a brain chondroitin sulfate proteoglycan, in association with the retinal vasculature in RCS rats. *Invest Ophthalmol Vis Sci,* 44**,** 1252-61.

ZHANG, Y. M., HARTZELL, C., NARLOW, M. & DUDLEY, S. C., JR. (2002) Stem cell-derived cardiomyocytes demonstrate arrhythmic potential. *Circulation,* 106**,** 1294-9.

ZHENG SHU, X., LIU, Y., PALUMBO, F. S., LUO, Y. & PRESTWICH, G. D. (2004) In situ crosslinkable hyaluronan hydrogels for tissue engineering. *Biomaterials,* 25**,** 1339-48.

ZHENG, Y. S., ZHANG, H., ZHANG, X. J., FENG, D. D., LUO, X. Q., ZENG, C. W., LIN, K. Y., ZHOU, H., QU, L. H., ZHANG, P. & CHEN, Y. Q. (2012) MiR-100 regulates cell differentiation and survival by targeting RBSP3, a phosphatase-like tumor suppressor in acute myeloid leukemia. *Oncogene,* 31**,** 80-92.

ZHOU, S., SHEN, D., WANG, Y., GONG, L., TANG, X., YU, B., GU, X. & DING, F. (2012) microRNA-222 targeting PTEN promotes neurite outgrowth from adult dorsal root ganglion neurons following sciatic nerve transection. *PLoS One,* 7**,** e44768.

Chapter 8: Appendices

8.1. Tables

8.1.1. Antibodies

Antibody	Raised in	Supplier	Catalogue no.	Dilution
B-actin	mouse	Sigma	A5316 (clone-AC-74)	1/5000
B-III-Tubulin	mouse	Millipore	MAB1637	1/100
BRN3B	goat	Santa Cruz	N-15 sc-31987	1/200
HUD	rabbit	Santa Cruz	sc-2536	1/500
ISLET-1	mouse	DSHB	39.4D5	1/50
Neurofilament 200	mouse	DSHB	RT97	1in 10
Notch 1 AND NICD	rabbit	Santa Cruz	C-20 sc-6014	1/100

8.1.2. Primers

Gene	Accession no.	Sequence	cDNA position	Annealing Temp.	Product size	Source
B-ACTIN F	NM_001101	CATGTACGTTGCTATCCAGGC	393	60		
B-ACTIN R		CTCCTTAATGTCACGCACGAT	642	60	250	primer bank (id:4501885a1)
BRN3B F	NM_004575	CAGGTTCGAGTCCCTCACAC	903	60		
BRN3B R		ATGGCAAAGTAGGCTTCGAGC	1100	60	198	primer bank (id:4758948a2)
HES1 F	NM_005524.2	AAGATAGCTCGCGGCATTCCA	200	60		
HES1 R		CGTTCATGCACTCGCTGAAG	358	60	160	self
HES5 F	NM_001010926.2	AAGCTGGAGAAGGCCGACAT	244	60		
HES5 R		CGAGTAGCCTTCGCTGTAGT	360	60	116	self
HEY2F	NM_012259	CAACCCCTTGTCGCCTCTC	620	60		
HEY2R		CCG TGG ATG GCA TTC GGAG	730	60	111	primer bank (id:6912414a3)
HUD F	NM_021952.2	GAAACTGTCCTTCTCCCATGC	310	64		
HUD R		GATTGAGGCAGAGCTCGGAC	611	64	301	self
ISL1 F	NM_002202	CAGGTTGTACGGGATCAAATGC	207	60		
ISL1 R		CACACAGCGGAAACACTCGAT	315	60	109	primer bank (id:4504737a2)
NOTCH1 F	NM_017617	GCTGGACTGGTGAGGACTG	977	60		
NOTCH1 R		AGCCCTCGTTACAGGGGTT	1153	60	180	primer bank (id:27894368a3)

8.2. Publications

Bhatia B, Jayaram H, Singhal S, **Jones MF**, Limb GA. Neurogenic and Proliferative Differences Between Müller Glia with Stem Cell Characteristics and the Ciliary Epithelium from the Adult Human Eye. Exp Eye Res 2011

Singhal S, Bhatia B**,** Jayaram H**,** Becker S, **Jones MF,** Cottrill PB, Khaw PT, Salt TE, Limb GA**.** Human Müller glia with stem cell characteristics differentiate into retinal ganglion cell (RGC) precursors in vitro and partially restore RGC function in vivo following transplantation. *Stem Cells* Transl Med. 2012 Mar;1(3):188-99.